

# Tumour promoting HER2 splice variant $\Delta 16$ HER2: Regulation and implication in breast cancer

**Anna-Lena Dittrich**

**2/22/2017**

A thesis submitted for the degree of Doctor  
of Philosophy



---

**Institute of  
Cellular Medicine**



## Abstract

Results from high-throughput studies of the last decade have shown an important connection between regulated pre-mRNA splicing and tumorigenesis as well as therapy resistance. To date only relatively few such interactions have been studied in depth. The human epidermal growth factor receptor 2 (HER2) is an important biomarker in cancer, especially in 20-30% of breast cancer cases. This subset of breast cancer patients are treated with HER2-targeting therapies in addition to chemotherapy. Although these therapies are very successful, in a subset of patients with primary tumours as well as in advanced metastatic breast cancer resistance occurs. The underlying mechanisms are not well understood; one potential cause is the alternative splicing of *HER2* pre-mRNA yielding protein variants which can evade or prevent action of these therapeutics. This PhD thesis details progress in understanding the mechanisms regulating the production of the HER2 variant  $\Delta 16$ HER2, which has been shown to have high oncogenic potential. Four key splicing factors that regulate this splicing event were identified as well as a specific RNA:protein binding site in the  $\Delta 16$ HER2 splicing region.

In addition, a potential novel HER2 mRNA transcript was identified involving retention of intron 25 (termed I25HER2). I25HER2 was shown to be expressed in both normal human tissues and breast cancer tissue samples. Interestingly, the expression level of I25HER2 is not proportional to wild type HER2 in all tissues. Although, I25HER2 would be expected to undergo nonsense-mediated decay, this study indicated that I25HER2 mRNA has similar stability to  $\Delta 16$ HER2 mRNA.

An ongoing challenge in both clinical and non-clinical studies is the inability to distinguish different HER2 protein variants. Initial results presented in this thesis, from a comparative study between immunohistochemistry (using three different HER2 antibodies, including the clinically used HercepTest™) and *HER2* gene amplification (using *HER2* CISH pharmDx™) in a cohort of primary human ductal carcinomas showed a subset of discordant cases. In a few of these tumours elevated levels of HER2 splice variants could be detected. The

possible implication for successful treatment of these patients' highlights the importance of linking the basic processing of HER2 transcripts and protein variants with pathological information from patients.

## Acknowledgement

*"A journey of a thousand miles begins with a single step"*

by Lao Tsu (604 BC - 531 BC)

I came across a poster with this quote in the first weeks of my PhD and it has kept me company throughout these three years. Step by step I completed this journey and with every step came new challenges, but also help from many wonderful new people.

First I would like to thank my supervisors, Dr Alison Tyson-Capper for giving me this opportunity, encouraging me and giving me the chance to explore my own ideas, and my second supervisor Dr Hannah Gautrey for her hands on help with my research and encouragement. This work would not have been possible without the breast tumour samples provided by the Breast Cancer Now Tissue Bank and the help of Dr Helen Kourea, with her experience in clinical pathology. My thanks also go to Dr John Brain for letting me use his microscope. Next I have to thank my annual review team Dr Jeremy Brown and Dr Xiao Wang for ripping my work apart to find any weakness, to challenge and encourage me to bring the best out of my work.

I couldn't imagine what this time would have been without the other members of our lab. First of all, Marco Silipo who started and finished his PhD with me. He was always there to bounce ideas off, to give a helping hand and to cheer me up. Helen Lawrence and Soulaf Kakel who were great colleagues and friends, as well as all our BSc and MSc students who brought in fresh air, some challenges but also some really good fun.

I had the most amazing time not last due to the John Kirby lab who basically adopted me. Letting me borrow reagents and equipment, inviting me to their Christmas parties as well as the lab drinks. You all were great colleagues to work with and amazing friends: Bea, Ben, Cat, Irene, Jose, Laura, Nina, Rachel, Rishab, Shameem and Tom. The people that can't be forgotten for the lovely company they were and the great source of knowledge, the wonderful team of technicians on our floor: Barbara, Grant, Julie, Kate, Nikki and Rachel.

Halfway along this journey I found a wonderful man who has stayed with me through all my ups and downs. Thank you for being there Mike!

Even across 1000s of miles I have been supported by my best friend. Thanks a ton Tita!

But nothing, not the first and surely not the last step on this journey to my PhD would have been possible without my family. Mama, Papa, Alex, Ihr seid die Besten!

## Table of contents

Abstract.....	ii
Acknowledgement.....	iv
Abbreviations .....	xii
List of Figures .....	xv
List of Tables.....	i
Chapter 1: Introduction .....	1
1.1. The Human Breast.....	1
1.2. Breast cancer.....	3
1.2.1. Breast cancer epidemiology .....	3
1.2.2. Breast cancer risk factors .....	3
1.2.3. Breast cancer categorisation .....	5
1.3. Oestrogen receptor .....	9
1.4. Progesterone receptor .....	11
1.5. Human epidermal growth factor receptor 2 .....	13
1.5.1. The regulation of HER2 gene expression.....	13
1.5.2. HER2 transcript and protein variants.....	15
1.5.3. The protein structure of HER2.....	16
1.5.4. HER2 signalling pathways.....	20
1.5.4.1. Co-receptors of HER2.....	22
1.5.4.2. The RAS/MAPK signalling pathway .....	23
1.5.4.3. The PI3K-AKT signalling pathway.....	24
1.5.5. The crosstalk between HER2 and the hormone receptors .....	26
1.5.6. Function of nuclear HER2 .....	28
1.6. Breast cancer therapy.....	29
1.6.1. HER2 targeting therapy.....	31

1.7.	Eukaryotic mRNA processing .....	34
1.7.1.	The importance of pre-mRNA splicing.....	35
1.7.2.	Basic mechanisms of splicing.....	37
1.7.3.	Assembly and function of the spliceosome .....	38
1.7.4.	Regulators of alternative splicing.....	40
1.8.	Alternative splicing and cancer .....	43
1.9.	HER2 splice variants and their role in cancer .....	44
1.10.	Anti-HER2 therapy resistance: Focus on HER2 splice variants.....	48
1.11.	Rationale, hypotheses and aims.....	51
1.11.1.	Study rationale .....	51
1.11.2.	Hypotheses .....	51
1.11.3.	Aims .....	52
Chapter 2:	General materials and methods .....	53
2.1.	Cell lines .....	53
2.2.	Cell culture.....	53
2.2.1.	Cell line maintenance .....	54
2.2.2.	Mycoplasma testing.....	54
2.2.3.	Cryopreservation of cells.....	55
2.2.4.	Cell counting.....	55
2.2.5.	Transient gene knockdown by siRNA transfection .....	56
2.3.	Human breast tissue .....	57
2.4.	Normal human tissue cDNA.....	57
2.5.	RNA isolation techniques.....	58
2.5.1.	Total RNA isolation.....	58
2.5.2.	mRNA isolation.....	59
2.5.3.	Isolation of Cytoplasmic and Nuclear RNA Fraction.....	60
2.6.	Polymerase chain reaction (PCR) based techniques .....	61
2.6.1.	Reverse transcription .....	61

2.6.2.	Conventional PCR.....	62
2.6.3.	Real-Time PCR: SYBR Green.....	64
2.6.4.	Real-Time PCR: TaqMan™ Assays .....	65
2.7.	Protein based techniques .....	66
2.7.1.	Protein isolation.....	66
2.7.2.	Protein quantification.....	67
2.7.3.	SDS-polyacrylamide gel electrophoresis (SDS-PAGE) .....	67
2.7.4.	Western blot .....	68
2.8.	Cloning and transformation in Escherichia coli ( <i>E.coli</i> ) .....	69
2.8.1.	PCR product isolation from agarose gel.....	70
2.8.2.	Ligation into pCR™4 TOPO® and transformation into E.coli .....	70
2.8.3.	Plasmid DNA isolation from E.coli .....	71
2.8.4.	Restriction digest.....	72
2.9.	Sanger sequencing.....	72
2.10.	<i>In-silico</i> prediction of RNA secondary structure .....	72
Chapter 3:	Investigating the regulation of the $\Delta$ 16HER2 splicing event.....	74
3.1.	Introduction .....	74
3.2.	Aims.....	76
3.3.	Methodology .....	77
3.3.1.	In-silico prediction of the splicing factor binding .....	77
3.3.2.	RNA chromatography assay.....	78
3.3.3.	$\Delta$ 16HER2-minigene construction .....	82
3.3.4.	Site-directed mutagenesis v.1 on $\Delta$ 16HER2-minigene.....	85
3.3.5.	Site-directed mutagenesis v.2 on $\Delta$ 16HER2-minigene.....	87
3.3.6.	Transfection of the $\Delta$ 16HER2-minigene with and without transient splicing factor knockdown.....	89
3.3.7.	Treatment of SKBR3 cells with lapatinib .....	89
3.3.8.	Treatment of cells with progesterone .....	90

3.3.9. Statistical analysis .....	90
3.4. Results.....	91
3.4.1. Describing the $\Delta$ 16HER2 mRNA transcript .....	91
3.4.2. In-silico predictions for the regulation of $\Delta$ 16HER2 splicing .....	95
3.4.3. Identification of splicing factors that bind the $\Delta$ 16HER2 splicing region	97
3.4.4. Verification by transient knockdown in HER+/- cell lines.....	99
3.4.5. Efficiency of the $\Delta$ 16HER2-minigene construct .....	107
3.4.6. Identification of regulatory sequences by site-directed mutagenesis	109
3.4.7. Regulation of splicing factor expression through HER2 .....	111
3.4.8. Progesterone induces HER2 expression.....	115
3.5. Discussion .....	117
3.5.1. Identification of the $\Delta$ 16HER2 splicing event regulating factors ..	118
3.5.2. Feedback-loop between HER2 and its splicing regulators? .....	125
3.5.3. Progesterone induced expression of HER2 .....	126
3.5.4. Summary.....	128
3.5.5. Future work .....	129
Chapter 4: Characterising HER2 in human breast tumours .....	132
4.1. Introduction .....	132
4.2. Aims.....	135
4.3. Specific methodology.....	135
4.3.1. Immunohistochemistry (IHC).....	135
4.3.2. HER2 chromogenic in-situ hybridisation (CISH).....	139
4.3.3. Scoring of HER2 CISH .....	142
4.4. Results.....	144
4.4.1. Immunohistochemistry for HER2 protein expression and localisation in human breast tumours .....	144
4.4.2. HER2 gene amplifications in human breast tumours.....	149

4.4.3.	Comparison of HER2 protein levels and HER2 gene amplification in a cohort of human breast tumours.....	153
4.4.4.	HER2 splice variant expression in selected, discrepant breast tumour cases.....	164
4.5.	Discussion .....	166
4.5.1.	Discrepant IHC and CISH staining in invasive ductal carcinomas 166	
4.5.2.	Possible role of HER2 splice variants in discrepant breast cancer cases 169	
4.6.	Summary .....	170
4.7.	Further work.....	171
Chapter 5:	Identification of novel HER2 splice variants .....	173
5.1.	Introduction .....	173
5.2.	Aims.....	175
5.3.	Specific methodology.....	175
5.3.1.	In-silico predictions of I25HER2 .....	175
5.3.2.	RNA stability assay .....	176
5.3.3.	Northern blot using NorthernMax <sup>®</sup> -Gly .....	176
5.4.	Results.....	180
5.4.1.	Identification of novel HER2 splicing events by PCR .....	180
5.4.2.	In-silico predictions for I25HER2 mRNA and protein.....	184
5.4.3.	Expression of I25HER2 in cell lines and tissue .....	188
5.4.4.	Stability of I25HER2 mRNA.....	191
5.5.	Discussion .....	195
5.5.1.	Intron 25 retention .....	195
5.5.2.	Summary .....	203
5.5.3.	Further work .....	203
Chapter 6:	Conclusion and outlook.....	205
6.1.	Conclusion .....	205

6.2. Outlook .....	207
References.....	208
Appendix.....	241
Publications .....	241
Presentations.....	241
Awards.....	242

## Abbreviations

<b>4E-BP1</b>	eIF4E binding protein 1
<b>ADCC</b>	antibody-dependent cellular cytotoxicity
<b>AR</b>	androgen receptor
<b>ATM</b>	ataxia telangiectasia mutated
<b>ATP</b>	adenosine triphosphate
<b>Bad</b>	B cell leukemia 2 antagonist of cell death
<b>BBP</b>	branch point bound protein
<b>BP</b>	branch point
<b>BPS</b>	branch point sequence
<b>BRCA1</b>	breast cancer early onset genes
<b>CDK</b>	cyclin dependent kinase
<b>cDNA</b>	complement DNA
<b>CEN-17</b>	chromosome 17 centromere
<b>CISH</b>	chromogenic <i>in situ</i> hybridization
<b>ck2</b>	casein-kinase 2
<b>Cox-2</b>	cyclooxygenase-2
<b>CTF</b>	c-terminal fragment
<b>DCIS</b>	ductal carcinoma in situ
<b>DNA</b>	deoxyribonucleic acid
<b>DMSO</b>	dimethyl sulphoxide
<b>ECD</b>	extracellular domain
<b>EJC</b>	exon junction complex
<b>Elk-1</b>	erythroblastosis virus E26 oncogene homolog 1 like gene 1
<b>EMT</b>	epithelial to mesenchymal transition
<b>ER</b>	oestrogen receptor
<b>ErbB</b>	erythroblastosis oncogene B
<b>ERE</b>	oestrogen response element
<b>ERK</b>	extracellular signal-regulated kinase
<b>ESE</b>	exonic splicing enhancers
<b>ESR 1/2</b>	oestrogen receptor 1/2
<b>ESS</b>	exonic splicing silencers
<b>FDA</b>	Food and Drug Administration
<b>FFPE</b>	formalin-fixed paraffin-embedded
<b>FISH</b>	fluorescent <i>in situ</i> hybridization
<b>FOXO3a</b>	forkhead box O3a
<b>GDP</b>	guanosine diphosphate
<b>GRB2</b>	growth factor receptor-bound protein 2
<b>GTP</b>	guanosine triphosphate
<b>HER 2</b>	human epidermal growth factor receptor 2
<b>hnRNP</b>	heterogeneous nuclear ribonucleoprotein
<b>HSP</b>	heat-shock protein
<b>ICD</b>	Intracellular domain

<b>IDC</b>	invasive ductal carcinoma
<b>IGF-IR</b>	insulin-like growth factor-I receptor
<b>IHC</b>	immunohistochemistry
<b>IKK</b>	I $\kappa$ B kinase
<b>ILC</b>	invasive lobular carcinoma
<b>INPP4B</b>	inositol polyphosphate 4-phosphatase type II
<b>ISE</b>	intronic splicing enhancer
<b>ISS</b>	intronic splicing silencers
<b>JM</b>	juxtamembrane
<b>LB</b>	lysogeny broth
<b>Mdm2</b>	mouse double minute 2
<b>MFE</b>	Minimum free energy
<b>miRNA</b>	micro RNA
<b>MAPK</b>	mitogen-activated protein
<b>MNK</b>	MAPK-interacting serine/threonine kinase
<b>MPA</b>	medroxyprogesterone acetate
<b>mRNA</b>	messenger RNA
<b>mTOR</b>	mammalian target of rapamycin
<b>mTORC2</b>	mammalian target of rapamycin complex 2
<b>MUC1</b>	mucin 1
<b>NCBI</b>	National Center for Biotechnology Information
<b>NMD</b>	nonsense-mediated mRNA decay
<b>NMR</b>	nuclear magnetic resonance
<b>NTP</b>	nucleoside triphosphate
<b>PBS</b>	phosphate buffered saline
<b>PDK1</b>	3-phosphoinositide-dependent kinase 1
<b>PI3K</b>	phosphoinositide-3-kinase
<b>PIP2</b>	phosphatidylinositol-4,5-bisphosphate
<b>PIP3</b>	phosphatidylinositol-3,4,5-triphosphate
<b>PLC</b>	pregnancy-lactation cycle
<b>PPT</b>	polypyrimidine tract
<b>PR</b>	progesterone receptor
<b>Prp5</b>	pre-mRNA-processing 5
<b>PTC</b>	premature stop/termination codon
<b>PTEN</b>	phosphatase and tensin homolog
<b>RACE</b>	rapid amplification cDNA ends
<b>RAS</b>	rat sarcoma
<b>Rb</b>	retinoblastoma
<b>RIPA buffer</b>	radioimmunoprecipitation assay buffer
<b>RNA</b>	ribonucleic acid
<b>RNAi</b>	RNA interference
<b>RRM</b>	RNA recognition motifs
<b>RS domain</b>	arginine-serine domain
<b>RSK</b>	p90 ribosomal S6 kinase
<b>S6K1/2</b>	p70 ribosomal protein S6 kinase 1/2

<b>SDS-PAGE</b>	sodium dodecyl sulfate polyacrylamide gel electrophoresis
<b>SF1</b>	splicing factor 1
<b>siRNA</b>	small interfering RNA
<b>snRNA</b>	Small nuclear RNA
<b>snRNP</b>	small nuclear ribonucleoprotein
<b>SOS</b>	son of sevenless
<b>SR proteins</b>	serine rich proteins
<b>ss</b>	splice sites
<b>TBS</b>	Tris-buffered saline
<b>T-DM1</b>	ado-trastuzumab emtansine
<b>TF</b>	transcription factor
<b>TM</b>	transmembrane domain
<b>TNM</b>	tumour-node-metastasis
<b>TSC2</b>	tuberous scelerosis 2
<b>U2AF</b>	U2 auxiliary factor
<b>UTR</b>	untranslated region
<b>VEGF</b>	vascular endothelial growth factor
<b>WHO</b>	World Health Organisation
<b>WT</b>	wild type

## List of Figures

Figure 1.1: Anatomy of the human breast. ....	2
Figure 1.2: The development of ductal carcinoma. ....	5
Figure 1.3: Oestrogen receptor variants.....	9
Figure 1.4: The oestrogen and oestrogen receptor (ER) signalling pathways...	10
Figure 1.5: The domains of the progesterone receptor. ....	12
Figure 1.6: HER2 protein variants.....	15
Figure 1.7: Structure and interaction of HER2 proteins.....	17
Figure 1.8: Intracellular structure of ErbB proteins and their interaction. ....	19
Figure 1.9: The main HER2 signaling pathways: Ras-MAPK and PI3K-AKT....	21
Figure 1.10: Canonical alternative splicing events. ....	36
Figure 1.11: Conserved exon and intron sequences.....	37
Figure 1.12: The splicing process. ....	39
Figure 3.1: The schematic depiction of the RNA chromatography assay.....	78
Figure 3.2: The design of $\Delta 16$ HER2-minigene.....	82
Figure 3.3: The exon 16 skipping event as part of a full length HER2 mRNA transcript.....	91
Figure 3.4: <i>In-silico</i> predicted secondary structure of wild type HER2 and $\Delta 16$ HER2 mRNA. ....	93
Figure 3.5: <i>In-silico</i> predicted secondary structure of wild type HER2 and $\Delta 16$ HER2 mRNA, focus on miRNA-155 binding site. ....	94
Figure 3.6: The three sequences covering the $\Delta 16$ HER2 splicing region: H1, H2, H3.....	96
Figure 3.7: Filtered prediction of splicing factors binding to three sequences covering the $\Delta 16$ HER2 splicing region (H1, H2, H3).....	97
Figure 3.8: The RNA chromatography assay followed by mass spectrometry and western blot.....	98
Figure 3.9: Transient knockdown of splicing factors measured on the mRNA and protein level in SKBR3 cells. ....	100
Figure 3.10: Transient knockdown of splicing factors measured on the protein level in SKBR3 cells.....	101
Figure 3.11: The effect of the transient knockdown of splicing factors (hnRNP A1, A/B, A2/B1 and D) on HER2 splicing in SKBR3 cells. ....	102

Figure 3.12: The effect of the transient knockdown of splicing factors (hnRNPs F, H and K) on HER2 splicing in SKBR3 cells.....	104
Figure 3.13: The effect of the transient knockdown of SRSF3 on HER2 splicing in SKBR3 cells. ....	105
Figure 3.14: The effect of the transient knockdown of SRSF3 and hnRNP K on HER2 splicing in MCF-7 cells.....	106
Figure 3.15: Effect of the transient knockdown of hnRNPs F/H and hnRNP K on HER2 splicing in MCF-7 cells.....	107
Figure 3.16: Expression of the $\Delta$ 16HER2-minigene products and the effect of the splicing factors on it.....	108
Figure 3.17: Depiction of splicing factor binding sites in the $\Delta$ 16HER2 splicing region.....	110
Figure 3.18: The $\Delta$ 16HER2-minigene expression after mutation of splicing factor binding sites. ....	111
Figure 3.19: The effect of HER2 transient knockdown on splicing factor gene expression.....	112
Figure 3.20: The effect of HER2 signalling inhibition by lapatinib on splicing factor protein expression.....	114
Figure 3.21: Effect of progesterone on HER2 expression and splicing in MCF-7 cells.....	116
Figure 3.22: The HER2 sequence of the $\Delta$ 16HER2-minigene. ....	119
Figure 3.23: The effect of SRSF3 on the splicing of p100 and $\Delta$ 16HER2. ....	121
Figure 3.24: Splicing factor binding motifs at the exon 15/intron 15 boundary of HER2 pre-mRNA. ....	125
Figure 4.1: Immunohistochemistry scoring scheme for HER2 status in breast tumours.....	139
Figure 4.2: <i>HER2</i> CISH pharmDx™ (DAKO) signal counting guide.....	143
Figure 4.3: C-terminal antibody controls. ....	144
Figure 4.4: N-terminal antibody controls. ....	145
Figure 4.5: HercepTest™ controls. ....	146
Figure 4.6: <i>HER2</i> CISH pharmDx™: no primary probe control .....	150
Figure 4.7: <i>HER2</i> CISH staining on normal breast tissue. ....	150
Figure 4.8: <i>HER2</i> CISH staining showing HER2 gene amplification on the HER2 3+ positive control tumours. ....	151
Figure 4.9: IHC and CISH images for the human breast cancer case IHC-1. .	157

Figure 4.10: IHC and CISH images for the human breast cancer case IHC-3. .....	158
Figure 4.11: IHC and CISH images for the human breast cancer case IHC-4. .....	159
Figure 4.12: IHC and CISH images for the human breast cancer case IHC-11. .....	160
Figure 4.13: IHC and CISH images for the human breast cancer case IHC-13. .....	161
Figure 4.14: IHC and CISH images for the human breast cancer case IHC-14. .....	162
Figure 4.15: IHC and CISH images for the human breast cancer case IHC-15. .....	163
Figure 4.16: HER2 splice variant levels in discrepant primary invasive ductal carcinoma cases. ....	164
Figure 5.1: Chromosomal location of <i>HER2</i> and surrounding genes. ....	173
Figure 5.2: Transcript profile of the <i>HER2 (ErbB2)</i> gene. ....	174
Figure 5.3: Depiction of the northern blot transfer assembly. ....	178
Figure 5.4: Expression of exons upstream of normal exon 1. ....	180
Figure 5.5: The retention of intron 25 in <i>HER2</i> transcripts. ....	181
Figure 5.6: Presence of intron 25 in <i>HER2</i> mRNA transcripts. ....	182
Figure 5.7: Presence of intron 25 in <i>HER2</i> mRNA transcripts. ....	183
Figure 5.8: <i>In-silico</i> predicted secondary structure of wild type <i>HER2</i> and I25HER2 mRNA. ....	185
Figure 5.9: Protein predictions for I25HER2. ....	186
Figure 5.10: Predicted secondary structures of wild type <i>HER2</i> and I25HER2. .....	187
Figure 5.11: Expression of I25HER2 in a panel of human breast cancer cell lines (A) and normal human tissues (B). ....	188
Figure 5.12: Expression of I25HER2 in breast tumour and breast reduction samples. ....	190
Figure 5.13: RNA stability assay for <i>HER2</i> transcripts. ....	191
Figure 5.14: Mouse GAPDH positive control for northern blot. ....	192
Figure 5.15: Northern blot for I25HER2 and wild type <i>HER2</i> . ....	194
Figure 5.16: Transcript profile of the <i>HER2</i> gene. ....	196
Figure 5.17: Promoter related signatures around <i>HER2</i> exons 17 to 19. ....	197



## List of Tables

Table 1.1: Breast cancer according to the TMN stage system. ....	7
Table 1.2: Transcription factors and co-regulators of the <i>HER2</i> gene. ....	14
Table 2.1: Transient knockdown with INTERFERin™ .....	56
Table 2.2: List of Silencer® Select siRNAs used. ....	56
Table 2.3: Reverse transcription reaction mix. ....	61
Table 2.4: PCR reaction mix. ....	62
Table 2.5: Number of PCR cycles used. ....	63
Table 2.6: List of PCR primers used. ....	63
Table 2.7: PCR reaction mix with QuantiFAST SYBR Green PCR Master Mix. ....	65
Table 2.8: TaqMan™ Assays. ....	65
Table 2.9: TaqMan™ Real-Time PCR reaction mix. ....	66
Table 2.10: Components of polyacrylamide resolving and stacking gels. ....	67
Table 2.11: Details to the antibodies used in western blotting. ....	69
Table 2.12: EcoR1 restriction digest reaction mix. ....	72
Table 2.13: Primers used for sequencing. ....	72
Table 3.1: <i>In-silico</i> prediction tools for splicing factor binding. ....	77
Table 3.2: The synthesised RNA oligonucleotides. ....	77
Table 3.3: DNA oligonucleotide for RNA synthesis. ....	79
Table 3.4: T7 RNA polymerase reaction mix (New England Biolabs). ....	80
Table 3.5: List of $\Delta$ 16HER2-minigene primers. ....	83
Table 3.6: Platinum Tag PCR Reaction for Minigene segments. ....	83
Table 3.7: Restriction digestion for the $\Delta$ 16HER2-minigene fragment. ....	84
Table 3.8: Primers for site directed mutagenesis. ....	85
Table 3.9: Q5® site-directed mutagenesis reaction. ....	86
Table 3.10: <i>Pfu</i> DNA polymerase site-directed mutagenesis reaction. ....	87
Table 3.11: <i>In-silico</i> prediction of RNA-binding proteins binding to the three sequences covering the exon 16 splicing region. ....	96
Table 3.12: Summarizing the binding of the splicing factors from the RNA chromatography assay. ....	109
Table 3.13: $\Delta$ 16HER2-minigenes splicing factor binding site mutants. ....	110
Table 3.14: Effect of HER2 signalling inhibition on splicing factor protein levels: densitometry of western blots. ....	114

Table 4.1: Table of FDA-approved HER2 assessment kits (FDA, 2016). .....	132
Table 4.2: Table detailing the epitope retrieval method and dilution of the antibodies.....	136
Table 4.3: List of breast cancer tissue sections used for CISH. ....	140
Table 4.4: Results from immunohistochemistry of 40 human primary ductal carcinomas.....	148
Table 4.5: Results of the <i>HER2</i> CISH staining for the human invasive ductal carcinomas.....	152
Table 4.6: Overview of results from HER2 IHC and CISH experiments. ....	156
Table 4.7: Summary of CISH and IHC results for samples used in PCR. ....	165
Table 5.1: Primers for the northern blot RNA probe DNA template.....	177
Table 5.2: The T7 reaction mix for Northern blot RNA probe generation. ....	177
Table 5.3: HER2 IHC and CISH score for four tumour samples used in intron 25 PCRs.....	200

## Chapter 1: Introduction

### 1.1. The Human Breast

The human breast is a bilateral organ overlaying the pectoralis major muscle located between the second and sixth rib. The mammary gland, the milk producing organ, is surrounded by adipose tissue and structurally stabilised and anchored to the pectoralis major muscle by Cooper's ligaments, a loose fibrous connective tissue (Cooper, 1840). The breast is supplied by the internal mammary artery and the lateral thoracic artery with blood (Vorherr, 1974). Lymphatic drainage occurs primarily through axillary lymph nodes and ipsilateral internal mammary lymphatics (Suami *et al.*, 2008).

The first steps in the development of the human breast occur in weeks seven to eight of gestation (Naccarato *et al.*, 2000). At birth the mammary gland consists of a basic ductal system. Until shortly before puberty the mammary gland remains in this resting state and little difference between the genders can be observed. Reaching puberty the female breast increases in size primarily through the growth of adipose tissue. More importantly, the hormonal changes of the menarche and the subsequent menstrual cycles induce the elongation of existing ducts and the branching into secondary ducts. At the termini of the secondary ducts lobules, clusters of bi-layered epithelial buds, also known as alveoli develop. After initial growth of the ductal system in puberty, a decreased growth continues until the age of ~35 (Russo and Russo, 2004; Hassiotou and Geddes, 2013).

Only with completion of the first pregnancy-lactation cycle (PLC) does the mammary gland develop into a mature and fully functional organ. The presence of competent mammary stem cells accounts for the ability of the mammary gland to repeatedly undergo structural and functional rearrangements through development, repeated PLC and post-menopausal regression (Hassiotou and Geddes, 2013). The increase in circulating hormones especially progesterone, oestrogen and prolactin in pregnancy induces the elongation and branching of

## Chapter 1: Introduction

the ductal system and the differentiation of the alveolar mammary epithelial cells into lactocytes (Pang and Hartmann, 2007). Although, a low level secretion of milk components can be observed around 24 weeks of gestation, within 48-72h after parturition the levels of secretion drastically increase. A suckling induced neuroendocrine reflex causes the release of oxytocin, which induces contraction of the myoepithelial cells surrounding the alveoli. The produced milk is drained from the alveoli into the main duct, from which it is transported via the lactiferous sinus onto the nipple surface (McManaman and Neville, 2003).

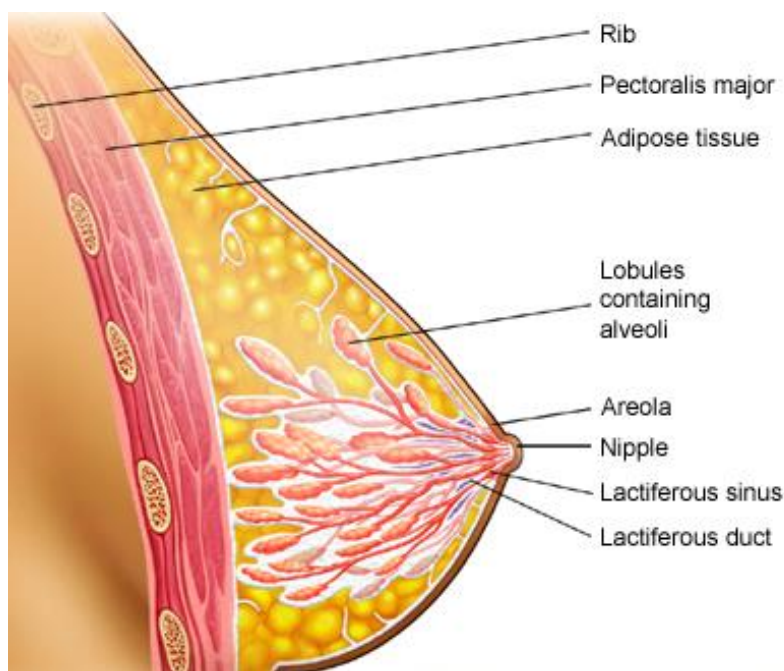


**Figure 1.1: Anatomy of the human breast.**

The image shows the structure of the female breast. The different parts are indicated. Image adapted from (*Anatomy of the human breast*).

As the demand for milk decreases or stops, milk production stops and the mammary gland returns to a resting state. This process is called post-lactational involution, wherein the mammary alveolar cells are removed (Hurley, 1989). As the ovary functions decline with the onset of menopause, the hormonal changes trigger post-menopausal regression of glandular tissue, which is replaced by adipose tissue (Hutson *et al.*, 1985).

## **1.2. Breast cancer**

### ***1.2.1. Breast cancer epidemiology***

According to numbers collected by the World Health Organisation (WHO) cancer remains one of the leading causes of morbidity and mortality with 14 million new cases and 8.2 million deaths in 2012 (World Health Organisation, 2015). Furthermore, the numbers of new cancer cases is expected to continuously increase (Maddams *et al.*, 2012; World Health Organisation, 2015). The most common cancer associated deaths are due to lung, liver, stomach, colorectal, breast and oesophageal cancer (World Health Organisation, 2015).

Given the ability of the mammary gland for repeated cycles of growth and regression as well as morphological changes, it is not surprising to find it as a common site for tumour development. In the UK alone nearly 50,000 women are diagnosed every year with cancer and 11,643 women died due to breast cancer in 2012 alone (Cancer Research UK, 2014b; Cancer Research UK, 2014c). Thanks to an early diagnosis and to improved treatment options the ten-year net survival rate has increased to 78.4% in the UK (Cancer Research UK, 2014d; World Health Organisation, 2014). In many less developed countries breast cancer is only diagnosed at a later stage and the five-year survival rate is therefore only around 10-40% (World Health Organisation, 2014).

### ***1.2.2. Breast cancer risk factors***

As most forms of cancer, breast cancer develops due to an accumulation of multiple genetic and environmental insults. This is also reflected in the increased occurrence of breast cancer with age. A steep increase in breast cancer cases can be found from the age of 30-34 onwards. In the UK 80% of cases occur in the age group over 50. These number are potentially slightly

## Chapter 1: Introduction

biased as they coincide with the onset of the breast cancer screening program (Cancer Research UK, 2014a).

Common cancer risk factors including lifestyle choices such as increased alcohol consumption and smoking, as well as environmental factors such as exposure to gamma and x-ray radiation are also risk factors of developing breast cancer (Parkin *et al.*, 2011). Another risk factor, is a history of benign breast disease with a proliferative lesion or atypical hyperplasia (Tice *et al.*, 2015).

Many risk factors for the development of breast cancer are associated with mammary gland development and circulating hormone levels. An early menarche and late menopause, therefore a long exposure to increased sex hormone levels are considered important risk factor for the development of hormone receptor overexpressing breast tumours (Collaborative Group on Hormonal Factors in Breast, 2012). On the other hand, early first pregnancy (<14 years after menarche), multiple PLCs and breast feeding are considered to reduce the risk of breast cancer (Collaborative Group on Hormonal Factors in Breast, 2002; Kubba, 2003).

Additionally, increased body weight, especially abdominal fat is considered an important risk factor for post-menopausal breast cancer (Gathirua-Mwangi *et al.*, 2015). The increased sex hormone production, especially oestrogen by adipose tissue is thought to increase breast cancer risk (Key *et al.*, 2003). Similarly, oral oestrogen-progesterone contraceptives and hormone replacement therapy increase the risk of tumour development. Ten years after the use of oral contraceptives is stopped, the risk has decreased back to a normal level (Collaborative Group on Hormonal Factors in Breast, 1996; Kubba, 2003; Gierisch *et al.*, 2013).

About 90 to 95% of breast tumours are classified as sporadic, with no disease relevant inherited genetic alteration. The majority of hereditary tumours, 10-20% are linked with mutations of the breast cancer early onset genes *BRCA1* and *BRCA2* (Rizzolo *et al.*, 2011; Aloraifi *et al.*, 2015). The *BRCA* genes are involved in cell cycle, apoptosis and DNA-repair after DNA double strand breaks (Yoshida and Miki, 2004). These functions make their deregulation an important

step in the development of hereditary breast tumours. Inherited mutations increase the risk of developing breast cancer by 79.5% for BRCA1 and 88% for BRCA2 (Evans *et al.*, 2008). Mutations in p53, STK11, CDH1 and PTEN (phosphate and tensin homolog) are also associated with a higher risk of developing breast cancer but are far less common (Aloraifi *et al.*, 2015). A moderate increase in risk can also be observed for mutations in proteins that are part of regulatory pathways like the BRCA signalling pathways, such as ATM (ataxia telangiectasia mutated), CHEK2, PALB2 and BRIP1 (Rizzolo *et al.*, 2011). Further mutations exist that are common in the population, but only confer a low increase in the risk of developing breast cancer (Aloraifi *et al.*, 2015).

### **1.2.3. Breast cancer categorisation**

Breast cancer is an umbrella term for multiple distinct tumour types originating from breast tissue. All tumours can be categorized according as to whether they are localised (*in situ*), if they have invaded surrounding tissue (invasive) or if they have formed metastasis at distal sites (metastatic).

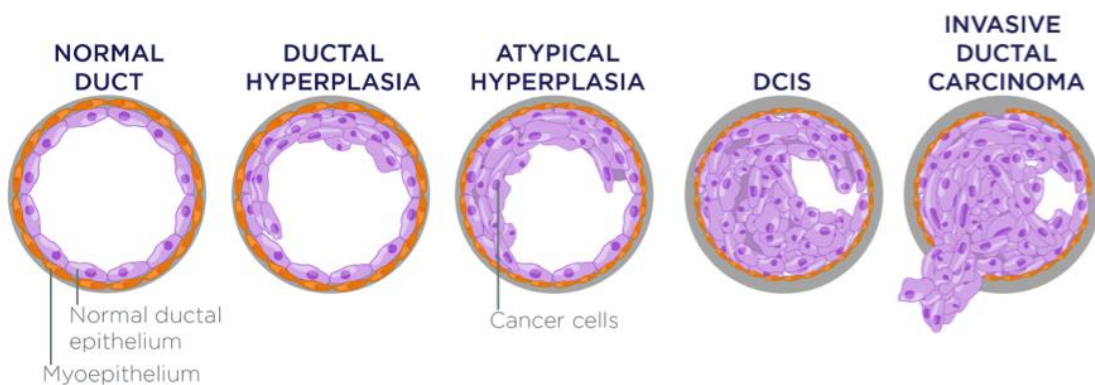


**Figure 1.2: The development of ductal carcinoma.**

The image shows the stages from a normal duct through hyperplasia and ductal carcinoma *in situ* (DCIS) to invasive carcinoma. Image extracted from (*Development of ductal carcinoma*, 2014).

## Chapter 1: Introduction

The development of cancer is not clearly defined. In most cancer cases multiple tumours of different stages surrounded by benign tissue can be observed within one breast cancer. Most tumours develop in the terminal ducts, not the lobules, making the ductal carcinomas the major type of breast cancer. As shown in figure 1.2, the first step in the development of ductal carcinomas is an increased proliferation of the ductal epithelial cells (ductal hyperplasia). Next abnormal, less well differentiated cells (atypical hyperplasia) emerge. These develop into non-invasive ductal carcinoma *in situ* (DCIS) and in a next step into infiltrating, invasive breast cancers.

Invasive tumours are categorized by their histological features. The major subtypes are invasive ductal carcinoma (IDC) (80%) and invasive lobular carcinoma (ILC) (5-15%). Further minor groups exist, such as adenoid cystic carcinoma, apocrine carcinoma, IDC with osteoclastic giant cells, medullary carcinoma, metaplastic carcinoma, micropapillary carcinoma, mucinous carcinoma, neuroendocrine carcinoma and tubular carcinoma (Weigelt *et al.*, 2008).

Additionally, a small proportion (1-5%) of breast tumours are characterised by cancer cells that block dermal lymph vessels and cause redness and swelling of the breast. These inflammatory breast cancers are very aggressive and fast progressing, and are mostly IDC tumours (Anderson *et al.*, 2005; National Cancer Institute, 2012).

### **1.2.3.1. Breast Cancer Grading and Staging**

As part of the clinical assessment of a tumour it is categorised according to grading and staging systems. Tumours are graded according to how closely they resemble the surrounding normal tissue.

Grade 1: well differentiated cells with slow growth

Grade 2: moderately differentiated cells with moderate growth

Grade 3: poorly differentiated cells with fast growth

## Chapter 1: Introduction

GX: grade cannot be determined

If the tumour consists of poorly differentiated cells this also means that the cells are more stem cell like and able to multiply and adapt to external influences much faster (Rakha *et al.*, 2010; Scimeca *et al.*, 2016). Ductal carcinoma *in situ* is differently graded. The grades are due to the nuclear grade, how abnormal the cancer cells appear, and the presence of necrosis (Pinder, 2010).

The tumour-node-metastasis (TNM) breast cancer staging system is a more complex categorisation system (Table). It takes into consideration the local extend and size of the tumour (T), the number and extent of affected regional lymph nodes (N) and the presence or absence of metastasis (M) (Singletary and Connolly, 2006).

**Table 1.1: Breast cancer according to the TMN stage system.**

(Singletary and Connolly, 2006; Cancer Research UK, 2014e)

<b>Tumour size (T)</b>	
<b>TX</b>	Cannot be assessed
<b>T0</b>	No tumour detected
<b>T1</b>	The tumour is $\leq 2$ cm
<b>T2</b>	The tumour is $\geq 2$ cm, but $\leq 5$ cm
<b>T3</b>	The tumour is $\geq 5$ cm
<b>T4</b>	a – The tumour has spread into the chest wall b – The tumour has spread into the skin and the breast may be swollen c – The tumour has spread to both the skin and the chest wall d – Inflammatory carcinoma – this is a cancer in which the overlying skin is red, swollen and painful to the touch
<b>Regional lymph nodes (N)</b>	
<b>NX</b>	Cannot be assessed
<b>N0</b>	No regional lymph node metastasis
<b>N1</b>	Movable ipsilateral axillary lymph nodes affected
<b>N2</b>	a – cancer cells in the lymph nodes in the armpit, which are stuck to each other and to other structures b – cancer cells in the lymph nodes behind the breast bone (the internal mammary nodes), which have either been seen on a scan or felt by the doctor. There is no evidence of cancer in lymph nodes in the armpit
<b>N3</b>	a – cancer cells in lymph nodes below the collarbone b – cancer cells in lymph nodes in the armpit and behind the breast bone c – cancer cells in lymph nodes above the collarbone
<b>Disease metastasis (M)</b>	
<b>MX</b>	Cannot be assessed
<b>M0</b>	No distant metastasis
<b>M1</b>	Distant metastasis

**1.2.3.2. Molecular Breast Cancer Categories**

A number of well-established biomarkers exist which are routinely measured in breast cancer patients. These are oestrogen receptor (ER) and progesterone receptor (PR) as well as the human epidermal growth factor receptor 2 (HER2). They are overexpressed in different combinations in 85-90% of all breast tumours. A tumour is referred to as being receptor positive, if the receptor is strongly overexpressed. Most common is the overexpression of ER, in 75% of all breast tumours, of these 55% are also PR positive. Generally ER/PR+ tumours occur more in postmenopausal women and have the lowest incidence of general metastases, but the highest incidence of bone metastasis. Bone metastases may also develop upward of 10-20 years after initial diagnosis (Chikarmane *et al.*, 2015). ER and/or PR+ tumours can further be grouped into two categories luminal A if HER2- and luminal B, if HER2 overexpressing. The 2011 St. Gallen International Expert Consensus proposed a change to the classification system. There, luminal A tumours are ER+ and PR+ and HER2- with a low cellular proliferation index (Ki-67 <14%). Luminal B can be ER+/- PR+/- and HER2-/+ with a high proliferative index (Eroles *et al.*, 2012).

In total 20-30% of breast tumours are HER2 overexpressing (Slamon *et al.*, 1987; Slamon *et al.*, 1989). 10-15% are hormone receptor negative and proliferation index high (Eroles *et al.*, 2012). HER2 overexpressing tumours are more common in younger women. The metastases generally occur within 5 years after initial diagnosis and are often found in the liver. Interestingly after the treatment with Trastuzumab, a HER2-targeting therapeutic agent, an increase in central nervous system metastasis can be observed (Chikarmane *et al.*, 2015).

Tumours that are negative for ER, PR and HER2 fall into three categories: basal-like or triple negative (ER-, PR- and HER2-, cytokeratine 5/6 and/or EGFR +, high proliferative index), Claudin-low (ER-, PR- and HER2-, cytokeratine 5/6 and/or EGFR +/-, high proliferative index) and normal breast like (ER-/+ , HER2-, cytokeratine 5/6 and/or EGFR +/-, low proliferative index) (Eroles *et al.*, 2012).

This categorisation is important in a clinical setting to devise the best possible treatment plan for each patient, especially with regards to the administration of ER-targeting therapy and HER2-targeting therapies.

### 1.3. Oestrogen receptor

The oestrogen receptor is an important breast cancer biomarker and therapeutic target. Oestrogen is involved in cell growth, reproduction, development and differentiation. In humans its most common form is 17 $\beta$ -oestradiol, although oestrone and oestriol can also be found. 17 $\beta$ -oestradiol is synthesised by the ovaries in premenopausal women. In postmenopausal women and men 17 $\beta$ -oestradiol is converted from testosterone and androstenedione at different site of the body including breast and adipose tissue (Jia *et al.*, 2015).

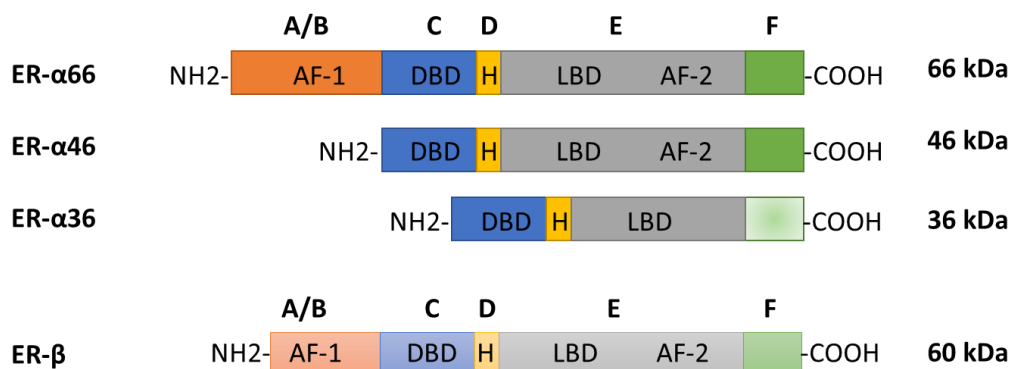


**Figure 1.3: Oestrogen receptor variants.**

Oestrogen receptor  $\alpha$  has two well studied splice variants ER- $\alpha$ 46 and 36. Common features between the ERs are the five domains. A/B: ligand-independent activation function (AF-1); C: DNA-binding domain (DBD); D: hinge domain (H) with a nuclear localisation signal; E: ligand-binding domain (LBD) and ligand-dependent transactivation function (AF-2); F: agonist/antagonist regulator.

Two highly homologous oestrogen receptors have been identified ER- $\alpha$  encoded by the oestrogen receptor 1 (ESR1) gene at position 6q25.1 and ER- $\beta$  encoded by the oestrogen receptor 2 (ESR2) gene at position 14q23.2. Both receptors belong to the nuclear receptor superfamily of ligand-inducible transcription factors (Chan *et al.*, 2015; Jia *et al.*, 2015). The ER proteins are

made up of five main domains (Figure 1.3): The N-terminal A/B region contains a ligand-independent activation function (AF-1), a DNA-binding domain (DBD) in region C, a hinge domain (H) with a nuclear localisation signal in region D, a ligand-binding domain (LBD) and the ligand-dependent transactivation function (AF-2) in region E. Lastly region F with an agonist/antagonist regulator (Marino *et al.*, 2006). In addition to wild type ER receptors both genes encode for a number of splice variants. Only the ER- $\alpha$ 46 and 36 variants have been studied in more depths. Studies have suggested contradictory roles for the two ERs. ER- $\alpha$  is thought to promote growth and survival of breast epithelial cells, whereas ER- $\beta$  is associated with growth inhibition (Chan *et al.*, 2015).

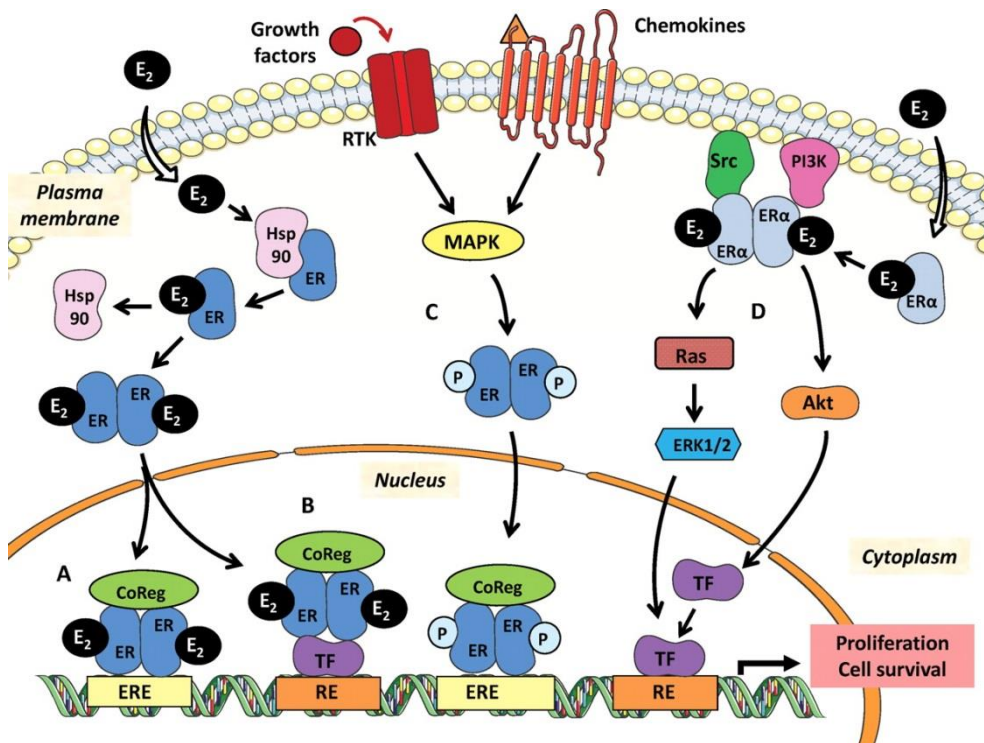


Figure 1.4: The oestrogen and oestrogen receptor (ER) signalling pathways.

Oestrogen and ER can induce transcription of target genes through multiple pathways. In the classical model, oestrogen bound ER is translocated to the nucleus, where it recognises and binds oestrogen response elements in target genes (A) or acts as co-transcription factor (B), and thereby regulates transcription. C, Alternatively, ER can be phosphorylated through growth factor receptors or chemokine receptors and translocate to the nucleus, to regulate the transcription of target genes. D, In the non-genomic pathway, oestrogen activated ER can activate the PI3K/AKT and RAS/MAPK signalling pathways. These signalling pathways regulate transcription factors of target genes. Image has been derived from (Le Romancer *et al.*, 2011).

Oestrogen activates a complex signalling pathway. The classical model involves the high-affinity binding of oestrogen to ER, conformational changes and disassociation from heat shock proteins and immunophilin chaperones

(Gougelet *et al.*, 2005). Following this, the ER dimers translocate into the nucleus, where ER recognises and binds to the oestrogen response element (ERE) within target genes (Figure 1.4). ER can indirectly affect transcription by causing the association or dissociation of components of coregulatory complexes, which regulate chromatin function and affect the transcription machinery (Kampa *et al.*, 2013). The ER signalling pathway also includes non-genomic activation (Figure 1.4). ER- $\alpha$  dimers localised in close proximity of the plasma membrane can be activated by oestrogen and in turn activate the phosphoinositide-3-kinase (PI3K)/AKT and rat sarcoma/mitogen-activated protein kinase (RAS/MAPK) signalling pathways. These pathways lead to cell proliferation, survival and control of cell cycle (Bjornstrom and Sjoberg, 2005; Le Romancer *et al.*, 2011). The activity of ER can also be initiated independently of oestrogen. Growth factor and chemokine receptors can phosphorylate and activate ER through RAS/MAPK pathway members. The activated ER can then perform its transcription regulation function on the target genes (Kato *et al.*, 1995; Rhodes *et al.*, 2011; Kampa *et al.*, 2013).

### **1.4. Progesterone receptor**

The steroid hormone progesterone is known for its essential function in normal female reproductive organs and the mammary gland, but it is also important in the normal function of the cardiovascular system, central nervous system and bones [reviewed in (Mulac-Jericevic and Conneely, 2004; Taraborrelli, 2015)]. Its main receptors are PR-A and B, but it can also act through other receptors such as the nuclear glucocorticoid receptor (Lei *et al.*, 2012). PR is essential in the normal female reproductive organ and mammary gland development (Mulac-Jericevic and Conneely, 2004). It also plays an important role in the development of breast cancer and is therefore an important biomarker for breast cancer therapy.

The two PR receptors, PR-A and PR-B are encoded by one gene from two alternative promoters (Kastner *et al.*, 1990). They are members of the ligand

## Chapter 1: Introduction

activated nuclear receptor superfamily of transcription factors. The PR-B protein contains two transactivation domain (AF-3, AF1) at the N terminus, followed by a DNA-binding domain, a ligand binding domain towards the C-terminus and another transactivation domain (AF2). PR-A differs from PR-B by lacking the AF3 domain, but containing an inhibitor domain at the N-terminus (Figure 1.5) (Leonhardt *et al.*, 2003). Additional PR variants which are due to alternative splicing have been described, but more extensive investigation is necessary to understand their actual role (Cork *et al.*, 2008).



**Figure 1.5: The domains of the progesterone receptor.**

The progesterone receptor gene encodes two proteins, PR-A and PR-B. The PR-B protein contains two transactivation domain (AF-3, AF1), followed by a DNA-binding domain (DBD), a ligand binding domain (LBD) and another transactivation domain (AF2). The PR-A differs from PR-B by lacking the AF3 domains, but containing an inhibitor domain at the N-terminus.

Interesting to note is the fact that PR is an oestrogen responsive gene (Cork *et al.*, 2008). Similar to ER, binding of the ligand, progesterone, induces a conformational change and dimerization of PR. Active and phosphorylated PR binds to progesterone-response-elements in the promoter of target genes. Activated PR can also, independently of progesterone-response elements, interact with co-activator/co-repressor proteins or general transcription factors to regulate transcription of target genes (Mulac-Jericevic and Conneely, 2004). Through the regulation of transcription, PR is involved in cell growth, apoptosis and protein and nucleic acid processing as well as metabolism (Richer *et al.*, 2002). The non-genomic action of PR can be mediated through its interaction with ER- $\alpha$  and initiation of the src/RAS/MAPK pathway which regulates cell proliferation and survival (Ballare *et al.*, 2003). Again similarly to ER, PR can act in a ligand independent manner. For example in breast cancer with increased levels of casein-kinase 2 (ck2), PR-B can be activated by phosphorylation through ck2 and in turn initiate downstream pathways (Hagan *et al.*, 2011).

## **1.5. Human epidermal growth factor receptor 2**

The human epidermal growth factor receptor 2 is a member of the erythroblastosis oncogene B family of receptor tyrosine kinases. It is also referred to as *ErbB2* or *NEU*. Other members of this protein family are *ErbB1* (HER1) better known as *EGFR*, *ErbB3* (*HER3*) and *ErbB4* (*HER4*). The members of this family are known to interact by dimerization and regulate a large network of signalling pathways, most notably the PI3K/AKT and the RAS/MAPK pathways, which control cell proliferation, growth and survival, as well as angiogenesis and cellular metabolism (Roskoski, 2013; Dittrich *et al.*, 2014). In about ~20% of primary breast cancers HER2 is overexpressed, its ability to induce these cellular process makes it a driver of tumour development and persistence (Slamon *et al.*, 1987; Slamon *et al.*, 1989).

### **1.5.1. The regulation of HER2 gene expression**

The *HER2* gene is located on chromosome 17q12-21. Transcription of the gene is regulated by a number of transcription factors (Table 1.2). Some transcription factors such as activator protein-2 (AP-2) induce *HER2* expression (Vernimmen *et al.*, 2003a; Vernimmen *et al.*, 2003b), others such as the Foxp3 are negative regulators (Zuo *et al.*, 2007).

In the past the *HER2* gene has been shown to give rise to a complex set of mRNA transcripts. In Ensembl a number of *HER2* transcripts have been collected. Most studies, including this research, considers ensembl transcript ERBB2-008 (ENST00000269571) the wild type transcript. It contains 27 exons and is 4.545 kb long.

The high number of transcripts can be partially attributed to multiple promoters. The first promoter was shown to have up to three mRNA start sites at 178, 244 and 257 nucleotides upstream of the translation initiation site in placenta tissue and the human HER2 positive breast carcinoma cell line SKBR-3. Additionally in the human breast cancer cell line MCF-7, which only expresses HER2 at a low level, two different mRNA start sites at 270 and 315 nucleotides upstream of the initiator ATG were found (Tal *et al.*, 1987). The second promoter was

## Chapter 1: Introduction

identified in conjunction with 4 additional exons upstream of the conventional exon 1, which is skipped if the upstream exons are used yielding a 5.2kb long mRNA transcript. They detected this transcript in the HER2-low MCF-7 cells, but not in HER2-positive SKBR-3 cells (Nezu *et al.*, 1999).

**Table 1.2: Transcription factors and co-regulators of the *HER2* gene.**

Name	Co-regulators	Type of regulation	References
<b>HER2 Transcription Factor</b>		Positive	(Vernimmen <i>et al.</i> , 2003a)
<b>Activator Protein</b>	Yin Yang 1; KU proteins	Positive	(Vernimmen <i>et al.</i> , 2003b; Allouche <i>et al.</i> , 2008; Nolens <i>et al.</i> , 2009)
<b>PEA3</b>	c-June & p300	Positive	(Vernimmen <i>et al.</i> , 2003b; Matsui <i>et al.</i> , 2006)
<b>EGR2/Krox20</b>	CITED1	Positive	(Dillon <i>et al.</i> , 2007)
<b>Y-box Binding Protein-1</b>		Positive	(Kalra <i>et al.</i> , 2010)
<b>Signal Transducer and Activator of Transcription 3</b>		Positive	(Qian <i>et al.</i> , 2006)
<b>Myc Promoter-binding Protein-1</b>	Histone deacetylase 1	Negative	(Contino <i>et al.</i> , 2013)
<b>ErbB3-Binding Protein 1</b>		Negative	(Ghosh <i>et al.</i> , 2013)
<b>Foxp3</b>		Negative	(Zuo <i>et al.</i> , 2007)
<b>PURA</b>		Negative	(Zhang <i>et al.</i> , 2012)
<b>Nucleolin</b>		Negative	(Zhang <i>et al.</i> , 2012)

Adapted from (Dittrich *et al.*, 2014).

A number of proteins associate with mRNA transcripts to stabilise it, facilitate its export and translation. HDAC5 has a stabilising effect on *HER2* mRNA in breast cancer cell lines (Scott *et al.*, 2008). Translational inhibition and degradation of mRNA can be regulated by microRNAs (miRNAs). In the breast cancer cell line SKBR-3 the overexpression of miR-125a and miR-125b downregulates *HER2* mRNA levels. As a consequence anchorage dependent growth, migration and invasion was inhibited (Scott *et al.*, 2007). This is supported by the observation that miR-125b is downregulated in some breast tumours (Ferracin *et al.*, 2013). Furthermore, miRNAs have been identified that target the *HER2* 3'untranslated region: miR-2559, 548d-3p (Chen *et al.*, 2009) and 331-3p (Epis *et al.*, 2009). Recently, miR-155 was found to down-regulate *HER2*. The miRNA can target HDAC2, a transcription activator of *HER2* and thereby downregulate the

expression of HER2. Additionally, miR-155 can directly target HER2 by binding in the coding region (He *et al.*, 2016).

### 1.5.2. HER2 transcript and protein variants

In addition to wild type HER2, three functionally distinct alternative splice variants have been identified (Sasso *et al.*, 2011; Jackson *et al.*, 2013). These are membrane-bound  $\Delta 16$ HER2 and the secreted proteins Herstatin and p100 (Doherty *et al.*, 1999a; Aigner *et al.*, 2001; Sasso *et al.*, 2011). To date only a small number of studies have investigated the effect of HER2 splice variants on cell signalling and their role in breast cancer development and therapy. In breast cancer the secreted proteins have been associated with a good prognosis, especially Herstatin (Aigner *et al.*, 2001; Hu *et al.*, 2005). In contrast  $\Delta 16$ HER2 has been associated with more aggressive tumours and in vitro resistance to some forms of targeted therapy (Castiglioni *et al.*, 2006; Mitra *et al.*, 2009).

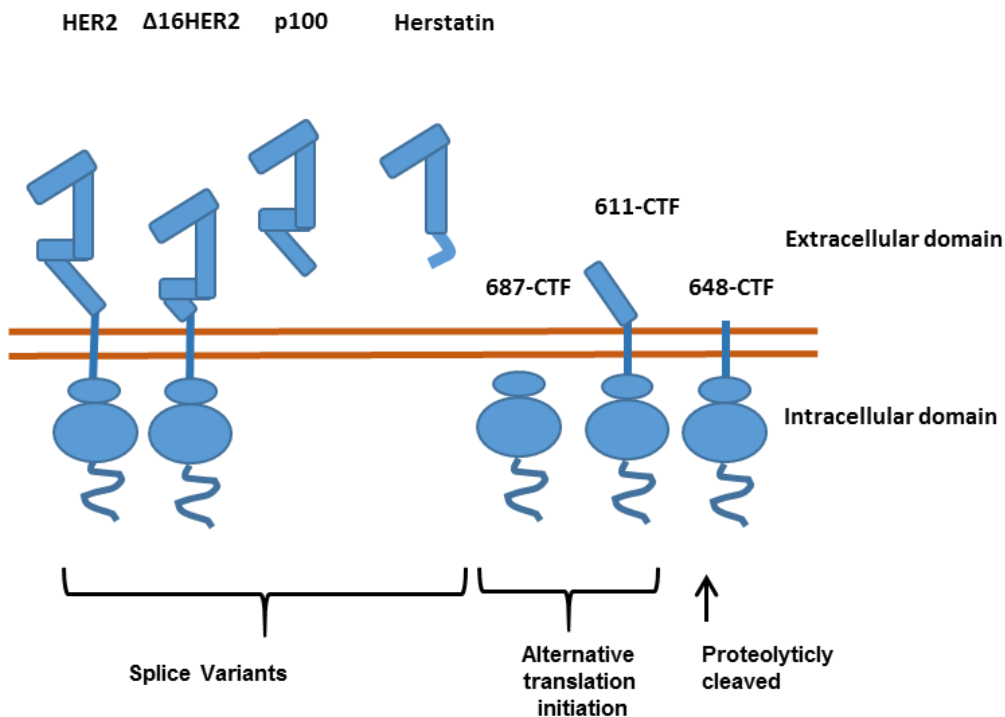


Figure 1.6: HER2 protein variants.

Protein variants of HER2 arise through different processes. Three are due to alternative splicing, these are  $\Delta 16$ HER2, p100 and Herstatin. Alternative translation initiation gives rise to 687-CTF and 611-CTF. Additionally proteolytic cleavage can produce a truncated membrane bound 648-CTF.

Additional HER2 protein variants can arise from the HER2 transcript through alternative translation initiation, these are the cytoplasmic 687-C-terminal fragment (p95cyto) and the membrane bound 611-CTF (p110) (Pedersen *et al.*, 2009). Furthermore, post-transcriptional HER2 protein cleavage gives rise to membrane bound 648-CTF (p95m) (Sasso *et al.*, 2011). Although these protein variants lack all or most of the extracellular domain, some studies have shown that they can induce downstream signalling and play a role in breast cancer outcome. Research showed 611-CTF to induce the transcription of metastasis associated genes and linked it to a poor prognosis (Pedersen *et al.*, 2009; Ward *et al.*, 2013). Similarly 648-CTF has also been linked to poor prognosis, through its constitutively active conformation and downstream signalling. It also lacks the epitope of the HER2 targeting therapeutic antibody Trastuzumab (Chandrapaty *et al.*, 2010; Tse *et al.*, 2012). Recently, a HER2 protein with a short alternative N-terminus was identified, although the underlying mechanisms have not been studied (Kuyama *et al.*, 2014).

### **1.5.3. The protein structure of HER2**

The ErbB protein family shares a common general protein structure. Most studies concerning the ErbB protein structure have focused on EGFR, especially concerning the highly conserved intracellular domain. The structure and function of the tyrosine kinase domain is generally accepted to be common between the EGFR and HER2. The 185kDa sized HER2 protein consists of an N-terminal extracellular domain, followed by a transmembrane domain and the intracellular C-terminal domain.

#### **The extracellular domain**

The extracellular domain consists of two leucine-rich ligand-binding domains I/LI and III/LII that facilitate ligand binding as well as two cysteine-rich domains II/CI and IV/CII which facilitate the formation of disulphide bonds (Figure 1.7). Traditionally, HER2 is considered an “ligand” orphan receptor with an active “open structural” conformation, which allows the formations of dimers with other family members after ligand binding, followed by transactivation and

downstream signalling via the intracellular tyrosine kinase domain (Roskoski, 2013). Only very recently a ligand for HER2 was identified. A study reported that prolidase binds to pre-existing HER2 homodimers. Its binding disrupts the intracellular association of Src with HER2 and thereby inhibits downstream signalling in HER2 overexpressing cells. This study also found that in cells expressing HER2 at a low level, HER2 monomers are bound by prolidase initiating dimerisation and normal downstream signalling (Yang *et al.*, 2014).

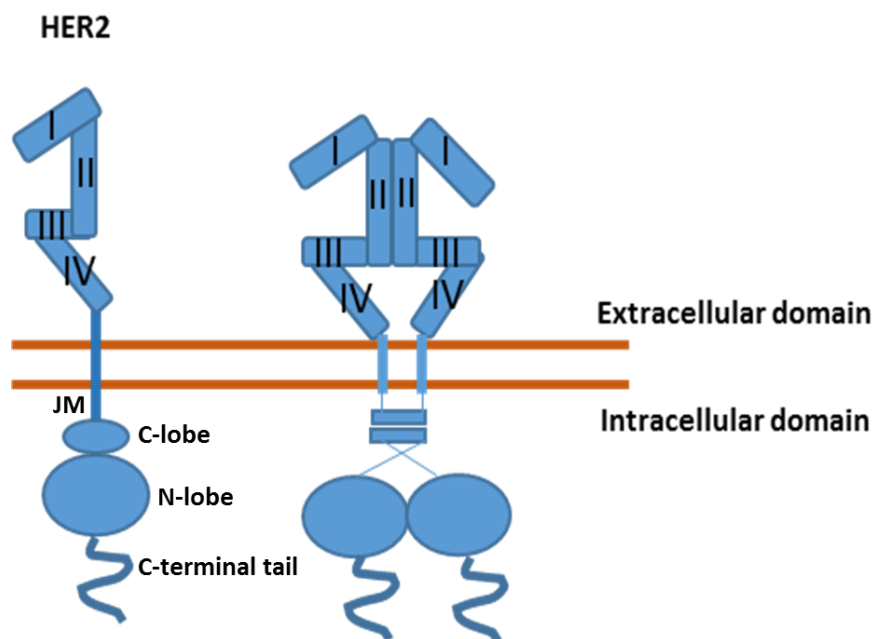


**Figure 1.7: Structure and interaction of HER2 proteins.**

The extracellular domain consists of two leucine-rich ligand-binding domains I and III that facilitate ligand binding, and two cysteine-rich domains II and IV which facilitate the formation of disulphide bonds. The domain II forms a  $\beta$ -hairpin dimerization loop which participates in the dimerisation. A short single-span  $\alpha$ -helix transmembrane segment connects the extracellular with the intracellular domain. The intracellular domain consists of the juxtamembrane (JM), followed by the tyrosine kinase domain which is comprised of the N-terminal lobe (N-lobe) and the C-terminal lobe (C-lobe). The protein ends in a non-catalytic C-terminal tail. Dimerization and activation of the receptor frees the JM segment from the negatively charged membrane. The first 20 amino acids form an antiparallel coiled-coil structures between dimerising receptors (Jura *et al.*, 2009; Roskoski, 2014).

The domain II forms a  $\beta$ -hairpin dimerization loop which participates in the dimerisation (Burgess *et al.*, 2003). HER2 primarily forms heterodimers with other members of its protein family, but in cells expressing high levels of HER2 the close proximity increases the level of homodimerisation significantly (Di Fiore *et al.*, 1987; Hudziak *et al.*, 1987).

### **The transmembrane (TM) domain**

The extracellular domain is connected by a short single-span  $\alpha$ -helix transmembrane segment with the intracellular domain. Solution NMR has shown that two ErbB protein TM domains associate in a right-handed  $\alpha$ -helical bundle. This is thought to be mediated by the double GG4-like motif T<sup>648</sup>G<sup>649</sup>X<sub>2</sub>G<sup>652</sup>A<sup>653</sup> and the glycine zipper motif T<sup>652</sup>X<sub>3</sub>S<sup>656</sup>X<sub>3</sub>G<sup>660</sup> (Escher *et al.*, 2009; Mineev *et al.*, 2010; Arkhipov *et al.*, 2013). Activating mutations in the TM domain can increase downstream signalling and thereby increase the risk to develop breast cancer, this under pins the importance of the TM domain (Segatto *et al.*, 1988; Xie *et al.*, 2000).

### **The intracellular domain**

The intracellular domain consists of the juxtamembrane (JM) segment which can be subdivided into A and B. This is followed by the tyrosine kinase domain which is comprised of the N-terminal lobe (N-lobe) with the helix  $\alpha$ C,  $\alpha$ C- $\beta$ 4 loop and the activation loop and the C-terminal lobe (C-lobe). The protein ends in a non-catalytic C-terminal tail.

In recent years, the accepted receptor dimerization mechanism has gone from a symmetric activation to an asymmetric interaction of the intracellular domains. One receptor takes up the role of the donor/activator, its C-lobe interacting with the N-lobe of the acceptor/receiver (Figure 1.7) [reviewed in (Kovacs *et al.*, 2015)]. In the case of a HER2 – ErbB3 heterodimer, HER2 takes on the role of the acceptor and HER3 the donor (Collier *et al.*, 2013).

Intracellularly a 40 amino acid long JM segment follows the transmembrane domain (Jura *et al.*, 2009; Roskoski, 2014). Dimerization and activation of the receptor frees the JM segment from the negatively charged membrane (Arkhipov *et al.*, 2013; Matsushita *et al.*, 2013). The first 20 amino acids make up the JM-A segments which forms an antiparallel coiled-coil structures between dimerising receptors. The N-terminal half of the JM-domain (JM-B) of the acceptor kinase interacts with the C-lobe of the donor kinase (Jura *et al.*, 2009; Roskoski, 2014).

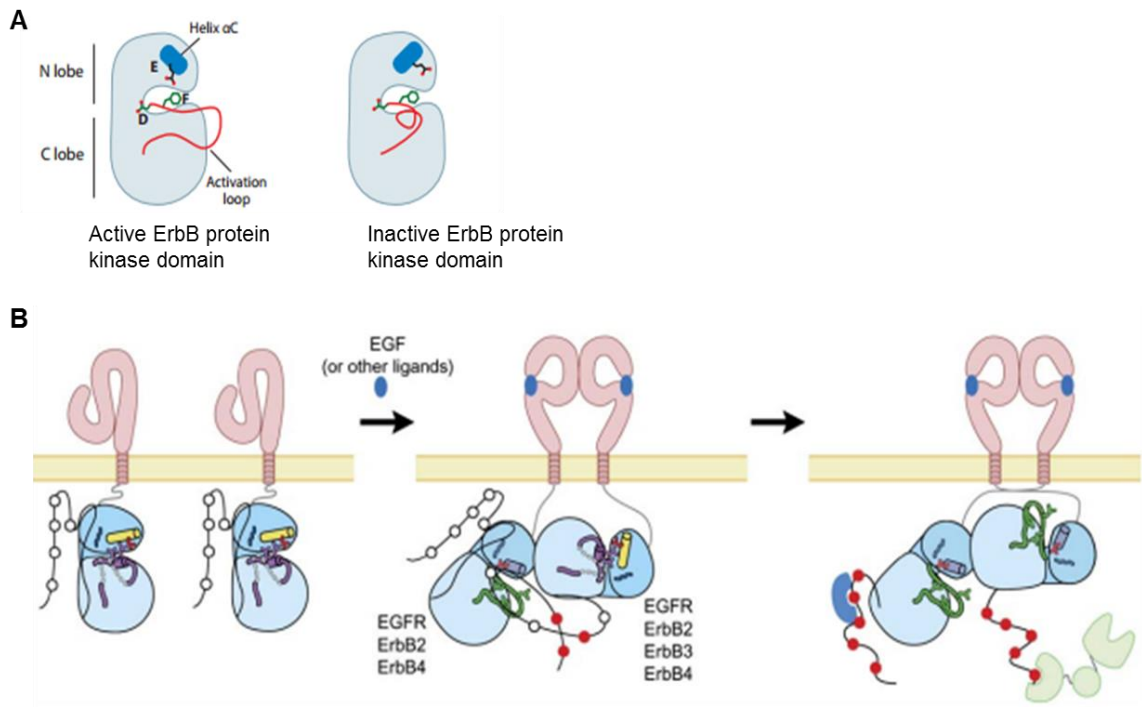


**Figure 1.8: Intracellular structure of ErbB proteins and their interaction.**

A, The tyrosine kinase domain is comprised of the N-terminal lobe (N-lobe) with the helix  $\alpha C$ ,  $\alpha C$ - $\beta 4$  loop and the activation loop and the C-terminal lobe (C-lobe). Its conformation changes dependent on activation. B, The dimerization of ErbB proteins is an asymmetric interaction of the intracellular domains. One receptor takes up the role of the donor/activator, its C-lobe interacting with the N-lobe of the acceptor/receiver. The JM segments interact and form an antiparallel coiled-coil structures between dimerising receptors. The C-lobe of the donor kinase interacts with the N-lobe of the acceptor kinase, this activates the acceptor kinase. The activated tyrosine kinase domain uses ATP to transphosphorylate the C-terminal tail. The phosphorylated C-terminal tail is essential for the recruitment of adaptor and effector proteins. Images adapted from (Collier *et al.*, 2013).

Fann *et al.* have suggested that HER2 has an autoinhibitory mechanism through the interaction of the  $\alpha C$ - $\beta 4$  loop in the N-lobe which forms a hydrophobic patch that interacts with the hydrophobic stripe of the activation loop, this keeps the helix  $\alpha C$  and activation loop in an inactive conformation. Receptor dimerization and conformational changes cause the activation loop to be in an open confirmation to allow access to the kinase substrate-binding pocket and the helix  $\alpha C$  to face the ATP-binding site (Fan *et al.*, 2008).

Controversial findings have been made concerning the importance of tyrosine phosphorylation of the activation loop in HER2, the study by Collier and colleagues suggest that this phosphorylation is not essential for tyrosine kinase activation (Collier *et al.*, 2013). The C-lobe of the donor kinase interacts with the N-lobe of the acceptor kinase, which activates the acceptor kinase. As part of

the receptor dimerization and activation the tyrosine kinase domain uses ATP for the transphosphorylation of the C-terminal tail loop [reviewed in (Kovacs *et al.*, 2015)]. The long C-terminal tail contains 6 tyrosine transphosphorylation sites, which are essential for the recruitment of adaptor (e.g. Grb2) and effector proteins (e.g. phospholipase C gamma – PLC $\gamma$ ) that contain src homology domain 2 (SH2) or phosphotyrosine binding (PTB) domains (Arteaga *et al.*, 1991; Dankort *et al.*, 1997; Dankort *et al.*, 2001; Hartman *et al.*, 2013). These proteins are essential for the downstream signalling as will be discussed later [reviewed in (Dittrich *et al.*, 2014)].

### **1.5.4. HER2 signalling pathways**

The most prominent signalling pathways activated by HER2 are the PI3K/AKT and RAS/MAPK pathways (Figure 1.9), which mediate cell proliferation, growth and survival, as well as angiogenesis and cellular metabolism [reviewed in (Dittrich *et al.*, 2014)]. In the last decade it was reported that the HER2 signalling network extends to include crosstalk with other receptors such as ER (Creighton *et al.*, 2006; Giuliano *et al.*, 2013; Grabinski *et al.*, 2014). Additionally, it was shown that HER2 can function as co-transcription factor of genes such as *cyclooxygenase-2 (Cox-2)* (Dillon *et al.*, 2008) and *cyclin D1* (Beguelin *et al.*, 2010; Diaz Flaque *et al.*, 2013). These are only a few examples which show the complexity of the HER2 network and its ability to regulate cell proliferation, growth and survival, as well as angiogenesis and cellular metabolism via different pathways [reviewed in (Dittrich *et al.*, 2014)]. It has to be noted that most studies only consider full length wild type HER2, not the other protein variants when studying the signalling pathways. The HER2 variant  $\Delta 16$ HER2 is an exception; work in cell lines and mouse models has elucidated a signalling pathway separate from wild type HER2 (Mitra *et al.*, 2009; Marchini *et al.*, 2011; Castagnoli *et al.*, 2014). It has been described that  $\Delta 16$ HER2 homodimerization induces the phosphorylation and translocation of the associated pSrc to the cell membrane (Mitra *et al.*, 2009; Castagnoli *et al.*, 2014). The non-receptor cytoplasmic tyrosine kinase, Src is a key signalling molecule a complex signalling network which regulates cell survival,

mitogenesis and cell motility. In cancer it has been further implied to be important in EMT and metastasis (Guarino, 2010; Castagnoli *et al.*, 2014).

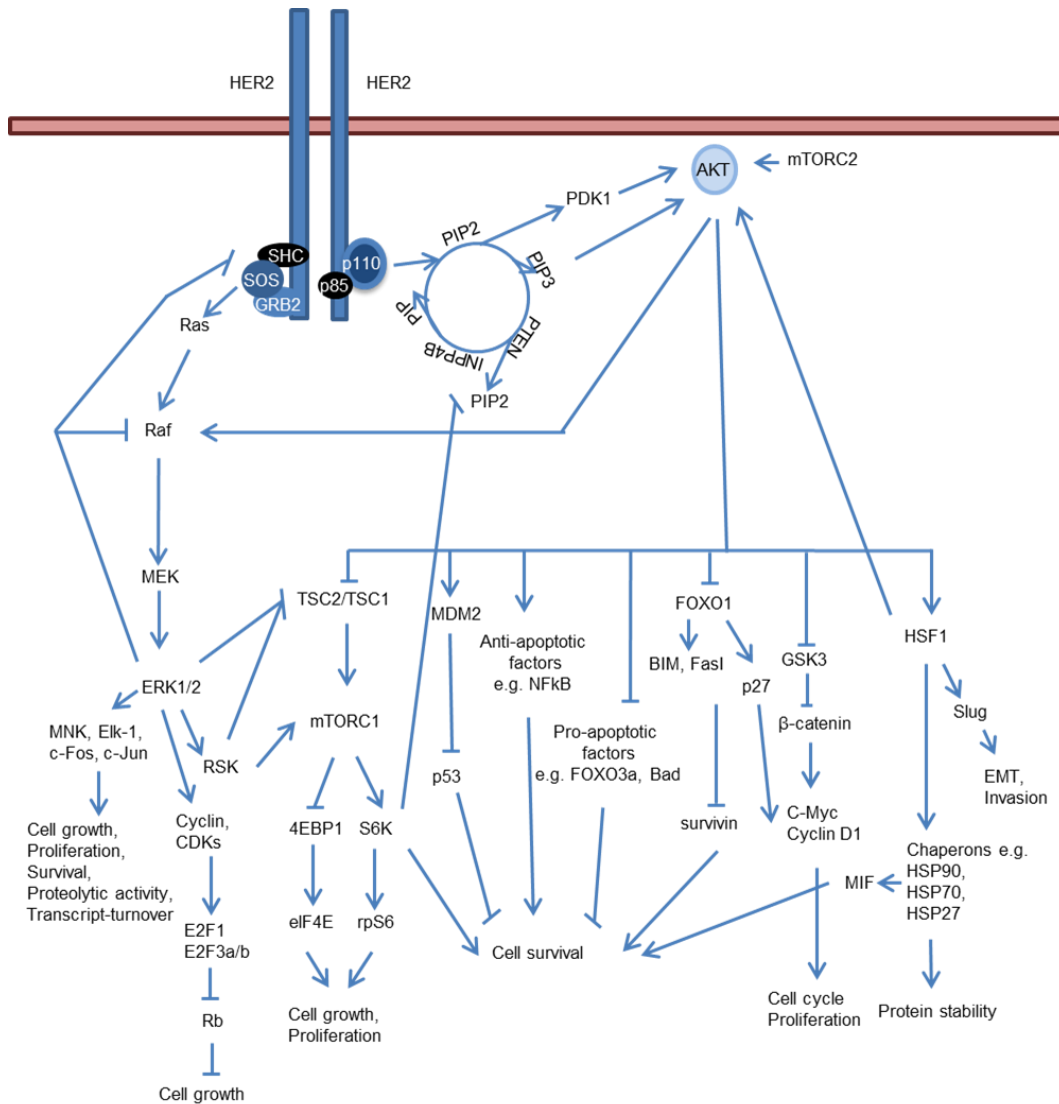


**Figure 1.9: The main HER2 signaling pathways: Ras-MAPK and PI3K-AKT.**

Dimerisation and transphosphorylation of HER2 initiates the Ras-MAPK and PI3K-AKT pathways. Adaptor proteins bind to HER2 initiating a signaling cascade via Ras, Raf and MEK to ERK1/2. ERK induces transcription factors involved in cell growth, proliferation, survival, proteolytic activity and transcript-turnover. The PI3K-AKT pathway is also initiated by the transphosphorylation of HER2. The recruitment of p85 releases p110 to recruit PI3K heterodimer to its substrate PIP2, this is phosphorylated into PIP3. AKT becomes translocated to the plasma membrane by PIP<sub>3</sub>. AKT regulates proteins involved in a number of cellular processes; cell survival, cell cycle, proliferation, protein stability, epithelial to mesenchymal transition and invasion. Additionally, a number of negative feedback loops regulate the pathways. Image derived from (Dittrich *et al.*, 2014).

**1.5.4.1. Co-receptors of HER2**

HER2 is traditionally considered to be an orphan receptor which has to dimerise with a ligand-binding, activated co-receptor to induce downstream signalling. Dimerisation primarily occurs with other members of the ErbB family - EGFR, HER3 and HER4 [reviewed in (Hurvitz *et al.*, 2013)]. They can bind a number of different ligands. Some ligands are receptor specific (Epithelial Growth Factor to EGFR) and others bind multiple receptors (Heregulin) [reviewed in (Barros *et al.*, 2010)]. In tumours overexpressing HER2, homodimerisation can also occur. EGFR and ErbB4 are able to bind ligands and induce downstream signalling through functional tyrosine kinase domains. In contrast ErbB3 is able to bind its ligands, but has a truncated tyrosine kinase domain [reviewed in (Barros *et al.*, 2010)].

Some studies have found HER2 to also interact with two receptors that are not part of the ErbB protein family. One is Ob-R, the receptor of the fat cell-derived peptide hormone leptin. Eisenberg *et al.* first showed that HER2 can be indirectly phosphorylated through Ob-R via JAK2 and initiate the RAS/MAPK pathway in human embryonic kidney HEK 293T cells (Eisenberg *et al.*, 2004). Similar findings were observed in the breast cancer cell line SKBR3 (Soma *et al.*, 2008). Only one study has shown a direct association between Ob-R and HER2, through co-immunoprecipitation (Fiorio *et al.*, 2008). If, and how, Ob-R acts as co-receptor of HER2 remains unclear.

The second unrelated co-receptor is Mucin 1 (MUC1), a protein heterodimer formed by an N-terminal extracellular and a C-terminal membrane bound subunit. The C-terminal subunit can interact with HER2 and other receptor tyrosine kinases [reviewed in (Kufe, 2013)]. It has been shown that Heregulin can induce a complex formation between MUC1 and HER2, which leads to the translocation of the C-terminal subunit of MUC1 together with  $\gamma$ -catenin to the nucleus (Li *et al.*, 2003). Nuclear localisation of C-terminal MUC1 is thought to be involved in the regulation of cell proliferation, differentiation and epithelial to mesenchymal transition through the co-regulation of WNT target genes (Huang *et al.*, 2003; Micalizzi *et al.*, 2010; Gangopadhyay *et al.*, 2013). The overexpression of MUC1 in breast and other cancers indicates that this

interaction with HER2 can have an important role in cancer cells (Mukhopadhyay *et al.*, 2011; Torres *et al.*, 2012).

### **1.5.4.2. The RAS/MAPK signalling pathway**

One of the two main signalling pathways induced by the dimerisation of HER2 and subsequent phosphorylation of the C-terminal tyrosines is the RAS-MAPK pathway. Major cellular functions are governed by this pathway, these include cell growth, survival, proliferation and migration [reviewed in (Castaneda *et al.*, 2010; Fruman and Rommel, 2014)].

The phosphorylated HER2 C-terminus acts as the docking site for proteins such as growth factor receptor-bound protein 2 (GRB2). GRB2 binding to the adaptor protein son of sevenless (SOS) activates it which in turn allows SOS to cause the exchange of guanosine diphosphate (GDP) to guanosine triphosphate (GTP) on RAS. The activation of RAS initiates the activation of a kinase cascade, at its end stands the phosphorylation and activation of extracellular signal-regulated kinases (ERK) 1 and 2 [reviewed in (Aksamitiene *et al.*, 2012; De Luca *et al.*, 2012)].

Activated ERK regulates a number of transcription factors through phosphorylation. These include the erythroblastosis virus E26 oncogene homolog 1 like gene 1 (Elk-1) (Yordy and Muise-Helmericks, 2000), p90 ribosomal S6 kinase (RSK) (Chen *et al.*, 1992), c-Fos and c-Jun (Sistonen *et al.*, 1989), as well as MAPK-interacting serine/threonine kinase (MNK) (Chrestensen *et al.*, 2007). The RAS-MAPK pathway regulates the expression of genes involved in cell growth, differentiation, proliferation, survival, migration as well as transcript turnover and proteolytic activity through these transcription factors [reviewed in (Aksamitiene *et al.*, 2012; De Luca *et al.*, 2012; Romeo *et al.*, 2012; Kasza, 2013)].

The ERK proteins can initiate a negative feedback loop by inhibiting the interaction of SOS with GRB2. This leads to a decreased activation of RAS. The subsequent inhibition of RAF negatively regulates the activation of MEK (Ueki *et*

*al.*, 1994; Lemmon and Schlessinger, 2010). The RAS signalling activates a complex of cyclins and cyclin dependent kinases (CDKs) which can release the well-known tumour suppressor retinoblastoma (Rb) (Leone *et al.*, 1997; Dimova and Dyson, 2005). Through the feedback loop this is inhibited.

### **1.5.4.3. The PI3K-AKT signalling pathway**

The other main signalling pathway of HER2 is the PI3K-AKT pathway. Similar to the RAS-MAPK pathway it regulates a number of important cellular functions, such as cell growth, survival, proliferation as well as protein synthesis, invasive properties and drug resistance [reviewed in (Burriss, 2013; Fruman and Rommel, 2014)]. As with the RAS-MAPK pathway the phosphorylation of the HER2 C-terminus recruits proteins, in this case p85. The recruitment of p85 disassociates it from p110. p110 is now free to recruit the PI3K heterodimer to its substrate phosphatidylinositol-4,5-bisphosphate (PIP<sub>2</sub>) at the cell membrane (Carpenter *et al.*, 1993). PIP<sub>2</sub> in turn is phosphorylated by the PI3K heterodimer into phosphatidylinositol-3,4,5-triphosphate (PIP<sub>3</sub>) [reviewed in (Castaneda *et al.*, 2010; De Luca *et al.*, 2012)]. This process is negatively regulated by the phosphatase and tensin homolog (PTEN) [reviewed in (Hopkins *et al.*, 2014)] and inositol polyphosphate 4-phosphatase type II (INPP4B) which dephosphorylate PIP<sub>3</sub> [reviewed in (Burriss, 2013)]. PIP<sub>3</sub> next causes the translocation of AKT, a central protein of this signalling pathway, to the plasma membrane and where it is phosphorylated by 3-phosphoinositide-dependent kinase 1 (PDK1) and mammalian target of rapamycin (mTOR) complex 2 (mTORC2) [reviewed in (Castaneda *et al.*, 2010)].

It is interesting to note that a study showed that of the three AKT isoforms, AKT1 and 3 levels seem to be increased in HER2 positive cells, but not AKT2. Knockdown of AKT 1 and 3 in these cells leads to reduced proliferation. Additionally, this study also suggested that the AKT isoform levels can affect the phosphorylation of HER2 and HER3. Depletion of AKT1 and 2 causing an increase of HER2 and HER3 phosphorylation, whereas the depletion of AKT3 has the opposite effect downregulating protein expression at a posttranscriptional level and decreasing tyrosine phosphorylation (Grabinski *et*

*al.*, 2014). This study suggests AKT3 as a more specific marker of HER2 specific initiation of the PI3K/AKT pathway.

### **Cell Survival**

This signalling pathway regulates cell survival through multiple channels. This includes the inhibition of pro-apoptotic proteins like B cell leukemia 2 antagonist of cell death (Bad) (Datta *et al.*, 1997) or of the transcription factors of pro-apoptotic proteins e.g. forkhead box O3a (FOXO3a) (Brunet *et al.*, 1999). AKT can phosphorylate and activate the antagonist of the tumour suppressor p53, mouse double minute 2 (Mdm2). This inhibits the p53 mediated pro-apoptotic pathway, cell-cycle arrest and senescence pathways as well as its modulation of autophagy (Mayo and Donner, 2001). Further, the NF- $\kappa$ B survival pathway can be activated through the phosphorylation of its positive regulator I $\kappa$ B kinase (IKK) (Fresno Vara *et al.*, 2004). Finally, survivin levels can be upregulated and the protein stabilised through the HER2-PI3K-AKT pathway (Wu *et al.*, 2010; Wu *et al.*, 2012; Chakrabarty *et al.*, 2013; Ju *et al.*, 2013; Lazrek *et al.*, 2013).

### **Cell Cycle Progression and Proliferation**

Another important cellular process regulated by the PI3K/AKT pathway is cell cycle progression and proliferation. AKT is able to regulate mTORC1 through tuberous sclerosis 2 (TSC2) and thereby the phosphorylation of eIF4E binding protein 1 (4E-BP1) and p70 ribosomal protein S6 kinase 1 and 2 (S6K1,2) (Inoki *et al.*, 2002). S6K1 plays a role in the initiation and control of mRNA translation as well as cell growth and proliferation [reviewed in (Proud, 2009)]. S6K2 has been shown to be essential in cell survival (Sridharan and Basu, 2011). Phosphorylation of 4E-BP1 releases the eukaryotic translation initiation factor 4E (eIF4E), which is incorporated into the translational machinery [reviewed in (Proud, 2009)].

Further, targets of AKT like FOXO1 inhibit p27 and increase cyclin D1 levels, this has been shown to cause an increased proliferation in breast cancer cell lines (Wu *et al.*, 2010).

### **The other central player: Heat-Shock Factor 1 (HSF1)**

The HER2/PI3K/AKT pathway has been linked to invasion and epithelial to mesenchymal transition (EMT), both central mechanisms in cancer development and progression, through the activation of HSF1 (Fresno Vara *et al.*, 2004; Yilmaz and Christofori, 2009; Carpenter *et al.*, 2014; Schulz *et al.*, 2014). HSF1 is considered a positive “master regulator” of a number of adaptor proteins and heat-shock chaperones including HSP90 $\alpha$ , HSP70 and HSP27. In cancer HSP chaperons are essential in stabilising oncogenes and other cellular proteins, as tumour cells generally suffer higher levels of stress due to aberrant cellular processes and the tumour microenvironment [reviewed in (Ciocca *et al.*, 2013)].

The role of HSF1 in EMT can be explained by its role as a transcription factor of Slug, which in turn is a transcriptional repressor of E-cadherin (Carpenter *et al.*, 2014). The downregulation of E-cadherin causes changes in the adhesive properties of cells, which increases the invasive and metastatic potential of tumour cells [reviewed in (Yilmaz and Christofori, 2009; Tania *et al.*, 2014)].

In addition, it has been indicated that HSF1 influence the expression of genes involved in the cell cycle regulation, metabolism, adhesion and translation (Mendillo *et al.*, 2012).

### **1.5.5. The crosstalk between HER2 and the hormone receptors**

#### **Oestrogen receptor (ER)**

Studies have found that different hormone receptors ‘crosstalk’, which is especially important in breast tumours in which hormone receptors are often overexpressed and drive tumorigenesis. A small percentage of breast cancer cases show expression of both HER2 and ER (Arpino *et al.*, 2008).

The two oestrogen receptors have been implied to have antagonistic functions with ER $\alpha$  inducing proliferation and survival of breast cancer cells (Giuliano *et al.*, 2013), and ER $\beta$  antagonising these functions (Omoto *et al.*, 2003; Lattrich *et*

al., 2013). HER2 signalling has been linked to ER through both the RAS/MAPK and PI3K/AKT pathways. HER2 downregulates the expression of ER $\alpha$  through the RAS/MAPK pathway (Oh et al., 2001; Creighton et al., 2006) and the phosphorylation of p38MAPK inhibits ER $\beta$  and thereby its function as TF (St-Laurent et al., 2005). The HER2/PI3K/AKT pathway causes phosphorylation and inactivation of FoxO3a through AKT and thereby also prevents or reduces ER $\alpha$  expression. This is supported by the finding that AKT3 depletion induces the protein expression of ER $\alpha$ . HER2 dependent signalling has been shown to be mainly mediated by AKT3, not AKT1 or 2 (Grabinski et al., 2014).

These links between HER2 and ER might indicate a mechanism underlying mono-therapy resistance of cells that switch from HER2+/ER- to HER-/ER+ (Giuliano et al., 2013).

### **Androgen receptor (AR)**

Less well understood is the link between HER2 and the androgen receptor (AR). The cross-regulation of steroid-response genes has been observed in a subgroup of HER2 positive molecular apocrine (ER-/AR+) breast cancer cell lines. The ligand heregulin is expected to induce target genes of HER2, 3 and 4, but a study found that it also induced AR target genes. The same cells when treated with testosterone, ligand of AR, showed the induction of HER2 target genes (Naderi and Hughes-Davies, 2008). Both signalling pathways act through phosphorylation of ERK (Naderi and Hughes-Davies, 2008). ERK and CREB1 are linked back to AR via a positive feedback loop. It has also been shown that AR can act as a transcription inducer of HER2 (Chia *et al.*, 2011). In the context of breast cancer it is interesting to note that a study has indicated that breast cancer patients which lack AR and ER, but overexpress HER2, have a poorer prognosis than patients that are also positive for AR and ER (Lin Fde *et al.*, 2012).

### **Insulin-like growth factor-I receptor (IGF-IR)**

Recently, studies have described crosstalk between HER2 and IGF-IR, which has been linked to drug resistance. Both HER2 and IGF-IR activate the PI3K/AKT pathway and thereby induce cell proliferation (Baxi *et al.*, 2012). There are likely to be multiple forms of interaction. It was found that targeting

either receptor can induce activation of the other receptor (Haluska *et al.*, 2008). In some Trastuzumab resistant breast cancer cell lines both a heterodimerisation of IGF-IR with HER2 (Nahta *et al.*, 2005) as well as a complex formation of IGF-IR with both HER2 and HER3 has been observed (Huang *et al.*, 2010). A study has also shown that HER2 can induce the IGF-IR pathway through the downregulation of IGF binding protein-3, which increases the secretion of the IGF-IR ligand IGF-1 (Worthington *et al.*, 2010).

### **1.5.6. Function of nuclear HER2**

Until now, HER2 has been described as a membrane bound receptor protein, but in the last ten years ErbB family proteins have been identified in the nucleus and been shown to affect transcription directly [reviewed in (Mills, 2012)]. Nuclear HER2 has been found in cell lines and primary tissues [reviewed in (Wang *et al.*, 2004)]. Interestingly, a study correlated dual nuclear and high membrane HER2 staining with a worse outcome for breast cancer patients (Schillaci *et al.*, 2012).

For the translocation into the nucleus an active tyrosine kinase domain is necessary. A short amino acid sequence (676-KRRQQKIRKYTMRR-689) located at the beginning of the intracellular domain has been suggested to act as a nuclear localisation signal (Wang *et al.*, 2004).

Target genes of nuclear HER2 are *COX-2*, *PRPK*, *MMP-16* and *DDX-10* (Wang *et al.*, 2004; Dillon *et al.*, 2008). Of these target genes only *COX-2* has been further studied. Its expression has been correlated to HER2 expression, but is not exclusively dependent on the HER2 induced RAS/MAPK pathway (Subbaramaiah *et al.*, 2002; Wang *et al.*, 2004). It has been observed that the correlation between HER2 and *COX-2* is stronger in metastatic tumours and with a poorer prognosis (Wang *et al.*, 2004; Dillon *et al.*, 2008).

HER2 has also been found to act as a co-transcription factor of PR in MCF-7 cells (Beguelin *et al.*, 2010). PR can regulate a number of cellular proteins lacking the progesterone response element (PRE). For these proteins PR

forms a complex with other transcription factors (Beguelin *et al.*, 2010). A well-studied case is the cyclin D1 gene. It has been found that the synthetic progestin medroxyprogesterone acetate (MPA) via ERK1/2 causes the translocation of c-Fos and c-Jun to the nucleus. PR co-localises with c-Fos and c-Jun, as the AP-1 complex on the cyclin D1 promoter (Diaz Flaque *et al.*, 2013). Furthermore, MPA cause the phosphorylation of STAT3 and HER2. These can then be found in a transcription complex on the STAT3 binding site of the cyclin D1 promoter (Beguelin *et al.*, 2010). These two transcription complexes assemble at the same time. The HER2 STAT2 complex only forms in the presence of c-Jun and c-Fos on the promoter. The treatment with MPA also induces chromatin structure favourable to gene transcription. It has been suggested that both AP-1 and nuclear HER2 are essential for progestin dependent growth (Beguelin *et al.*, 2010; Diaz Flaque *et al.*, 2013).

### **1.6. Breast cancer therapy**

The treatment of breast cancer is designed on a case-to-case basis depending not only the patient's age, health, medical history, the characteristics of the tumour and the patient's preferences, but also on resources and practice in different hospitals. In most cases a combination therapy is used.

Typically, a surgical intervention is performed to remove the tumour mass and some of the surrounding normal tissue. Practise has mostly moved away from whole breast removal (mastectomy) to surgeries that remove the tumour but keep as much as possible of the normal breast intact. During surgery sentinel lymph node biopsy might be performed, to remove potentially abnormal lymph nodes. Before surgery, following ultrasound, fine needle aspiration or biopsy might be performed on potentially abnormal axillary lymph nodes to determine spread of the tumour. The excised tumour tissues and lymph nodes are used to determine follow up treatment (NICE, 2009; Cancer Research UK, 2014d). In patients above 70 with health problems a surgery might not be possible and hormone therapy will be recommended (primary endocrine therapy) (Cancer Research UK, 2014c).

## Chapter 1: Introduction

If cancer cells have spread to the axillary lymph nodes the remaining axillary lymph nodes will most probably be removed too. Depending on the risk and extent of the cancer, radiotherapy might be applied to lymph nodes (Cancer Research UK, 2014d). Recently it has become possible to perform a rapid test, RD-100i OSNA, during surgery to determine whether cancer cells have spread to lymph nodes (NICR, 2013; Cancer Research UK, 2014d).

Radiotherapy generally follows breast conserving surgeries, but can also be necessary after mastectomy to remove any remaining cancer cells (NICR, 2013; Cancer Research UK, 2014d). It has been shown that radiation decreases the likelihood of recurrence of cancer in the treated breast tissue and surrounding lymph nodes (Early Breast Cancer Trialists' Collaborative et al., 2011). In addition chemotherapy and hormone therapy might be performed before or following surgery. Treatment before surgery whether it is chemotherapy or hormone therapy is referred to as neo-adjuvant therapy. Neo-adjuvant therapy is mostly performed in locally metastatic breast cancer or large tumours, to reduce the size of the tumour before surgery (Cancer Research UK, 2014a). Adjuvant therapy follows after surgery and is performed to reduce the risk of recurrence. The treatment options will depend on the age and health of the patients and the category of tumour. In cases of small localised tumours adjuvant therapy might not be necessary (Cancer Research UK, 2014a).

### **Targeted therapies**

Current national guidelines recommend that early oestrogen positive tumours should be treated with hormone/endocrine therapy following surgery. In younger ER positive patients hormone therapy is often combined with chemotherapy. As mentioned before ER is often found to be overexpressed in breast tumours and to act as a driver of the tumour, therefore in premenopausal women treatments that stop oestrogen production might be suggested (Cancer Research UK, 2014c). Tamoxifen is the most common anti-ER drug, it binds to the AF-2 domain of ER and blocks interaction with ER as well as its co-activator complex. Toremifene, droloxifene, idoxifene, TAT-59 and GW5638 are similar to Tamoxifen in regard to their chemical structure and function. Raloxifene although similar in function belongs to a different SERM family (Osborne et al., 2000). Fulvestrant is another common anti-ER drug, which blocks the

interaction with ER and causes its degradation (Osborne et al., 2000; Dahlman-Wright et al., 2006). In patients with metastasis or in post-menopausal patients with tamoxifen resistance other types of drugs might be used, such as aromatase inhibitors, which stop the synthesis of oestrogen (Ali and Coombes, 2002). However, despite the several endocrine treatments which have been developed, more than 50% of patients with metastatic disease do not respond to endocrine therapy (Giuliano et al., 2013).

As discussed earlier a subset of tumours is characterised through the overexpression of HER2. These patients will be given HER2 targeting agents such as the monoclonal antibody Trastuzumab (Herceptin). In more advanced cancers tyrosine kinase inhibitors such as Lapatinib will also be considered (Cancer Research UK, 2014b).

### **Chemotherapies**

Chemotherapeutic agents are cytotoxic drugs that target all growing and proliferating cells. The main problem with these agents is that they do not differentiate between normal dividing cells and tumour cells. The impaired self-repair mechanisms in cancer cells, increase the efficiency of these drugs in cancer cells. In addition to adjuvant and neoadjuvant settings, chemotherapy is also used on metastatic cancer. In many cases they are administered in combination. The main drugs used are: Cyclophosphamide, Epirubicin, Fluorouracil (5FU), Methotrexate, Mitomycin, Mitozantrone, Doxorubicin, Docetaxel and Gemcitabine (Cancer Research UK, 2014a).

#### ***1.6.1. HER2 targeting therapy***

Through the development of HER2 targeting drugs, the prognosis of HER2 positive patients has strongly improved (Hurvitz et al., 2013). At present time four anti-HER2 drugs for breast cancer have been approved by either the U.S. Food and Drug Administration (FDA) or National Health Service (NHS) or both; these are trastuzumab, trastuzumab emtansine, pertuzumab and lapatinib.

### **Trastuzumab**

Both trastuzumab and pertuzumab are humanized monoclonal antibodies targeting the extracellular domain of HER2. Trastuzumab has been approved by FDA and NHS for adjuvant therapy of both lymph node positive and negative, HER2-positive breast cancer (NICE, 2002; NICE, 2009; NIH, 2013). The FDA has also approved trastuzumab in combination with pertuzumab and docetaxel for use in neoadjuvant inflammatory or early stage breast cancer (Amiri-Kordestani *et al.*, 2014). It is to be used in combination with one or multiple chemotherapeutic drugs, such as cyclophosphamide, doxorubicin, paclitaxel, docetaxel and carboplatin. It can also be applied as a single agent following multi-modality anthracycline based therapy. In metastatic HER2-overexpressing breast cancer it is indicated for first line treatment in combination with paclitaxel or as single agent after previous chemotherapy for metastatic disease (NICE, 2002; NICE, 2009; NIH, 2013). By targeting the extracellular domain of HER2, trastuzumab blocks the dimerization of HER2 with other ErbB family members and thereby down-regulates HER2 signalling. The antibody has also been shown to induce apoptosis by mediating antibody-dependent cellular cytotoxicity (ADCC), as well as complement mediated cytotoxicity in breast cancer cells (Tai *et al.*, 2010; Bianchini and Gianni, 2014). In humans the main effect of trastuzumab is through the engagement of the immunsystem. In clinical studies it has been observed that in patients responding to trastuzumab containing therapies the levels of lymphocytes are increased (Bianchini and Gianni, 2014).

Recently an antibody drug conjugate of trastuzumab, ado-trastuzumab emtansine (T-DM1) has been approved by the FDA as single agent treatment of HER2-overexpressing, metastatic breast cancer, which had previously been treated with trastuzumab and taxane (U.S. Food and Drug Administration, 2013). Due to low cost-effectiveness it is not recommended in the UK (National Institute for health and Care Excellence, 2015). The maytansinoid anti-microtubule agent DMT1 is bound to trastuzumab and thereby directly delivered to HER2 overexpressing cells (Zardavas *et al.*, 2013). The HER2-T-DM1 complex is internalized after binding and the drug is released in the cytoplasm. Once there DM1 can cause the degradation of microtubules. In addition, the

abilities of Trastuzumab to block the HER2 signalling and mediate ADCC are retained (Lewis Phillips *et al.*, 2008).

### **Pertuzumab**

The second monoclonal antibody which has been approved for breast cancer treatment is pertuzumab. Similarly to trastuzumab the antibody binds an extracellular domain of HER2 by which it inhibits dimerization with its co-receptors and down regulates HER2 signalling. Pertuzumab also mediates ADCC. It has to be noted that the binding domain of pertuzumab does not overlap with the epitope of trastuzumab. The antibody is indicated for use with trastuzumab and docetaxel for therapy of patients with HER-2 overexpressing metastatic breast cancer, which have not received previous anti-HER2 treatment or chemotherapy for metastatic cancer (U.S. Food and Drug Administration, 2012; National Health Service, 2013). In 2014 this therapy was also approved for the neo-adjuvant use in patients with locally advanced, inflammatory or early stage breast cancer (Amiri-Kordestani *et al.*, 2014).

### **Lapatinib**

A different class of targeted therapeutics are tyrosine kinase inhibitors. At the moment only lapatinib is approved for the treatment of advanced or metastatic HER2-positive breast cancer (U.S. Food and Drug Administration, 2007; Dillon, 2012; Hurvitz *et al.*, 2013). Lapatinib is given after prior therapy with anthracycline, taxane and trastuzumab. In patients with advanced or metastatic HER2-positive breast cancer lapatinib is used in combination with capecitabine and in postmenopausal women with ER+/HER2+ metastatic breast cancer it is applied in combination with letrozol (U.S. Food and Drug Administration, 2007; Dillon, 2012). This tyrosine kinase inhibitor interrupts the signalling of both EGFR and HER2. Lapatinib binds reversibly to the ATP-binding domain of the receptor inhibiting the tyrosine phosphorylation (Tai *et al.*, 2010). Studies showed that lapatinib is able to interrupt the signalling of HER2 and EGFR, inhibit growth and IGF-1R signalling as well as inducing apoptosis (Konecny *et al.*, 2006; Tai *et al.*, 2010).

### **Pre-approval anti-HER2 drugs**

Research for new HER2 targeting therapies is on-going. A number of molecules downstream of the HER2 receptor are being targeted. Further, monoclonal antibodies that target the dimerization site of HER2 are under investigation. One example is ertumaxomab, a trifunctional bispecific monoclonal antibody targeting HER2 and the T-cell specific CD3 antigen. Its epitope does not overlap with trastuzumabs and pertuzumabs. It has been shown to induce ADCC and antibody-dependent cellular phagocytosis (Diermeier-Daucher *et al.*, 2012). Novel tyrosine inhibitors are also under investigation. Neratinib and afatinib bind irreversibly to HER1, HER2 and HER4 as well as mutated HER2 (Zardavas *et al.*, 2013). Additionally, tumour vaccines against HER2 are being investigated (Hurvitz *et al.*, 2013; Zardavas *et al.*, 2013). The E75 HER2/neu peptide based vaccine was designed based on an epitope other than the one trastuzumab and pertuzumab bind to. It induces an immune system response of antibodies, helper T-cells and cytotoxic T-cells, which recognise cells expressing the immunogenic peptide on their surface and induce their lysis (Mittendorf *et al.*, 2008).

Although these and other new therapeutic agents have shown promising results, more research is required and clinical data has to be collected to determine their efficiency in the clinic.

### **1.7. Eukaryotic mRNA processing**

The complex mechanism of transcription and mRNA regulation is essential for the translation of fixed genetic information in a flexible, circumstance- and cell-specific manner into cellular proteins.

The process of mRNA transcription begins with changes in chromatin that allow the assembly of a transcription complex, containing RNA polymerase II [reviewed in (Hahn, 2004)]. A number of genes poses multiple promoters, through context specific DNA binding proteins and the chromatin structure, one will be selected for transcription initiation [review in (de Klerk and t Hoen,

2015)]. The different mRNA synthesis and processing steps e.g. transcription initiation and elongation, 5' capping, splicing, transcription termination and polyadenylation are tightly interwoven [reviewed in (Cramer *et al.*, 2001)].

As the mRNA is being synthesised, the 5'-end of the transcript is modified, capped, by a methylated GTP linked through a 5' to 5' triphosphate bridge to the pre-mRNA. Termination of transcription is followed by polyadenylation at the 3' end of the transcript. The typical recognition sequence for polyadenylation is AAUAAA, 11-30 nucleotides downstream an endonuclease cuts the mRNA and the polyA polymerase adds several hundred adenines [reviewed in (Cramer *et al.*, 2001)].

Genes encode exonic (exons) and intronic sequences (introns), both sequences are transcribed into pre-mRNA, but introns are generally removed from the sequence; spliced out. Leaving exons as the protein coding sequences. This was first described by Gilbert in 1978 (Gilbert, 1978). In humans, exons are generally between 50 and 300 nt (Berget, 1995). Introns can range in size from a few dozen nucleotides to over a megabase, with a median size of 1520 bases in coding genes (Hube and Francastel, 2015). Most eukaryotic pre-mRNAs contain short exons and long introns [reviewed in (Matera and Wang, 2014)].

### **1.7.1. The importance of pre-mRNA splicing**

Alternative splicing was first described approximately 40 years ago (Berget *et al.*, 1977; Chow *et al.*, 1977). It is an essential cellular process in most organisms. In recent years studies have indicated that over 95%, possible up to 100% of human transcripts are alternatively spliced, giving rise to a vastly increased proteome [reviewed in (Lee and Rio, 2015)]. Changes in the pattern of alternative splicing, can be observed for example in the development of an organism or in response to the environment [reviewed in (Zhang *et al.*, 2007; Pagliarini *et al.*, 2015)].

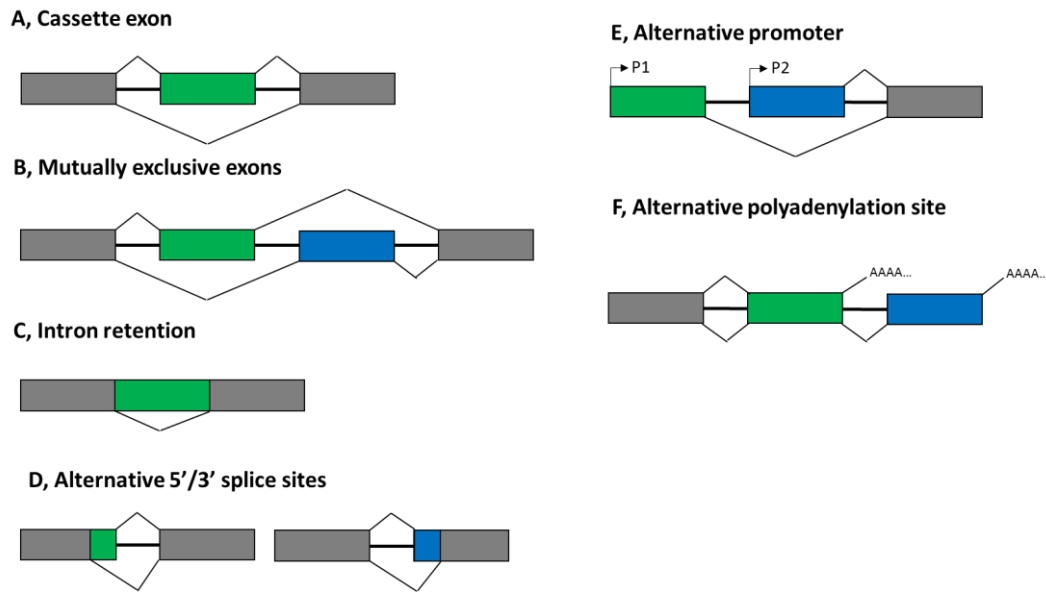


**Figure 1.10: Canonical alternative splicing events.**

A, Cassette exon. B, Mutually exclusive exons. C, Intron retention. D, Alternative 5'/3' splice sites. E, Alternative promoter. F, Alternative polyadenylation site.

Splicing and alternative splicing occurs mostly while the pre-mRNA is still being transcribed, but can also occur in the nucleus post-transcriptionally. The basic principle of splicing lies in the recognition of specific nucleotide sequences within the pre-mRNA which are recognised as introns (intergenic regions) and excised, whereas the exons (expressed regions) are assembled together (Sharp, 2005). Introns are mostly degraded in the nucleus and the mature mRNA is exported to the cytoplasm. Alternative splicing is the deviation from this basic pattern of exon inclusion and intron exclusion.

Different forms of alternative splicing can be observed, as illustrated in figure 1.10. These are the exclusion of an exon or the use of mutually exclusive exons, as well as the retention of introns. Further, alternative 5' or 3' splice sites (ss) within an exon as well as alternative promoters or polyadenylation sites can be used in mRNA processing [reviewed in (Tazi *et al.*, 2009)].

1.7.2. Basic mechanisms of splicing

The boundaries of exons and introns are highly conserved. The donor or 5' ss is the boundary between an exon ending on AG and an intron generally starting with "GURAGU", where the R indicates a purine. The acceptor or 3' ss is defined by an intron/exon junction of YAG/G, Y being a pyrimidine. Additional conserved sequence motifs are the branch point (BP), which is an adenine as part of a "YNYURAY" sequence, which is located 18 to 40 nucleotides upstream of the 3' splice site. The polypyrimidine tract (PPT), which consists of 15 to 20 consecutive uracils and cytosins between 5-40 nucleotides upstream of the 3' splice site and downstream of the BP [reviewed in (Burge *et al.*, 1999; Cartegni *et al.*, 2002)]. These sequences are of high importance in the recognition by and assembly of the spliceosome (Figure 1.11). The spliceosome is the catalytic unit that mediates the two-step trans-esterification that underlies splicing [reviewed in (Jurica and Moore, 2003; Will and Luhrmann, 2011)].

In the first step the phosphodiester bond between the last nucleotide of the exon and the first intronic nucleotide, at the 5' ss (AG\GU) is broken. The now freed phosphate group of the guanosine interacts with the adenosine of the branch point (YNYURAY). As a consequence the lariat, an intron loop is formed. The 3'-hydroxyl (OH) group of the last nucleotide of the exon interacts with the phosphate group of the first nucleotide of the following exon, at the 3'ss (YAG/G). The second trans-esterification step joins the two exons and releases the lariat [reviewed in (Moore and Sharp, 1993; Sharp, 1994)].

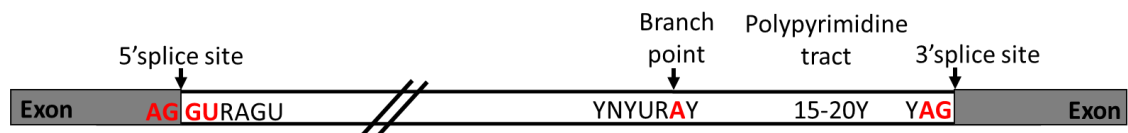


Figure 1.11: Conserved exon and intron sequences.

The 5' splice site is the boundary between an exon "AG" and an intron "GURAGU", where the R indicates a purine. The 3' splice site is defined by an intron/exon junction of YAG/G, Y being a pyrimidine. The branch point is an adenine as part of a "YNYURAY" sequence, which is located 18 to 40 nucleotides upstream of the 3' splice site; and the polypyrimidine tract, which consists of 15 to 20 consecutive uracils and cytosines between 5-40 nucleotides upstream of the 3' splice site and downstream of the BP.

### **1.7.3. Assembly and function of the spliceosome**

The spliceosome is the catalytic macromolecular complex that undertakes the above described splicing process. Throughout the splicing process it undergoes changes in its composition, structure and function (Figure 1.11). The spliceosome can consist of more than 170 proteins and 5 small nuclear ribonucleoproteins (snRNPs) [reviewed in (Jurica and Moore, 2003; Will and Luhrmann, 2011)]. The snRNPs consist of small nuclear RNAs and proteins that recognise the before discussed conserved signal sequences in the pre-mRNAs (Figure 1.11) [reviewed in (Matera and Wang, 2014)].

Splicing has been most extensively studied in yeast, but the processes are very well conserved in humans. A main difference lies in the length of human introns. Where in yeast introns tend to be short, in humans they are usually long with shorter exons (Fox-Walsh *et al.*, 2005). The first step for the splicing of shorter introns, is intron definition (Berget, 1995). The first weak complex is ATP-independent and has to be stabilised by the cap-binding complex and trans-elements, proteins bound to specific sequences on the pre-mRNA. The early complex (complex E) is formed through base pairing of U1snRNP with the 5'ss of the intron, this is aided by the C-terminal domain of the polymerase in co-transcriptional splicing. Following this splicing factor 1 (SF1), also known as BBP (branch point bound protein) binds to the BPS and interacts with the U2snRNP which recognises and binds the 3'ss of the intron (Berglund *et al.*, 1997). U2snRNP is associated with the U2 auxiliary factor (U2AF) heterodimer. U2AF binds to both the PPT with its 65kDa subunit and to the 3'ss of the intron with its 35kDa subunit (Merendino *et al.*, 1999; Wu *et al.*, 1999; Zorio and Blumenthal, 1999). In the next step which is an ATP-dependent reaction DExD/H helicases pre-mRNA-processing 5 (Prp5) and Sub2 catalyse the recognition of the BP by U2snRNP. Prp5 has been suggested to have a BPS proofreading and stabilising function (Liang and Cheng, 2015). SF1 is removed and U2snRNP interacts with U1snRNP to form the complex A [reviewed in (Matera and Wang, 2014)].

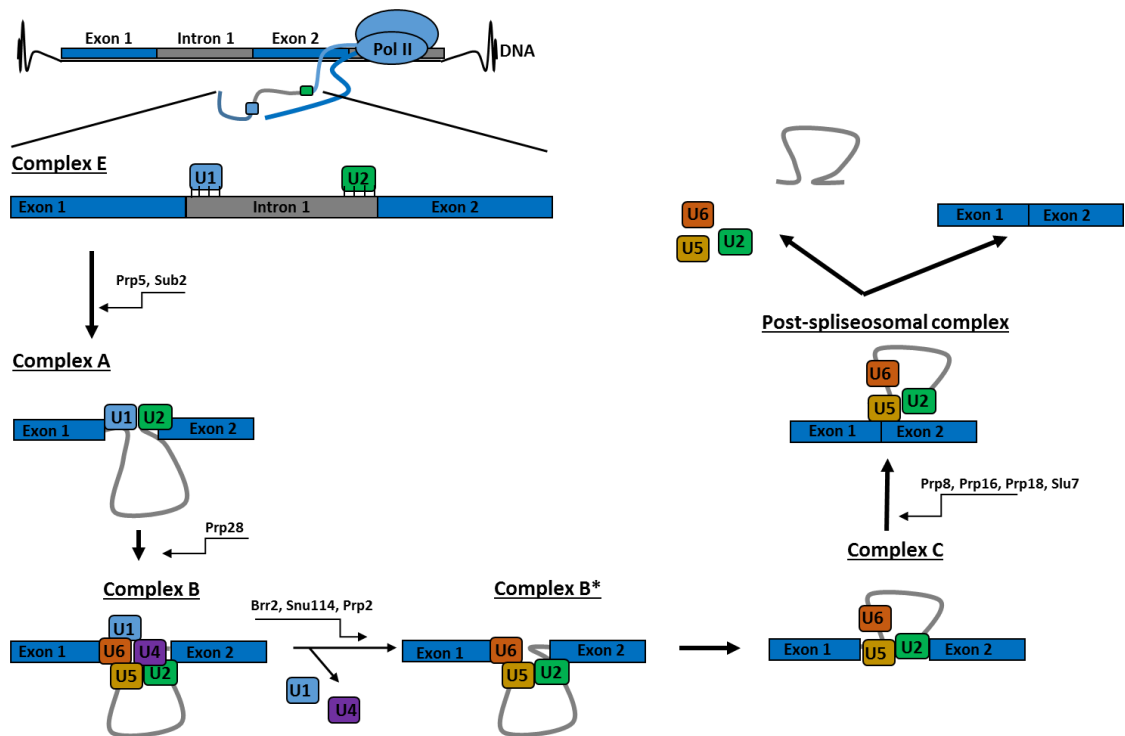


**Figure 1.12: The splicing process.**

A rough depiction of the essential steps in the splicing process. Complex E is formed through base pairing of U1snRNP with the 5'ss and U2snRNP with the 3'ss of the intron. Prp5 and Sub2 interact with the mRNA and cause a re-arrangement whereby U1 and U2snRNP interact. Prp28 catalysis the addition of U4/U6.U5 tri-snRNP complex to form Complex B. Extensive remodelling produces the active complex B\*. In complex C the lariat is formed and the exons joined together. The lariat is then degraded and the snRNPs recycled.

In the case of long introns, typical for mammals, the initial steps are less well understood. The exons become recognised through the exon definition complex, a pairwise interaction of U1 and U2snRNPs across the exon (Robberson *et al.*, 1990). The subsequent rearrangement yields an intron definition complex, which is considered to be equivalent to the complex A (Sharma *et al.*, 2008).

The spliceosomal B complex is formed by the recruitment of the preformed U4/U6.U5 tri-snRNP complex. This is catalysed by Prp28 (Sun and Manley, 1995; Matera and Wang, 2014). A number of helicases and snRNP components are necessary for the extensive remodelling of complex B into the catalytically active Complex B\*. As a result U1 and U4 snRNPs disassociate (Raghunathan and Guthrie, 1998).

On addition of ATP and Prp2 to the B\* complex, the 2'-OH of the branch point adenosine attacks the phosphodiester bond at the 5'ss to produce a free 5' exon and a lariat structure connected to 3' exon within the spliceosomal C complex. The lariat is removed and the two exons joined through another ATP-dependent reaction. This reaction is dependent on Prp8, Prp16 and synthetic lethal with U5 snRNP 7 (Slu7). The remaining snRNPs are released by RNA helicases in an ATP-dependent manner and recycled (Fourmann *et al.*, 2013) [reviewed in (Matera and Wang, 2014)].

### **1.7.4. Regulators of alternative splicing**

The efficiency of splicing and the occurrence of alternative splicing is dependent on a number of factors. As discussed before the important signalling sequences in the definition of an intron are well conserved. The splice site and correct splicing might be inhibited, depending on the extent of divergence from the consensus of these sequences (Kelemen *et al.*, 2013). The total length of exons and introns can also influence the efficiency of splicing. In exons that are shorter than 50nt the splice sites and splicing factor binding sites come into close proximity and thereby can sterically inhibit each other. On the other hand exons larger than 300nt are less likely to be recognised in an exon definition complex, and might therefore be spliced out (Fox-Walsh *et al.*, 2005). Just as important is the length of the introns for the recognition of exons and proper splicing. Long introns, especially upstream introns impair exon recognition (Fox-Walsh *et al.*, 2005; Wang *et al.*, 2014).

The secondary structures of the pre-mRNA itself can mask recognition sequences such as splice sites and inhibit splicing factor binding and spliceosome assembly. The opposite can also be observed, where secondary structures promote the recognition of a splice site and the correct splicing of an exon (Graveley, 2005; Kralovicova *et al.*, 2015). It has been suggested that a high GC content around the splice sites stimulates the formation of stabilising secondary structures that promote correct splicing (Zhang *et al.*, 2011).

### ***Cis-* and *trans-*acting elements**

The most well studied factors regulating pre-mRNA splicing are referred to as *cis-* and *trans-*acting elements. *Cis*-elements are sequences encoded into the pre-mRNA sequence that are recognition sites for *trans*-acting elements. Depending on localisation and effect, recognition sequences can be described as exonic splicing enhancers (ESE) and exonic splicing silencers (ESS) as well as intronic splicing enhancer (ISE) and intronic splicing silencers (ISS) (Fairbrother and Chasin, 2000; Faustino and Cooper, 2003; Srebrow and Kornblihtt, 2006).

*Trans*-acting elements, splicing factors, can help recognition of a splice site by the spliceosome, stabilise it and promote splicing or they can mask a splice site and inhibit splicing. Some of these *trans*-elements will remain on the pre- and mature mRNA to regulate further processes such as the transport into the cytoplasm, translation and mRNA decay (David and Manley, 2010; Twyffels et al., 2011). Traditionally arginine and serine rich (SR) proteins have been considered to enhance exon recognition (Cartegni *et al.*, 2002). They have two main motifs. One is a RS domain which contains repetitions of arginine-serine in the C-terminus and mediates protein-protein interactions. The second is one or more RNA recognition motifs (RRM) in the N-terminus contains (Twyffels *et al.*, 2011). Opposed to SR proteins heterogeneous nuclear ribonucleoproteins (hnRNPs) have been thought to inhibit exon recognition, although shown opposing functions have also been observed (Venables *et al.*, 2008). Similarly to SR proteins hnRNPs contain one or more RNA binding domains and a protein-protein interaction domain (Dreyfuss *et al.*, 1993; Geuens *et al.*, 2016). Diverse mechanisms by which hnRNPs inhibit exon recognition have been proposed. The first mechanism is by hnRNPs competing with SR proteins for binding sites on the pre-mRNA, and thereby inhibiting recognition and assembly of the spliceosome. The second mechanism is through hnRNPs interacting with each other and altering the structure of the pre-mRNA and thereby masking some regions of the pre-mRNA (Cartegni *et al.*, 2002; Venables *et al.*, 2008; Geuens *et al.*, 2016). The pre-mRNAs are generally occupied by a large number of splicing regulating proteins (splicing factors) which affect each

other's function, antagonizing or enhancing. This can occur locally, but also over a larger distance (Cartegni *et al.*, 2002).

### **Alternative splicing is linked to chromatin structure and transcription**

As splicing mostly occurs co-transcriptionally, chromatin structure and transcription is strongly linked with alternative splicing. Two models have been described to explain the effect of chromatin on splicing. The kinetic model links the transcription elongation rate to alternative splicing. Fast transcription elongation is likely to inhibit the recognition of alternative exons with weak splice sites by the spliceosome in favour of stronger downstream exons. Decreased velocity of transcription increases the likelihood of inclusion of a weak exon into the mature mRNA (de la Mata *et al.*, 2003; Fong *et al.*, 2014). Additionally, it has been suggested that an optimal velocity is necessary for correct splicing and change of elongation rate in either direction can lead to the same patterns of incorrect splicing (Fong *et al.*, 2014).

Transcription elongation rate dependent splicing has also been linked to nucleosome assembly. Exons of highly expressed genes are associated with an increased number of nucleosomes. Transcription by RNA polymerase II is slowed down by the nucleosome, this promotes exon inclusion (Naftelberg *et al.*, 2015). It has been shown that gene regions encoding exons tend to be more highly DNA methylated than introns. It was shown that about 22% of studied alternative exons are regulated by DNA methylation. Again this has been linked to the transcription elongation rate, but also to a recruitment of splicing factors by heterochromatin protein 1 [reviewed in (Lev Maor *et al.*, 2015)]. This is also referred to as the recruitment model (Naftelberg *et al.*, 2015). Lastly, changes to the transcription termination also influence the splicing of the last intron of the pre-mRNA (Niwa and Berget, 1991).

### **1.8. Alternative splicing and cancer**

Given the importance of alternative splicing in the normal homeostasis of cells and organisms, it is not surprising that changes to alternative splicing patterns are also important factors in the development and maintenance of cancer. There are multiple ways in which aberrant splicing can occur in cancer. Epigenetic changes can affect transcription linked to the previously discussed kinetic and recruitment model. An example is the skipping of exon 8 in the tumour suppressor gene *CDH1* in gastric cancer that is linked to the methylation pattern of the exon encoding gene region (Li *et al.*, 2015b). The changes can affect the normal equilibrium of splice variants of one gene or cause the production of splice variants that are not normally expressed in the cell type or which are altogether novel [reviewed in (Pal *et al.*, 2012)].

In cancer common targets of aberrant alternative splicing are genes that are important in signalling pathways such as cell survival and growth or metastasis [reviewed in (Siegfried *et al.*, 2013)]. One example is the tumour suppressor *BRCA1*, which main role is in DNA repair, not only plays an important role in developing hereditary cancer when mutated, but is also a target of alternative splicing [reviewed in (Orban and Olah, 2003)]. One splicing factor involved in its aberrant splicing is SRSF1. It is the most extensively studied splicing factors in breast cancer and has been considered a proto-oncogene 2 [reviewed in (Silipo *et al.*, 2015)]. Deregulated SRSF1 causes changes to the alternative splicing pattern of a number of important genes such as cell cycle protein cyclin D1, vascular endothelial growth factor (VEGF) a promoter of angiogenesis and apoptosis regulator Bcl-2 [reviewed in (Silipo *et al.*, 2015)]. Another study showed how members of the hnRNP family cause changes in the alternative splicing pattern of apoptotic genes promoting breast cancer development (Venables *et al.*, 2008).

### **1.9. HER2 splice variants and their role in cancer**

As mentioned previously, three functionally distinct alternative splice variants of HER2 have been identified; the membrane bound  $\Delta 16$ HER2 and the two secreted proteins Herstatin and p100 (Doherty *et al.*, 1999a; Aigner *et al.*, 2001; Sasso *et al.*, 2011). These three HER2 protein variants have been studied to different extents in the context of cancer and much of their function is still not understood.

#### **P100**

In 1993 Scot and colleagues identified a short HER2 transcript. This transcript encodes the first 2.1 kb of the otherwise 4.6 kb long wild type HER2 transcript. The transcript is compromised of the first 15 exons and a part of the following intron (Scott *et al.*, 1993). This causes the use of an in-frame stop codon and an early alternative poly(A) site within intron 15 (Scott *et al.*, 1993; Aigner *et al.*, 2001). The partial intron 15 inclusion gives rise to a novel 20 amino acid long C-terminal tail. Once translated this transcript produces a 633 amino acid long and 100 kDa sized glycosylated protein that only contains the extracellular domain of HER2 and can be found both in cells and as a secreted protein. Due to its size it was termed p100 (Scott *et al.*, 1993).

First identified in breast cancer cell lines, this transcript was also found to be expressed in other HER2 overexpressing gastric and ovarian cell lines (Scott *et al.*, 1993; Aigner *et al.*, 2001). This HER2 variant was later also found to be expressed at varying levels in breast cancer tissue and metastasis samples (Gebhardt *et al.*, 1998) as well as gastric cancer (Aigner *et al.*, 2001).

Studies into its role in cancer have given rise to controversial results. Initially it was shown that if cells overexpressed p100, the effect of HER2 targeting growth-inhibiting antibodies was decreased. Presumably, because the antibody binds p100 instead of wild type HER2, and as p100 is not able to induce signalling the antibody loses its effect (Scott *et al.*, 1993). A later study showed that the overexpression of p100 causes a decrease of cell proliferation in the breast cancer cell line MCF-7. It was also shown that p100 overexpression reduces heregulin dependent HER4 activation and thereby inhibits the induction

of the important cellular MAPK pathway. Additionally, it reduced the colony forming ability on soft agar of the gastric cancer cells MKN7. These observations were supported by an inverse association of p100 expression with advanced gastric cancer (Aigner *et al.*, 2001). Most studies do not distinguish between different secreted extracellular domain (ECD) HER2 proteins. Although, some studies have found ECD HER2 expression to be a good prognostic factor for patients treated with trastuzumab, others have associated it with a bad prognosis. A meta-analysis has not been able to show any clear associations (Lennon *et al.*, 2009). Interestingly, a recent study has shown that patients with an elevated ECD HER2 level benefit from lapatinib treatment (Lee *et al.*, 2016).

### **Herstatin**

Herstatin is the second secreted HER2 isoform arising from alternative splicing. It was first described by Doherty and colleagues in 1999 in an ovarian carcinoma cell line. The Herstatin mRNA transcript differs from WT HER2 through the inclusion of intron 8. From the 274bp of the intron 237bp are translated and the translation is terminated by an alternative stop codon in the intron. The arising protein is 68 kDa and consists of the extracellular domain of HER2 and a novel 79 amino acid long C-terminus. The novel C-terminal domain has been termed ECDIIIa. Herstatin is a minor HER2 protein variant (<5% of all HER2) in breast and ovarian cell lines as well as fetal tissue. Anti-sera was raised against Herstatin and endogenous Herstatin could be detected both in cell lysate and supernatant from the embryonic kidney cell line HEK-293 (Doherty *et al.*, 1999a). Herstatin inhibits WT HER2 signalling by binding to HER2 and disrupting dimer formation with EGFR, HER3 and HER4, this inhibits tyrosine phosphorylation and consequently anchorage-independent growth (Doherty *et al.*, 1999a; Azios *et al.*, 2001; Justman and Clinton, 2002; Shamieh *et al.*, 2004) and proliferation in general (Jhabvala-Romero *et al.*, 2003). It has also been shown that HER2 and Herstatin can be found co-localised in the endoplasmic reticulum and cytoplasm, and this complex formation seems to prevent HER2 from transitioning to the cell surface (Hu *et al.*, 2006).

Herstatin has been found both in cancerous and adjacent normal tissue both at mRNA and protein level. Interestingly, in 75% of the cancer tissue samples the mRNA levels did not predict the protein levels. Relative ratio between Herstatin

and HER2 were similar in cell lines and tissue, but generally lower in tissue. The same study also shows that about 20% of the HER2+ tumours studied also expressed relatively high Herstatin levels. In the surrounding normal tissue only relative low levels of Herstatin could be detected. This subgroup of tumours was further characterised by a high level of cytoplasmic phospho-AKT/p21 proteins. Such high cytoplasmic phospho-AKT/p21 levels in combination with HER2 overexpression have also been associated with an adverse prognosis in breast cancer and poor therapy outcome (Koletsa *et al.*, 2008). Although the mechanisms in Herstatin high breast cancer are still not well understood, Herstatin is generally considered to act as an autoinhibitor of HER2 and function as a tumour suppressor in cancer.

### **Δ16HER2**

The third HER2 splice variant, Δ16HER2, was first described by Kwong and Huang in 1998 as well as Siegel and colleagues in 1999. It is produced by the in-frame deletion of the 48 bp long cassette exon 16. This exon encodes 16 amino acids that are part of the extracellular domain (IV) directly preceding the transmembrane domain (Kwong and Hung, 1998; Siegel *et al.*, 1999). Earlier research had identified a deletion mutant of the HER2 orthologue Neu in mice to cause a loss of the same amino acids (Guy *et al.*, 1992; Siegel *et al.*, 1994; Siegel and Muller, 1996). The loss of cysteine residues in this region of the extracellular domain causes a conformational change, which gives rise to a continuously active conformation and promotes homo-dimerization by intermolecular disulphide bonds as well as strong association with HER3 (Siegel *et al.*, 1999). Depending on the study Δ16HER2 mRNA has been found to make up 5% to 9% of the total HER2 mRNA transcripts (Siegel *et al.*, 1999; Castiglioni *et al.*, 2006). Δ16HER2 has been found expressed in both cancerous and non-cancerous breast tissue, but it has been found at increased levels in cancerous breast (Siegel *et al.*, 1999; Castiglioni *et al.*, 2006). Another study found that 89% of local lymph node-positive and HER2-positive breast cancer patients expressed Δ16HER2 (Mitra *et al.*, 2009). It has been suggested that the gene amplification of HER2 in breast cancer may cause the elevation of Δ16HER2 expression over a threshold, where the splice variant contributes to the progression of the tumour (Siegel *et al.*, 1999; Castiglioni *et al.*, 2006).

## Chapter 1: Introduction

Already in initial studies exogenous  $\Delta 16$ HER2 was shown to have a six-fold stronger downstream signalling ability than exogenous WT HER2 when transiently transfected into cell lines. Furthermore,  $\Delta 16$ HER2 has been shown to have an increased transforming capability compared to wild type HER2 (Kwong and Hung, 1998; Siegel *et al.*, 1999; Mitra *et al.*, 2009; Sasso *et al.*, 2011). This transforming capability has been shown in 3D cell culture models using the normal-like mammary cell line MCF-10A that only formed invasive structures when  $\Delta 16$ HER2 was overexpressed, but not with WT HER2 overexpression (Alajati *et al.*, 2013) and in mice models (Castiglioni *et al.*, 2006; Marchini *et al.*, 2011; Alajati *et al.*, 2013). In mice models injected with WT HER2 transfected human cells no tumour growth could be observed. When the same experiments were performed with cells transfected with  $\Delta 16$ HER2, tumour growth and lung metastasis could be observed (Castiglioni *et al.*, 2006; Marchini *et al.*, 2011; Alajati *et al.*, 2013). This ability to induce tumour formation has been suggested to be due to the ability of  $\Delta 16$ HER2 to induced the expression of genes that mediate the endothelial to mesenchymal transition (Alajati *et al.*, 2013). Similar to previous studies Castagnoli *et al.*, showed that  $\Delta 16$ HER2-positive mice develop tumours faster and at a higher rate than WT HER2-positive mice. Interestingly, they observed changes in FISH analysis of the mice tumour tissues. They found WT HER2 mice tissues to have a near-tetraploid karyotype, but  $\Delta 16$ HER2 mice tissue to retain a diploid karyotype. Furthermore, they found WT HER2 tumours to be histologically very homogeneous, whereas  $\Delta 16$ HER2 tumours seemed to have three different zones with morphological differences in the cells (Castagnoli *et al.*, 2014).

Different studies have indicated that  $\Delta 16$ HER2 induces, at least partially, a different signalling pathway than WT HER2. Microarray expression profiling showed an expression profile that is typical for ER-negative, high-grade metastatic primary tumours, not HER2 positive tumours (Alajati *et al.*, 2013).  $\Delta 16$ HER2 has been shown to directly interact with the proto-oncogene Src.  $\Delta 16$ HER2 induces the translocation of the associated Src to the cell membrane, Src induces AKT, MAPK and cell motility regulating focal adhesion tyrosine kinase (FAK) pathways. Inhibition of Src caused destabilization of  $\Delta 16$ HER2 and decreased tumorigenicity (Mitra *et al.*, 2009). This was supported by a

study that found a direct correlation between Src phosphorylation and  $\Delta 16$ HER2 expression in a panel of breast tumours (Castagnoli *et al.*, 2014).

First studies in human cell lines indicated that  $\Delta 16$ HER2 might play a role in resistance to trastuzumab therapy (Castiglioni *et al.*, 2006; Mitra *et al.*, 2009). It was shown that although the therapeutic antibody trastuzumab could bind  $\Delta 16$ HER2 and cause its downregulation, the downstream signalling was not affected. Opposed to the WT HER2 model the tumour suppressor PTEN was also not induced in the  $\Delta 16$ HER2 model in response to trastuzumab (Mitra *et al.*, 2009). However, in the last seven years research has moved to study  $\Delta 16$ HER2 *in vivo*. Some studies injected mice with  $\Delta 16$ HER2/WT HER2 human cancer cells (Alajati *et al.*, 2013) and in other studies transgenic mouse models were used (Marchini *et al.*, 2011; Castagnoli *et al.*, 2014). In the *in vivo* study by Castagnoli *et al.*  $\Delta 16$ HER2 positive tumours were shown to be associated with an increased susceptibility to trastuzumab therapy (Castagnoli *et al.*, 2014). Additionally, using a method to infer  $\Delta 16$ HER2 levels through the expression of its downstream targets ( $\Delta 16$ HER2 metagene) Castagnoli and colleagues studied therapy resistance and prognosis in  $\Delta 16$ HER2 positive patients. They observed a positive association between the  $\Delta 16$ HER2 metagene and susceptibility to trastuzumab treatment (Castagnoli *et al.*, 2014).

### **1.10. Anti-HER2 therapy resistance: Focus on HER2 splice variants**

As encouraging as HER2 targeting therapeutics are, resistance against them in HER2 positive tumours has been observed. It was shown that in cases of metastatic breast cancer up to 74% of the patients were resistant to treatment with trastuzumab (Vogel *et al.*, 2002). Moreover, in 50% of the cases there was no response to combining trastuzumab with chemotherapy (Slamon *et al.*, 1989; Hurvitz *et al.*, 2013). The treatment with lapatinib alone yields similar percentages of resistant tumours. It has been suggested that an improved outcome could be attained when combining trastuzumab with lapatinib (Gampenrieder *et al.*, 2013). Studies have indicated that a treatment of pertuzumab in combination with trastuzumab and chemotherapy yields a

## Chapter 1: Introduction

pathologic complete response rate of 60%, and up to 90% have at least a partial response (Schneeweiss *et al.*, 2013).

As can be deduced from the numbers above, patients with an intrinsic or acquired resistance are not uncommon. A number of different mechanisms have been implied to be responsible for this resistance. Studies showed that often the aberrant activation of the HER2 signalling pathway, downstream of the receptor is the cause of resistance against therapy both with antibodies and lapatinib (Garrett and Arteaga, 2011). An example for this is the gain of function mutation to the PI3K subunit p110alpha (Campbell *et al.*, 2004). Another mechanism of resistance that has been suggested to be mediated by HER3, as trastuzumab seems to inhibit the heterodimerization of HER2 with EGFR, but not with HER3 (Junttila *et al.*, 2009; Hurvitz *et al.*, 2013). Additionally, targeting of HER2 seems to activate HER3 via an AKT-mediated feedback loop (Hurvitz *et al.*, 2013). Furthermore, trastuzumab resistance has also been observed to be caused by the masking of HER2 by increased expression of the membrane-associated mucin MUC4 (Nagy *et al.*, 2005).

Another potential reason for therapy resistance is the expression of a truncated version of HER2, p95HER2. This protein consists of the intracellular domain of HER2 and is mostly membrane bound. Trastuzumab has no effect on it as it lacks the extracellular domain which contains the epitope of trastuzumab (Aigner *et al.*, 2001). The tyrosine kinase inhibitor lapatinib is effective as the intracellular domain is intact. Similarly, as the intracellular domain of  $\Delta 16$ HER2 is also intact, it is also expected to be an effective target of lapatinib (Mitra *et al.*, 2009).

The cross-talk between ER and HER2 pathways has also been shown to affect drug treatment (Hurvitz *et al.*, 2013). The success of tamoxifen therapy, a competitive antagonist of oestrogen in ER-positive breast cancer, is strongly influenced by the co-expression of HER2. Studies showed that half of ER-positive breast cancer patients also express HER2 and up to 70% of these are resistant to tamoxifen therapy. This can be linked to the ability of HER2 and ER positive tumours to acquire oestrogen-independence. A study found that in up to 30% of the ER-positive breast tumours  $\Delta 16$ HER2 is expressed, and that  $\Delta 16$ HER2, not WT HER2 is responsible for increased oestrogen independent

## Chapter 1: Introduction

growth and resistance against tamoxifen. The following mechanism has been described. In response to tamoxifen, resistant cells upregulate the expression of the anti-apoptotic protein B-cell lymphoma-2 (BCL-2). This has been shown to be due to  $\Delta 16$ HER2 mediated downregulation of miRNAs 15a and 16, which normally target BCL-2 and cause its degradation (Cittelly *et al.*, 2010a; Cittelly *et al.*, 2010b).

Although it has been speculated that the binding of trastuzumab to  $\Delta 16$ HER2 could be inhibited by the epitope of the antibody lying in close proximity of the deleted region, it has been shown that trastuzumab is still able to bind  $\Delta 16$ HER2. Until recently studies indicated that  $\Delta 16$ HER2 was associated with trastuzumab resistance probably mediated by Src signalling (Mitra *et al.*, 2009), but recently a study showed  $\Delta 16$ HER2 expressing mice tumours to be increasingly susceptible to trastuzumab compared to WT HER2 expressing tumours (Castagnoli *et al.*, 2014).

**1.11. Rationale, hypotheses and aims**

**1.11.1. Study rationale**

When breast cancer is diagnosed the hormone receptor and HER2 status is assessed to determine the best possible treatment. HER2-positive breast cancers can be treated with HER2-targeting therapies (Hurvitz *et al.*, 2013). However their efficiency has been shown to be impacted by the presence of HER2 protein variants (Scott *et al.*, 1993; Aigner *et al.*, 2001; Mitra *et al.*, 2009; Lee *et al.*, 2016). Clinically the presence of HER2 protein variants is not assessed. Additionally, the mechanisms regulating the production of important HER2 splice variants has not been sufficiently studied.

Furthermore, although a number of HER2 protein variants have been identified, findings of our research group indicate the presence of additional HER2 protein variants. It has been shown by western blot and transient knockdown of HER2 that there are additional HER2 protein bands that cannot be attributed to known HER2 protein variants (Gautrey *et al.*, 2015).

**1.11.2. Hypotheses**

We hypothesize that:

- The production of HER2 splice variant  $\Delta 16\text{HER2}$  is primarily regulated through specific *cis*-and *trans*-acting elements.
- The presence of HER2 protein variants affects the HER2 status assessment and the subsequent therapy.
- Novel HER2 protein variants exist as a result of alternative splicing.

**1.11.3. Aims**

The aims of this project were to:

- Investigate the mechanisms regulating the  $\Delta 16$ HER2 splicing event
- Identify RNA-binding proteins that bind to the  $\Delta 16$ HER2 splicing region and regulate its splicing, and the RNA sequences they bind to
- Investigate a potential feedback loop between HER2 and its splicing regulators
- Study the effect of progesterone on HER2 expression and splicing
  
- Characterise a cohort of breast tumours for HER2 protein expression and localisation as well as the *HER2*-gene copy number
- Characterise breast tumours with discordant HER2 status results
- Study the HER2 splice variant levels in discrepant breast tumour samples
  
- To identify any potential novel HER2 splice variants
- To characterise any novel HER2 splice variant and their expression in normal and cancerous human tissues

## **Chapter 2: General materials and methods**

### **2.1. Cell lines**

Three breast cancer cell lines were used in this study, these were MCF-7 (ATCC® HTB-22™), MDA-MD-231 (ATCC® HTB-26™) and SKBR3 (ATCC® HTB-30™). The cell lines were acquired from the American Type Culture Collection (ATCC) and LGC Standards, Europe. All cell lines are adherent.

#### MCF-7

This cell line is an epithelial cell line derived from the metastatic site of a breast adenocarcinoma of a Caucasian 69 year old female. It is considered to be a model for early stage, non-invasive breast cancer (Soule *et al.*, 1973). MCF-7 is ER/PR positive and HER2 negative (Subik *et al.*, 2010).

#### MDA-MB-231

The MDA-MB-231 cell line is an epithelial cell line derived from the metastatic site of a breast adenocarcinoma of a Caucasian 51 year old female. The cell line is considered to be an invasive (Cailleau *et al.*, 1974) triple negative cell line (ER/PR/HER2 negative) (Subik *et al.*, 2010).

#### SKBR3

This cell line is an epithelial cell line derived from the metastatic site of a breast adenocarcinoma of a Caucasian 43 year old female (Trempe, 1976). This non-invasive cell line is ER/PR negative, but HER2 positive (Subik *et al.*, 2010).

### **2.2. Cell culture**

Cell culture techniques were performed under aseptic conditions in a Class II laminar flow microbiological safety cabinet. All cell lines were routinely cultured in 75 cm<sup>2</sup> or 25 cm<sup>2</sup> tissue culture flasks (Greiner) in a humidified atmosphere

## Chapter 2: General Materials and Methods

containing 5% CO<sub>2</sub> at 37°C. The MCF-7 and MDA-MB-231 cells were cultured in phenol-red free Dulbecco's Modified Eagles medium (DMEM) (Sigma-Aldrich), supplemented with 10% foetal bovine serum (FBS) (Sigma-Aldrich), 2 mM L-Glutamine (Sigma-Aldrich) and 100 units/ml penicillin and 0.1mg/ml streptomycin (Sigma-Aldrich). SKBR3 cells were grown in McCoy's 5A (modified) medium + GlutaMAX™ (Life Technologies) supplemented with 10% FBS (Sigma-Aldrich) and 100 units/ml penicillin and 0.1mg/ml streptomycin (Sigma-Aldrich).

### **2.2.1. Cell line maintenance**

The cells were grown to 70-80% confluency, passaged every 3 to 5 days. For cell passaging the medium was removed and the cells rinsed with Dulbecco's phosphate buffered saline (PBS) (Sigma-Aldrich) and incubated with 2mM trypsin-EDTA (Sigma-Aldrich) for 5 minutes at 37°C. To neutralise the trypsin complete growth medium was added and the cells were centrifuged at 200 x g for 5 min. The supernatant was discarded and the cells re-suspended in complete growth medium and passage at a ratio of 1:3-1:4.

### **2.2.2. Mycoplasma testing**

To ensure that the cells used in the experiments were not contaminated with Mycoplasma. Mycoplasma testing was routinely carried out using the MycoAlert™ PLUS Mycoplasma Detection kit (Lonza). Briefly, supernatants were collected from cells after a minimum of 48h of growth. The reagents were re-constituted and kept at RT for 20 min before use. The supernatants were centrifuged for 2.5 min at 2000 x g. The MycoAlert™ PLUS Reagent was added to the samples and incubated for 20 min. The absorbance was measured on a TD-20/20 Luminometer DLReady (Turner Designs), set for 1 sec (integrated). The first measurement 'A' was taken. Then MycoAlert™ PLUS Substrate was added to the samples and incubated for 30 min. The second reading 'B' was

taken. The ratio of 'B'/'A' was calculated. It was considered negative at < 1, borderline between 1 and 1.2, and contaminated at >1.2.

### **2.2.3. Cryopreservation of cells**

Cells were frozen at passages 10-20 for a continuous stock of cells. Cells were collected during routine cell passaging as described before (see section 2.2.1). The cell pellet was resuspended in 1 ml of undiluted FBS with 10% dimethyl sulphoxide (DMSO) (Sigma-Aldrich). The re-suspended cells were transferred to a cryo-vial (Gibco) and frozen down to -80°C in a Mr. Frosty™ Freezing Container, after which they were transferred to liquid nitrogen.

When needed, cells were brought up from liquid nitrogen and thawed at 37°C in a water bath. The cells were pelleted with the addition of complete growth medium at 200 x g for 5 min. The DMSO containing supernatant was removed and the cells re-suspended in complete growth medium and plated into tissue culture flasks.

### **2.2.4. Cell counting**

The cells were counted to plate the appropriate number of cells. An improved Neubauer chamber haemocytometer (Hawksley) was used to count cells. For this 10 µL of completely re-suspended cells in complete growth media were applied to the haemocytometer. The number of cells were counted for the four large squares (16 small squares) of the grid using a 10 x magnification on an inverted microscope (Leica). The average of four large squares was calculated. To calculate the number of cells per mL, the counted average was multiplied by 10<sup>4</sup>. The appropriate amount of cells depending on the experiment was then plated.

**2.2.5. Transient gene knockdown by siRNA transfection**

For transient gene knockdown experiments Silencer® Select siRNAs from Life Technologies were used (Table 2.2). The INTERFERin™ siRNA Transfection Reagent (Polyplus-Transfection) was used to transfect the siRNAs into the cells. The protocol was based on the manufacturers' instruction, with minor changes. Volumes used are indicated in table 2.1. For experiments where proteins were to be isolated 24 well plates were used and for RNA isolation 12 or 6 well plates were used. Cells were seeded 24 h before transfection. For the untreated control only Opti-MEM® medium (Life Technologies) was added to the cells. The target specific siRNAs or scrambled negative control siRNA were added to Opti-MEM® medium. INTERFERin™ was added and immediately vortexed for 10 sec. After 10 minutes incubation at RT the transfection mix was added to the cells. Beforehand, the complete medium was removed and antibiotic-free complete medium was added. The medium was exchanged for complete medium 24h later. To measure the effect of the gene knockdown on the mRNA level RNA was isolated 48 h post-transfection. For the protein level effect, the proteins were collected 72 h post-transfection. Additionally, to measure the effect on downstream targets of the knocked down gene, RNA was collected 72 h post-transfection.

**Table 2.1: Transient knockdown with INTERFERin™.**

	<b>24 well plate</b>	<b>12 well plate</b>	<b>6 well plate</b>
<b>Number of cells</b>	3.5 x 10 <sup>4</sup>	7 x 10 <sup>4</sup>	1.75 x 10 <sup>4</sup>
<b>Opti-MEM® medium</b>	100 µL	150 µL	200 µL
<b>siRNA (2nM)</b>	1.25 µL	2.5 µL	6.25 µL
<b>Interferin</b>	2 µL	4 µL	10 µL
<b>Antibiotic-free complete medium</b>	0.4 mL	0.85 mL	1.8 mL

**Table 2.2: List of Silencer® Select siRNAs used.**

<b>Name</b>	<b>siRNA ID</b>	<b>Custom designed siRNA sequences</b>
<b>GAPDH</b>	AM4622	
<b>HER2 (a)</b>	s611	
<b>HER2 (b)</b>	s613	
<b>hnRNP A1</b>	ASO20R9L	Sense: CUUUGGUGGUGGUCGUGGAgg Antisense: UCCACGACCACCACCAAGtt

## Chapter 2: General Materials and Methods

<b>hnRNP A/B</b>	s6716	
<b>hnRNP A2B1</b>	s6713	
<b>hnRNP D</b>	s6722	
<b>hnRNP F (1)</b>	s6727	
<b>hnRNP F (2)</b>	s6725	
<b>hnRNP FH</b>	ADVI3QW	Sense: GGAAGAAAUUGUUCAGUUCtt Antisense: GAACUGAACAAUUUCUUCctt
<b>hnRNP H1 (1)</b>	s6728	
<b>hnRNP H1 (2)</b>	s6729	
<b>hnRNP K (1)</b>	s6737	
<b>hnRNP K (2)</b>	s6739	
<b>Negative Control #1</b>	4390843	
<b>SRSF3 (1)</b>	s12733	
<b>SRSF3 (2)</b>	s12731	

### **2.3. Human breast tissue**

Breast tumour tissue samples were obtained by an award from the Breast Cancer Now Tissue Bank. The samples were collected with full patient consent and ethical approval was taken from the Breast Cancer Now Tissue Bank (reference: TR000027). The samples are from primary invasive ductal carcinoma breast tumours, grade 3.

RNA was isolated by research technician Amy Keelty and cDNA generated with the Superscript III Reverse Transcriptase (Life Technologies). The cDNA was stored at -20°C.

### **2.4. Normal human tissue cDNA**

Normal human tissue cDNA from cerebellum, testis, heart, muscle and lung was kindly provided by Dr Julian Venables. RNA was originally procured from Clontech and each sample was pooled from 5 individuals. The cDNA was generated by Dr Venables group using Superscript III Reverse Transcriptase and stored at -20°C.

## **2.5. RNA isolation techniques**

### **2.5.1. Total RNA isolation**

Total RNA was isolated from cells with the RNeasy Mini kit (Qiagen) for the PCR based mapping of HER2 (chapter 5.3.2) and the transient knockdown experiments in SKBR3 cells (chapter 3.3.4). For other experiments the ReliaPrep™ RNA Cell Miniprep (Promega) was used. This change was performed as the Promega kit was shown to produce comparable quality RNA and was more cost effective. Especially at small sample sizes the ReliaPrep™ RNA Cell Miniprep was superior to the RNeasy Mini kit.

Both kits follow the same technical principals. They were used according to the manufacturer's protocol.

The RNeasy Mini kit, direct lysis of the adherent cells was performed on plates after the medium was removed. Lysis buffer was added and the cells lysed by mixing. The lysate was collected into 1.5 mL tube and homogenized using a 20-gauge needle (BD Microlance). One volume of 70% ethanol was added and mixed. This was applied to the RNeasy spin columns. Centrifugation steps were performed at  $\geq 8000 \times g$ . The spin columns were centrifuged for 15 sec. The columns were washed with Buffer RW1 and centrifuged for 15 sec. The RNAs were treated with DNase I (Qiagen) to remove genomic DNA for 15 min at RT. This was followed by a wash with Buffer RW1 and then Buffer RPE. The columns were washed again with Buffer RPE and centrifuged for 2 min. The columns were placed into new tubes and spun down for 1 min. The columns were then placed into collection tubes and 25-35  $\mu$ L of nuclease-free water was added. After one minute incubation the columns were centrifuged for 1 min. The RNAs were stored at  $-80^{\circ}\text{C}$ .

The ReliaPrep™ RNA Cell Miniprep, direct lysis of cells was performed. Medium was removed and cells washed twice with PBS. The BL + TG lysis Buffer was added and the cells lysed by mixing. The lysate was collected into 1.5 mL tube and homogenized using a 20-gauge needle in case of 6 well plate derived samples or vortexed for smaller sample sizes. 100% isopropanol was

added according to sample size (see manufacturers protocol) and mixed by vortexing. This was applied to the Minicolumns and centrifuged for 30 sec. Centrifugation steps were performed at 13000 x g. The columns were washed with RNA Wash Solution and centrifuged. A 15 min DNase I treatment was performed to remove genomic DNA, followed by a wash with Column Wash Solution and then RNA Wash Solution. The columns were placed into new tubes, washed again with RNA Wash Solution and centrifuged for 2 min. The columns were then placed into collection tubes and 25-30  $\mu$ L of nuclease free water was added. After one minute incubation the columns were centrifuged for 1 min. The RNA samples were stored at -80°C.

### **2.5.2. mRNA isolation**

To isolate an RNA fraction strongly enriched for polyadenylated mRNA the GenElute Direct mRNA Miniprep kit (Sigma-Aldrich) was used. The RNA was isolated according to the manufacturer's guidelines.

An 80% confluent 75 cm<sup>2</sup> flask of cells was used on two columns. All centrifugation steps were performed at 16000 x g. Cells were pelleted and treated with the Proteinase K containing lysis solution. After vortexing, the cell lysates were applied to filtration columns and spun down. The columns were incubated for 10 min at 65°C to eliminate RNase. 5 M NaCl and oligo (dT) beads were added to the samples according to the manufacturers protocol and vortexed. The mix was incubated for 10 min at RT, then the beads were pelleted. The supernatants were removed carefully. To concentrate the mRNA the beads were re-suspended in lysis-buffer and 5 M NaCl. This was followed by a 5 min incubation step at 65°C and then 5 min at RT. The beads were pelleted for 2 minutes and the supernatant carefully removed. The beads were then re-suspended in wash solution and transferred to a spin column. The column was spun down for 2 min and the flow-through was discarded. The wash step was repeated with a low salt wash solution. The column was placed into a new collection tube. Pre-warmed elution solution was added and the

samples incubated at 65°C for 5 min. The enriched mRNA was collected by centrifuging for 2 min. The elution was repeated.

An ethanol precipitation step was performed to concentrate the mRNA. For this 20 µg of glycogen (Fermentas), 0.1 volume of 3M sodium acetate buffer pH 5.2 (Sigma-Aldrich) and 3 volumes of ice cold absolute ethanol were added. The mRNA was precipitated overnight at -20°C. The mRNA was centrifuged at maximum speed for 15 min at 4°C. The supernatant was carefully removed and the pellet air dried. The mRNA was resuspended in 20µL nuclease-free water. The mRNA was stored at -80°C until use.

### ***2.5.3. Isolation of Cytoplasmic and Nuclear RNA Fraction***

Nuclear and cytoplasmic RNA fractions were isolated using the Cytoplasmic and Nuclear RNA Purification kit (NORGEN BIOTEK Corp.). For the RNA isolation the manufacturer's instructions were followed.

Cells were detached from plates with trypsin, collected, counted and RNA was isolated from  $1 \times 10^6$  cells. The cells were pelleted at 200 x g for 10 min and lysed using the Lysis Buffer J. The pellet was homogenized by vortexing. The lysate was centrifuged at maximum speed for 3 minutes. The supernatant, the cytoplasmic RNA, was collected in a new tube. Buffer SK was added to the cytoplasmic RNA and vortexed for 10 sec. Then 100% ethanol was added and again mixed by vortexing. This mix was applied to the column and spun down at 3500 x g for 1 min. The same was performed for the pellet, the nuclear RNA fraction.

DNase [concentration: 2.73 Kunits/µL] (Qiagen) was used to treat the RNA fractions. For each column 100 µL 0.25 Kunits/µL was prepared in DNase Buffer. After addition of the Wash solution, the columns are centrifuged at 14000 x g for 2 min. Then the DNase mix was added to the columns and centrifuged for 1 min at 14000 x g. The flow-through was applied back onto the columns and incubated for 15 min at RT. Then the columns were washed with Wash solution and spun down for 2 min at 14000 x g. The columns were placed

## Chapter 2: General Materials and Methods

into fresh tubes and 25  $\mu\text{L}$  elution buffer E added. The columns were centrifuged at 200 x g for 2 min and 1 min at maximum speed. The RNA samples were stored at  $-80^{\circ}\text{C}$ .

### **2.6. Polymerase chain reaction (PCR) based techniques**

#### **2.6.1. Reverse transcription**

RNA quantity and quality was assessed using the NanoDrop1000 (ThermoScientific). Reverse transcription was performed using the SuperScript III Reverse Transcriptase kit (Invitrogen). For each sample a reaction containing all reagents except the SuperScript III reverse transcriptase was performed as a negative (-ve) control to check for genomic contamination. Additionally a control containing all reagents but no template was used as an RT- control.

**Table 2.3: Reverse transcription reaction mix.**

<b>Reaction mix components</b>	<b>For a 50 <math>\mu\text{L}</math> reaction</b>
<b>5x First Strand buffer</b>	10 $\mu\text{L}$
<b>Oligo (dT) primers (0.5 <math>\mu\text{g}/\mu\text{L}</math>)</b>	1 $\mu\text{L}$
<b>dNTP mix (25 mM each)</b>	0.8 $\mu\text{L}$
<b>DTT (0.1 M)</b>	1 $\mu\text{L}$
<b>RNaseOUT (40 unts/<math>\mu\text{L}</math>)</b>	1 $\mu\text{L}$
<b>SuperScript III reverse transcriptase</b>	1 $\mu\text{L}$
<b>RNA</b>	(0.2 to ) 1 $\mu\text{g}$
<b>Nuclease free water</b>	Make up to 50 $\mu\text{L}$

For each reaction (0.2 to) 1  $\mu\text{g}$  of RNA was used, the amount was kept consistent in each set of experiments. The reagents, except the reverse transcription enzyme, were pipetted together with the RNA and made up to a total volume of 49  $\mu\text{L}$  (Table 2.4). Lastly the reverse transcription enzyme was added. The sample was then incubated in a BioRad or G-storm thermocycler for 59 min at  $50^{\circ}\text{C}$  and 15 min at  $70^{\circ}\text{C}$ . Synthesised cDNA was stored at  $-20^{\circ}\text{C}$ .

**2.6.2. Conventional PCR**

For conventional PCR the 2 x PCR Master Mix (Promega) was used. The reaction mix was prepared according to the manufacturer’s instructions (Table 2.4). Only for Intron 25 detection the primer amount used was decreased to 0.2 µL each and the annealing temperature set for 60°C. The full list of primers is shown in table 2.8. The PCRs were undertaken using either a BioRad or a G-storm thermocycler, the cycle number of the basic programs was adjusted according to the gene to be amplified and cDNA source (Table 2.5).

Orange G loading dye [50% Glycerol, 60mM EDTA, 10mM Tris-HCl, 0.15% Orange G (Sigma-Aldrich)] was added to the PCR products which were then separated on 2% agarose (Bioline) gels with 0.04 µL/mL ethidium bromide in 0.5 x crystal TBE running buffer (Bioline). The voltage used was dependent on the size of tank and gel used. It was visualised under UV light on a Biospectrum®500 Imaging system (UVP) with the VisionWorks LS software (UVP).

Basic PCR Program

95°C	2 min		
95°C	30 sec	}	x cycles
55°C	30 sec		
72°C	30 sec - 1.5 min		
72°C	5 min		
12°C	∞		

**Table 2.4: PCR reaction mix.**

	For a 25 µL reaction
<b>2x Master Mix</b>	12.5 µL
<b>(0.5 µg/µL) Forward/Reverse Primer</b>	0.25 µL
<b>Nuclease-free water</b>	11 µL
<b>cDNA</b>	1 µL

## Chapter 2: General Materials and Methods

**Table 2.5: Number of PCR cycles used.**

	<b>SKBR3 cDNA</b>	<b>MCF-7 / MDA-MD-231 cDNA</b>	<b>Human Tissue cDNA</b>	<b>Breast Tumour cDNA</b>
<b>Δ16HER2</b>	27	30	N/A	35
<b>B-actin</b>	N/A	N/A	25	25
<b>GAPDH</b>	20	20	20	N/A
<b>Herstatin</b>	N/A	N/A	N/A	35
<b>hnRNP A1</b>	35	N/A	N/A	N/A
<b>hnRNP A2B1</b>	25	N/A	N/A	N/A
<b>hnRNP F</b>	26	N/A	N/A	N/A
<b>hnRNP H</b>	28	N/A	N/A	N/A
<b>hnRNP K</b>	25	N/A	N/A	N/A
<b>I12HER2</b>	30	N/A	N/A	N/A
<b>I25HER2</b>	30	32	32	35
<b>P100</b>	N/A	N/A	N/A	35
<b>SRSF3</b>	24	N/A	N/A	N/A
<b>Wild type HER2</b>	23	25	32	32

**Table 2.6: List of PCR primers used.**

<b>Name</b>	<b>Sequence</b>
<b>Novel exon 1 Forward</b>	CGAGGCGATAGGGTTAAGGG
<b>Novel exon 6 Forward</b>	ATTCCAGAAGATATGCCCCG
<b>Exon 1 Forward</b>	TCCTCCTCGCCCTCTTGC
<b>Exon 2 Forward</b>	CCAGCCTGTCCCTCCTGC
<b>Exon 3 Forward</b>	CGCTGAACAATACCACCCCT
<b>Exon 3 Reverse</b>	AGGGGTGGTATTGTTTCAGCG
<b>Exon 5 Forward</b>	CTCCGATGTGTAAGGGCTCC
<b>Exon 6 Forward</b>	CCACTGACTGCTGCCATGAG
<b>Exon 9 Reverse</b>	TGCCAGGCTCCCAAAGATC
<b>Exon 10 Forward</b>	GAGACTCTGGAAGAGATCAC
<b>Exon 12 Forward</b>	GGCCAGAGGACGAGTGTG
<b>Intron 12 Forward</b>	CCCTTCCTCCTCACTGCAG
<b>Exon 14 Forward</b>	AGTGACCTGTTTTGGACCG
<b>Exon 16 Exclusion Reverse</b>	CGTCAGAGGGGAGTGGGT
<b>Exon 16 Inclusion Reverse</b>	GGACCTGGATGACAAGGG
<b>Exon 16 Inclusion Forward (3Fa)</b>	GTGTGGACCTGGATGACAAGGG
<b>Exon 16 Exclusion Forward (3Fb)</b>	CACCCACTCCCCTCTGAC
<b>Exon 16 Reverse (3R)</b>	GCTCCACCAGCTCCGTTTCCTG
<b>Exon 17 Forward (F1)</b>	CATTCTGCTGGTCGTGGTCT
<b>Exon 18 Reverse (R1)</b>	CCGTCTCTTTCAGGATCCGC
<b>Exon 19 Reverse (R2)</b>	TGGCTTTGGGGGATGTGTTT
<b>Exon 20 Reverse (R3)</b>	AGAGGCAGCCATAGGGCATA
<b>Exon 20 Forward (F2)</b>	GGTGACACAGCTTATGCCCT
<b>Exon 21 Reverse (R4)</b>	GCACATCCTCCAGGTAGCTC

## Chapter 2: General Materials and Methods

<b>Exon 22 Reverse (R5)</b>	CCACACATCACTCTGGTGGG
<b>Exon 23 Reverse (R6)</b>	AGGTTTGGCCCCAAAAGTCA
<b>Exon 23 Forward (F3)</b>	GGCCAAACCTTACGATGGGA
<b>Exon 24 Reverse (R7)</b>	GCGGGAGAATTCAGACACCA
<b>Exon 25 Reverse (R8)</b>	TGGGCCCAAGTCCTCATT
<b>Exon 25 Forward (F4)</b>	CACCGCAGCTCATCTACCAG
<b>Exon 26 Reverse (R9)</b>	CCCATTCCCAGGTCACCATC
<b>Exon 27 Reverse (R10)</b>	CCTTTCCAGAGTGGCACCAG
<b>HER2_n3UTR_R</b>	CAGAAGTCAGGCCTTCCCTG
<b>HER2_3UTRv1_R</b>	GAAGATTCCCAGCCACTCCC
<b>HER2_3UTRv2_R</b>	GGACAGCTGGTGTCTCCAA
<b>HER2_Intron 24_F</b>	GAGGGTGGGAAGGAGAGATGAG
<b>HER2_Intron 24_R</b>	GCCTGGCATACTGGACTCAT
<b>New Herstatin Forward</b>	CCTGTCCTATCCTTCCTCAGAC
<b>Intron 25 qPCR Forward</b>	GCTCATCTACCAGGGTCAGT
<b>Intron 25 qPCR Reverse</b>	TGGGGTTTCCTTGAGAGGTG
<b>hnRNP A1 Forward</b>	CCAGAGAAGATTCTCAAAGACC
<b>hnRNP A1 Reverse</b>	CTTCAGTGTCTTCTTTAATGCC
<b>hnRNP A2B1 Forward</b>	TTTGATGACCATGATCCTGT
<b>hnRNP A2B1 Reverse</b>	CTCTGAACTTCTTGCATTTCC
<b>hnRNP F Forward</b>	GAGGGAGGTGAAGGCTTTGT
<b>hnRNP F Reverse</b>	CGGCCCCATCATGAATCGT
<b>hnRNP H Forward</b>	TCCTGACACGGCCAATGATC
<b>hnRNP H Reverse</b>	TTGGCACGATTTCCAACCCT
<b>hnRNP K Forward</b>	GTGCACAGCCTTATGATCCC
<b>hnRNP K Reverse</b>	ACCAGGAGGCATTCTGTCAA
<b>P100 Forward</b>	TGGACCGGAGGCTGACCAG
<b>P100 Reverse</b>	AGACCGTTGGACTCACGAGTGG
<b>GAPDH Forward (conv. PCR)</b>	CTGCCGTCTAGAAAAACC
<b>GAPDH Reverse (conv. PCR)</b>	CCAAATTCGTTGTCATACC
<b>GAPDH (2) Forward (qPCR)</b>	CCACCCATGGCAAATTCC
<b>GAPDH (2) Reverse (qPCR)</b>	GATGGGATTTCCATTGATGACA

### **2.6.3. Real-Time PCR: SYBR Green**

For HER2 splice variant expression studies, the cDNA samples derived from SKBR-3 cells were diluted 1:10 because of the high HER2 expression level and from the MCF-7 cells the cDNA samples were diluted 1:2 due to low HER2 expression levels. The QuantiFAST SYBR Green PCR Master mix was used. The primers for wild type HER2 (3Fa, 3R),  $\Delta$ 16HER2 (3Fb, 3R) and p100 are listed in table 2.6. For normalisation the housekeeping gene GAPDH was used. The reaction mix was prepared as detailed in table 2.7. Triplicates were applied

## Chapter 2: General Materials and Methods

to MicroAmp Optical 96-Well Reaction Plates (Applied Biosystems®). Negative control reactions were included for each primer pair. The sealed plates were spun down for 5 min at 500 x g, to remove any air bubbles. A fast comparative CT ( $\Delta\Delta CT$ ) program with a melting curve was run on a StepOnePlus™ Real-Time PCR System.

The real-time PCR program:

95°C	5 min	
95°C	10 sec	} 40 cycles
60°C	30 sec	

Melting curve was set to have a 0.5°C ramp rate.

**Table 2.7: PCR reaction mix with QuantiFAST SYBR Green PCR Master Mix.**

	For a total volume of 25 $\mu$ L
<b>2x QuantiFast SYBR Green PCR Master Mix</b>	12.5 $\mu$ L
<b>10 <math>\mu</math>M Forward/Reverse Primer</b>	2.5 $\mu$ L
<b>cDNA (1 to 100 ng)</b>	1 $\mu$ L
<b>Nuclease-free water</b>	6.5 $\mu$ L

### ***2.6.4. Real-Time PCR: TaqMan™ Assays***

Where available real-time PCR with TaqMan™ assay (Life Technologies) was performed. The TaqMan™ assays used are listed in table 2.9. For TaqMan™ real-time PCR reactions 1:10 diluted SKBR3 cDNA samples were used. The reaction mix was prepared following the manufacturers protocol (Table 2.10).

**Table 2.8: TaqMan™ Assays.**

	TaqMan™ Assay ID
<b>GAPDH</b>	Hs0258991_g1
<b>hnRNP H1</b>	HS01033855_g1
<b>hnRNP F</b>	Hs01855422_s1
<b>hnRNP K</b>	Hs03989611_gH
<b>SRSF3</b>	Hs00751507_s1

## Chapter 2: General Materials and Methods

Four replicates were plated onto MicroAmp Optical 96-Well Reaction Plates and negative controls for each TaqMan™ assay were included. The sealed plates were spun down for 1-2 min at 500 x g, to remove any air bubbles. The standard program for a standard comparative CT ( $\Delta\Delta CT$ ) program on the StepOnePlus™ Real-Time PCR System was used.

**Table 2.9: TaqMan™ Real-Time PCR reaction mix.**

	<b>For 10 <math>\mu</math>L total volume</b>
<b>20x TaqMan Gene Expression Assay</b>	0.5 $\mu$ L
<b>2x TaqMan Gene Expression Master Mix</b>	5 $\mu$ L
<b>cDNA template (1 to 100 ng)</b>	2 $\mu$ L
<b>RNase-free water</b>	2.5 $\mu$ L

### **2.7. Protein based techniques**

#### **2.7.1. Protein isolation**

Protein lysate was prepared following transient knockdown using 2 x SDS lysis/loading buffer [30% Urea, 2.5% SDS, 35 $\mu$ l/ml Mercaptoethanol, 0.1% Bromophenol Blue in 0.5M Tris pH 6.8 (Sigma Aldrich)]. After direct lysis of cell with SDS lysis buffer, the protein extract was denatured by incubation at 10min at 95°C.

After lapatinib treatment cells grown in 12 well plates were collected in radioimmunoprecipitation assay (RIPA) buffer. After removing the medium and washing with 1 x PBS, 200 $\mu$ L of RIPA buffer (25mM Tris-HCL, 150mM NaCl, 5mM EDTA, 1% NP-40 substitute, 1% sodium deoxycholate, 0.1% sodium dodecyl sulfate [Sigma Aldrich]) supplemented just before use with 2% protease inhibitor (Sigma Aldrich) and 1% phosphatase inhibitor cocktail III (Sigma Aldrich) was added. The cells are lysed and scraped in the buffer. The cell lysate is collected and centrifuged for 15 min at 14000 x g. The supernatant was collected, frozen in liquid nitrogen and transferred to a -80°C freezer. For western blot 30  $\mu$ g samples were prepared. To the appropriate amount of protein sample 10  $\mu$ L of 2 x SDS lysis/loading buffer was added and the protein sample denatured through a 10 min incubation at 95°C.

### **2.7.2. Protein quantification**

To quantify proteins the colourimetric DC Protein Assay (Bio-rad) was used. For this a protein standard was prepared from bovine serum albumin (BSA) in the same buffer as the proteins were isolated into. The protein quantification was performed according to the manufacturer's protocol. The absorbance was read at 750nm on a SpectraMax 190 microplate reader (Molecular Devices) using the parameters set for the Lowry assay on the SoftMax Pro software (Molecular Devices). The standard curve was plotted and the equation of the linear trend line used to calculate the protein concentrations of the samples.

### **2.7.3. SDS-polyacrylamide gel electrophoresis (SDS-PAGE)**

To size separate proteins SDS-PAGE was performed. The samples were denatured and prepared with SDS-lysis buffer as loading dye and applied to a polyacrylamide gel (Table 2.8). If not otherwise indicated, reagents were bought from Sigma-Aldrich. The SDS-PAGE was performed in a Mini-PROTEAN III system (Bio-Rad) with a 1 x electrophoresis buffer (25 mM Tris-HCl pH 8.3, 190 mM glycine, 0.1% SDS). A PageRuler™ Prestained protein ladder or a PageRuler™ Plus Prestained protein ladder (Thermo Scientific) was used as a reference molecular weight marker. Electrophoresis was performed at 175V for 1h, or as necessary using a PowerPAC 3000 system (Bio-Rad). The gel was immediately used for protein transfer.

**Table 2.10: Components of polyacrylamide resolving and stacking gels.**

<b>For a volume of 20 mL</b>	<b>7.5%</b>	<b>10%</b>	<b>12%</b>	<b>4% stacking gel</b>
<b>40% Acrylamide/Bis solution (Bio-Rad)</b>	3.76 mL	5 mL	6 mL	500 µL
<b>H<sub>2</sub>O</b>	10.94 mL	9.7 mL	8.7 mL	3.2 mL
<b>1.5 M Tris HCl pH 8.8</b>	5 mL	5 mL	5 mL	N/A
<b>SDS</b>	200 µL	200 µL	200 µL	50 µL
<b>TEMED</b>	10 µL	10 µL	10 µL	5 µL
<b>10% Ammonium persulphate</b>	100 µL	100 µL	100 µL	25 µL
<b>0.5 M Tris HCl pH 6.8</b>	NA	NA	NA	1.26 mL

**2.7.4. Western blot**

A wet transfer was performed to transfer the proteins from the SDS-gels to Immun-Blot<sup>®</sup> PDVF membranes (Thermo Scientific). The transfer was performed in 1 x transfer buffer (25 mM Tris-HCl pH 8.3, 150 mM glycine, 10% methanol) at 90 V for 90 min in the case of small to medium sized proteins and for 2 h for large proteins using the PowerPAC 200 system (BioRad). The run was performed under constant cooling.

The membrane was blocked with 10% not-fat milk powder (Marvel) in 1 x PBS (Sigma Aldrich) for 1 h. This was followed by overnight incubation with the primary antibody at 4°C. The antibody was prepared in the recommended or optimised concentration in 1% milk powder (Table 2.9). Following incubation the antibody was recovered and the membrane washed three times for 10 min in 1 x PBS. The appropriate horseradish peroxidase (HRP) conjugated secondary antibody (Dako) (Table 2.9) was diluted 1:3000 in 1 x PBS and applied to the membrane for 1h at RT under agitation. The membrane was then washed three times with 1 x PBS for 10 min. To detect the proteins through chemiluminescence an ECL detection was used. With normal abundant proteins Pierce ECL Western Blotting Substrate (Thermo Scientific) was used and for increased sensitivity Amersham<sup>™</sup> ECL Select<sup>™</sup> Western Blotting detection reagent (GE Healthcare) was used. X-ray films (Kodak) were exposed to the membranes and developed.

Alternatively, if phosphorylated proteins were to be detected the membranes were blocked with 5% Albumin, serum bovine (BSA) (Sigma-Aldrich) in 1x TBS. The primary antibodies were prepared in 5% BSA, 1 x TBS with 0.1% Tween<sup>®</sup>20 (Sigma-Aldrich) and the secondary antibody in 1 x TBS. The washes before the secondary antibody were alternatively performed with 1x TBS or 1 x TBS-Tween<sup>®</sup>20. After the secondary antibody the washes were performed with 1 x TBS and once with 1 x PBS.

**Table 2.11: Details to the antibodies used in western blotting.**

Antibody	Company	Western Blot antibody ratio	2 <sup>nd</sup> Antibody
GAPDH (FL335)	Santa Cruz	1:1000	rabbit
HER2/ErbB2 (c-terminal)	Cell Signaling	1:1000	rabbit
HER2/ErbB2 (D8F12) XP™	Cell Signaling	1:1000	rabbit
Phospho-HER2/ErbB2 (Tyr1221/1222) (6B12)	Cell Signaling	1:1000	rabbit
hnRNP 1	GeneTex	1:3000	rabbit
hnRNP A1	GeneTex	1:3000	mouse
hnRNP A/B	GeneTex	1:3000	rabbit
hnRNP A2B1	GeneTex	1:10000	rabbit
hnRNP D / AUF1	GeneTex	1:3000	rabbit
hnRNP H	GeneTex	1:3000	rabbit
hnRNP K	GeneTex	1:3000	rabbit
SRp40/p55/p75 (H-180)	Santa Cruz	1:1000	mouse
SRSF3	Zymed	1:1000	mouse
Akt (pan) (C67E7)	Cell Signaling	1:1000	rabbit
phospho-Akt (Ser473) (D9E) XP®	Cell Signaling	1:2000	rabbit
Anti-MAP kinase 1/2 (Erk1/2)	Merck Millipore	1:1000	rabbit
phospho-p44/42 MAPK (Erk1/2) (Thr202/Tyr204) (D13.14.4E) XP®	Cell Signaling	1:2000	rabbit

## 2.8. Cloning and transformation in *Escherichia coli* (*E.coli*)

To verify the identity of PCR amplified sequences, the PCR products were excised from gels after size separation, purified and cloned into the pCR™4-TOPO® vector, which contains an Ampicillin resistance gene for selection. *E.coli* were transfected with plasmids and a colony picked for plasmid isolation. To verify the sequences plasmids were sent for sequencing. The detailed steps are described in the next subsections.

**2.8.1. PCR product isolation from agarose gel**

To recover PCR products after size separation from a 1% agarose gel, the GeneJET Gel Extraction and DNA Cleanup Micro Kit (Thermo Scientific) was used. The recovery was performed as recommended by the manufacturer. Briefly, under UV light the PCR band was excised from the gel and placed into a 1.5 mL tube. Maximum 200 mg of gel was used on one column. Next Extraction Buffer was added and mixed by pipetting. The gel was dissolved over 10 min at 50-58°C with inversions to homogenise the solution. Then ethanol (96-100%) was added and mixed. The solution was added onto DNA Purification Micro Columns and centrifuged for 1 min at 14000 x g. The flow-through was discarded and the column was washed with prewash Buffer and centrifuged again. This was repeated twice with Wash Buffer. The column was dried by centrifuging for 1 min at 14000 x g. The column was placed into a new tube and the DNA eluted in 10 µL H<sub>2</sub>O by centrifuging for 1 min at 14000 x g. The DNA was used immediately for the best results. The concentration was determined using a NanoDrop1000.

**2.8.2. Ligation into pCR<sup>TM</sup>4 TOPO<sup>®</sup> and transformation into *E.coli***

The previously purified PCR product was cloned into the pCR<sup>TM</sup>4 TOPO<sup>®</sup> vector. The TOPO TA Cloning<sup>®</sup> Kit for Sequencing (Life Technologies) was used for this. To 4 µl of PCR product 1 µl of Salt Solution and 1 µl of the pCR<sup>TM</sup>4 TOPO<sup>®</sup> vector were added. This was incubated for 30 min at RT. Then 4 µL of the mix was added to 25 µL of One Shot<sup>®</sup> Chemically Competent *E.coli* thawed on ice. After a 30 min incubation on ice the *E.coli* were heat shocked for 30 sec at 42°C and placed back onto ice. To the *E.coli* 250 µL of S.O.C. medium (Life Technologies) was added and they were grown at 37°C in an orbital shaker at 7 x g for 1 h. LB agar plates were prepared with 100 mg/mL of Ampicillin and pre-warmed before the *E.coli* were plated. From the transformed *E.coli* 50-150 µL were plated and grown for 14 h. Colonies were picked and

## Chapter 2: General Materials and Methods

grown in 3 mL sterilised lysogeny broth (LB) [1% peptone, 0.5% yeast extract, 1% NaCl, pH 7.5 (Sigma-Aldrich)] for 12-16 h.

### **2.8.3. Plasmid DNA isolation from *E.coli***

Before plasmids were isolated 500 µL of transformed *E.coli* were frozen away as stocks. For this 500µL of 50% Glycerol (Sigma-Aldrich) were added to the *E.coli* and vortexed. They were then stored at -80°C.

The plasmid DNAs were extracted using the PureYield™ Plasmid Miniprep System (Promega). The plasmid isolation was performed according to the manufacturer's guideline. Briefly, for all centrifugation steps 16900 x g was used. The *E.coli* were pelleted into 1.5 mL tubes in two parts for 30 sec each. The pellet was dissolved in 600 µL of nuclease-free water. Then the cell Lysis Buffer was added and the tubes inverted six times. Then the ice cold Neutralizing Solution was added and mixed by inverting. The cell lysate was centrifuged for 3 min. The supernatant was carefully transferred onto the PureYield™ Minicolumn and centrifuged for 1 min. The flow-through was discarded and the column was washed with the Endotoxin Removal Wash (ERB) and centrifuged for 15 sec, and then washed with Column Wash Solution (CWC) and centrifuged for 30 sec. After discarding the flow-through the column was shortly spun down to remove any remaining liquid. To elute the plasmid 26 µL of nuclease-free water was added and the column incubated at RT for one minute. To elute the plasmids the column was placed into a new tube and centrifuged for 30 sec. The DNA concentration was measured using the NanoDrop1000.

#### **2.8.4. Restriction digest**

To verify that the insert was in the isolated plasmids a restriction digest was performed using the EcoR1 restriction enzyme (Promega) and buffer H (Promega). The reaction mix was prepared (Table 2.12) and digested for 2 h at 37°C. The mix was size separated on a 1% agarose gel to verify the excision of the insert.

**Table 2.12: EcoR1 restriction digest reaction mix.**

	<b>For a 10 µL reaction mix</b>
<b>EcoRI</b>	0.5 µL
<b>10 x Buffer H</b>	1 µL
<b>Nuclease-free water</b>	6 µL
<b>Plasmid DNA</b>	2.5 µL

#### **2.9. Sanger sequencing**

The plasmids were send for DNA sequencing to Source BioScience Lifesciences Services. As by requirement of the company the samples were diluted to 100ng/µL and were sequenced with primers supplied by the company (Table 2.13).

**Table 2.13: Primers used for sequencing.**

	<b>Primer</b>
<b>pCR™4 TOPO® vector</b>	M13 Forward
	M13 Reverse
<b>pcDNA™3.1(-) vector</b>	T7 Forward
	BGH Reverse

#### **2.10. *In-silico* prediction of RNA secondary structure**

Online predictive tools were used to predict the secondary structure folding of HER2, I25HER2 and Δ16HER2 mRNA sequences. The RNAfold web server (<http://rna.tbi.univie.ac.at/>) from the University of Vienna was used for the

## Chapter 2: General Materials and Methods

prediction (Lorenz *et al.*, 2011). The full length mRNA sequences were used excluding the polyA-tail, as the length of it is unknown. Two models were used for prediction the standard minimum free energy (MFE) and the newer centroid prediction model. A stable RNA secondary structure with the lowest energy state is predicted by the MFE model (Zuker and Stiegler, 1981; Lorenz *et al.*, 2011). The algorithm for the centroid model calculates the statistically most likely Boltzmann weighted ensemble of predicted secondary structures. This is informed by structures of comparative sequence analysis (Ding *et al.*, 2005).

## **Chapter 3: Investigating the regulation of the $\Delta$ 16HER2 splicing event**

### **3.1. Introduction**

HER2 is an important growth factor receptor that induces signalling of the PI3K/AKT and the RAS/MAPK pathways, which control cell proliferation, growth and survival as well as cellular metabolism (Roskoski, 2013; Dittrich *et al.*, 2014). HER2 is overexpressed in about ~20% of primary breast cancers, where due to its ability to induce these cellular process it acts as a driver of tumour development and persistence (Slamon *et al.*, 1987; Slamon *et al.*, 1989). The *HER2* gene encodes for a number of alternative splice variants (Jackson *et al.*, 2013). In this chapter the HER2 splice variant  $\Delta$ 16HER2 was investigated. It arises when 48 bp long cassette exon 16 is not recognised during pre-mRNA processing and is spliced out. At the protein level this translates to a HER2 protein variant ( $\Delta$ 16HER2) which lacks 16 amino acids of the extracellular domain (IV) directly preceding the transmembrane domain (Kwong and Hung, 1998; Siegel *et al.*, 1999).  $\Delta$ 16HER2 can be expressed in both normal and cancerous tissues. The relative expression ratio compared to wild type HER2 varies, but generally  $\Delta$ 16HER2 mRNA is a minor transcript making up 2 to 10% of all HER2 transcripts (Siegel *et al.*, 1999; Castiglioni *et al.*, 2006; Turpin *et al.*, 2016). Despite it being a minor transcript, studies have shown  $\Delta$ 16HER2 to be a driver of tumour formation (Mitra *et al.*, 2009; Alajati *et al.*, 2013; Turpin *et al.*, 2016). It has been hypothesized that as a consequence of gene amplification events in breast cancer  $\Delta$ 16HER2 expression might be elevated above a threshold, whereby the splice variant contributes to the progression of the disease (Siegel *et al.*, 1999; Castiglioni *et al.*, 2006).  $\Delta$ 16HER2 has been shown to have a continuously active conformation which promotes homo-dimerization and downstream signalling (Siegel *et al.*, 1999). It has been reported to induce signalling pathways separate from normal wild type HER2 (Alajati *et al.*, 2013). Strong evidence exists that suggests that  $\Delta$ 16HER2 as opposed to wild type HER2 induces tumour formation (Kwong and Hung, 1998; Siegel *et al.*, 1999; Mitra *et al.*, 2009; Sasso *et al.*, 2011). Contradictory results exist on the

importance of  $\Delta$ 16HER2 in the resistance of breast cancer cells to the therapeutic antibody trastuzumab (Mitra *et al.*, 2009; Castagnoli *et al.*, 2014). Initially, *in vitro* studies had shown  $\Delta$ 16HER2 to be resistant to trastuzumab (Mitra *et al.*, 2009), however in *in vivo* studies, in mouse models,  $\Delta$ 16HER2 overexpressing tumours showed an increased susceptibility to trastuzumab therapy (Castagnoli *et al.*, 2014). Using a method to infer  $\Delta$ 16HER2 levels through the expression of its downstream targets (metagene) has been used to study therapy resistance and prognosis in  $\Delta$ 16HER2 positive patients. Through this it was observed that patients with the  $\Delta$ 16HER2 metagene were more likely to respond to trastuzumab treatment (Castagnoli *et al.*, 2014). This effect is likely mediated by trastuzumab causing an immune response against the tumour cells (Bianchini and Gianni, 2014; Triulzi *et al.*, 2016). Research, to date, has focused on defining the role of the oncogenic  $\Delta$ 16HER2 protein in breast cancer progression and drug resistance (Kwong and Hung, 1998; Siegel *et al.*, 1999; Mitra *et al.*, 2009; Sasso *et al.*, 2011; Castagnoli *et al.*, 2014), however the mechanisms that regulate production of  $\Delta$ 16HER2 mRNA and protein have not been investigated.

#### **Link between hormones and alternative splicing**

It is well established that breast cancer is a disease that is influenced by the female sex hormones oestrogen and progesterone (*Breast Cancer, A Lobular Disease*, 2011). Recently, progesterone and PR came back into focus in breast cancer research, because PR was shown to regulate the function of ER- $\alpha$  in favour of a tumour inhibiting signalling pathway (Mohammed *et al.*, 2015). This highlighted the need for further investigations into the role of progesterone and PR in breast cancer biology. Previous studies have reported crosstalk between wild type HER2 and both ER and PR (Beguelin *et al.*, 2010; Diaz Flaque *et al.*, 2013; Giuliano *et al.*, 2013). It has also been shown that oestrogen can affect alternate splicing in breast cancer cell lines, specifically the splicing of the type 1 corticotropin-releasing hormone receptor (Lal *et al.*, 2013). Previous research in our group suggests that oestrogen does not affect *HER2* mRNA expression in breast cancer cell lines (unpublished data). In light of the role that hormones can play in alternative splicing, and the new findings on the roles of

progesterone and PR in breast cancer, we wished to investigate whether progesterone affects *HER2* expression and alternative splicing.

### **3.2. Aims**

The aims of this chapter are to:

- Investigate the mechanisms regulating the  $\Delta$ 16HER2 splicing event
- Identify RNA-binding proteins that bind to the  $\Delta$ 16HER2 splicing region and regulate its splicing
- Identify the regulating RNA sequences of the  $\Delta$ 16HER2 splicing event
- Design and construct a  $\Delta$ 16HER2-minigene
- Investigate a potential feedback loop between HER2 and its splicing regulators
- Study the effect of progesterone on HER2 expression and splicing

### 3.3. Methodology

#### 3.3.1. *In-silico* prediction of the splicing factor binding

Freely available online *in-silico* tools were used to determine RNA-binding proteins that could potentially bind the splicing region of  $\Delta$ 16HER2. The programs that were used are shown in table 3.1. The *in-silico* predictions were performed on the pre-mRNA sequences that were subsequently studied by experimental *in-vitro* approaches (Table 3.2). The sequences studied reached from the last 75 bp of intron 15, over exon 16 to the first 74 bp of intron 16. The software predicted the binding of RNA-binding proteins to protein specific RNA-binding motifs present in the query sequence.

**Table 3.1: *In-silico* prediction tools for splicing factor binding.**

Name	Website
<b>SpliceAid</b>	<a href="http://www.introni.it/splicing.html">http://www.introni.it/splicing.html</a>
<b>Human Splice Finder</b>	<a href="http://www.umd.be/HSF3/HSF.html">http://www.umd.be/HSF3/HSF.html</a>
<b>SFmap</b>	<a href="http://sfmap.technion.ac.il/">http://sfmap.technion.ac.il/</a>

**Table 3.2: The synthesised RNA oligonucleotides.**

Name	Region covered	Synthesised RNA oligonucleotide sequence (exon 16 in red)
<b>H1</b>	Intron 15 (21 bp) – Exon 16 (48 bp) – Intron 16 (14 bp)	AUGAGACUGUUUCUCCUGCAG <b>CUGUGUGGACCU</b> <b>GGA</b> <b>UGACAAGGGCUGCCCCGCCGAGCAGAGAGCCAG</b> GUU GGCCUGGACCC
<b>H2</b>	Intron 15 (75 bp) – Exon 16 (8 bp)	GUUGUUGUGAGGCUGGAAAGGUGGUCCCAAGAGGGU GGUUCCCAGAAUUGUUGAUGAGACUGUUUCUCCUGCA <b>G</b> CUGUGUG <b>G</b>
<b>H3</b>	Exon 16 (9 bp) – Intron 16 (74 bp)	<b>GAGAGCCAG</b> GUUGGCCUGGACCCAGGAUGUACCCU UCAUUGCCCUUCACUCCCCACUGGAUGCUGGGUGG UCACUGCUGUA

### 3.3.2. RNA chromatography assay

To identify RNA-binding proteins that bind the sequence of interest a RNA chromatography assay (RNA-assisted protein pull-down) was performed [adopted from (Michlewski and Caceres, 2010)]. Briefly, single stranded RNA was synthesised that covers the region of interest. This was incubated with nuclear proteins. Stringent washing removed unbound proteins. The RNAs are digested and the previously RNA bound proteins collected (Figure 3.1). These were separated out on a SDS-PAGE from which protein bands of interest were cut out and sent for mass spectrometry. In addition these protein extracts were applied in a western blot experiment to validate the identity of the RNA-binding proteins.

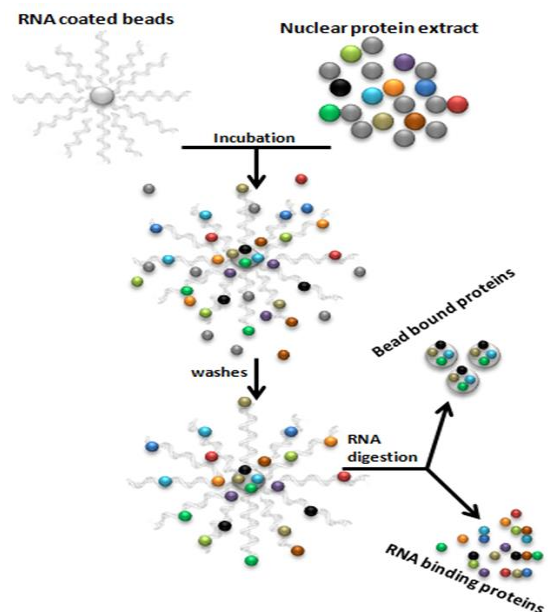


**Figure 3.1: The schematic depiction of the RNA chromatography assay.**

Agarose beads coated with single stranded RNAs were incubated with a nuclear protein extract. This is followed by stringent washing. The RNA is digested and the previously RNA bound proteins can be collected separately from proteins that bound the agarose beads.

#### Nuclear protein extract

Nuclear proteins were extracted from SKBR3 breast cancer cells as a protein source for the RNA chromatography assay. These cells were used as they express all known HER2 splice variants. The nuclear protein extract is also a highly enriched source of nuclear RNA-binding proteins.

Three 75 cm<sup>2</sup> flasks of SKBR3 cells near confluency were used. The cells were washed with ice cold PBS and then collected by scraping into PBS. The cell suspension was centrifuged at 173 x g for 5 min at 4°C. The cell pellet was re-suspended in 500  $\mu$ L of Buffer A (10 mM HEPES pH 7.9, 1.5 mM MgCl<sub>2</sub>, 10 mM

### Chapter 3: Investigating the regulation of the $\Delta$ 16HER2 splicing event

KCl, 0.5 mM DTT, 5  $\mu$ L/mL protease inhibitor cocktail in H<sub>2</sub>O) and incubated for 15 min on ice. NP-40 substitute was added to the cell lysate to give a final concentration of 0.5% and then vortexed for 10 sec. The cell lysate was centrifuged at 4487 x g for 1 min. This centrifuged the nuclei into a pellet. The supernatant could be recovered as cytoplasmic cell lysate fraction and stored at -80°C. The nuclear pellet was re-suspended in 150  $\mu$ L of Buffer C (20 mM HEPES pH 7.9, 1.5 mM MgCl<sub>2</sub>, 420 mM NaCl, 0.2 mM EDTA, 25% (V/V) Glycerol, 5  $\mu$ L/mL protease inhibitor cocktail in H<sub>2</sub>O) and incubated for 30 min at 4°C under vigorous agitation. The nuclear lysate was centrifuged at 15294 x g for 10 min at 4°C. The supernatant, the nuclear fraction, was recovered and stored at -80°C until use.

#### **RNA synthesis**

Three DNA templates were designed for the synthesis of RNA single strands that correspond to the splicing region of interest (Table 3.2). Table 3.3 shows the DNA templates with the T7 promoter sequence (indicated in bold). These were annealed to DNA oligonucleotides that contained the complementary sequence to the T7 promoter in a 2:1 ratio. The reaction was performed in an annealing buffer (10 mM Tris, pH 7.5 - 8.0, 50 mM NaCl, 1 mM EDTA). Annealing was undertaken by heating the reaction mix up to 95°C and slowly cooling down to room temperature. RNA was synthesised by overnight *in-vitro* transcription with T7 RNA polymerase (New England Biolabs). The manufacturer's protocol was adapted; 3  $\mu$ L of DNA template mix were added to the reaction mix (Table 3.4) and incubated overnight at 37°C. The template DNA was degraded by TURBO™ DNase (Ambion) for 30 min at 37°C and the RNA was purified by phenol-chloroform extraction.

**Table 3.3: DNA oligonucleotide for RNA synthesis.**

Name	DNA oligonucleotide for RNA synthesis
H1	GGGTCCAGGCCAACCTGGCTCTCTGCTCGGCGGGGCAGCCCTTGTCATCC AGGTCCACACAGCTGCAGGAGAAACAGTCTCATT <b>TATAGTGAGTCGTATTA</b>
H2	CCACACAGCTGCAGGAGAAACAGTCTCATCAACAATTCTGGGAACCAACCCT CTTGGGAACCAACCTTTCCAGCCTCACAACA <b>ACTTATAGTGAGTCGTATTA</b>
H3	TACAGCAGTGACCACCCAGCATCCAGTGGGGGAGTGAAGGGCAATGAAGG GTACATCCTGGGGTCCAGGCCAACCTGGCTCT <b>TATAGTGAGTCGTATTA</b>

**Table 3.4: T7 RNA polymerase reaction mix (New England Biolabs).**

	<b>Total volume of 40 <math>\mu</math>L</b>
<b>DNA template mix</b>	3 $\mu$ L
<b>10 x T7 Polymerase Buffer (New England Biolabs)</b>	4 $\mu$ L
<b>25 mM NTP mix (Thermo Scientific)</b>	0.8 $\mu$ L
<b>RNaseOUT (Ambion)</b>	2 $\mu$ L
<b>T7 RNA Polymerase (New England Biolabs)</b>	4 $\mu$ L
<b>RNase-free water</b>	26.2 $\mu$ L

### **Phenol-chloroform extraction**

To purify the RNA, 230  $\mu$ L RNase-free water and 30  $\mu$ L Ammonium Acetate Stop Solution (5 M Ammonium acetate, 100mM EDTA in RNase-free water) were added to the RNA and mixed. An equal volume of Phenol:Chloroform 5:1 (Sigma Aldrich) was added and mixed by vortexing. The RNA mix was then centrifuged at 14000 x g for 5 min at 4°C. The upper aqueous phase was recovered and an equal volume of chloroform (Sigma Aldrich) was added. After vortexing, the mix was centrifuged at 14000 x g for 5 min at 4°C. The upper aqueous phase was recovered and one volume of 2-propanol (Sigma Aldrich) was added. After mixing, the 2-propanol-RNA mix was incubated for 30 min at -20°C. This was followed by a 15 min 16900 x g centrifugation step at 4°C. The supernatant was removed and the pellet washed with 70% ice cold ethanol. This was followed by centrifugation at 16900 x g for 15 min at 4°C. The ethanol was removed and the pellet air dried for 15 min. The pellet was then resuspended in 11  $\mu$ L of RNase-free water.

### **RNA chromatography**

For the RNA chromatography 1 nmole of each synthesized RNA was used. The RNA was prepared by adding 360  $\mu$ l 5 mM sodium-m-periodate solution (Sigma Aldrich) in 0.1 M sodium acetate (NaOAc) pH 5 to maximum of 40  $\mu$ L of RNA. RNase-free water was added for a final volume of 400  $\mu$ L. The mix was incubated for 1 h in the dark on a rotator. Next the RNA was ethanol precipitated. For this 1/10 volume 3M NaOAc (pH 5.2) and 2.5 volumes 100%

### Chapter 3: Investigating the regulation of the $\Delta$ 16HER2 splicing event

ethanol were added to the RNA. The RNA mix was incubated at  $-80^{\circ}\text{C}$  for 2 h. Next the RNA mix was centrifuged at  $16900 \times g$  for 30 min at  $4^{\circ}\text{C}$ . The supernatant was removed and 1 mL of ethanol was added to the RNA pellet. The pellet was centrifuged at  $16900 \times g$  for 5 minutes at  $4^{\circ}\text{C}$ . Then the ethanol was removed and the pellet air dried for 15 min. At last the RNA was resuspended in 100  $\mu\text{L}$  of 0.1 M NaOAc pH 5.

Adipic dihydrazide agarose beads 50% (Sigma Aldrich) were prepared for incubation with the RNA. 100  $\mu\text{L}$  of beads per RNA were washed four times with 10 mL 0.1 M NaOAc pH5. Finally the beads were resuspended in 300  $\mu\text{L}$  0.1 M NaOAc pH 5. A RNA-free control was also included. The RNA or control were incubated with the beads overnight at  $4^{\circ}\text{C}$  on a rotator. The following day the bead-RNA mix was washed three times with 2 M KCl by incubating on a rotator for 5 min and centrifuging at  $3824 \times g$  for 5 min. This was followed by four washes with Buffer D (20 mM Tris HCl (pH 8), 20% (V/V) Glycerol, 0.1 M KCl, 0.2 mM EDTA, 0.5 mM DTT, 0.2 mM PMSF in  $\text{H}_2\text{O}$ ). Then 300  $\mu\text{L}$  nuclear protein extract mix (40% nuclear proteins, 1.5 mM  $\text{MgCl}_2$ , 5 mM ATP in RNase-free water) was added and incubated for 30 min at  $37^{\circ}\text{C}$ . To remove any unbound proteins the mix was washed four times with Buffer D with added 1.5 mM  $\text{MgCl}_2$ . Additionally, the Bead-RNA mix was washed twice with nuclease-free water. The beads were then incubated with an RNase reaction mix (10 mM 0.1 Tris HCl (pH 7.2), 1 mM  $\text{MgCl}_2$ , 40 mM NaCl, 8.33% A/T1 RNase (Ambion)) for 30 min at  $37^{\circ}\text{C}$  and mixed to digest the RNA. The supernatant containing the now unbound proteins was collected and denatured with 30  $\mu\text{L}$  of 2 x SDS lysis buffer/loading dye at  $95^{\circ}\text{C}$  for 10 min.

The collected proteins were separated on a 4-12% NuPage pre-cast polyacrylamide gel (Invitrogen, Life Technologies) alongside the PageRuler™ Prestained protein ladder and 10  $\mu\text{L}$  of nuclear protein. SimplyBlue Safestain (Invitrogen, Life Technologies) was used to visualise the protein bands after size separation. Bands up to the size of  $\sim 100\text{kDa}$  were excised and sent for Mass spectrometry (Prof Gary Black and Andrew Porter at Northumbria University). The RNA chromatography was repeated and used for Western blotting as described previously.

### 3.3.3. $\Delta 16\text{HER2}$ -minigene construction

A minigene is a manipulable experimental system which can be used to study the regulation of splicing. A  $\Delta 16\text{HER2}$ -minigene was designed and constructed by cloning the splicing region of  $\Delta 16\text{HER2}$  into the pcDNA3.1- expression plasmid. It was not possible to clone the whole region from intron 14 to exon 18 into the vector, due to the size of intron 15 (2306 bp) and intron 16 (3484 bp). Therefore three fragments were generated and cloned into pcDNA<sup>TM</sup> 3.1- (Figure 3.2).

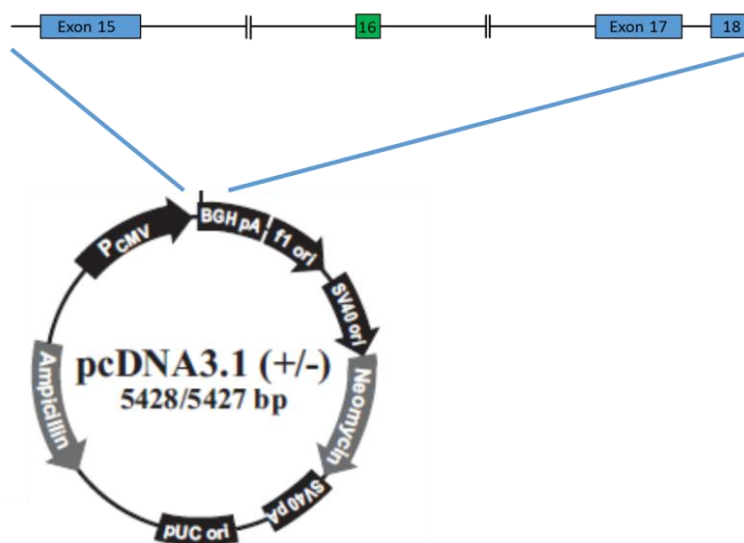


**Figure 3.2: The design of  $\Delta 16\text{HER2}$ -minigene.**

The  $\Delta 16\text{HER2}$  splicing region was cloned into the pcDNA3.1- vector in three parts. The large middle parts of the two introns are not included in the  $\Delta 16\text{HER2}$ -minigene.

The fragments were labelled MG15, MG16 and MG17. They contained the following regions:

- MG15 contains 76 bp of intron 14, the whole exon 15 (161 bp) and 191 bp of the beginning of intron 15.
- MG16 contains 285 bp of the end of intron 15, exon 16 (48 bp) and 263bp of the beginning of intron 16.
- MG17 contains 272 bp of the end of intron 16, exon 17 (139 bp), intron 17 (80 bp) and exon 18 (137 bp).

#### **Amplification and cloning of $\Delta 16\text{HER2}$ -minigene fragments**

Genomic DNA (isolated by PhD student Marco Silipo) from SKBR3 cells was used in PCRs to amplify the above described regions. The primers used are listed in table 3.5.

Chapter 3: Investigating the regulation of the  $\Delta$ 16HER2 splicing event

**Table 3.5: List of  $\Delta$ 16HER2-minigene primers.**

Primer name	Restriction site	Sequence
AL_MG_F15 in intron 14	NheI	<u>GCTAGCCCCAACTAAGGGCCTGATCC</u>
AL_MG_R15 in intron 15	XbaI	<u>TCTAGATTAACAGTGGGGATAGAAGCTGCT</u>
AL_MG_F16 in intron 15	XbaI	<u>TCTAGAGAGGGGAATAGTTGAGCTCCCG</u>
AL_MG_R16 in intron 16	XhoI	<u>CTCGAGTGTGTCCCTCACAAGGCATC</u>
AL_MG_F17 in intron 16	XhoI	<u>CTCGAGATTGTTGAAGCCCTAAGCCAGAG</u>
AL_MG_R17 in exon 18	HindIII	<u>AAGCTTGACCTGGCCCTGACCTTGTAG</u>
AL_MG_Plasmid_R		CTTCCAGGGTCAAGGAAGGC

A Platinum Taq High Fidelity Polymerase (Invitrogen) was used to ensure amplification without mutations. The PCR was performed according to the manufacturer's instructions on a BioRad thermocycler (Table 3.6). The product was run out on a 2% agarose gel with ethidium bromide for visualization. The bands were excised and a gel elution step was performed to recover the PCR product from the gel. The GeneJet gel extraction and DNA clean up Micro kit (Thermo Scientific) was used for PCR product recovery (see chapter 2.8.1).

**Table 3.6: Platinum Tag PCR Reaction for Minigene segments.**

Reaction mix components	Volume for a 50 $\mu$ L reaction
10 x High Fidelity PCR Buffer	5 $\mu$ L
50 mM MgSO <sub>4</sub>	2 $\mu$ L
25 mM dNTP mix	0.4 $\mu$ L
Primer Frw./Rev. (10 $\mu$ M)	each 1 $\mu$ L
Genomic DNA	500 ng
Platinum Taq DNA polymerase High Fidelity	0.2 $\mu$ L
Nuclease-free water	Fill up to 50 $\mu$ L

PCR program:

94°C	1 min	
94°C	15 sec	} 35 cycles
55°C	30 sec	
68°C	30 sec	
12°C	$\infty$	

### Chapter 3: Investigating the regulation of the $\Delta$ 16HER2 splicing event

The isolated PCR product was cloned into pCR<sup>TM</sup>4-TOPO<sup>®</sup> vector and transfected into competent *E.coli* as described before in section 2.8.1. Transformed *E.coli* were plated on agar plates with ampicillin, colonies were picked after ~12 h and grown in LB media with ampicillin (see section 2.8.2). The plasmids were isolated with the PureYield<sup>TM</sup> Plasmid Miniprep System and 100 ng/ $\mu$ l plasmid DNA was sent for sequencing to Source BioScience Lifesciences Services (see section 2.9).

#### **Assembly of the $\Delta$ 16HER2-minigene**

The three  $\Delta$ 16HER2-minigene fragments were digested out of the pCR<sup>TM</sup>4-TOPO<sup>®</sup> vector with the appropriate enzymes and buffers (Promega) at 37°C for 2-3 h (Table 3.7). The digested  $\Delta$ 16HER2-minigene fragments were size separated on a 1% agarose gel and gel eluted (see section 2.8.1). At the same time the pcDNA<sup>TM</sup> 3.1(-) vector was digested with the same restriction enzymes, so that the  $\Delta$ 16HER2-minigene fragment could be ligated in. The digested pcDNA<sup>TM</sup> 3.1(-) was also size separated and the appropriate band of the double digested vector was gel eluted.

As the restriction sites of MG15 NheI and XbaI produce compatible ends, they had to be treated with CIP (alkaline phosphatase, calf intestinal) (New England BioLabs) to prevent self-ligation of the vector. After digestion, the heat inactivation was performed at 65°C for 20 min. To 20  $\mu$ L of vector for the  $\Delta$ 16HER2-minigene fragment 1  $\mu$ L of CIP was added and incubated for 10 min at 37°C. Again the product was size separated and gel eluted.

**Table 3.7: Restriction digestion for the  $\Delta$ 16HER2-minigene fragment.**

<b><math>\Delta</math>16HER2-minigene fragment</b>	<b>Restriction enzymes</b>	<b>Restriction enzyme buffer</b>
<b>MG15</b>	NheI and XbaI	10 x CutSmart Buffer (NEB)
<b>MG16</b>	XbaI and XhoI	10 x Buffer H
<b>MG17</b>	XhoI and HindIII	10 x Buffer C

### Ligation with T4 (5U) Ligase (Invitrogen)

The reaction was performed according to the manufacturer's guidelines. A 3:1 vector to insert ratio was used. The reaction was performed at RT for 1-2 h. 5U of T4 ligase per 20  $\mu$ L reaction was used. Of the ligation product 2  $\mu$ L were used to transform 25  $\mu$ L of *E.coli*. The transformed *E.coli* were plated on ampicillin containing agar plates, colonies were picked the next day and grown in LB media with ampicillin. The plasmids were isolated with the PureYield™ Plasmid Miniprep System and sent for sequencing to Source BioScience Lifesciences Services. For details see sections 2.8.2, 2.8.3 and 2.9.

Sequentially all  $\Delta$ 16HER2-minigene fragments were cloned into the same pcDNA™ 3.1(-) backbone. The end product was sent for sequencing. The clone MG-3 was shown to contain all  $\Delta$ 16HER2-minigene fragments in the correct orientation.

#### 3.3.4. Site-directed mutagenesis v.1 on $\Delta$ 16HER2-minigene

Site-directed mutagenesis was performed on the  $\Delta$ 16HER2-minigene to identify the binding site of RNA-binding proteins. For this the Q5 site-directed mutagenesis kit (New England Biolabs) was used. Primers were designed using the base changer web tool (<http://nebasechanger.neb.com/>) as suggested by the kit manufacturer. The reactions were performed as suggested by the manufacturer. Three site directed mutations were performed (Table 3.8). Briefly, a PCR was performed using the  $\Delta$ 16HER2-minigene as DNA template (Table 3.9) and the primers listed in table 3.6.

**Table 3.8: Primers for site directed mutagenesis.**

	<b>Forward Primer</b>	<b>Reverse Primer</b>	<b>T(An) °C</b>
<b>MGMut-2</b>	GGAGTATTTACGGTAAACTG	TTGACGTCAATGGAAAGTC	59
<b>MGMut-4</b>	CCAGGATGTAcgcttgATTGCCCTTCAC	GGTCCAGGCCAACCTGGC	69
<b>MGMut-5</b>	TGGTTCCCAAtagcGTGGTTCCCAG	CCTTCCAGCCTCACAAC	63

### Chapter 3: Investigating the regulation of the $\Delta$ 16HER2 splicing event

Table 3.9: Q5<sup>®</sup> site-directed mutagenesis reaction.

Reaction mix components	Volume for a 25 $\mu$ L reaction
Q5 Hot Start High-Fidelity 2x Master Mix	12.5 $\mu$ L
10 $\mu$ M Forward/Reverse Primer	1.25 $\mu$ L each
Template DNA - $\Delta$ 16HER2-minigene (10ng/ $\mu$ l)	1 $\mu$ L
Nuclease-free water	9 $\mu$ L

#### PCR program:

98°C	30 sec		
98°C	10 sec	}	25 cycles
x °C	30 sec		
72°C	3.5 min		
72°C	2 min		
10°C	$\infty$		

Following the PCR reaction 1  $\mu$ L of the PCR product was used in a reaction which causes the linear mutated  $\Delta$ 16HER2-minigene to be ligated into a circular plasmid. It also causes the degradation of any remaining original DNA template. To the PCR product 5  $\mu$ L 2x KLD Reaction Buffer, 1  $\mu$ L 10x KLD Enzyme Mix and 3  $\mu$ L nuclease-free water was added, mixed and incubated for 5 minutes at RT. A vial of NEB 5-alpha Competent *E.coli* cells was thawed on ice and half of the enzyme reaction was added to the cells. After 30 min incubation on ice the cells were heat shocked for 30 sec at 45°C. After a further 5 min on ice 950  $\mu$ L SOC medium was added to the cells and they were then incubated at 37°C and 220 rpm shaking for 1 h. 100-200  $\mu$ L of the transformed *E.coli* were then plated on ampicillin containing agar plates. After overnight incubation colonies were picked and grown in ampicillin containing LB medium for 6-14 h. Plasmid isolation was performed using the PureYield<sup>™</sup> Plasmid Miniprep System. For details see sections 2.8.2, 2.8.3 and 2.9. 100 ng/ $\mu$ l plasmid DNA was send for sequencing to Source BioScience Lifesciences Services. Initially, T7 forward and BGH reverse primers were requested to be used for the sequencing of the mutated  $\Delta$ 16HER2-minigene. Recurrent issues with incomplete or failed sequencing reactions led us to use the dGTP chemistry in the sequencing

reactions for MGMut6. The dGTP chemistry produced improved sequencing results on samples that could not be sequenced using the conventional method.

### 3.3.5. Site-directed mutagenesis v.2 on $\Delta 16\text{HER2}$ -minigene

As the site-directed mutagenesis v.1 had a high percentage rate of unspecific mutations an alternative approach was used for MGMut-6. Overlapping primers were designed with the desired mutation embedded in them. The MGMut-6 forward primer was used in combination with the MG16 reverse primer, and the MG16 forward primer with the MGMut-6 reverse primer to amplify the MG16 region of the  $\Delta 16\text{HER2}$  minigene region while incorporating the point mutations. For the PCR the *Pfu* DNA Polymerase (Promega) was used (Table 3.10).

**Table 3.10: *Pfu* DNA polymerase site-directed mutagenesis reaction.**

Reaction mix components	Volume for a 50 $\mu\text{L}$ reaction
<i>Pfu</i> DNA Polymerase 10x Buffer with $\text{MgSO}_4$	5 $\mu\text{L}$
25 mM dNTP mix	4 $\mu\text{L}$
Forward/Reverse Primer (0.5 $\mu\text{g}/\mu\text{L}$ )	0.25 $\mu\text{L}$
DNA Template	200 ng
<i>Pfu</i> DNA Polymerase	1.25 $\mu\text{L}$
Nuclease-free water	Fill up to 50 $\mu\text{L}$

#### PCR program:

95°C	1.5 min		
95°C	1 min	}	35 cycles
55°C	30 sec		
72°C	1.50 min		
72°C	5 min		
12°C	$\infty$		

The PCR products were run out on a 1% agarose gel and gel extracted (section 2.8.1). To combine the two PCR products into the full MG16 fragment another PCR was performed. The PCR reaction was performed using the *Pfu* DNA

### Chapter 3: Investigating the regulation of the $\Delta$ 16HER2 splicing event

Polymerase. The same reaction mix as described above was prepared, with 375 ng of DNA from each PCR reaction. Initially no primers were added. The PCR program was run for 5 cycles with a 45 sec annealing period and 2 min elongation. Then 0.25  $\mu$ L of the forward and reverse primer MG16 were added and the PCR run for an additional 15 cycles with a 30 sec annealing period.

The PCR product was run out on a 1% gel and a gel extraction was performed. 1  $\mu$ g of the  $\Delta$ 16HER2-minigene was digested with the restriction enzymes XhoI and XbaI (see sections 2.8.4 and 3.3.3 for details). The digested  $\Delta$ 16HER2-minigene was size separated on a 1% gel and gel extracted. The mutated fragment was inserted into the  $\Delta$ 16HER2-minigene by T4 ligation (see section 3.3.3 Ligation with T4 (5U) Ligase for details).

Competent *E.coli* were transfected with the ligation product and plated on ampicillin containing agar plates. After overnight incubation colonies were picked and grown in ampicillin containing LB medium. The plasmids were isolated with the PureYield™ Plasmid Miniprep System. For details see sections 2.8.2, 2.8.3 and 2.9. 100 ng/ $\mu$ l plasmid DNA was send for sequencing to Source BioScience Lifesciences Services. As the basic sequencing reaction using the T7 forward primer and BGH reverse primer have yielded a high number of incomplete or failed sequencing reactions, the MG16 forward primer was used. The  $\Delta$ 16HER2-minigene has been sequenced previously and the length of the mutated MG16 fragment was expected to be covered by a single sequencing reaction.

#### PCR program:

95°C	1 min		
95°C	30 sec	}	5/15 cycles
55°C	45/30 sec		
72°C	1.50 min		
72°C	5 min		
12°C	$\infty$		

**3.3.6. Transfection of the  $\Delta$ 16HER2-minigene with and without transient splicing factor knockdown**

The  $\Delta$ 16HER2-minigene or mutants of it (described in 3.3.5) were transfected into breast cancer cells. For this  $7 \times 10^4$  MCF-7 or SKBR3 cells/well were seeded onto 12 well plates. After 24 h they were transfected using FuGeneHD Transfection reagent (Promega). The transfection was performed according to the manufacturer's guidelines. Briefly, the experiment was scaled up to 10 x 96 well plate reaction size. 350 ng of plasmid DNA was added to Opti-MEM<sup>®</sup> medium and mixed. Then 1.5  $\mu$ L of the transfection reagent was added and mixed. The total reaction volume was 20  $\mu$ L. The mix was incubated for 10 min at RT and then added to the cells. The plates were swirled to promote even distribution of the transfection mix. The medium on the cells was not exchanged. The RNA was collected 24 h after transfection of the  $\Delta$ 16HER2-minigene.

To determine if the previously identified splicing factors affect the  $\Delta$ 16HER2-minigene, the splicing factors were transiently knocked down by RNAi followed by  $\Delta$ 16HER2-minigene transfection. The knockdown was prepared as described previously (section 2.2.5.). On day 2 after the siRNA transfection the minigene was transfected (see above). RNA was isolated 24 h later (see 2.5.1).

**3.3.7. Treatment of SKBR3 cells with lapatinib**

To study the effects of HER2 signalling inhibition HER2 overexpressing SKBR3 cells were treated with the HER2 tyrosine kinase inhibitor lapatinib. Lapatinib was dissolved in DMSO and diluted to a 1mM stock solution. On 12 well plates  $1.5 \times 10^5$  SKBR3 cells/well were seeded. After 24 h the treatment was performed. The cells were treated with 1  $\mu$ M lapatinib, and control cells for each time point were treated with an equal volume of DMSO. Proteins were collected after 15 min, 6 h, 12 h and 24 h. For the 15 min time point a control of untreated cells was also collected. Three independent experiments were carried out. The proteins were used in western blot experiments to study the effect of the

treatment on protein levels and phosphorylation status (see section 2.7.4). To measure and compare the band intensities densitometry was performed on the western blots of all three experiments (time points 6 h - 24 h). The ImageJ program (National institute of Health) was used. GAPDH was used for normalisation and for each time point the DMSO control was set to one.

### **3.3.8. Treatment of cells with progesterone**

For the treatment of cells with progesterone,  $1.4 \times 10^5$  MCF-7 cells/well were seeded in 6 well cell culture plates and grown for ~ 26 h. The medium was exchanged for serum-free phenol-free DMEM medium 14 h before treatment. Complete DMEM medium as described previously supplemented with 10% charcoal stripped FCS (Life Technologies) instead of normal FCS was used in the next step. Normal FCS contains hormones that could mask the effect of the progesterone treatment. Therefore the charcoal stripped FCS was used. Progesterone (Sigma-Aldrich) was dissolved in 100% ethanol for stock concentrations of 1  $\mu$ M, 10  $\mu$ M and 100  $\mu$ M. From these appropriate amounts were added to the culturing medium for final concentrations of 1 nM, 10 nM and 100 nM. Control cells were treated with the vehicle ethanol alone. Three independent experiments were carried out. Cell lysate was collected after 3, 6, 12 or 24 h depending on the experiment and RNA was isolated (see section 2.5.1). Reverse transcription and qPCR was performed as previously described in section 2.6.

### **3.3.9. Statistical analysis**

Different statistical analyses were used depending on experiments. GraphPad Prism 6 was used for all statistical analyses. For the transient knockdown experiments paired t-tests between specific gene knockdowns and the negative controls were performed. For the progesterone dose response experiment one way ANOVA with Dunnett's multiple comparisons tests and for the time line experiment one way ANOVA with Sidak's multiple comparisons tests were performed. The mean of 3 experiments with +/- standard deviation is indicated. Statistical significance is shown as, \*  $\leq 0.05$ , \*\*  $\leq 0.01$ , \*\*\*  $\leq 0.001$ .

### 3.4. Results

#### 3.4.1. Describing the $\Delta 16$ HER2 mRNA transcript

$\Delta 16$ HER2 had first been described in the late 1990s (Kwong and Hung, 1998; Siegel *et al.*, 1999) and has since been studied by a number of research groups in regards to its function in breast cancer (Castiglioni *et al.*, 2006; Mitra *et al.*, 2009; Sasso *et al.*, 2011; Alajati *et al.*, 2013; Castagnoli *et al.*, 2014). Little is known, however, about the processing of the  $\Delta 16$ HER2 mRNA. Searching genome browser (<http://ucscbrowser.genap.ca>), NCBI AceView (<http://ncbi.nlm.nih.gov/IEB/Research/Acembly/index.html>) and Ensembl (<http://www.ensembl.org>) one cannot find any mRNA transcripts corresponding to  $\Delta 16$ HER2. Only one transcript shows exon 16 skipping, but this consists of only 6 exons (Ensembl: Erbb2-018). We therefore wished to verify that exon 16 skipping is part of a full length HER2 transcript.

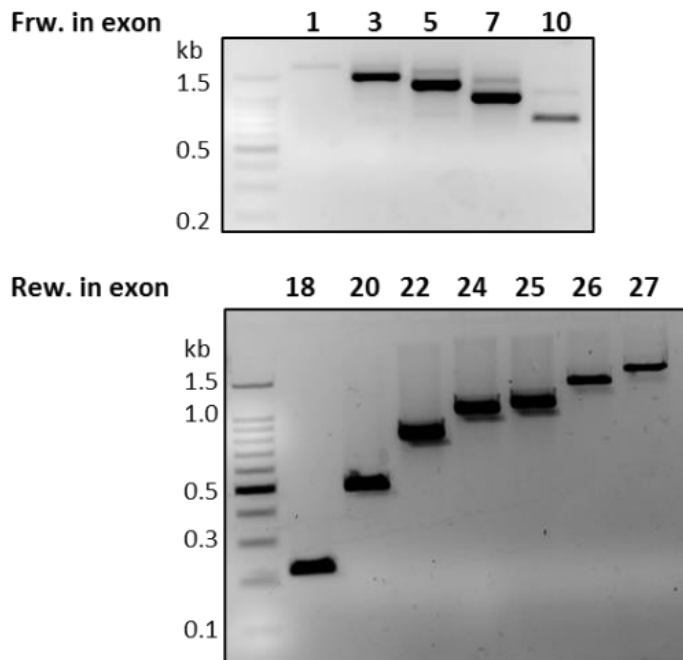


**Figure 3.3: The exon 16 skipping event as part of a full length HER2 mRNA transcript.**

The gel images show the products from PCRs with primers specific for exon 16 skipping in combination with primers specific for up and downstream exons. Exon 27 being the last exon of the HER2.

### Chapter 3: Investigating the regulation of the $\Delta 16$ HER2 splicing event

To verify the exact exon usage for  $\Delta 16$ HER2 in SKBR3 cells, a PCR based approach was used. It could be observed, using primers specific for the exon skipping event in combination with forward and reverse primers in up- and down-stream exons, that exon 16 skipping is part of a transcript spanning conventional exon 3 to exon 27. Only a very faint line appears when amplifying from exon 1 to exon 16 skipping. A very faint additional band can be observed when amplifying from exons 5, 7 or 10 to exon 16 skipping (Figure 3.3). This is thought to be caused by intron 12 retention. An event that was observed by fellow PhD student Marco Silipo.

It is difficult to predict the impact of the presence or absence of exon 16 on the processing of the HER2 mRNA transcript. *In-vivo* mRNAs are assembled into a complex with several hundred proteins. This complex formation determines the processing of the mRNA. Predicting this is nearly impossible, without knowing the proteins involved. To gain some insight into how wild type HER2 and  $\Delta 16$ HER2 might be differentially processed an *in-silico* mRNA secondary structure prediction was performed using both the standard minimum free energy (MFE) and the newer centroid prediction model from Vienna RNA Package 2 (Lorenz et al., 2011).

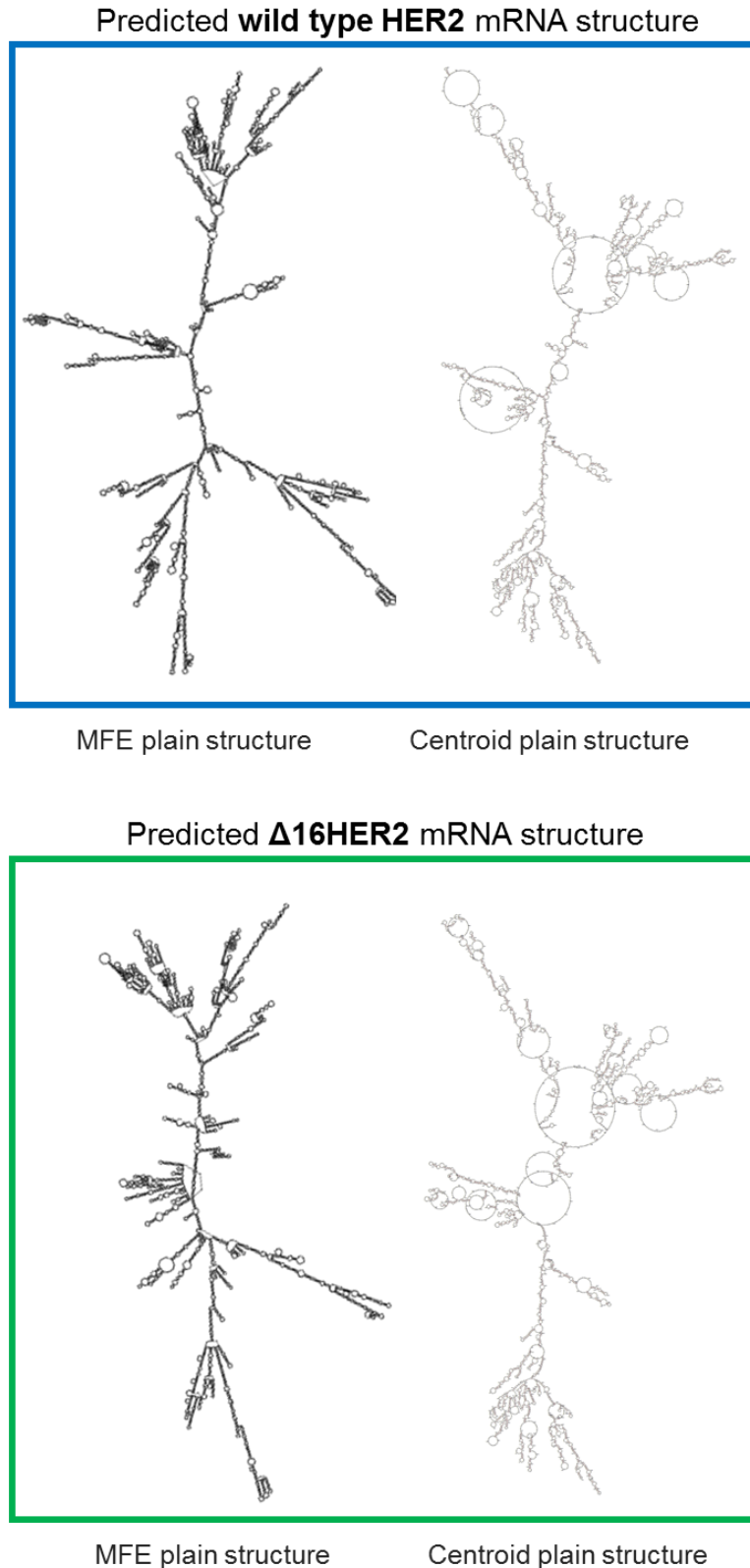


**Figure 3.4:** *In-silico* predicted secondary structure of wild type HER2 and  $\Delta 16\text{HER2}$  mRNA.

The predicted secondary structure is shown for the full length mRNA transcripts (lacking the poly A tail). Predictions from two methods are shown the minimum free energy (MFE) plain and the centroid plain. Images were generated by the RNAfold web server (Lorenz *et al.*, 2011).

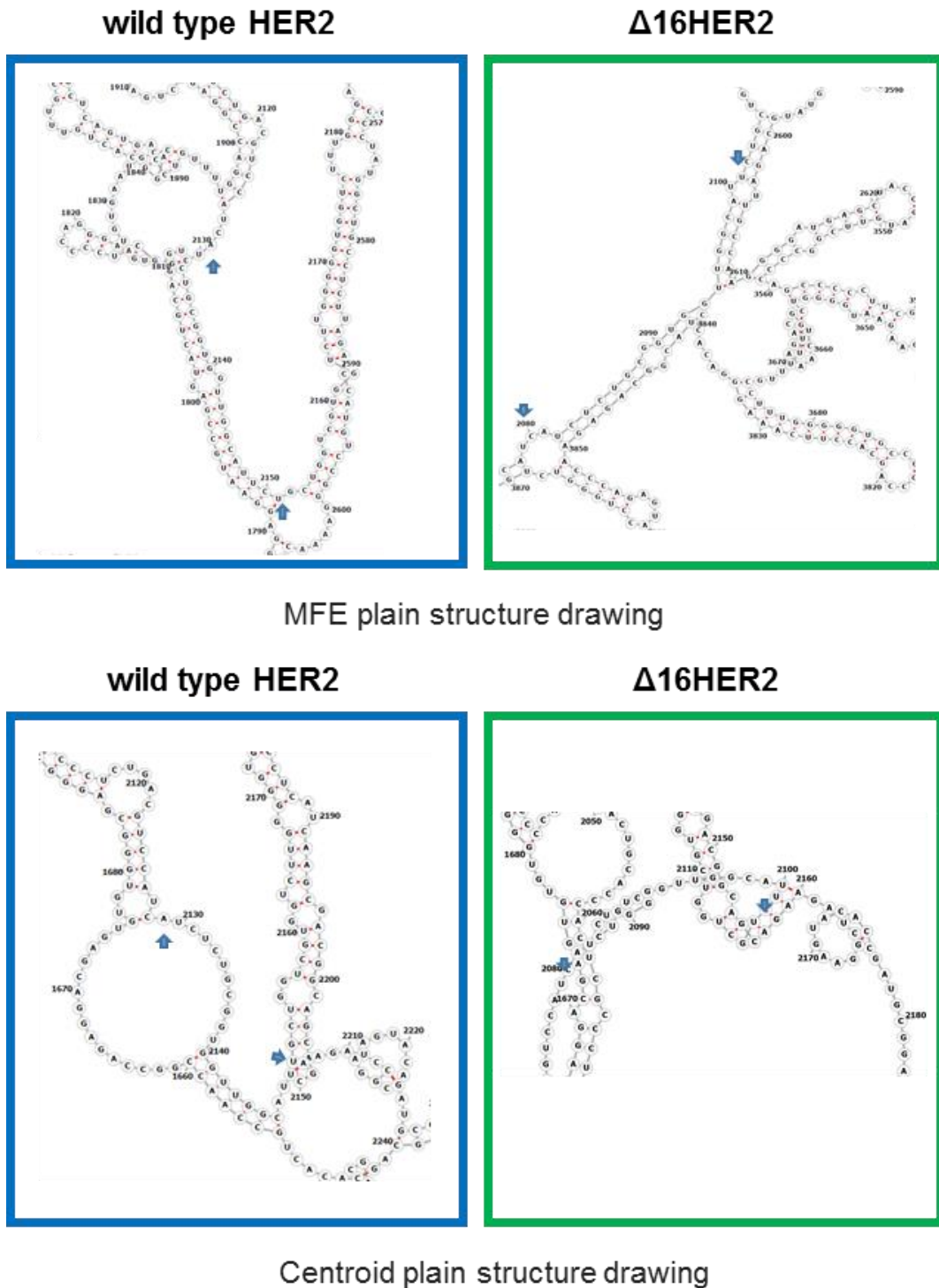


**Figure 3.5:** *In-silico* predicted secondary structure of wild type HER2 and  $\Delta 16$ HER2 mRNA, focus on miRNA-155 binding site.

Magnification of predicted secondary structures of wild type HER2 and  $\Delta 16$ HER2 are shown. The upper panels shows the minimum free energy (MFE) plain predictions and the lower panels the centroid plain predictions. The binding sequence of miRNA-155 on exon 17 is indicated by the arrows. The arrows show the first and last nucleotide of the binding sequence. Images were generated by the RNAfold web server (Lorenz *et al.*, 2011).

The conventional MFE model is based on algorithms that calculate a stable RNA secondary structure with the lowest energy state (Zuker and Stiegler, 1981; Lorenz *et al.*, 2011). The centroid model is generated by an algorithm that produces the statistically most likely Boltzmann weighted ensemble of predicted secondary structures. Predictions are informed by structures determined from comparative sequence analysis. This method has shown under certain circumstances to have an increased probability to predict the correct secondary structure of a RNA with less errors (Ding *et al.*, 2005). As it is not known how long the poly(A)-tail is, this could not be taken into consideration when performing the prediction. The predictions from both models showed that the presence/absence of exon 16 affects the overall secondary structure of *HER2* mRNA (Figure 3.4). The MFE model shows a higher number of branches and loops for  $\Delta 16$ HER2. The centroid model shows a lesser number of changes to the secondary structure, but not a less complex alteration.

Recently a publication described the binding site of miRNA-155 within the coding region of the *HER2* mRNA (He *et al.*, 2016), this binding site is located in exon 17 of *HER2*, within few nucleotides of exon 16. Both models predicted the secondary structures of the binding site to be structurally different between wild type *HER2* and  $\Delta 16$ HER2 (Figure 3.5). The centroid plain prediction for  $\Delta 16$ HER2 shows the binding site sequence to be located on a large loop, but broken up by number of pseudoknots and single nucleotide interactions. Additional loping of the different structures makes this predicted secondary structure very different and potentially hard to access (Figure 3.5).

#### **3.4.2. *In-silico* predictions for the regulation of $\Delta 16$ HER2 splicing**

To study the binding of RNA-binding proteins to the  $\Delta 16$ HER2 splicing region *in-silico* predictions were performed. The predictions were performed on the three sequences that were subsequently used for the experimental identification of RNA-binding proteins that bind the  $\Delta 16$ HER2 splicing region (see 3.3.1 and figure 3.6).

### Chapter 3: Investigating the regulation of the $\Delta$ 16HER2 splicing event

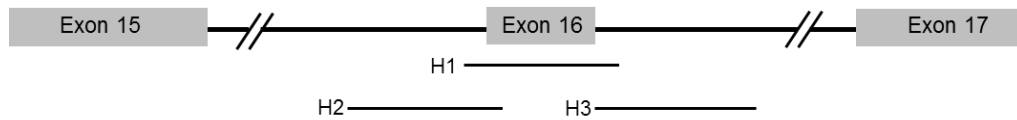


**Figure 3.6: The three sequences covering the  $\Delta$ 16HER2 splicing region: H1, H2, H3.**

Table 3.11 shows the initial predictions of RNA-binding proteins that were predicted to bind the region of  $\Delta$ 16HER2 splicing. Overall 30 proteins were predicted to bind this region. When comparing the predictions only few overlap at least partially, close to none overlap fully with all three programs. Figure 3.7 shows a schematic depiction of the binding sites predicted by at least two programs. The splicing factors that were predicted by at least 2 programs number only ten: hnRNP A1, hnRNP F, hnRNP H, SF2/ASF, sc35, SRp40, SRp55, SRSF3, CUG-BP and 9G8. The highest number of binding sites were found in the region covering exon 16.

**Table 3.11: *In-silico* prediction of RNA-binding proteins binding to the three sequences covering the exon 16 splicing region.**

	H1	H2	H3
<b>Human Splice Finder</b>	9G8, hnRNP A1, SRp40, SRp55, sc35, SF2/ASF	hnRNP A1, SRp40, 9G8, SRp55, Tra2beta, sc35, SF2/ASF	hnRNP A1, SF2/ASF, 9G8, sc35, SRp40,
<b>SFmap</b>	Tra2beta, SRp20, CUG-BP, hnRNP U, MBNL2, hnRNP F, FOX1, sc35, hnRNP A2B1	CUG-BP, sc35, MBNL1, hnRNP A2B1, hnRNP F, hnRNP M, hnRNP U, SRp20, SF2/ASF, Tra2beta	FOX1, sc35, MBNL, SRp20, hnRNP A2B1, hnRNP A1
<b>Splice Aid</b>	ETR-3, HuB, TIA-1, TIAL1, SRp40, CUG-BP, Nova-1, TDP43, SRp55, SRp30c, hnRNP H, MBNL1	ETR-3, ZRANB2, RBM5, hnRNP F, hnRNP H, HuB, SF2/ASF, hnRNP A1, SRp40, hnRNP K, hnRNP P, TIA-1, TIAL1, Nova-1, TDP43, CUG-BP	Sc30c, MBNL1, SRp40, RBM5, ZRANB2, KSRP, hnRNP P, hnRNP H, SRp30c, SF2/ASF, hnRNP K, Nova-1

## Chapter 3: Investigating the regulation of the $\Delta 16\text{HER2}$ splicing event



**Figure 3.7: Filtered prediction of splicing factors binding to three sequences covering the  $\Delta 16\text{HER2}$  splicing region (H1, H2, H3).**

This figure shows schematically splicing factors predicted by at least two programs to bind the three  $\Delta 16\text{HER2}$  splicing region covering sequences. The three programs used were Splice Aid, Human Splice Aid and SFmap.

### **3.4.3. Identification of splicing factors that bind the $\Delta 16\text{HER2}$ splicing region**

In the previous section an *in-silico* approach was used to determine binding sites of RNA-binding proteins to the  $\Delta 16\text{HER2}$  splicing region. A high number of possible candidates were thereby identified. To narrow down the number of possible splicing regulators an experimental approach was used. An RNA chromatography assay was performed for the  $\Delta 16\text{HER2}$  splicing region. This assay identifies proteins that bind to a RNA of interest. Synthetic RNAs covering exon 16 and the intron/exon boundaries were used to pull down proteins binding specifically to the RNA (Figure 3.7 A). Stringent washing steps were performed to reduce unspecific binding. At the end the RNAs were digested and the previously RNA bound proteins were size separated on an SDS-PAGE. In figure 3.8 B, the SimplyBlue Safestain stained protein bands from the RNA chromatography assay can be seen. It shows the different patterns of proteins for the three RNA strands. Protein bands were excised and send for identification by mass spectrometry. The proteins identified were: hnRNP 1 (PTB), hnRNP A1, hnRNP A/B, hnRNP A2B1, hnRNP D, hnRNP K and YBX1.

The RNA chromatography assay was repeated, followed by a western blot. In addition to antibodies specific for the proteins identified by mass spectrometry a

panel of antibodies against other splicing factors was also used. This also included a pan-SR-protein antibody. Of the seven previously identified proteins YBX1 could not be verified by western blot. The other splicing factors (hnRNP 1, A1, A/B, A2B1, D and K) could be verified to bind one or more of the synthesised RNAs (Figure 3.8 C). Two additional splicing factors were identified to bind to the RNA strands, hnRNP H and SRSF3. SRSF3 was the only SR-protein that could be identified to bind these synthesised RNAs.

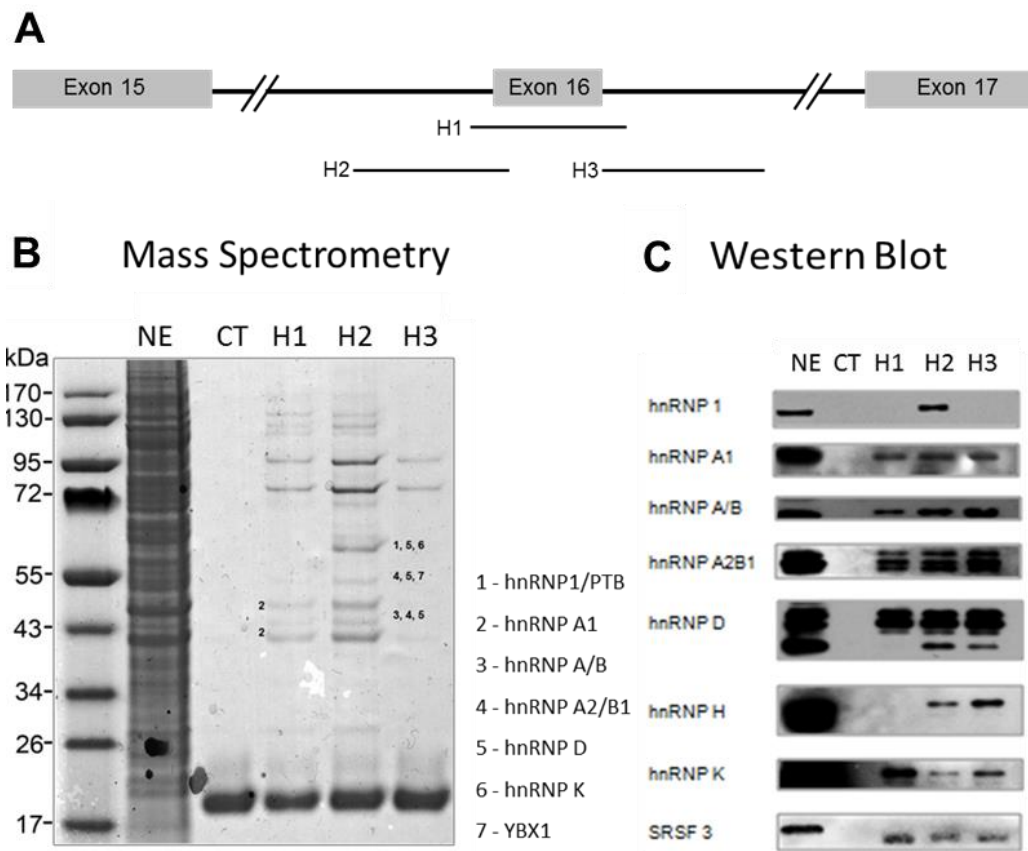


**Figure 3.8: The RNA chromatography assay followed by mass spectrometry and western blot.**

A, The depiction of the  $\Delta 16$ HER2 splicing region indicates the regions covered by the synthetic RNAs (H1, H2, H3) used in the RNA chromatography assay. B, The proteins collected from the RNA chromatography were size separated in a SDS-PAGE. NE indicates nuclear protein extract alone and CT, indicates the no RNA bead control. The numbers indicate the proteins identified by mass spectrometry (Professor Gary Black, Northumbria University). C, Western blots were performed with proteins from the RNA chromatography. A panel of antibodies against splicing factors were used.

**3.4.4. Verification by transient knockdown in HER $\pm$  cell lines**

The RNA chromatography assay identified eight splicing factors that bind the  $\Delta$ 16HER2 splicing region represented by synthetic RNAs. To study if these splicing factors affect the HER2 splicing pattern transient knockdowns were performed. As a model of HER2-overexpressing breast cancer the SKBR3 cell line was used. These cells were transfected with siRNAs targeting the genes of interest. To observe successful knockdown of target genes the mRNA levels were measured 48 h and the protein levels 72 h post-transfection. This was done twice, one representative blot is shown here (Figure 3.9 and 3.10). A GAPDH targeting siRNA was included to verify successful knockdown. In the initial experiments untreated cells (UT) as well as controls for the vehicle (V) and a negative control (NC) siRNA were included. In the following experiments, that were performed to determine the effect of splicing factor knockdown on HER2 splicing patterns, the scrambled siRNA was used as the negative control, as it mimics the conditions of the specific gene knockdowns best. For initial screening one siRNA for each splicing factor was used. If an effect on the HER2 splicing pattern was observed a second siRNA was used to verify the effect.

The knockdowns were performed in collaboration with Dr Hannah Gautrey and fellow PhD student Marco Silipo (Tyson-Capper Laboratory, Newcastle University). The knockdown of hnRNP 1 was attempted by M. Silipo. The levels of hnRNP 1 were too low in SKBR3 cells as to successfully perform a transient knockdown (data not shown). The detection of hnRNP 1 in the RNA chromatography assay can be explained by strong enrichment of nuclear proteins for the assay. The two siRNAs against hnRNP H and SRSF3 were tested by Dr. H Gautrey, and showed to work effectively (Gautrey *et al.*, 2015). HnRNP H and F are highly homologous, therefore hnRNP F was studied in addition to hnRNP H. Additionally, an siRNA targeting both hnRNPs F and H (F/H) was used.

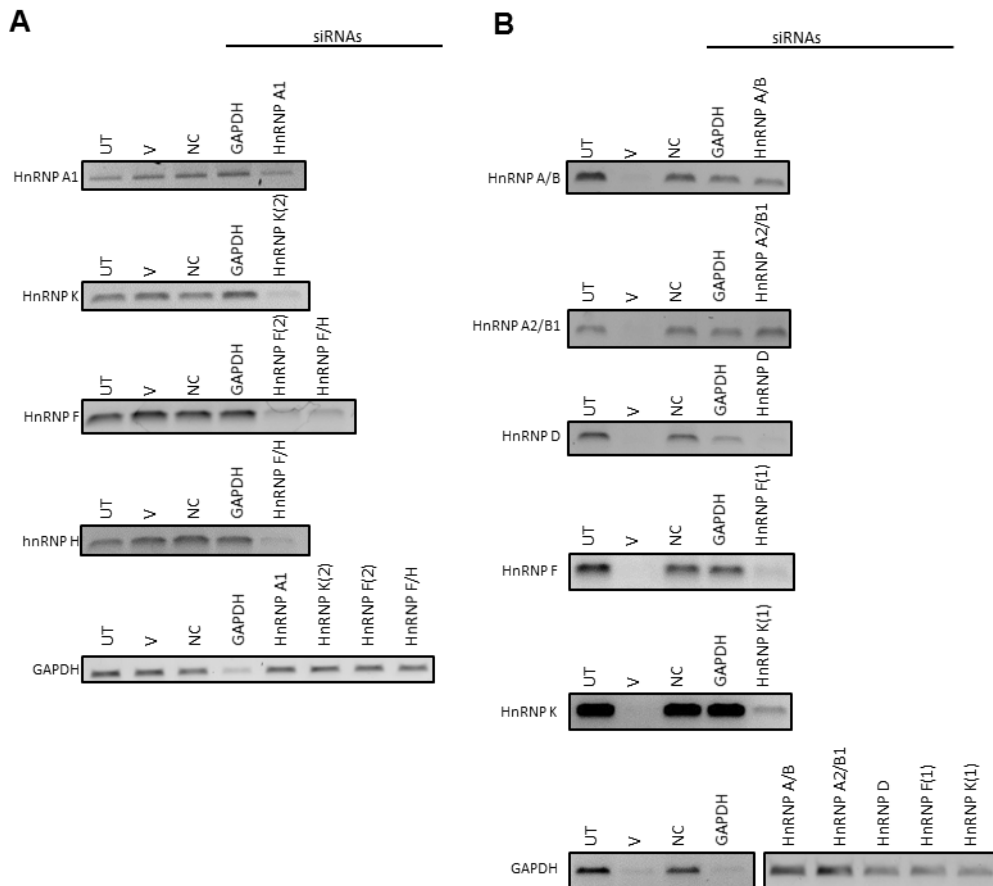


**Figure 3.9: Transient knockdown of splicing factors measured on the mRNA and protein level in SKBR3 cells.**

Transient knockdowns were performed in SKBR3 cells. RNA was collected 48 h post-transfection. Controls included were untreated (UT), vehicle (V), negative control (NC) scrambled siRNA and GAPDH siRNA. As housekeeping gene GAPDH expression was measured. The experiments were performed twice, on example is shown. A, PCR products for the expression of specific genes after transient knockdown of hnRNP A1, K (2), F(2) and a double knockdown of hnRNPs F and H with and siRNA targeting both. B, images provided by M. Silipo. PCR product for the expression of specific genes after transient knockdown of hnRNPs A/B, A2/B1, D, F (1) and K(1).

Figure 3.9 shows the effect of the transient knockdowns of hnRNPs A1, A/B, A2B1, K, F, F/H and D on the mRNA level. The experiments in panel B were primarily performed by M. Silipo. The vehicle control in this experiment did not work, probably due to bad quality of the RNA, however all other controls works as expected. The knockdowns of hnRNPs D, K(1, 2), F(1, 2) and F/H were successful. For hnRNP A1 only a partial knockdown at the mRNA level could be observed. Our research group has previously attempted to knockdown hnRNP A1 with no success. No obvious knockdown on the mRNA level could be observed for hnRNPs A/B and A2/B1. However on the protein level the

knockdowns of hnRNPs A/B, A2/B1, D, F, F/H, K and the double knockdown of hnRNPs F and H was successful. For hnRNP A1 a partial knockdown could be observed. It should be noted that the antibody against hnRNP H (56 kDa) also binds to hnRNP F (53 kDa). Our research group previously observed that knockdown of hnRNP F or H, causes an increase in the level of hnRNP H or F, respectively (data unpublished). This is likely linked to the high level of homology and overlapping actions of hnRNPs F and H (Caputi and Zahler, 2001; Wang *et al.*, 2012a).

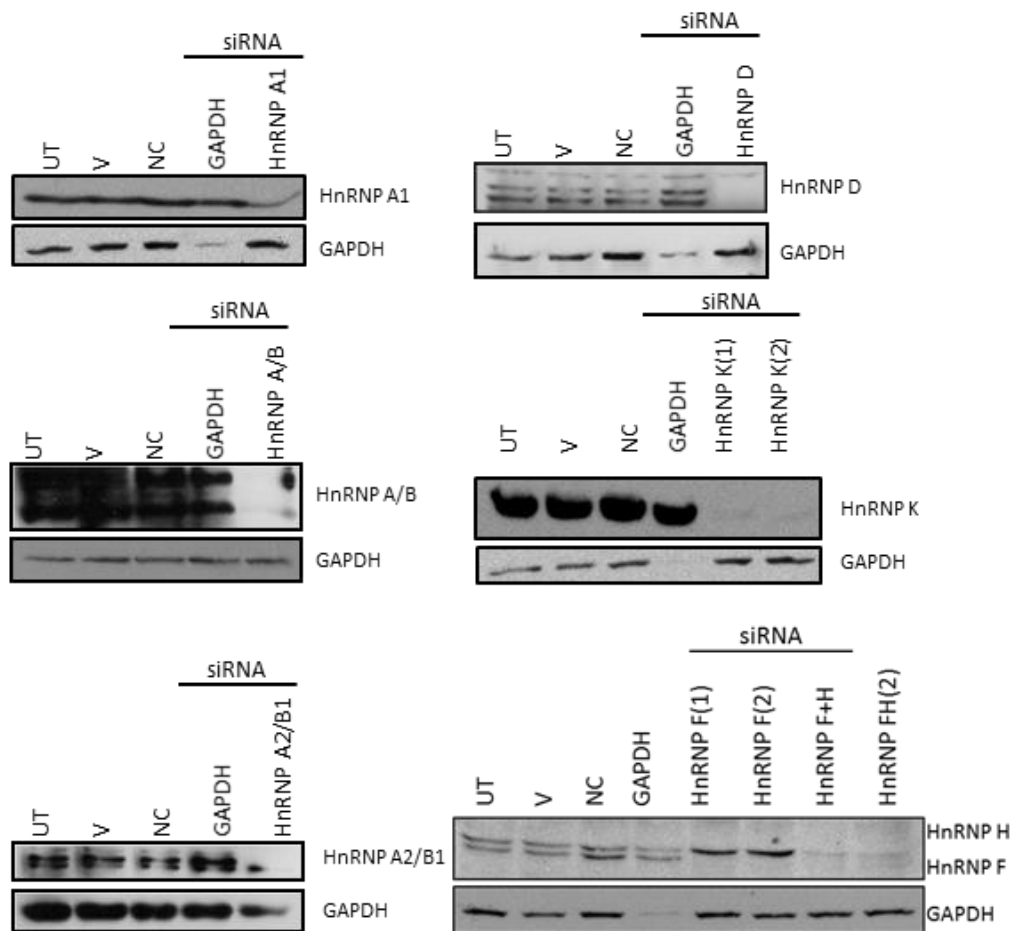


**Figure 3.10: Transient knockdown of splicing factors measured on the protein level in SKBR3 cells.**

Transient knockdowns were performed in SKBR3 cells. Proteins were collected 72 h post-transfection. Controls included were untreated (UT), vehicle (V), negative control (NC) scrambled siRNA and GAPDH siRNA. The experiments were performed twice, on example is shown. Western blot probed with antibodies for the knocked down genes and GAPDH as endogenous control are shown. The antibody against hnRNP H also binds hnRNP F.

To measure the effect of splicing factor knockdown on the splicing pattern of HER2 RNA was collected 72 h post-transfection. The siRNA target splicing factors are estimated to be knocked down at the protein level after 48 h, therefore HER2, the target of the splicing factors, is expected to be affected after 72 h on the mRNA level. The relative expression of wild type HER2 (exon 16 inclusion),  $\Delta$ 16HER2 (exon 16 skipping) and p100 (partial intron 15 retention) was measured by SYBR green qPCR, normalized with GAPDH. p100 was measured as it arises from a splicing event located in close proximity to the  $\Delta$ 16HER2 splicing region. The average of three independent experiments is shown in figures 3.11 to 3.13. The knockdown of the splicing factors hnRNP A1, A/B, A2/B1 and D did not significantly affect the splicing pattern of HER2. Only a slight, but not significant decrease in the expression of wild type HER2 and  $\Delta$ 16HER2 was observed in the knockdowns of hnRNP A/B, A2/B1 and D (Figure 3.11).

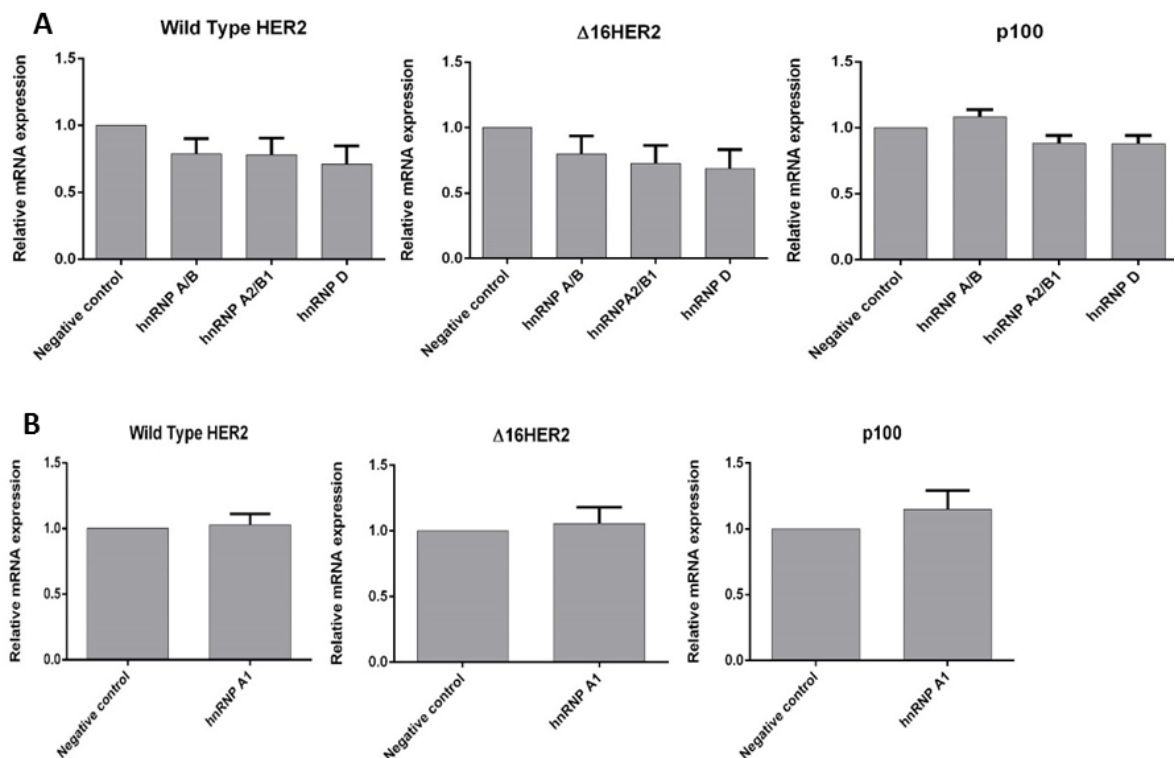


**Figure 3.11: The effect of the transient knockdown of splicing factors (hnRNP A1, A/B, A2/B1 and D) on HER2 splicing in SKBR3 cells.**

The knockdown of splicing factors was performed in SKBR3 cells and the RNA was collected 72h post-transfection. The graphs show the relative mRNA expression of wild type HER2,  $\Delta$ 16HER2 and p100 after gene specific knockdowns compared to the negative control knockdown. The average of three biological replicates is shown. Paired t-test was performed. Knockdowns were performed for hnRNPs A/B, A2/B1 and D (A) and hnRNP A1 (B).

As mentioned previously the initial knockdown of hnRNP H was performed by Dr. H. Gautrey and was shown to cause an increase in  $\Delta$ 16HER2 expression with no effect on p100 expression (Gautrey *et al.*, 2015). The here shown results for the second siRNA against hnRNP H were also published in this article (Gautrey *et al.*, 2015). In the first lane of figure 3.12 A, the knockdown with siRNAs hnRNP H (2), hnRNP F (1) and the double knockdown with both siRNAs is shown. A slight, but not statistically significant increase in the  $\Delta$ 16HER2 level can be observed with hnRNP H (2) and hnRNP F (1) siRNAs. The double knockdown showed a borderline significant increase in the  $\Delta$ 16HER2 level. The hnRNP F (1) siRNA causes a small statistically significant decrease in the p100 level. However this stands in contrast with the trend for hnRNP H (2) and the double knockdown. The second line of figure 3.12 A, shows the effect of the second hnRNP F siRNA and the siRNA targeting both hnRNP F and H. Both siRNAs show a statistically significant increase to the  $\Delta$ 16HER2 level. Opposed to the result with the hnRNP F (1) siRNA, p100 is clearly upregulated in these knockdowns. The double knockdown of hnRNPs F and H has an additive effect on the p100 levels but a cumulative effect on the  $\Delta$ 16HER2 levels.

Figure 3.12 B, shows the effect of hnRNP K knockdown with two siRNAs. Both siRNAs targeting hnRNP K caused a statistically significant downregulation of  $\Delta$ 16HER2 and p100 mRNA levels. Additionally, the first siRNA also causes a smaller but significant downregulation of wild type HER2 expression.

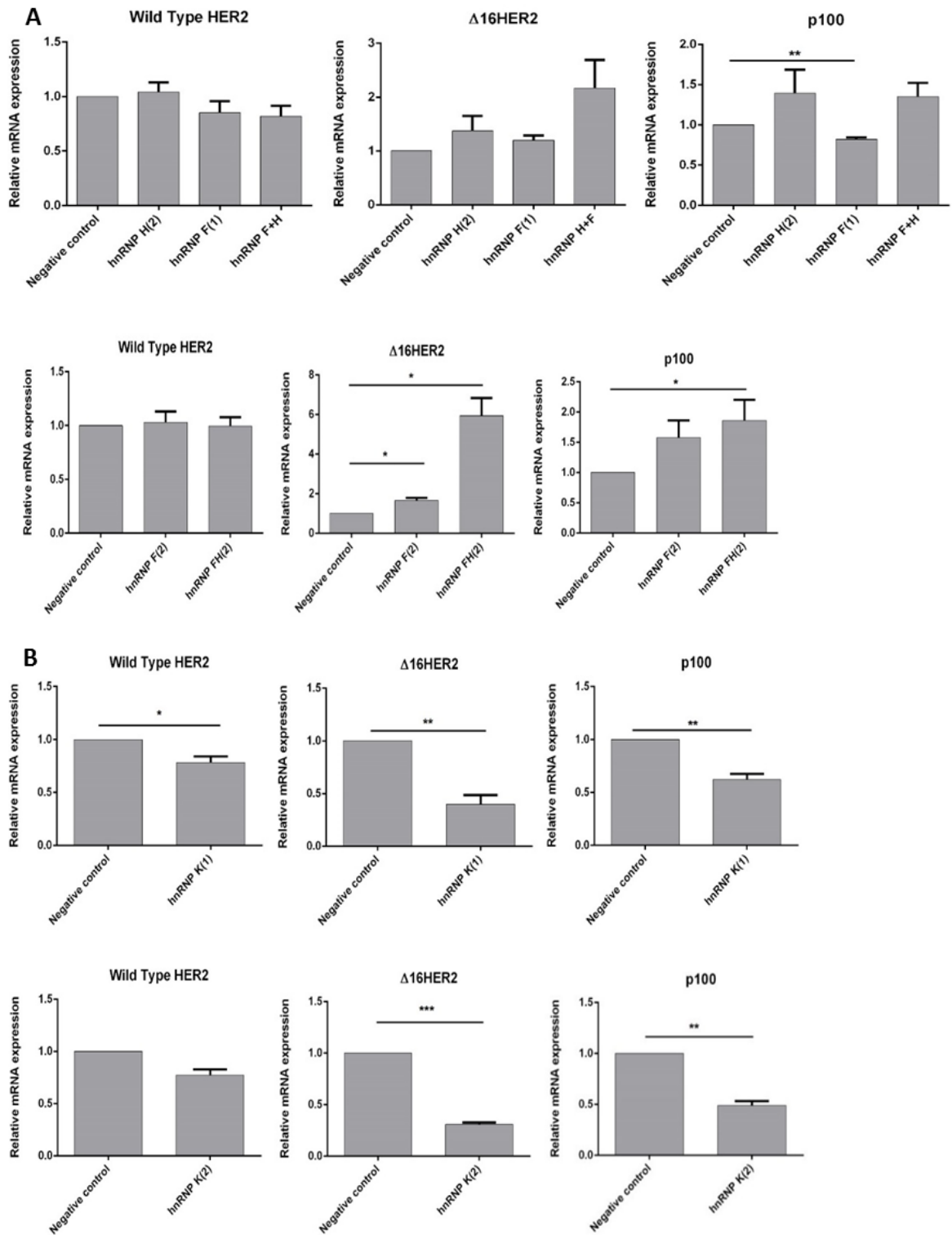


**Figure 3.12: The effect of the transient knockdown of splicing factors (hnRNPs F, H and K) on HER2 splicing in SKBR3 cells.**

The knockdown of splicing factors was performed in SKBR3 cells and the RNA was collected 72 h post siRNA transfection. The graphs show the relative mRNA expression of wild type HER2,  $\Delta 16$ HER2 and p100 after gene specific knockdowns compared to the negative control knockdown. The average of three biological replicates is shown. Paired t-test was performed, \*  $\leq 0.05$ , \*\*  $\leq 0.01$ , \*\*\*  $\leq 0.001$ . A, One siRNA was used against hnRNP H, two against hnRNP F and for the double knockdown of hnRNPs F/H siRNAs hnRNP H (1) and hnRNP F (1) were used and a siRNA targeting both hnRNPs F/H (2). B, Two siRNAs were used against hnRNP K.

In previous work by a member of our research group, Dr H. Gautrey studied the effect of SRSF3 on HER2 splicing with a focus on  $\Delta 16$ HER2 and p100. It was shown that the knockdown of SRSF3 causes the downregulation of  $\Delta 16$ HER2 and the upregulation of p100 expression. No significant effect on wild type HER2 expression was observed (Gautrey *et al.*, 2015). Figure 3.13 shows one repetition of this experiment, it was performed in the HER2 positive cell line SKBR3. The same general trend was observed, but as this experiment was only performed once no statistical analysis was performed. It was purely to observe the reproducibility of the previous work.

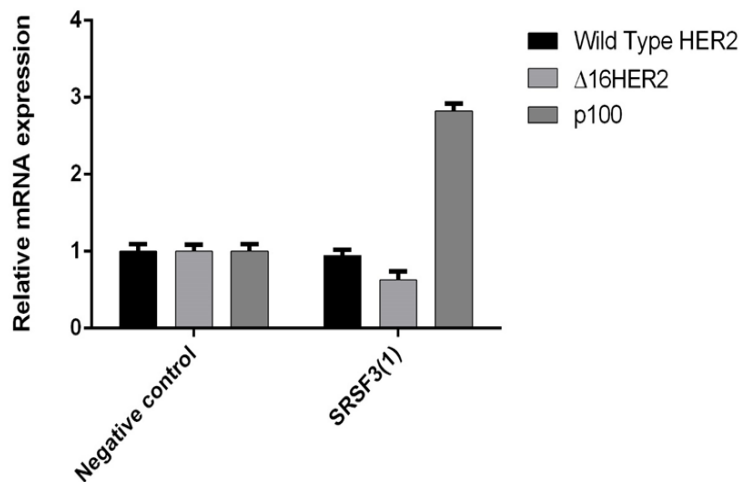


**Figure 3.13: The effect of the transient knockdown of SRSF3 on HER2 splicing in SKBR3 cells.**

SRSF3 was transiently knocked down in SKBR3 cells, the RNA was collected 72 h post-transfection (n=1). The graph shows the relative mRNA expression of wild type HER2,  $\Delta 16$ HER2 and p100 compared to the negative control knockdown.

Leading on from this we wished to observe whether the effect hnRNP F/H, K and SRSF3 were restricted to the HER2 overexpressing cell line SKBR3 or if the same mechanisms could be observed in the HER2 low MCF-7 cell line. For this SRSF3 and hnRNP K were transiently knocked down in MCF-7 cells (Figure 3.14 A). In addition, a double knockdown of SRSF3 and hnRNP K was performed to study if the absence of SRSF3 and hnRNP K had a cumulative effect on the alternative splicing of HER2. Opposed to the observations in SKBR3 cells, in MCF-7 cells the level of wild type HER2 was significantly induced by the knockdown of SRSF3 and the double knockdown. The level of  $\Delta 16$ HER2 was not downregulated in the SRSF3 knockdown compared to the negative control, but the relative expression level compared to wild type HER2 did decrease (Figure 3.14 B). The knockdown of hnRNP K showed the same downregulation of  $\Delta 16$ HER2 as observed in SKBR3 cells. No increased effect

### Chapter 3: Investigating the regulation of the $\Delta 16$ HER2 splicing event

was observed for the double knockdown. The knockdown of SRSF3 increased the level of p100 as observed in SKBR3 cells. The results are borderline significant. It has to be noted that p100 levels are very low in MCF-7 cells. Low copy numbers of target cDNAs in SYBR green qPCR can increase the variability between experiments.

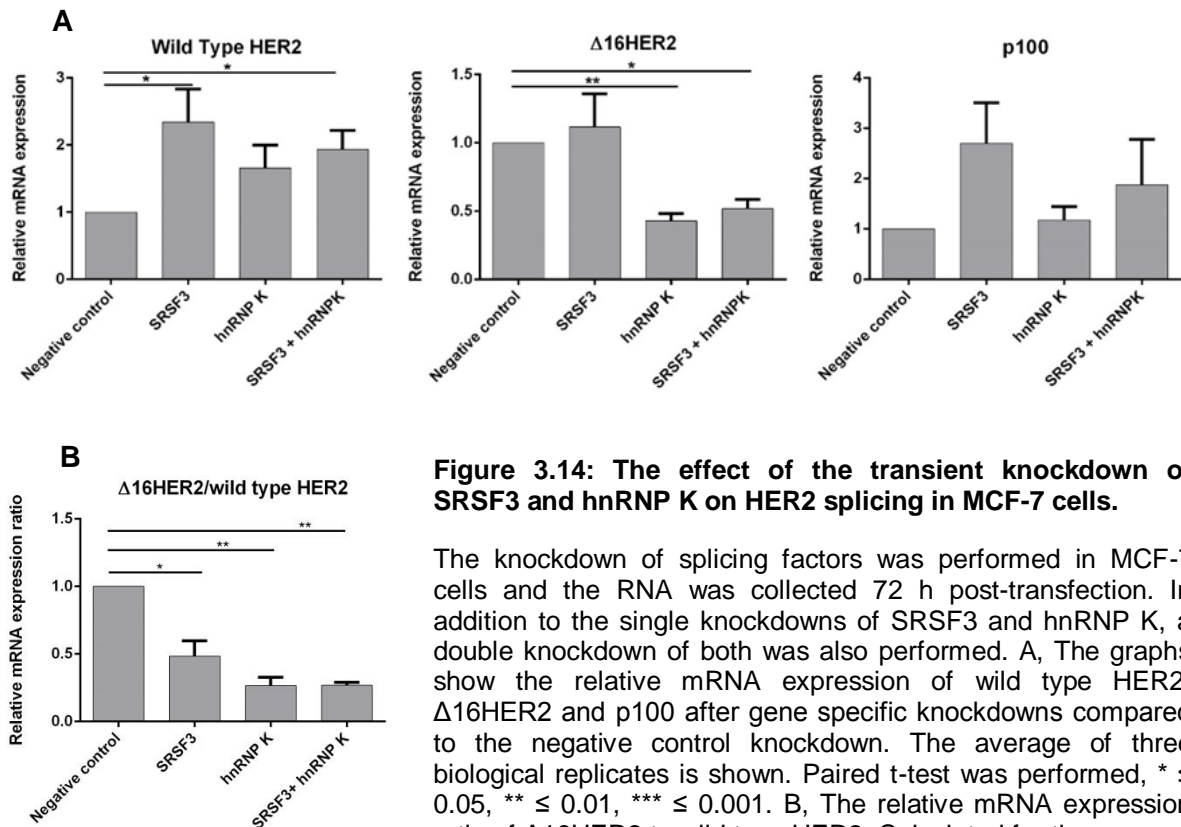


**Figure 3.14: The effect of the transient knockdown of SRSF3 and hnRNP K on HER2 splicing in MCF-7 cells.**

The knockdown of splicing factors was performed in MCF-7 cells and the RNA was collected 72 h post-transfection. In addition to the single knockdowns of SRSF3 and hnRNP K, a double knockdown of both was also performed. A, The graphs show the relative mRNA expression of wild type HER2,  $\Delta 16$ HER2 and p100 after gene specific knockdowns compared to the negative control knockdown. The average of three biological replicates is shown. Paired t-test was performed, \*  $\leq 0.05$ , \*\*  $\leq 0.01$ , \*\*\*  $\leq 0.001$ . B, The relative mRNA expression ratio of  $\Delta 16$ HER2 to wild type HER2. Calculated for the average of three biological replicates.

As part of a separate study in our laboratory knockdowns of hnRNP K and hnRNPs F/H were performed in MCF-7 cells. Dr. H. Gautrey kindly provided cDNA from these experiments. The knockdowns have been carried out to the same standard protocol as used in this study. The levels of  $\Delta 16$ HER2 and wild type HER2 compared to GAPDH was measured by conventional PCR in three independent experiments, one representative image is shown in figure 3.15. These knockdowns confirmed the observation from figure 3.14 that hnRNP K strongly decreases the expression of  $\Delta 16$ HER2. The effect of hnRNP F/H double knockdowns is very pronounced; it strongly upregulates the  $\Delta 16$ HER2

levels. The levels of wild type HER2 and GAPDH were not obviously affected by the knockdowns.

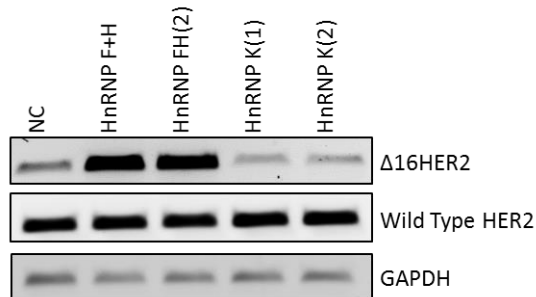


**Figure 3.15: Effect of the transient knockdown of hnRNPs F/H and hnRNP K on HER2 splicing in MCF-7 cells.**

The knockdowns were performed in MCF-7 cells and the RNA was collected 72 h post siRNA transfection. Two siRNAs against hnRNP K were used, and for the double knockdown of hnRNPs F/H siRNAs hnRNP F (1) and hnRNP H (1) were transfected together and a siRNA targeting both hnRNP F and H was used (2). PCRs were performed with gene specific primers for  $\Delta 16$ HER2, wild type HER2 and the housekeeping gene GAPDH. NC stands for the negative control scrambled siRNA.

#### **3.4.5. Efficiency of the $\Delta 16$ HER2-minigene construct**

The  $\Delta 16$ HER2-minigene construct was designed to study the  $\Delta 16$ HER2 splicing event in more detail. The construct covers the region from exon 15 to exon 18. Due to size limitations the whole introns 15 and 16 could not be included into the  $\Delta 16$ HER2-minigene. The  $\Delta 16$ HER2-minigene was transfected into MCF-7 cells, which are low in endogenous HER2. The PCR was performed with primers specific for the  $\Delta 16$ HER2-minigene and therefore no endogenous HER2 should be amplified. The PCR products were verified to be transcripts produced by the  $\Delta 16$ HER2-minigene through sequencing. In addition to the expected band corresponding to exon 16 inclusion (wild type-like HER2) there is also a band that corresponds to the retention of intron 17. A similar extra band due to the retention of intron 17 can be observed with the  $\Delta 16$ HER2 minigene primers for the exon 16 exclusion product ( $\Delta 16$ HER2-like). No p100-like minigene product is transcribed from this  $\Delta 16$ HER2-minigene, as it lacks the necessary upstream region (data not shown).

To investigate whether the  $\Delta 16$ HER2-minigene contained the binding sites for the previously identified splicing factors (hnRNP F/H, K and SRSF3) which affect HER2 splicing, transient knockdowns were performed. Both the HER2-overexpressing SKBR3 cells and HER2-low MCF-7 cells (n=3) were transfected

with the  $\Delta$ 16HER2-minigene following transient knockdown of the splicing factors (Figure 3.16). The experiments were performed three times in both cell lines. One experiment in the SKBR3 cell line did not yield results due to bad RNA quality. However the observed splicing pattern was consistent across the experiments. The knockdown of SRSF3 had no obvious effect on the expression pattern of the  $\Delta$ 16HER2-minigene product. However, the knockdown of hnRNP K caused an increased expression of the wild type HER2 and a decrease of  $\Delta$ 16HER2-like minigene product. The strongest effect on the splicing of the  $\Delta$ 16HER2-minigene can be observed when hnRNP F/H is knocked down. After hnRNP F/H knockdown wild type-like HER2 expression is strongly decreased and an unspecific amplification of plasmid DNA can be observed in cDNA from MCF-7 cells. At the same time the  $\Delta$ 16HER2-like minigene product is expressed strongly.

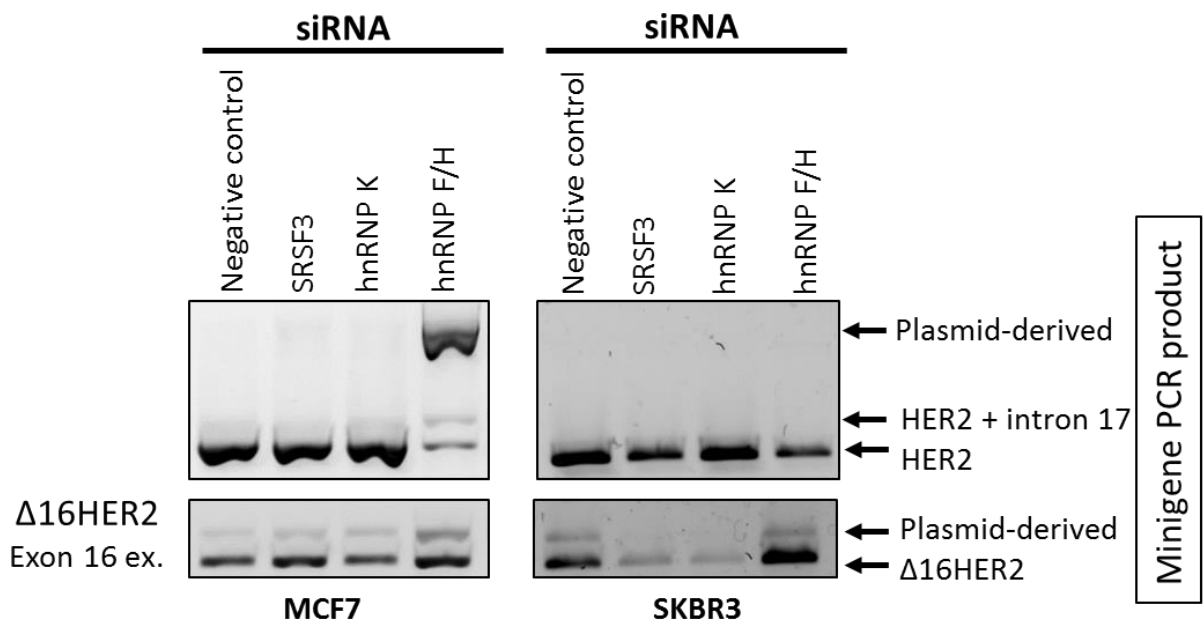


**Figure 3.16: Expression of the  $\Delta$ 16HER2-minigene products and the effect of the splicing factors on it.**

Transient knockdown of SRSF3, hnRNP K and hnRNPs F/H was performed in MCF-7 and SKBR3 (n=3) cells. 48 h after siRNA transfection the  $\Delta$ 16HER2-minigene was transfected. RNA was isolated 24 h later. A negative control siRNA was also transfected in both cell lines with the  $\Delta$ 16HER2-minigene. PCR was performed with an exon 16 inclusion or exon 16 skipping ( $\Delta$ 16HER2) specific forward and minigene product specific reverse primer.

**3.4.6. Identification of regulatory sequences by site-directed mutagenesis**

To further study the mechanisms regulating the  $\Delta$ 16HER2 splicing event the binding sites of the identified splicing regulators was investigated. From the four splicing factors regulating the  $\Delta$ 16HER2 splicing event only hnRNP K and hnRNPs F/H were shown to affect the splicing of the  $\Delta$ 16HER2-minigene. In the RNA chromatography assay hnRNP K was found to bind all three synthesised RNAs. Strongest binding was seen on the exon 16 covering RNA (H1) and least to the intron 16 covering RNA (H3). HnRNP H only bound to the intron 15 and 16 covering RNAs (H2 and H3).

**Table 3.12: Summarizing the binding of the splicing factors from the RNA chromatography assay.**

	<b>H1</b> (exon 16)	<b>H2</b> (intron 15)	<b>H3</b> (intron 16)
<b>HnRNP K</b>	+ (stronger)	+	+ (fainter)
<b>HnRNP H</b>	-	+	+ (stronger)

*In-silico* analysis suggested a number of binding sites for hnRNPs F/H and two for hnRNP K (Figure 3.17). Interestingly, no hnRNP K binding site on exon 16 was predicted. Only one binding site for hnRNP H in intron 16 was predicted. A number of binding sites overlapping with the polypyrimidine tract and the branch point were also predicted. It has been shown that the binding of hnRNPs F/H in the 3' intron could regulate exon recognition (Xiao *et al.*, 2009; Wang *et al.*, 2012a). Therefore the hnRNP H binding site in intron 16 was first point mutated (mut 2).

It was not possible to design a mutation for the cluster of hnRNPs F/H binding sites around the branch point that was not predicted to interfere with normal exon recognition. Instead the hnRNPs F/H binding site in intron 15 that is upstream of the branch point was mutated, this binding site also contains the more typical recognition motive of triple G (mut 5). In addition, the binding site

### Chapter 3: Investigating the regulation of the $\Delta 16$ HER2 splicing event

was also predicted by two predictive programs. Subsequently both the intron 15 and 16 hnRNP K binding sites (mut 4 and 6) were mutated.

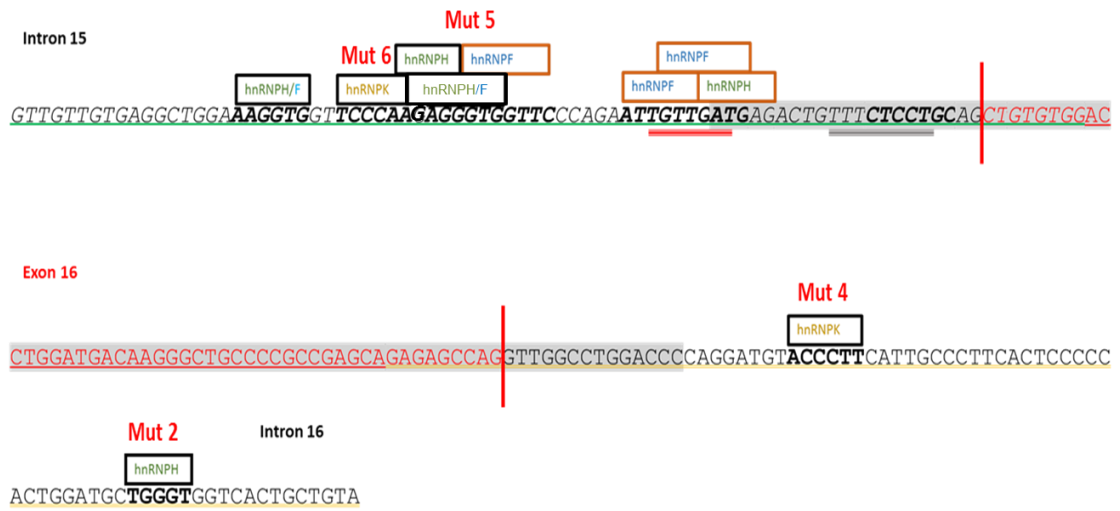


**Figure 3.17: Depiction of splicing factor binding sites in the  $\Delta 16$ HER2 splicing region.**

*In silico* predictions for the binding of hnRNPs F/H and hnRNP K filtered for the binding region identified in the RNA chromatography assay are shown. The green underlining indicates RNA H2, the grey shaded sequences are covered by H1 and the yellow underlined is covered by H3. The red line indicates the boundary of exon 16. The sites at which site-directed mutagenesis was performed are indicated (Mut).

The types of mutations carried out are shown in table 3.13. The mutated  $\Delta 16$ HER2-minigenes and the unchanged  $\Delta 16$ HER2-minigene were transfected into SKBR3 cells. Figure 3.18 shows the expression pattern of the HER2-like minigene product. Mut 4 showed an increase in wild type-like levels and a decrease in  $\Delta 16$ HER2-like levels. This reflects the downregulation of  $\Delta 16$ HER2 by hnRNP K knockdown. The hnRNP F/H mutants showed no increase in the  $\Delta 16$ HER2-like transcript level, contrarily it showed a very small decrease in  $\Delta 16$ HER2-like transcript level. The second hnRNP K mutant 6, showed overall decrease levels of  $\Delta 16$ HER2-minigene transcripts.

**Table 3.13:  $\Delta 16$ HER2-minigenes splicing factor binding site mutants.**

	Mut 2	Mut 4	Mut 5	Mut 6
<b>Mutation</b>	Deletion TGGGT	ACGCTTGA	TAGCGTG	TCGCA
<b>Binding site for</b>	hnRNP H	hnRNP K	hnRNP F/H	hnRNP K

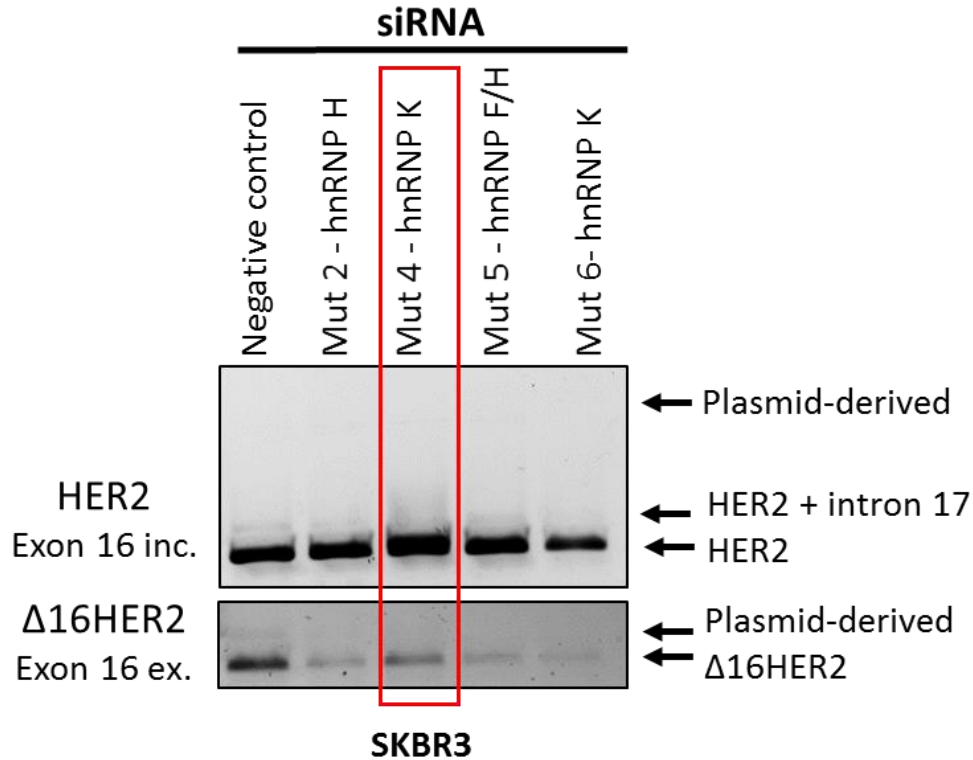


**Figure 3.18: The  $\Delta 16$ HER2-minigene expression after mutation of splicing factor binding sites.**

The  $\Delta 16$ HER2-minigene and the splicing factor binding site mutants were transfected into SKBR3 cells ( $n=3$ ). RNA was collected 24 h after transfection. The PCR was performed with an exon 16 inclusion or exon 16 skipping ( $\Delta 16$ HER2) specific forward and  $\Delta 16$ HER2-minigene product specific reverse primer. The red rectangle marks a change in expression ratio.

### 3.4.7. Regulation of splicing factor expression through HER2

In the previous section the regulation of HER2 splicing by RNA-binding factors was investigated. Often regulatory pathways show complex feedback-loops to auto-regulate themselves. Unpublished work by Dr Evrim Besray Unal (Charite, Berlin) indicated regulation of hnRNP family proteins through the ras-MAPK signalling pathways in the breast cancer cell line MCF-7. This finding made us interested in defining whether HER2 initiated ras-MAPK signalling to regulate the four splicing regulators (SRSF3, hnRNP H, hnRNP F, hnRNP K) of HER2. HnRNP K expression has previously been shown to be induced by growth factors/growth factor receptors (Mandal *et al.*, 2001). Additionally, hnRNP K expression has been shown to be induced by AKT in prostate cancer cells

(Ciarlo *et al.*, 2012). AKT is a part of the PI3K-AKT pathway, which is one of the main HER2 signalling pathways [reviewed in (Dittrich *et al.*, 2014)].

To observe the effect of HER2 signalling on the mRNA expression of the splicing factors, HER2 was transiently knocked down with two specific siRNAs in SKBR3 cells. A partial knockdown of HER2 mRNA could be observed by conventional PCR even 72 h after transfection (Figure 3.19, A), when the effect on the splicing factor expression was measured. A strong down regulation of HER2 on the protein level has been shown for these siRNAs by MSc student S. Satam (data not shown). Changes in expression were measured by qPCR with gene specific TaqMan probes. No change in the expression level of SRSF3 could be observed after transient knockdown of HER2. A statistically significant increase in the expression of hnRNPs H, F and K was observed, but the increase is small (Figure 3.19, A).

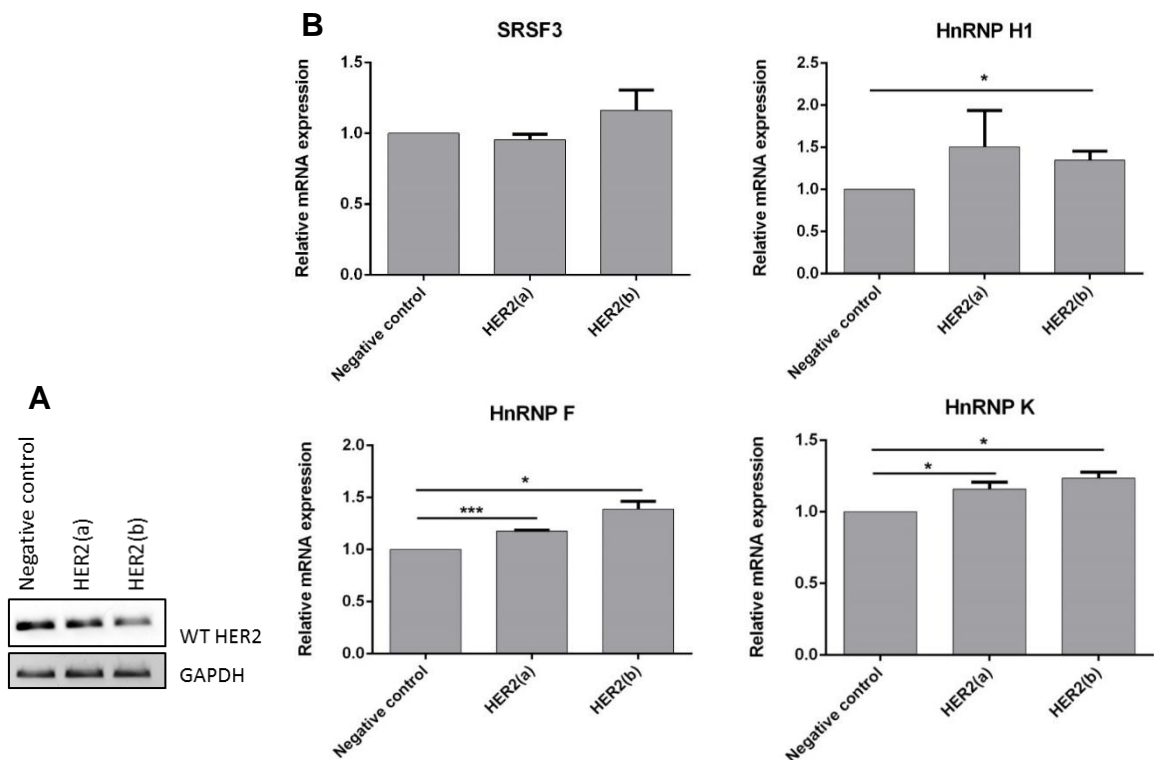


**Figure 3.19: The effect of HER2 transient knockdown on splicing factor gene expression.**

Two siRNAs targeting HER2 were transfected into SKBR3 cells. RNA was collected 72h post-transfection. A, PCRs were performed for the housekeeping gene GAPDH and HER2 to confirm the partial knockdown of HER2 expression. B, The graphs show the relative mRNA expression of the splicing factors SRSF3, hnRNP, hnRNP F and hnRNP K after HER2 knockdown compared to the negative control knockdown. The average of three biological replicates is shown. Paired t-test was performed, \*  $\leq 0.05$ , \*\*\*  $\leq 0.001$ .

Both the work by Dr Unal and in the two studies on hnRNP K (Mandal *et al.*, 2001; Ciarlo *et al.*, 2012) detected an effect on the protein level of the splicing factors. To study a possible effect of HER2 signalling on the protein level of the splicing factors, the HER2 overexpressing SKBR3 cells were treated with the HER2 tyrosine kinase inhibitor lapatinib. Using lapatinib it was possible to measure the splicing factor protein levels at specific time points after inhibition of signalling. Three independent experiments were carried out, from which one representative experiment is shown in figure 3.20. Literature suggests treatments should be performed with a 1  $\mu$ M concentration of lapatinib (O'Neill *et al.*, 2013; Venturutti *et al.*, 2016). To verify that lapatinib inhibits HER2 signalling, proteins were collected after 15 min lapatinib treatment. For this time point an untreated and DMSO vehicle control was also taken. The treatment of SKBR3 cells with lapatinib showed no changes to the total protein levels of HER2 nor its downstream effectors AKT and ERK1/2. However, lapatinib treatment inhibited the phosphorylation of AKT (Ser473) and ERK (Thr202/Tyr204) (Figure 3.20).

After confirming for each experiment that the HER2 signaling pathway was inhibited, the protein levels of the previously studied splicing factors SRSF3, hnRNP K and hnRNP H/F were measure (Figure 3.20). The time points used were 6, 12 and 24 h post lapatinib treatment. A DMSO vehicle control was included. GAPDH levels are shown for normalisation. Densitometry was performed to compare the three experiements (Tables 3.14). The protein levels of the splicing factors fluctuate slightly experiments and time points. The results for the 24 h treatment were the most consistent, with a slight trend towards downregulation of the splicing factors.

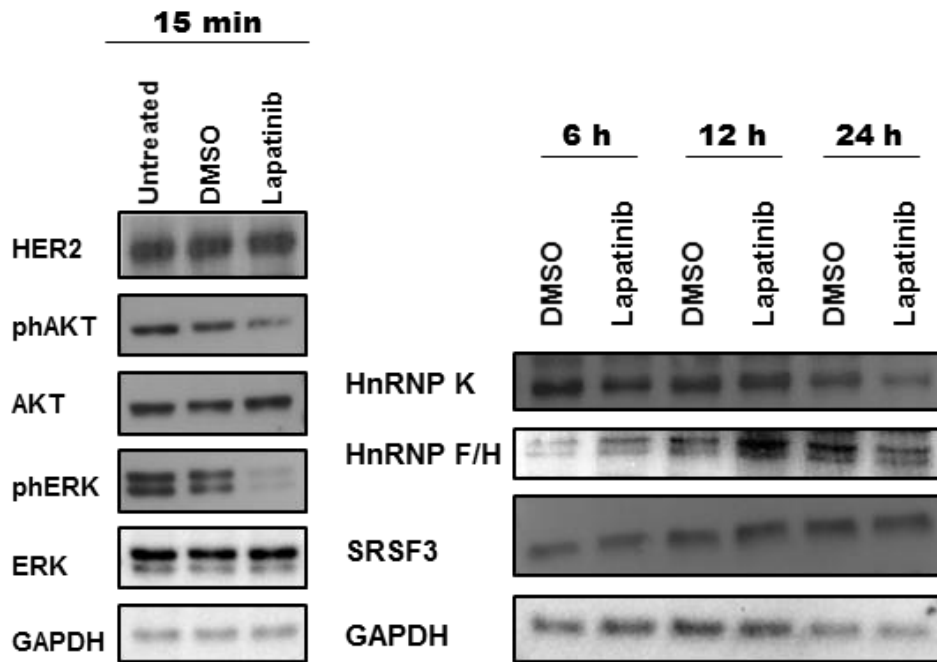


Figure 3.20: The effect of HER2 signalling inhibition by lapatinib on splicing factor protein expression.

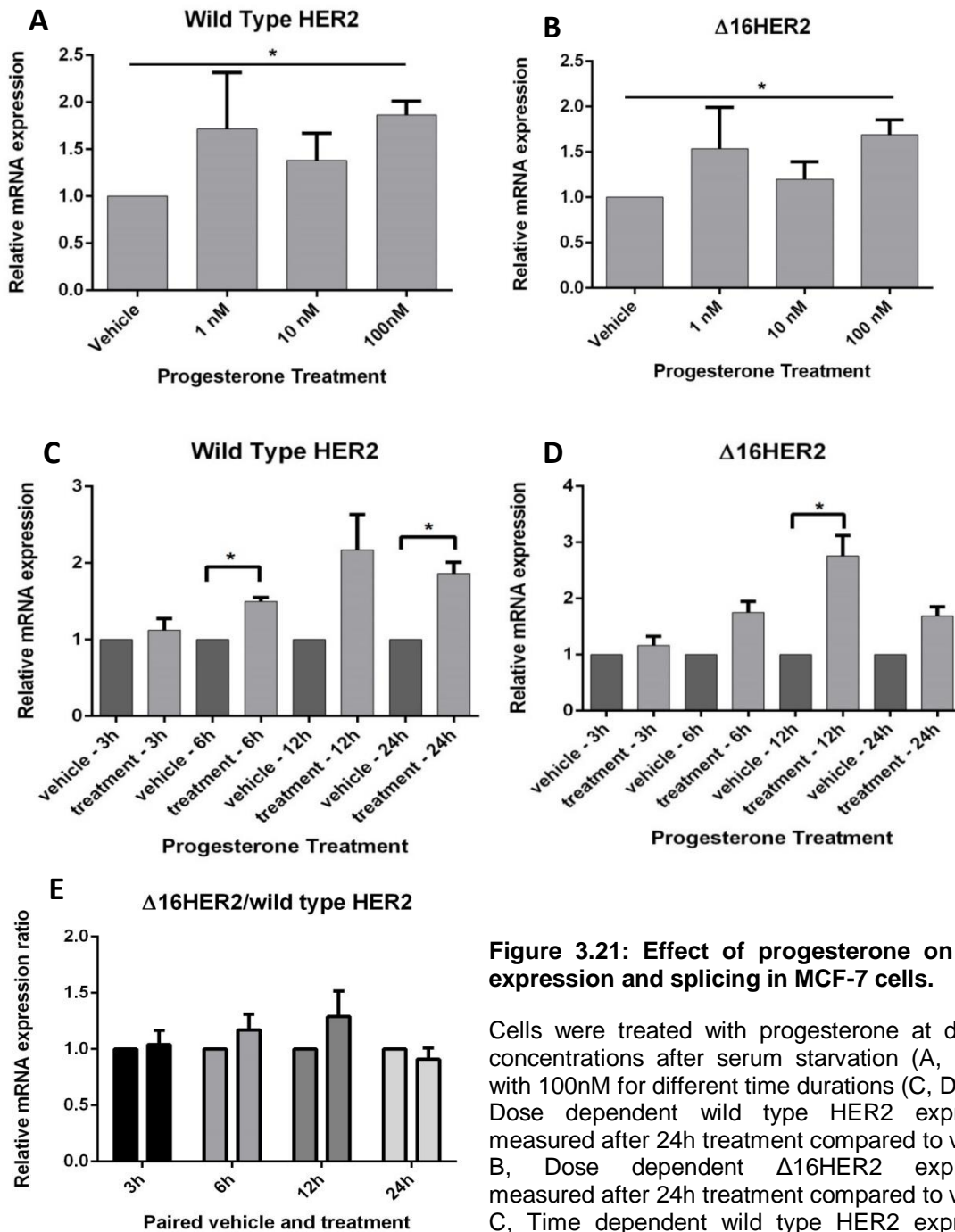
SKBR3 cells were treated with 1  $\mu$ M lapatinib for 15 min, 6, 12 and 24 h. After 15 min the protein levels of HER2, phospho-AKT (Ser473), AKT, phospho-ERK (Thr202/Tyr204), ERK and GAPDH were determined by western blot. Untreated, DMSO vehicle control and lapatinib treatment are shown. DMSO vehicle control and lapatinib treatments are shown for the other time points. Protein levels of hnRNP K, hnRNPs F and H as well as SRSF3 and the housekeeping gene GAPDH is shown. The experiment was performed 3 times, one representative experiment is shown.

Table 3.14: Effect of HER2 signalling inhibition on splicing factor protein levels: densitometry of western blots.

HnRNP K	6 h		12 h		24 h	
	DMSO	Lapatinib	DMSO	Lapatinib	DMSO	Lapatinib
Experiment 1	1	0.47	1	1.37	1	0.77
Experiment 2	1	1.18	1	0.91	1	0.83
Experiment 3	1	0.71	1	0.55	1	0.71
Average	1	0.79 $\pm$ 0.36	1	0.94 $\pm$ 0.41	1	0.77 $\pm$ 0.06
hnRNP F/H	6 h		12 h		24 h	
	DMSO	Lapatinib	DMSO	Lapatinib	DMSO	Lapatinib
Experiment 1	1	4.08	1	2.1	1	0.81
Experiment 2	1	0.87	1	1.33	1	0.49
Experiment 3	1	1.27	1	1.03	1	0.80
Average	1	2.07 $\pm$ 1.75	1	1.49 $\pm$ 0.54	1	0.70 $\pm$ 0.18
SRSF3	6 h		12 h		24 h	
	DMSO	Lapatinib	DMSO	Lapatinib	DMSO	Lapatinib
Experiment 1	1	1	1	1.36	1	0.75
Experiment 2	1	0.74	1	0.5	1	0.8
Experiment 3	1	0.54	1	0.93	1	0.49
Average	1	0.76 $\pm$ 0.23	1	0.93 $\pm$ 0.43	1	0.68 $\pm$ 0.17

### **3.4.8. Progesterone induces HER2 expression**

As mentioned in the introduction of this chapter hormones have been shown to be able to regulate the splicing of receptor proteins (Lal *et al.*, 2013). Previous work of our research group showed that oestrogen does not affect the expression or splicing of HER2 (unpublished). The other main hormone studied in the context of breast cancer is progesterone. Here the effect of progesterone on HER2 splicing was studied. The HER2 negative but ER and PR positive breast cancer cell line MCF-7 was used for this part of the study. The cells were treated for 24 h with a range of progesterone concentrations (1 nM, 10 nM, 100 nM) to determine the effect of progesterone on the expression of wild type HER2 and  $\Delta$ 16HER2. RNA was collected and following reverse transcription SYBR Green qPCR was performed to measure HER2 and  $\Delta$ 16HER2 expression. Figure 3.21 A and B show the relative mRNA expression compared to the vehicle. Both wild type HER2 and  $\Delta$ 16HER2 expression increases with progesterone treatment. At 1 nM of progesterone the deviation of expression levels between three experiments was large. A reproducible and statistically significant increased expression could only be measured at 100nM treatment, both for wild type HER2 and  $\Delta$ 16HER2. No significant difference in wild type HER2 and  $\Delta$ 16HER2 mRNA expression could be observed. The hereby determined optimal progesterone dose of 100 nM was used to treat the cells for 3, 6, 12 and 24 hours. This was undertaken to determine the optimal time point at which progesterone starts to affect the expression and when the expression peaks. The average relative wild type HER2 and  $\Delta$ 16HER2 mRNA expression compared to time paired vehicle controls is shown in figure 3.21 C and D. The expression increases steadily, peaking roughly at 12 h, followed by a slight decrease at 24 h. Only 6 h and 24 h post-treatment could a statistically significantly increased expression of wild type HER2 be observed. The standard deviation between the three independent experiments for the 12 h treatment is increased, and no statistical significance is reached, although the average expression is peaked here. The highest level of  $\Delta$ 16HER2 expression and only statistically significant time point is reached at 12 h. No significant change in the expression of ratio between  $\Delta$ 16HER2 and wild type HER2 could be observed (Figure 3.21 E).



**Figure 3.21: Effect of progesterone on HER2 expression and splicing in MCF-7 cells.**

Cells were treated with progesterone at different concentrations after serum starvation (A, B) and with 100nM for different time durations (C, D, E). A, Dose dependent wild type HER2 expression measured after 24h treatment compared to vehicle. B, Dose dependent  $\Delta 16$ HER2 expression measured after 24h treatment compared to vehicle. C, Time dependent wild type HER2 expression measured after 3, 6, 12 and 24h treatment. Shown compared to paired vehicle control. D, Time dependent  $\Delta 16$ HER2 expression measured after 3, 6, 12 and 24h treatment. Shown compared to paired vehicle control. E, Cells were treated with 100nM progesterone for 3, 6, 12 and 24h. Paired vehicle control was taken for each time point. The relative mRNA expression ratio between  $\Delta 16$ HER2 and wildtype HER2 is shown. N=3 for all experiments, standard deviation is indicated. One-way anova with multiple comparison by – was used for A and B. Paired t-test was used for C, D and E. Statistical significance is indicated, \*  $\leq 0.05$ .

### 3.5. Discussion

$\Delta 16$ HER2 is one of the three very well-studied HER2 splice variants. It has been extensively studied with regards to its ability to induce tumour formation (Mitra *et al.*, 2009; Alajati *et al.*, 2013; Turpin *et al.*, 2016), its distinct signalling pathway and the types of breast tumours formed (Alajati *et al.*, 2013; Castagnoli *et al.*, 2014). However little is known about the mechanisms involved in its production and regulation. Here the mechanisms regulating the alternative splicing mechanism that produces  $\Delta 16$ HER2 were investigated. Although  $\Delta 16$ HER2 is accepted to be a full length mRNA variant which only lacks exon 16, there is no supporting mRNA sequence logged with any of the publicly available databases. Here it was confirmed by conventional PCR, that exon 16 skipping is part of a transcript that reaches at least from exon 3 to the last exon 27. The variations of amplification strengths of the various PCR products can be explained by differences of primer efficiencies and the length of the transcripts.

Using two RNA secondary structure prediction tools wild type HER2 and  $\Delta 16$ HER2 were compared. The absence of exon 16 is predicted to affect the secondary structure. Both models showed changes to the structure. The MFE model showed a higher number of branches and loops for  $\Delta 16$ HER2, whereas the centroid model showed a lesser number of changes to the secondary structure, but not a less complex alteration. Changes to the secondary structure are especially interesting when considering a recent publication. He and colleagues described a miRNA-155 binding site within the coding region of the HER2 mRNA (He *et al.*, 2016). This binding site was found to be located in exon 17, within few nucleotides of exon 16. Both models predicted the secondary structures of the binding site to be different between wild type HER2 and  $\Delta 16$ HER2. The most severe change was predicted by the centroid plain model, which predicted the binding site sequence in  $\Delta 16$ HER2 to be located on a large loop, but broken up by number of pseudoknots and single nucleotide interactions. Additional loping of the different structures could make this potentially hard to access by miRNA-155. The previously mentioned study showed that miRNA-155 was upregulated by treatment of cells with trastuzumab. MiRNA-155 in turn represses HER2 expression by targeting

HDAC2, a transcriptional activator of HER2 and by binding in the coding region of HER2 (He *et al.*, 2016). Work in cell lines, showed  $\Delta 16$ HER2 to be resistant to trastuzumab treatment (Castiglioni *et al.*, 2006; Mitra *et al.*, 2009), however *in vivo* work has shown the opposite; that  $\Delta 16$ HER2 positive tumour cells are increasingly susceptible to trastuzumab (Castagnoli *et al.*, 2014). Here we suggest that due to the absence of exon 16 the secondary structure of the miRNA-155 binding site in  $\Delta 16$ HER2 is obscured and  $\Delta 16$ HER2 is thereby less affected by miRNA-155 and thereby trastuzumab in *in vitro* models.

### **3.5.1. Identification of the $\Delta 16$ HER2 splicing event regulating factors**

The most prominent mechanism of splicing regulation is through RNA-binding proteins that affect the recognition of exons and introns by the spliceosome. Most regulatory signals are found in close proximity to the exon/intron boundaries [reviewed in (*RNA and Cancer*, 2013)]. Initially the intron boundary area of exon 16 and the exon itself was studied using three *in silico* predictive tools. These predicted 30 proteins to potentially bind the exon 16 splicing area. Comparing the results from the 3 software packages showed a list of ten splicing factors that were at least predicted by 2 tools for overlapping binding sites. These were hnRNP A1, hnRNP F, hnRNP H, SF2/ASF, sc35, SRp40, SRp55, SRSF3, CUG-BP and 9G8. A major limitation is that these programs have been produced at different times and are not all up to date in regard to more novel splicing factors and binding sites. *In-silico* predictions often differ strongly from what can be found in cells. To further narrow down the number of possible splicing regulators an experimental approach was used. The RNA chromatography assay combined with mass spectrometry and western blot confirmed some of the *in-silico* predicted splicing factors: hnRNP A1, hnRNP H, hnRNP F and SRSF3, as well as factors that were only predicted by one or none of the predictive programs. To verify if these proteins affect the splicing of  $\Delta 16$ HER2, transient knockdowns were performed. Besides  $\Delta 16$ HER2 the effect on p100, another HER2 splice variant was also measured. The close proximity is likely to link the splicing events; p100 is due to a partial intron 15 retention and  $\Delta 16$ HER2 is due to exon 16 skipping. The knockdowns showed that only

SRSF3 and the hnRNPs K, F and H affect the splicing of  $\Delta$ 16HER2. This could be observed in both HER2-high SKBR3 and HER2-low MCF-7 cells and supports previous findings by our group (Gautrey et al., 2015). The splicing factors SRSF3 and hnRNP K were shown to repress the recognition of exon 16 and promote the production of  $\Delta$ 16HER2. HnRNPs F and H downregulate both  $\Delta$ 16HER2 and p100 production. As both p100 and  $\Delta$ 16HER2 are minor transcripts in the cell lines used, changes to their level only minimally affect the wild type HER2 levels. Interestingly, SRSF3 was found to upregulate the production of  $\Delta$ 16HER2, but downregulates the production of p100.  $\Delta$ 16HER2 has been shown to promote tumour development and aggressiveness of the disease (Kwong and Hung, 1998; Siegel *et al.*, 1999; Mitra *et al.*, 2009; Sasso *et al.*, 2011), whereas p100, although not extensively studied, has been associated with a tumour suppressing function (Aigner *et al.*, 2001). Therefore in this model SRSF3 promotes a tumourigenic phenotype by promoting of  $\Delta$ 16HER2 and inhibition of p100 splicing.

To show that these splicing factors act specifically on the exon 16 splicing region and to identify the mRNA binding sites, a  $\Delta$ 16HER2-minigene was constructed. When transfected into breast cancer cells the  $\Delta$ 16HER2-minigene gave rise to both wild type HER2-like and  $\Delta$ 16HER2-like transcripts. The knockdown of the hnRNPs, but not SRSF3 had an effect on the  $\Delta$ 16HER2-minigene expression pattern. As mentioned previously our group has identified a SRSF3 binding site in exon 15 (Gautrey et al., 2015). Given the size constraints of a minigene, the  $\Delta$ 16HER2-minigene only contains exon 15 and a small portion of intron 14 (Figure 3.20). This is expected to affect how exon 15 and the binding site in it are recognised. Also no p100-like transcript is produced from the  $\Delta$ 16HER2-minigene (data not shown).



**Figure 3.22: The HER2 sequence of the  $\Delta$ 16HER2-minigene.**

The  $\Delta$ 16HER2-minigene contains a short segment of intron 14, followed by exon 15, intron 15, exon 16, intron 16, exon 17, intron 17 and exon 18. A large middle part of the introns 15 and 16 were not included.

Comparing the combined *in-silico* predictions with the results from the RNA chromatography assay gave a starting point to identify binding sites of hnRNP F/H and hnRNP K. Four site-directed mutagenesis were performed for predicted binding sites. The mutations were carefully designed to not impair the normal exon recognition. However some additional predicted binding sites were also abolished: for hnRNP F/H mutant 2 binding motifs for RBM5, hnRNP P, KSRP and ZRANB2, for hnRNP K mutant 4 a potential Nova-1 binding motif and for hnRNP F/H mutant 5 potential binding motifs hnRNP P and RBM5. Additionally, hnRNP F/H mutant 2 gained a binding motif for MBNL1, hnRNP K mutant 4 gained a potential binding motif for MBNL1 and hnRNP K mutant 6 gained a potential binding motif for ZRANB2. None of these splicing factors have been previously implied play a role in exon 16 splicing. However an effect of artificially produced binding motifs or deletion of potential binding sites could affect the splicing of the  $\Delta 16$ HER2-minigene.

Of the two hnRNP F/H and two hnRNP K binding sites only mutation 4 had an effect on the splicing pattern. This binding site was located on intron 15 slightly upstream of the branch point. Similar to the knockdown of hnRNP K, the mutation of its binding site also causes the reduced expression of  $\Delta 16$ HER2-like products in favour of wild type HER2-like products. HnRNP F/H was found to be a factor that promotes the recognition of exons 16, but none of the mutated sites affected the alternative splicing pattern. A cluster of binding sites were predicted that overlap the branch point. It was not possible to mutate the binding site without also stopping exon 16 recognition.

#### **The role of SRSF3 in alternative splicing of $\Delta 16$ HER2**

SRSF3 is a well-studied SR protein which is overexpressed and acts as an oncogene in a number of cancers including breast cancer (Jia *et al.*, 2010; Silipo *et al.*, 2015). One study showed an increase in SRSF3 expression to be positively correlated with the stage of breast cancer (Stickeler *et al.*, 1999). If SRSF3 is elevated above the normal tissue specific threshold it can promote tumour development and tumour maintenance. This is mediated by SRSF3's role in regulating the expression and alternative splicing of key proteins in the

cell cycle especially the G2/M phase transition and apoptosis (Jia *et al.*, 2010). SRSF3 plays not only a role in alternative splicing, but also in transcription (Cui *et al.*, 2008), RNA processing (Park and Jeong, 2016) and translation (Kim *et al.*, 2014; Park and Jeong, 2016). One of its best studied targets is the tumour suppressor p53. Decreased levels of SRSF3 cause the increased inclusion of exon i9 which causes the production of the p53 splice variant p53 $\beta$ , which is responsible for cellular senescence activity (Tang *et al.*, 2013).

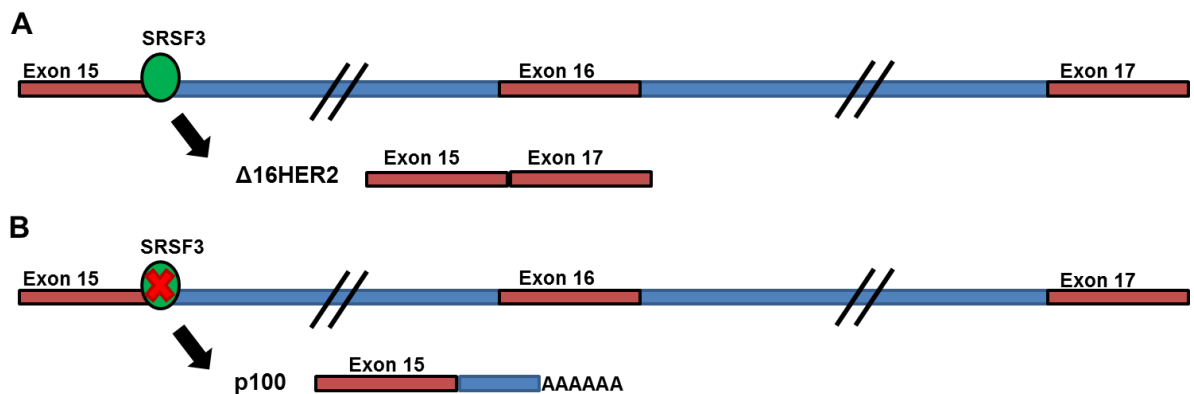


**Figure 3.23: The effect of SRSF3 on the splicing of p100 and  $\Delta 16$ HER2.**

A, if SRSF3 is present and binds to the HER2 mRNA  $\Delta 16$ HER2 is produced. Binding site is based on (Gautrey *et al.*, 2015). B, If SRSF3 does not bind to exon 15 the expression of p100 is increased.

In this study previous findings of our research group, that showed SRSF3 affects the alternative splicing of HER2 splice variants  $\Delta 16$ HER2 and p100 were reproduced (Gautrey *et al.*, 2015). SRSF3 was shown to inhibit exon 16 recognition and partial intron 15 retention (Figure 3.21). This is likely mediated by the previously identified SRSF3 binding site in exon 15 (Gautrey *et al.*, 2015). Although SRSF3 seemed to bind the exon 16 splice region in the RNA chromatography assay, SRSF3 had no effect on the  $\Delta 16$ HER2-minigene splicing. The reduced size of the  $\Delta 16$ HER2-minigene, the absence of chromatin factors or other factors associated with normal endogenous HER2 might cause SRSF3 to not interact with  $\Delta 16$ HER2-minigene. It is also possible that the binding of SRSF3 in the RNA chromatography assay was unspecific and SRSF3 act through the binding motif in exon 15. Indeed a similar mode of

action has been observed in Caspase 2 mRNA, where SRSF3 was shown to bind exon 8 and promote the skipping of downstream exon 9 (Jang *et al.*, 2014).

#### **The role of hnRNP K in alternative splicing of $\Delta 16$ HER2**

The ~66 kDa sized hnRNP K is comprised of three DNA-RNA binding homology domains, a K-protein-interactive region and a C-terminal protein kinase-binding domain (Dejgaard and Leffers, 1996) [reviewed in (Barboro *et al.*, 2014)]. It also contains a nuclear-localisation signal and a nuclear shuttling domain that are important for its functions in the nucleus and cytoplasm (Barboro *et al.*, 2014). HnRNP K has been shown to be highly expressed in a number of cancer types, the studied cancer types did not include breast cancer (Barboro *et al.*, 2014). However, in a small cohort of human breast tumour samples hnRNP K was expressed at higher levels in high grade human breast tumours than in low grade tumours (Mandal *et al.*, 2001). HnRNP K has been shown to play a role in transcription (Takimoto *et al.*, 1993; Zheng *et al.*, 2016), RNA processing (Venables *et al.*, 2008; Song *et al.*, 2016) and translation (Ostareck *et al.*, 1997; Notari *et al.*, 2006). Until 2008 only few hnRNP K regulated alternative splicing events had been described. In the large scale study by Venables and colleagues, they studied alternative splicing events that are regulated by hnRNP proteins (Venables *et al.*, 2008). They found hnRNP K to be associated with the largest number alternative splicing events out of the studied hnRNP proteins. In general, downregulation of hnRNP K was shown to promote both exon skipping and exon inclusion events. Specific targets of hnRNP K include apoptotic peptidase activating factor 1 (APAF1) and protein tyrosine kinase 2 (PTK2B), where it acts as an exon recognition factor, and NLR family, pyrin domain containing 1 (NALP1) where it is an exon silencer (Venables *et al.*, 2008). In the alternative splicing event producing  $\Delta 16$ HER2 hnRNP K was found to act as an exon silencer.

Additionally, hnRNP K has been shown to regulate splice site selection of Bcl-x, where it inhibits the production of the pro-apoptotic Bcl-x<sub>s</sub> splice form (Revil *et al.*, 2009). Another study showed hnRNP K was able to regulate intron retention of glucose-6-phosphate dehydrogenase (G6PD) in response to starvation signals.

In this study hnRNP K was found to bind C-rich motifs in the exon and promote intron retention, leading to a G6DP alternative splice variant that is not translated. In our work hnRNP K was also shown to promote the retention of partial intron 15 and thereby the production of p100. However, exon 16 does not contain the type of C-rich motif that has been identified to bind hnRNP K. It was also shown that SRSF3 and hnRNP K can compete for the same motif (defined pre-mRNA sequence) (Cyphert *et al.*, 2013). Indeed, the functional hnRNP K binding site (mutant 4) which was identified by mutagenesis, was also *in-silico* predicted to be a binding site of SRSF3. However SRSF3 does not affect splicing of the  $\Delta$ 16HER2-minigene model and therefore such a mechanism could not be detected in this system. It can only be speculated as to whether SRSF3 might be able to substitute hnRNPK at this binding site in endogenous HER2.

#### **The role of hnRNPs F and H in alternative splicing of $\Delta$ 16HER2**

HnRNPs F and H are very closely related proteins, sized 53 and 56 kDa, respectively (Honore *et al.*, 1995). They are expressed in most normal tissues. HnRNP F is predominantly found located in the cytoplasm and hnRNP H is more commonly found in the nucleus (Honore *et al.*, 2004). HnRNPs H and F have been found overexpressed in some cancers (Honore *et al.*, 2004; Balasubramani *et al.*, 2006) and have been implied in malignant transformation (Balasubramani *et al.*, 2006; Lefave *et al.*, 2011). Not all studies agree that hnRNPs F and H are bad prognostic factors in cancer, in one study hnRNP H nuclear staining was correlated with good prognosis in colorectal cancer (Hope and Murray, 2011). These two splicing factors, like the previously discussed splicing factors, are not only involved in alternative splicing (Uren *et al.*, 2016) but also in transcription (Wei *et al.*, 2005), mRNA transport (White *et al.*, 2012) and translation (Song *et al.*, 2012). In the study by Venables it was found that only ~ 30% of alternative splice events that were regulated by one hnRNP (F or H) were also regulated by the second hnRNP (F or H). In 80% of hnRNP F/H mediated splicing events identified by this study, hnRNP F/H act as exon defining factors (Venables *et al.*, 2008). This coincides with the findings of this thesis, where hnRNP F/H was observed to promote recognition of exon 16 in

HER2. In the initial work with Dr Gautrey, only knockdowns of hnRNP H were performed and an effect on p100 splicing was not observed (Gautrey et al., 2015). However as the work was extended to also include hnRNP F, hnRNP F/H was found to not only inhibit  $\Delta$ 16HER2 but also p100 production. In the mutagenesis work it was not possible to identify the binding site of hnRNP F/H. Given the binding pattern observed in the RNA chromatography assay and the *in-silico* predictions hnRNP F/H was expected to bind in the intron surrounding the exon 16. As expected nothing indicates binding to the exon, as other studies have found binding to the exon to be associated with exon skipping (Rahman et al., 2015). HnRNP F/H has mostly been suggested to bind to the intron containing the 5'ss to promote the recognition of the upstream exon, but it has now also been found to act when binding to the upstream intron containing the 3'ss (Wang et al., 2012b). Additionally, hnRNP F/H has been suggested to define an exon by binding to the beginning and end of an intron, thereby define the intron and promoting the correct splicing of both the intron and exon (Martinez-Contreras et al., 2006). Indeed there is a large cluster of hnRNP F and H binding sites predicted at the beginning of intron 15 (Figure 3.24). If hnRNP F/H bound the intron at these predicted binding sites as well as at the end of intron 15 it would possibly improve the intron 15 recognition and thereby also promote the recognition of exon 16. HnRNP F/H also inhibits the production of p100, therefore if hnRNP F/H acts through defining intron 15 it could impair both p100 and  $\Delta$ 16HER2 production.

We suggest here that hnRNP F/H might bind to a sequence that overlaps with the branch point upstream of exon 16. One might assume that binding of hnRNP F/H at this site would mask the branch point and impair the assembly of the spliceosome. However, hnRNP F/H has been shown in the alternative splicing of RE1-silencing transcription factor (REST) to bind near the 5'ss of the alternative exon N50 and be displaced by the spliceosome assembly factor U2AF65 (Ortuno-Pineda et al., 2012). Therefore hnRNP F/H could similarly bind across the branch point and be displaced if necessary by SF1/BBP or U2AF. Here the most likely binding sites for hnRNP F/H based on experimental evidence, *in-silico* predictions and the current subject knowledge were studied. However there are also further potential binding sites further away in the introns 15 and 16.

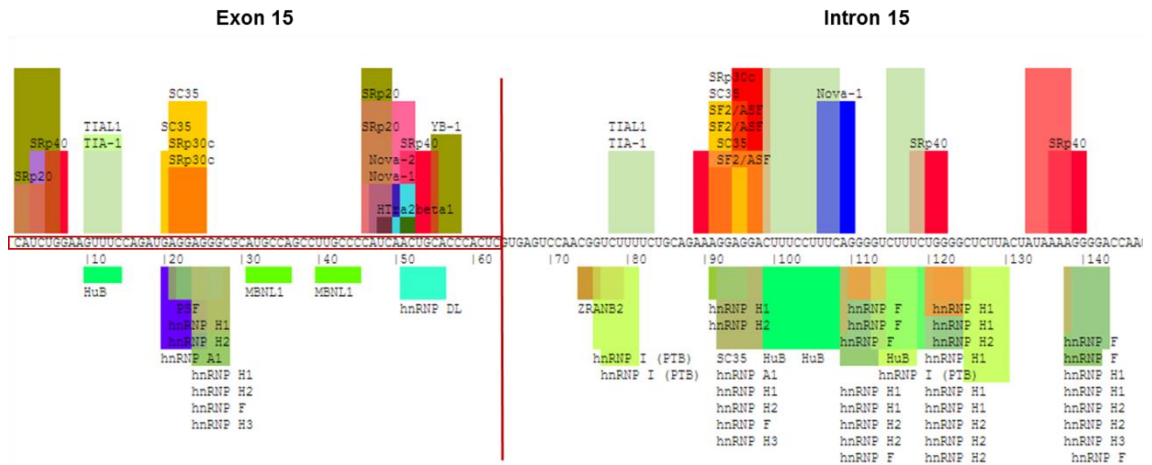


**Figure 3.24: Splicing factor binding motifs at the exon 15/intron 15 boundary of HER2 pre-mRNA.**

The image shows the splicing factors predicted to bind the boundary sequence of exon 15 and intron 15. The red line indicates the exon intron boundary. A large number of hnRNP H and F binding sites have been predicted for this part of intron 15. The image was generated by SpliceAid (<http://www.introni.it/splicing.html>).

### 3.5.2. Feedback-loop between HER2 and its splicing regulators?

HER2 is known to regulate a complex signalling network, the two main pathways being the ras-MAPK and the PI3K-AKT pathways. These pathways are known to have complex crosstalk and feedback mechanisms [reviewed in (Dittrich *et al.*, 2014)]. Unpublished work by Dr Unal indicated the regulation of the hnRNP family of splicing factors through the ras-MAPK signalling pathway. This observation and studies showing hnRNP K could be induced by growth factor signalling, lead us to question whether HER2 mediated signalling could regulate the four identified splicing factors (SRSF3, hnRNP H, hnRNP F, hnRNP K) in our cell model (Mandal *et al.*, 2001; Ciarlo *et al.*, 2012). A transient knockdown of HER2 was performed to investigate the effect on the gene expression of the splicing factors. No change in the expression level of SRSF3 could be observed, but for the expression of hnRNPs H, F and K a statistically significant increase was observed. Still the change was relatively small and should not be considered conclusive. They also contradict the previous observations in other cell lines that hnRNP K is induced by growth factor

signalling (Mandal *et al.*, 2001; Ciarlo *et al.*, 2012). SKBR3 cells were only used by Mandal *et al.* for initial experiments, where they observed that inhibiting HER2 with a monoclonal antibody decreased hnRNP K mRNA levels slightly. Due to the small changes observed, SKBR3 cells were not used in the further experiments in that study (Mandal *et al.*, 2001). To study any changes to the protein level of the splicing factors, SKBR3 cells were treated with the HER2 tyrosine kinase inhibitor lapatinib. As expected treatment with lapatinib inhibited ras-MAPK and PI3K-AKT signalling. The splicing factor protein levels were measured over 24 h and a small downregulation of all splicing factors after 24 h lapatinib treatment was observed. The work by Unal *et al.*, suggested that the signalling pathways might additionally affect the phosphorylation status of the splicing factors. However, currently there is no phospho-hnRNP F/H antibody available. To assess the phosphorylation status of the splicing factors without specific antibodies, a column based phospho-protein separation kit could be used. As the last batch of hnRNP K and F/H antibodies showed a high number of unspecific bands, new antibodies would be needed to produce meaningful results in such an assay.

From these findings it can be conclude that in the HER2-high SKBR3 cell line HER2 signalling might slightly downregulate the hnRNPs K, F and H at the mRNA level. However, it induces the expression of all four splicing factors at the protein level. It will be interesting to further study the effect of PI3K-AKT and ras-MAPK signalling on phosphorylation of splicing factors, as studies have shown that AKT mediated phosphorylation of splicing factors, namely hnRNP L and A2 can be an important step in alternative splicing regulation (Guha *et al.*, 2010; Vu *et al.*, 2013).

#### **3.5.3. Progesterone induced expression of HER2**

Breast cancer as a predominantly female disease, has been closely linked to the two main female reproductive hormones oestrogen and progesterone (*Breast Cancer, A Lobular Disease*, 2011). Recent research, that showed PR to regulate the function of ER- $\alpha$  in favour of a tumour inhibiting signalling pathway

(Mohammed *et al.*, 2015), has brought progesterone and progesterone receptor back into the focus of research. A number of studies have shown both oestrogen/ER and progesterone/PR to be part of a complex network of interactions and crosstalk with HER2 (Beguelin *et al.*, 2010; Diaz Flaque *et al.*, 2013; Giuliano *et al.*, 2013). As previously mentioned, recent research has shown oestrogen to affect the alternate splicing of the type 1 corticotropin-releasing hormone receptor (Lal *et al.*, 2013). This link between oestrogen and alternative splicing opens up a number of further possibilities as to how hormones might affect alternative splicing. Previous research in our group suggests that oestrogen does not affect *HER2* mRNA expression in breast cancer cell lines (unpublished). In light of the role of the new findings on the roles of progesterone and PR in breast cancer, we wished to investigate whether progesterone affects *HER2* expression and alternative splicing.

It was determined that 100 nM progesterone is the optimal dose for treatment of the ER/PR positive cell line MCF-7. A time dependent effect of progesterone on the expression of HER2 and  $\Delta 16$ HER2 was observed. Progesterone induced the expression of both HER2 variants from 6 h to 24 h of treatment, roughly peaking at 12 h. Both wild type HER2 and  $\Delta 16$ HER2 followed the same trend. The ratio between wild type HER2 and  $\Delta 16$ HER2 did not significantly change. Taking these findings together, this work shows that progesterone induces the expression of HER2, but does not alter the alternative splicing pattern. MCF-7 cells are rich in PR and low in HER2, therefore the significant, but relatively small effect on the expression raises the question of the importance of this interaction. This might be in part due to the dependence of the cell line on growth hormones and the extreme stress they suffer when starved in preparation to the progesterone treatment. Progesterone mediated effects on the transcription of splicing factors of HER2 are not likely to be observed in the 24 h time frame of this experiment. Simply extending the time period cannot be considered a good solution, as this would prolong the stress situation and is very likely to cause unspecific effects on splicing and expression.

#### **3.5.4. Summary**

In this chapter, four key splicing factors were identified, that regulate the  $\Delta$ 16HER2 splicing event. Of these SRSF3 and hnRNP K were shown to act as splicing silencers, inhibiting exon 16 recognition. At the same time SRSF3 inhibits p100 production, but hnRNP K promotes p100 production. Knockdowns of hnRNPs F and H were shown to have an additive effect on the splicing events studied here. HnRNP F/H was shown to act as splicing enhancers for both exon 15 and 16, inhibiting  $\Delta$ 16HER2 and p100 production. A  $\Delta$ 16HER2-minigene was successfully designed and constructed, and showed to be responsive to splicing factors hnRNPs K, F and H. However, the  $\Delta$ 16HER2-minigene was not responsive to SRSF3. This is likely due to the lack of exons upstream of exon 15, which may also prevent  $\Delta$ 16HER2-minigene from producing p100. Through mutagenesis of the  $\Delta$ 16HER2-minigene a number of predicted splicing factor binding sites were eliminated and one binding site for hnRNP K was identified.

Based on published (Mandal *et al.*, 2001; Ciarlo *et al.*, 2012) and unpublished (Dr. Unal) work it was decided to investigate a feedback loop between HER2 and its splicing factors. HER2 knockdown was observed to increase the mRNA expression of hnRNPs F, H, and K. However, only very small changes to the protein level of the splicing factors were observed.

At last, a potential effect of progesterone on *HER2* expression and alternative splicing was investigated. This was brought on by a recent study highlighting a new role of PR in breast cancer (Mohammed *et al.*, 2015). Indeed progesterone was observed to inducing HER2 expression, but there were no changes to the splicing ratio of  $\Delta$ 16HER2 and wild type HER2. The observed effect of progesterone on HER2 expression warrants further investigation.

### **3.5.5. Future work**

In this chapter it was possible to answer a number of questions, but it has also given rise to more questions and ideas. As has been discussed in the beginning of this chapter, all work on  $\Delta 16$ HER2 is based on the assumption that it is part of a full length *HER2* transcript. However, the PCR work showed a very faint first exon. Verification of the promoter and transcription start site would be of great interest. Additionally, little is known about the 3'UTR of *HER2* and any changes to its length and the poly(A) site used, could impact on its stability and processing.

After identifying key splicing regulators of the  $\Delta 16$ HER2 splicing event, the binding sites of these factors was investigated by mutagenesis. One predicted, but unlikely binding site for hnRNP F/H has to still be tested. In the here described work the main focus was on the immediate area surrounding exon 16. It would be of interest to further investigate G-tracts in introns 15 and 16, as those could act as hnRNP F/H binding sites. Further, investigation should be extended to the exon 15/intron 15 and intron 16/exon 17 boundaries. As exon 16 recognition is dependent on intron 15 and 16 recognition. Additional, interesting factors to consider are SNPs in the splicing region and such that overlap with splicing factor binding sites. It would be of interest to observe if these have an effect on the splicing mechanism or binding of splicing factors.

Although, the  $\Delta 16$ HER2-minigene used in this study has worked well it is an artificial system that cannot account for the more complex transcriptional processes and the normal working of cells. The next step would be to design antisense morpholino oligonucleotides that target splicing factor binding sites. There are a number of uses for this.  $\Delta 16$ HER2 has been extensively studied with regards to its function (Kwong and Hung, 1998; Siegel *et al.*, 1999; Mitra *et al.*, 2009; Sasso *et al.*, 2011; Castagnoli *et al.*, 2014), however in all studies cells were transfected with  $\Delta 16$ HER2 plasmids or  $\Delta 16$ HER2 transgenic mice models were used. To account for RNA-processing associated effects and to produce a less artificial system it would be suggested to use alternative techniques. Using antisense morpholino oligonucleotides or a CRISPR/Cas9 system the *HER2* splicing could be switched in favour of  $\Delta 16$ HER2 production.

### Chapter 3: Investigating the regulation of the $\Delta 16$ HER2 splicing event

This could be a less artificial model to use for studying downstream signalling and drug resistance as well as migration and its behaviour in a 3D environment. Switching the splicing from  $\Delta 16$ HER2 to wild type HER2 or even the tumour suppressor p100 on the other hand would be of great interest for a potential therapy.

Further, the ability of HER2 signalling to regulate splicing factor expression was investigated. In a next step it would be of interest to study the impact of  $\Delta 16$ HER2 induced src signalling on the splicing factors, especially in regard to the  $\Delta 16$ HER2 splicing event regulating factors.

For future work it would be very interesting to consider different models for HER2-positive breast cancer. In a recent publication  $\Delta 16$ HER2 levels were assessed in a number of breast cancer cell lines (Turpin *et al.*, 2016). The SKBR3 cell line used for most of this study, was shown by Turpin and colleagues to have one of the lowest  $\Delta 16$ HER2/total HER2 ratios of all HER2-positive breast cancer cell lines studied. The highest  $\Delta 16$ HER2/total HER2 ratio in a HER2-positive cell line was observed for ZR7530, where the level of  $\Delta 16$ HER2 was ~12% of total HER2 transcripts. In this study a number of basal and luminal cell lines showed similar levels of  $\Delta 16$ HER2. The overall highest  $\Delta 16$ HER2/total HER2 ratio was observed in the basal cell line SUM149PT. However, the total  $\Delta 16$ HER2 expression level was the highest in HER2-positive cell lines, especially in SUM225CWN (Turpin *et al.*, 2016). The high  $\Delta 16$ HER2/total HER2 ratio in basal cell lines is interesting, as  $\Delta 16$ HER2 tumours in mice have shown a very heterogenous histology and their expression profile was found to be typical for ER-negative, high-grade metastatic primary tumours, not HER2 positive tumours (Alajati *et al.*, 2013). This opens up the possibility of a new role of  $\Delta 16$ HER2 in triple negative breast cancers.

Another avenue of research is based on the work by He *et al.*, where it was shown that miRNA-155 binds in the coding region of the *HER2* mRNA (He *et al.*, 2016). This binding sequence is located in exon 17, within few nucleotides of exon 16. This study also showed that miRNA-155 expression is induced by the therapeutic antibody trastuzumab (He *et al.*, 2016). Our work suggests that the secondary structure of  $\Delta 16$ HER2 might obscure the miRNA-155 binding

### Chapter 3: Investigating the regulation of the $\Delta$ 16HER2 splicing event

site.  $\Delta$ 16HER2 expressing cells have been shown to be resistant to trastuzumab treatment in cell line models (Castiglioni *et al.*, 2006; Mitra *et al.*, 2009), the mechanisms however has remained unclear. The potential ability of  $\Delta$ 16HER2 to evade recognition by trastuzumab induced miR-155 could be a new mechanism of resistance in cell line models.

## Chapter 4: Characterising HER2 in human breast tumours

### 4.1. Introduction

In the previous chapter the mechanisms that regulate  $\Delta 16$ HER2 mRNA splicing were studied. In this chapter the focus lies on linking HER2 alternative splice variants to more clinically relevant aspects. HER2, as an important biomarker for breast cancer, is routinely clinically assessed to determine the subtype of breast cancer and to accordingly plan therapy. The HER2 status can be determined by a number of methods. Immunohistochemistry (IHC) is the most commonly used technique. It determines the protein expression and localisation in breast tumour tissue sections. Alternatively, fluorescence/chromogenic *in situ* hybridization (FISH/CISH) can be performed to determine *HER2* gene amplification. For all three methods a number of companies provide FDA approved reagents (Table 4.1). The methods can be performed on fresh, frozen or formalin-fixed paraffin-embedded (FFPE) tissue sections.

**Table 4.1: Table of FDA-approved HER2 assessment kits (FDA, 2016).**

Assay type	Product name	Company
<b>Immunohistochemistry</b>		
<b>Semi-quantitative IHC</b>	HercepTest™	DAKO
<b>IHC</b>	PATHWAY® Anti-HER2/Neu (4B5) Rabbit Monoclonal Primary antibody	Ventana Medical Systems Inc
<b>IHC</b>	InSite® HER2/Neu Kit	Biogenex Laboratories Inc
<b>Semi-quantitative IHC</b>	Bond Oracle™ HER2 IHC system	Leica Biosystems
<b>Fluorescence <i>in situ</i> hybridization</b>		
<b>FISH</b>	INFORM <i>HER2/Neu</i>	Ventana Medical Systems Inc
<b>FISH</b>	PathVysion® HER2 DNA Probe Kit	Abbott Molecular Inc
<b>FISH</b>	<i>HER2</i> FISH PharmDx™ Kit	DAKO
<b>Chromogenic <i>in situ</i> hybridization</b>		
<b>CISH</b>	SPoT-Light® <i>HER2</i> CISH kit	Life Technologies Inc
<b>CISH</b>	INFORM <i>HER2</i> dual ISH DNA probe cocktail	Ventana Medical Systems Inc
<b>CISH</b>	<i>HER2</i> PharmDx™	DAKO

Depending on the intensity and extent of IHC staining the tumours are grouped. If a tissue section is scored 0 or 1, the case is classified as HER2-negative. In case of a score of 2+, which is considered to be equivocal, the *HER2* gene amplification status will be determined. The tumour is classified as HER2-positive with a score of 3+. The majority of tumours are grouped accordingly and therapy can commence (Rakha *et al.*, 2015).

These current, and routinely used, methods of HER2 assessment have a relatively high rate of accuracy [reviewed in (Sapino *et al.*, 2013)]. However two challenges remain, these are tumour heterogeneity and deviations between HER2 assessment methods (Miller *et al.*, 2004; Vance *et al.*, 2009; Sapino *et al.*, 2013; Carvajal-Hausdorf *et al.*, 2015)]. *HER2* genetic heterogeneity in a tumour was defined as a tumour with 5-50% of infiltrating tumour cells with a 2.2 ratio of *HER2* gene amplification to chromosome 17 centromere (HER2/CEN-17) (Vance *et al.*, 2009). The *HER2* genetic heterogeneity has been reported for 5% (Vance *et al.*, 2009) to 15% (Ohlschlegel *et al.*, 2011) of tested tumours. They are most common in HER2 (2+) equivocal breast cancer cases and have been associated with an overall negative *HER2* amplification status, but a significant number of cells with *HER2* amplification (Ohlschlegel *et al.*, 2011). It has been proposed that HER2 heterogeneity should be subdivided into categories (Sapino *et al.*, 2013). The first group of tumours is characterised by the presence of two distinct populations of cells, one clearly HER2-negative and the other HER2-positive. This group would be associated with the discordant results between IHC and FISH results, observed by Miller and colleagues. They found focal *HER2* amplification to be present in 21% of IHC 0-1/FISH-amplified and 30% of IHC 2+/FISH amplified breast tumour cases (Miller *et al.*, 2004). The second group is characterized by dispersed presence of HER2-positive cells in HER2-negative breast tumours (Sapino *et al.*, 2013). The implication of focal and diffuse *HER2* amplification on trastuzumab therapy has been assessed in a sub-study of the N9831 study. They reported that trastuzumab therapy can be beneficial for some patients with both focal and diffuse *HER2* amplification [reviewed in (Oakman *et al.*, 2010)].

In the introduction (section 1.10), the occurrence of HER2 therapy resistance and the lack of understanding the underlying mechanisms were discussed

(Vogel *et al.*, 2002; Nagy *et al.*, 2005; Junttila *et al.*, 2009; Garrett and Arteaga, 2011; Hurvitz *et al.*, 2013). When HER2 status is clinically determined the expression of HER2 protein variants is not taken into consideration. A recent study showed antibodies for the extracellular domain (ECD) and intracellular domain (ICD) of HER2 to give discordant results in 15% of assessed breast tumours. This study was also able to associate expression ratios between ECD and ICD with the length of disease free survival. Showing a high ECD/ICD level to be associated with an increased disease free survival (Carvajal-Hausdorf *et al.*, 2015). One could propose that increased levels of ECD mean high level of secreted HER2, such as HER2 splice variants p100 and Herstatin.

Furthermore, one could hypothesize that there are cases of breast tumours which are classified as HER2-positive, but express a substantial amount of other HER2 protein variants that will not respond to anti-HER2 therapies. Alternatively, tumours with low levels of wild type HER2, but elevated levels of undetected HER2 protein variants could be classified as HER2-negative. This could prevent patients from being offered and treated with anti-HER2 therapies, although they might well benefit from receiving this treatment.

The work presented in this chapter is part of a larger program of research investigating the importance of HER2 splice variants in breast cancer patients. To assist with the research we have obtained a well characterised cohort of breast tumour samples from the Breast Cancer Now Tissue Bank. The aim of the overall study is to assess differences between HER2 antibodies for different epitopes in IHC on breast tumours and compare these with the *HER2* gene amplification status measured by CISH. Those observations will be combined with quantitative measurement of HER2 splice variant expression in the same cohort of breast tumours and correlated with the clinical data available for the patients.

## 4.2. Aims

The aims of this chapter were to:

- Characterise HER2 protein expression and localisation in a cohort of breast tumour samples
- Assess *HER2* gene amplification by CISH in a small cohort of breast tumour samples
- Compare HER2 protein expression and *HER2* gene amplification
- Characterise breast tumours with discordant IHC and CISH results
- Study the HER2 splice variants levels in discrepant breast tumour samples

## 4.3. Specific methodology

### 4.3.1. Immunohistochemistry (IHC)

As part of a larger study, HER2 protein expression and localisation in human breast cancer tissue samples was assessed. Tissue sections from grade 3 invasive ductal carcinomas were received from the Breast Cancer Now Tissue Bank, which collected them with full patient consent and ethical approval under the number: BCNTB000027. For each breast cancer group, ER+/HER2+, ER+/HER2-, ER-/HER2+ and ER-/HER2-, tumour sections from 10 cases were received. Additionally, tissue samples from reduction mammoplasty, 10 cases, were received. From each tumour block serial sections were received from the Breast Cancer Now Tissue Bank and stained with a C-terminal [HER2/ErbB2 antibody #2242] (Cell Signalling) and an N-terminal HER2 antibody [HER2/ErbB2 (D8F12) XP™ Rabbit Antibody #4290] (Cell Signalling) as well as the HercepTest™ (Dako). The formalin-fixed paraffin embedded (FFPE) sections were immunostained by Research Technician Grant Richardson and initially analysed by our collaborator clinical pathologist Dr Helen Kourea (Associate Professor of Pathology, University of Patras, Patras, Greece).

**4.3.1.1. IHC with C- and N-terminal HER2 antibodies**

Forty cases were studied. For each tissue 4 µm thick sections were cut. Known HER2 3+ tumour section positive controls (provided by the Pathology Department at the University of Patras, Patras, Greece) as well as no primary antibody controls were included. As the Breast Cancer Now Tissue Bank sections were coated in a very thick layer of wax to preserve the tissue, the slides were incubated for 1 h at 60°C to help remove the wax. The sections were then dewaxed using xylene and rehydrated through graded ethanol (99%-70%). They were then treated with a water/hydrogen peroxide block for 10 min and rinsed in water. Depending on the antibody the appropriate pre-treatment was used (Table 4.2.).

**Epitope retrieval: citrate buffer/microwave pre-treatment**

The slides were microwaved for 5 minutes in citrate buffer pH 6, the citrate buffer was exchanged for fresh hot citrate buffer and the slides microwaved again for 5 min. The sections were left to cool in fresh hot citrate buffer. After washing with water the slides were kept in TBS pH 7.6.

**Epitope retrieval: EDTA buffer/pressure cooker pre-treatment**

The pressure cooker was filled with 1.5 L of EDTA buffer pH 8. After the buffer was brought to a boil, the slides were immersed and the lid locked in place. The cooker was kept on heat for 2 min after pressure was reached. The pan was rapidly cooled under water and the slides were removed. The slides were washed under running water.

**Table 4.2: Table detailing the epitope retrieval method and dilution of the antibodies.**

	<b>C-terminal [HER2/ErbB2 antibody #2242] Lot 8 (Cell Signalling)</b>	<b>N-terminal HER2 antibody [HER2/ErbB2 (D8F12) XP™ Rabbit Antibody #4290]] Lot 2 (Cell Signalling)</b>
<b>Pre-treatment</b>	Citrate microwave pre-treatment	EDTA and pressure cooking
<b>Antibody concentration</b>	1/50	1/50

### **Antibody incubation and staining procedure**

For the following steps the rabbit IgG VECTASTAIN Elite<sup>®</sup> ABC kit (VECTOR Laboratories) was used. The sections were incubated in TBS pH 7.6 for 5 min, following this they were blocked with goat serum for 10 min. The blocking serum was replaced by the appropriate primary antibodies in TBS pH 7.6, except for the no primary antibody control, where the primary antibody was replaced by TBS and incubated, overnight.

The slides were then washed in TBS pH 7.6 twice for 5 min. Next, all slides were covered with the anti-rabbit secondary antibody (VECTASTAIN ABC kit) for 30 min. The slides were washed as before and the tertiary antibody (VECTASTAIN ABC kit) was added and incubated for 30 min. The slides were washed again.

The VECTOR<sup>®</sup> NovaRED<sup>™</sup> peroxidase substrate kit (Vector Laboratories) was used to stain the tissue sections at RT. After 4 min staining, the slides were washed in water. Next they were counterstained in Mayers Haematoxylin (Haematoxylin 2g, Potassium alum 100g, Sodium alum 0.4g, Chloral hydrate 100g, citric acid 2g in 2 L distilled water) for 30 sec. This was followed by washing of the slides under running water. The slides were dehydrated through graded alcohols (70%-99%) and mounted with DPX mounting medium (Sigma Aldrich).

#### **4.3.1.2. HercepTest<sup>™</sup>**

The staining of the matched forty cases was performed using the HercepTest<sup>™</sup>. As in the previous IHC staining protocol, HER2 3+ graded tumour section positive controls (provided by the Pathology Department at the University of Patras, Patras, Greece) and no primary antibody controls were included in every experiment. The staining was performed according to the manufacturers protocol.

Briefly, the tissue slides were deparaffinised in xylene and then placed in absolute ethanol. Next they were incubated twice in 95% ethanol for 3 min and washed in distilled water. The sections were then immersed in the pre-heated

(to 95-99 °C) Epitope Retrieval Solution and incubated for 40 min at 95-99 °C. The slides were allowed to cool in the Epitope Retrieval Solution for 20 min at RT. They were then rinsed in diluted Wash Buffer. After tapping off excess buffer and carefully removing any remaining liquid around the tissue, the tissue section was encircled with a Dako Pen. Three drops of Peroxidase-Blocking Reagent were added to cover the specimen and incubated for 5 min. The specimens were gently rinsed with distilled water and placed in fresh buffer. Excess buffer was taped off and the slides wiped as before. Specimens were covered with 3 drops of Anti-HER2 Protein or Negative Control Reagent and incubated for 30 min. Again they were rinsed with Wash Buffer and placed in fresh buffer. The excess buffer was taped off and the slides wiped. The specimens were next covered with 3 drops of Visualization Reagent and incubated for 30 min. The slides were rinsed and wiped as before. The specimens were then covered with 3 drops of the Substrate-Chromogen Solution (DAB). After 10 min incubation, the slides were gently rinsed with distilled water. The slides were counterstained with hematoxylin and rinsed in distilled water. Lastly the slides were mounted and a coverslip applied.

#### **4.3.1.3. Scoring of immunohistochemistry (IHC)**

The sections were assessed according to the standard recommendation for HER2 assessment in breast cancer, depicted by figure 4.1 (Rakha *et al.*, 2015). A score of 0 was assigned if no membrane staining or only incomplete membrane staining in <10% of invasive tumour cells was observed; 1+ was assigned for faint incomplete membrane staining of >10% of tumour cells. Both scores are considered HER2-negative. The score of 2+ was given when a weak to moderate complete membrane staining was observed in >10% of tumour cells or strong complete membrane staining in  $\leq 10\%$  of tumour cells. This score is considered borderline and a second test such as FISH or CISH for *HER2* gene amplification should be performed. If the borderline scoring remains an alternative tumour section should be assessed. A HER2-positive or 3+ scoring was given to tumour sections with a strong (intense and uniform) complete membrane staining in >10% of invasive tumour cells.

The tissue sections were examined and scored by our collaborator Dr Helen Kourea (University of Patras, Patras, Greece). Images were taken at a number of magnifications in the clinical pathology at Royal Victoria Infirmary, Newcastle with a BX51 Olympus microscope, by Dr H. Kourea. Some images were also taken on a BX43 laboratory microscope (Olympus).

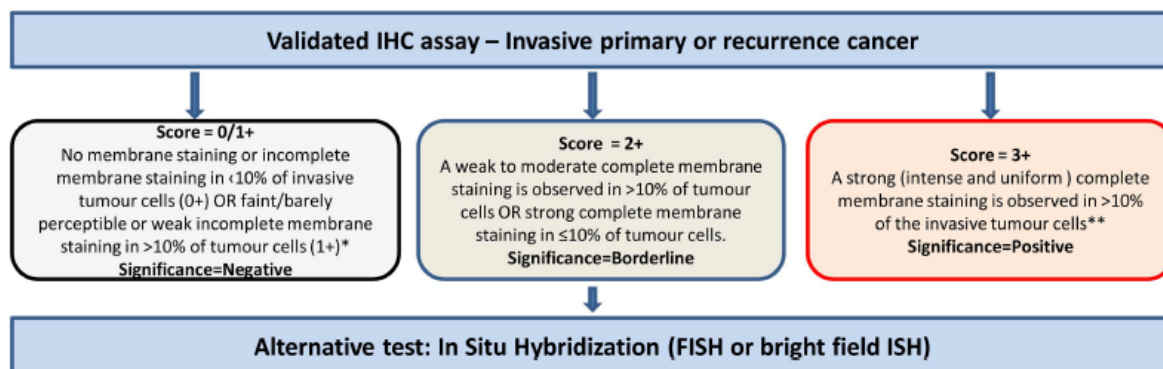


Figure 4.1: Immunohistochemistry scoring scheme for HER2 status in breast tumours.

Adapted from (Rakha *et al.*, 2015).

### 4.3.2. HER2 chromogenic in-situ hybridisation (CISH)

A total of 19 slides were stained using the *HER2* CISH pharmDx kit (Dako) (Table 4.3). These tissue sections were chosen as they had been identified as discrepant cases, in regard to the results obtained by the three different IHC antibodies, by Dr H. Kourea. Additionally, cases were included which showed no discrepancy to initial clinical assessment.

The *HER2* CISH pharmDx kit stains tissue sections for the *HER2* gene with a red chromogenic signal and the centromeric region of chromosome 17 with a blue chromogenic signal. The *HER2* probe is a Texas Red-labeled DNA probe that covers a 218 kb region which includes the *HER2* gene on chromosome 17. A mixture of fluorescein-labeled peptide nucleic acid probes were used to target the centromeric region of chromosome 17 (CEN-17). The fluorescent probe signals were converted to chromogenic signals. The probes were bound by antibodies; anti-FITC conjugated with horseradish peroxidase (HRP) and anti-Texas Red conjugated with alkaline phosphatase (AP). Incubation with the

substrates, Red and Blue Chromogen solutions yielded the red and blue signals at the probe site.

The 19 stained tissue sections included a primary probe negative control and two HER2 3+ positive controls (provided by the Pathology Department of the University of Patras, Patras, Greece). The tissue sections used here were derived from the same tumours as used in section 4.3.1 for IHC. The tissue sections were provided by the Breast Cancer Now Tissue Bank and had been previously clinically assessed. Their original grading is indicated in table 4.3. Four samples were originally grouped as ER/HER2+ (group 2), 3 each were grouped ER/HER2- and ER+/HER2- (group 3 and 4). Five samples were grouped ER-/HER2+ (group 5). Additionally, one section from a reduction mammoplasty was included. Similar to the IHC staining here too 4 µm sections were used.

**Table 4.3: List of breast cancer tissue sections used for CISH.**

<b>Group</b>	<b>IHC-ID</b>
<b>Group 2</b> ER+, HER2+ Grade 3 <b>Primary</b> NST/IDC	IHC-1
	IHC-2 *
	IHC-3
	IHC-4
<b>Group 3</b> ER-,HER2- Grade 3 <b>3 Primary</b> NST/IDC	IHC-5
	IHC-6
	IHC-7
<b>Group 4</b> ER+, HER2- Grade 3 <b>Primary</b> NST/IDC	IHC-8
	IHC-9
	IHC-10
<b>Group 5</b> ER-, HER2+ Grade 3 <b>Primary</b> NS/IDC	IHC-11
	IHC-12
	IHC-13
	IHC-14
	IHC-15
<b>Reduction mammoplasty</b>	IHC-16
<b>Positive control</b>	IHC-C1
	IHC-C2
<b>No primary antibody</b>	IHC-N1

The '\*\*' sample was not considered discrepant by IHC.

#### Chapter 4: Characterising HER2 in human breast tumours

The staining was performed according to the manufacturer's protocol. Briefly, the tissue slides were incubated at 60°C for 1h, then deparaffinised in a xylene bath and rehydrated stepwise in ethanol baths, last placed into Wash Buffer 1. For the pre-treatment a microwave oven was used. The slides were placed into a plastic jar filled with pre-treatment solution and microwaved 2 x 5 min. Then the slides were placed into a second preheated jar of pre-treatment solution and left to cool under light agitation for 15 min. The slides were then washed twice with Wash Buffer 1. After removal of any excess Wash Buffer 1 from the tissue sections, 5 drops of ice-cold pepsin were added to each slide. The slides were then incubated at 37°C for 2 min. The pepsin was removed and the tissue sections washed twice with Wash Buffer 1. Next the sections were dehydrated stepwise in ethanol baths from 70-95%. The slides were then left to air dry. Using a fume hood the HER2/CEN-17 Probe Mix was put onto the middle of the tissue section, a glass coverslip was placed on top and all air bubbles removed. Coverslip Sealant was used to seal the coverslip. The slides were then placed in a humid chamber and denatured for 15 min at 82°C. Hybridization with the probes was allowed to occur, with the slides incubating overnight at 45°C overnight in a humid chamber.

Jars of Stringent Wash Buffer were preheated in a water bath to 65 ( $\pm 2$ ) °C. After removing the slides from the hybridisation chamber, the Coverslip Sealant and the cover slips were removed. The slides were then incubated in the Stringent Wash Buffer at 65 ( $\pm 2$ ) °C for exactly 10 min. The slides were then placed in Wash Buffer for 3 minutes at RT, the wash was repeated. The wash was then repeated with Wash Buffer 2.

Excess buffer was removed and Peroxidase Block was added onto the slides. After 5 min incubation the slides were washed twice in Wash Buffer 2. Again, excess buffer was removed and CISH Antibody Mix was added onto the slides. After 30 min incubation in a humid chamber, the slides were washed twice in Wash Buffer 2.

The excess buffer was removed and the tissue sections covered with Red Chromogen Solution. After 10 min incubation in a humid chamber, two washes in Wash Buffer 2 were performed. The specimen were covered with Blue Chromogen Solution and incubated for 10 min, after excess buffer was

removed. The slides were washed twice in Wash Buffer 2. The tissue sections were counterstained, by immersing them for 1min 10 sec in hematoxylin. The slides were then rinsed in Wash Buffer 2 and washed for 5 min in fresh Wash Buffer 2. This was followed by two 3 min washes in water. The sections were dried at 37°C for approximately 30 min. The coverslips were mounted with CISH Mounting Medium and left to dry at RT for ~ 1 h. The slides were stored under dry conditions until analysis.

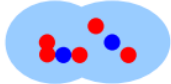
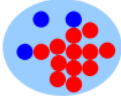
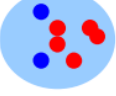
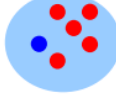
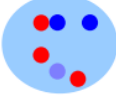
### **4.3.3. Scoring of HER2 CISH**

The whole tissue sections were scanned by the Leica SCN400 Slide Scanner and Autoloader system in the Newcastle Biobank facility. Areas of interest were identified and images up to 40 x magnification were gained from the scanning images. Matching images were taken to ones obtained by IHC. To count the exact number of stained probes per cell the slides were observed at 40 x magnification on a BX43 laboratory microscope (Olympus). The manufacturers signal counting guide (Figure 4.2) was used to guide scoring of tissue sections. Twenty distinct nuclei were counted from the main tumour area. For each the red *HER2* gene signals and the blue chromosome 17 centromere signals were counted. The *HER2*/Cen-17 signal ratio is calculated. In addition the average *HER2* signal was taken into consideration.

The final *HER2* score was assigned according to the updated (2013) recommendation for *HER2* assessment in breast cancer in the UK and USA (Rakha *et al.*, 2015). A *HER2*/Cen-17 signal ratio <2.0 and an average *HER2* copy number <4.0 signals per cell should be considered as *HER2* negative. According to the *HER2* CISH pharmDx™ (DAKO) signal counting guide, which is based on the pre-2013 recommendations, a *HER2*/Cen-17 signal ratio between 1.80 - 2.20 is considered borderline and another 20 nuclei were counted. Rakha *et al.* recommend additional cells to be counted for a ratio between 1.80 - 1.99. Additionally, they consider a ratio of <2.0 with an average *HER2* copy number between 4.0 - 6.0 as borderline (Rakha *et al.*, 2015). Borderline cases should be re-examined with a second method and possibly an

## Chapter 4: Characterising HER2 in human breast tumours

additional section of the tumour should be studied. The tumour is considered HER2 positive by the *HER2* CISH pharmDx™ signal counting guide with a ratio above 2.2. The new guidelines suggest the cut off to be at 2.0. Furthermore, they suggest to consider cases with a *HER2* copy number  $\geq 6.0$ , independent of the *HER2*/Cen-17 ratio to be HER2-positive.

	Do not count. Nuclei are overlapping, not all areas of nuclei are visible.
	Two blue signals, do not score nuclei with signals of only one color.
	Count as 3 blue and 12 red signals (cluster estimation).
	Count as 2 blue and 1 red signal. Signals that appear to have more than one centre of origin, should be counted as two signals.
	Do not count (over- or under digested nuclei) Missing signals in the centre of nuclei.
	Count as 2 blue and 5 red signals. Signals that appear to have more than one centre of origin, should be counted as two signals.
	Count as 1 blue and 5 red signals.
	Count as 3 blue (1 blue out of focus) and 3 red signals.
	Cluster of red signals hiding blue signals. Go to a higher level of magnification to confirm presence or absence of blue signals. In case of doubt, do not count.

**Figure 4.2: *HER2* CISH pharmDx™ (DAKO) signal counting guide.**

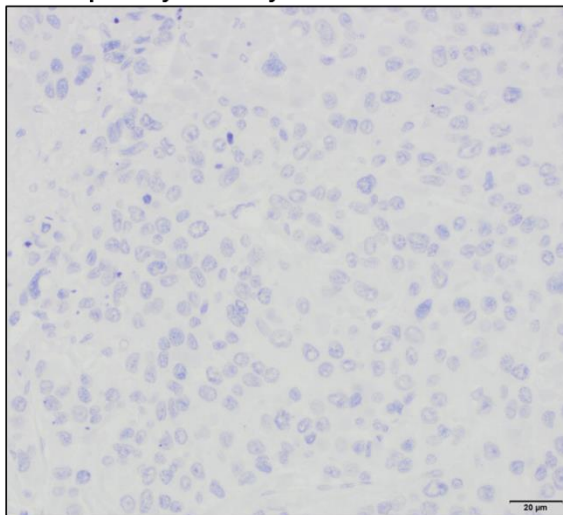
The red dots indicate the *HER2* gene amplification signals and the blue dots the centromeric region of chromosome 17 (CEN-17) signals. The image was extracted from *HER2* CISH pharmDx™ signal counting guide (DAKO).

#### 4.4. Results

##### **4.4.1. Immunohistochemistry for HER2 protein expression and localisation in human breast tumours**

The serial tissue sections from 40 tumours from the Breast Cancer Now Tissue Bank as well as HER2 3+ graded positive controls were stained with the C-terminal and N-terminal antibodies as well as the HercepTest™. The specific epitope for the N-terminal antibody has not been disclosed, although the product datasheet indicates it to bind near the N-terminus. The C-terminal HER2 antibody binds to an epitope around amino acid 1222 and the HercepTest™ was shown to bind to the C-terminus of HER2, at amino acids 1244 to 1254 (Schrohl *et al.*, 2011). The tissue sections were examined by a clinical pathologist Dr H. Kourea (Associate Professor of Pathology, University of Patras, Patras, Greece).

**A – No primary antibody control**



**B – HER2 3+ positive control**

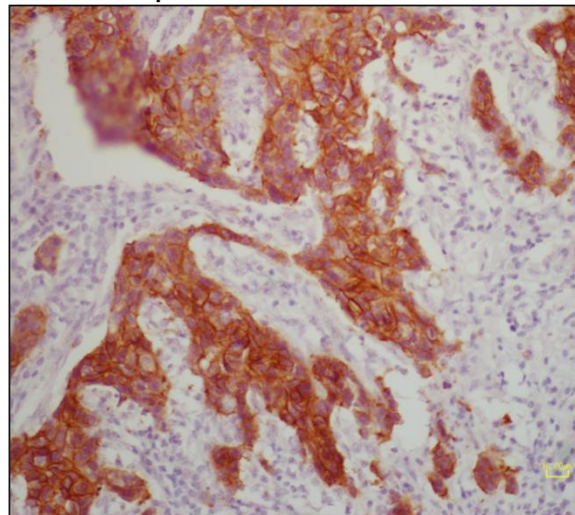
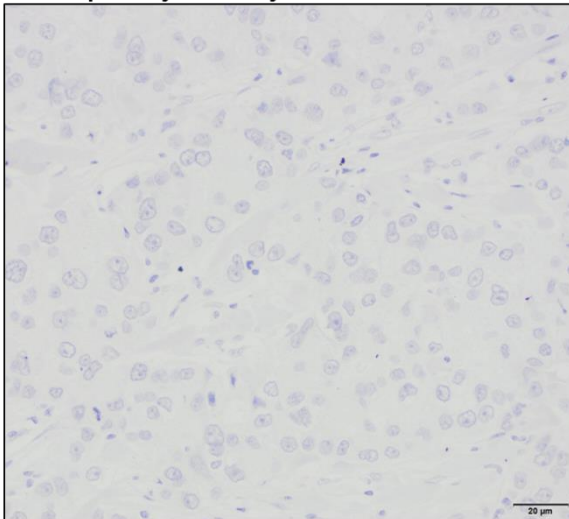


**Figure 4.3: C-terminal antibody controls.**

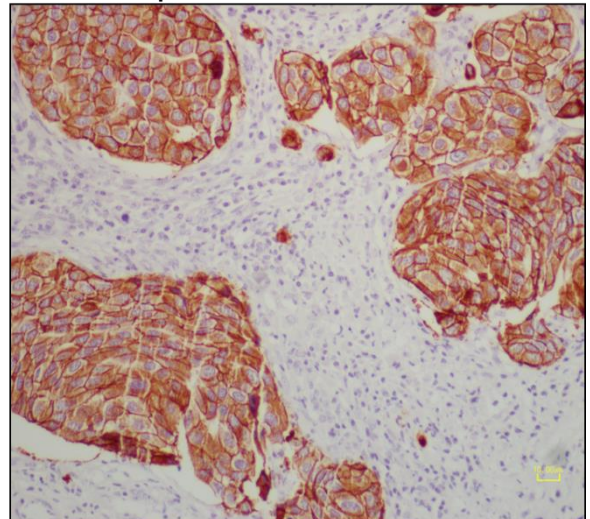
Examples of the controls used with each experiment are shown. A, shows the no primary antibody control. B, HER2-positive control on HER2 3+ graded tumour section.

Figure 4.3 A, shows the no primary antibody control and B, the 3+ positive control case with the C-terminal antibody. No staining was observed for the no primary antibody control, but a strong membrane staining was observed in the positive control. Similarly, figure 4.4 A, shows the no primary antibody control and B the positive control for the N-terminal antibody. The antibody worked as expected, giving a strong membrane staining in the positive control. The controls for the HercepTest™ are shown in figure 4.5. For the no primary antibody control a colon tissue section was used (provided by the Pathology of the Royal Victoria Infirmary, Newcastle). No unspecific staining can be observed in the no primary antibody control (Figure 4.5 A) and the positive control shows strong complete membrane staining (Figure 4.5 B). The manufacturer supplied controls were also used (Figure 4.5 C, D, E). The controls consisted of three cell lines. HER2-overexpressing SKBR3 cells showed complete membrane staining in all cells (Figure 4.5 C). In figure 4.5 D weak partial membrane staining of MDA-175 cells can be observed typical for 1+ HER2 cells, and the MDA-231 cell line shows no HER2 staining.

**A – No primary antibody control**



**B – HER2 3+ positive control**



**Figure 4.4: N-terminal antibody controls.**

Examples of the controls used with each experiment are shown. A, shows the no primary antibody control. B, HER2 3+ staining for the HER2 positive control tumour case.

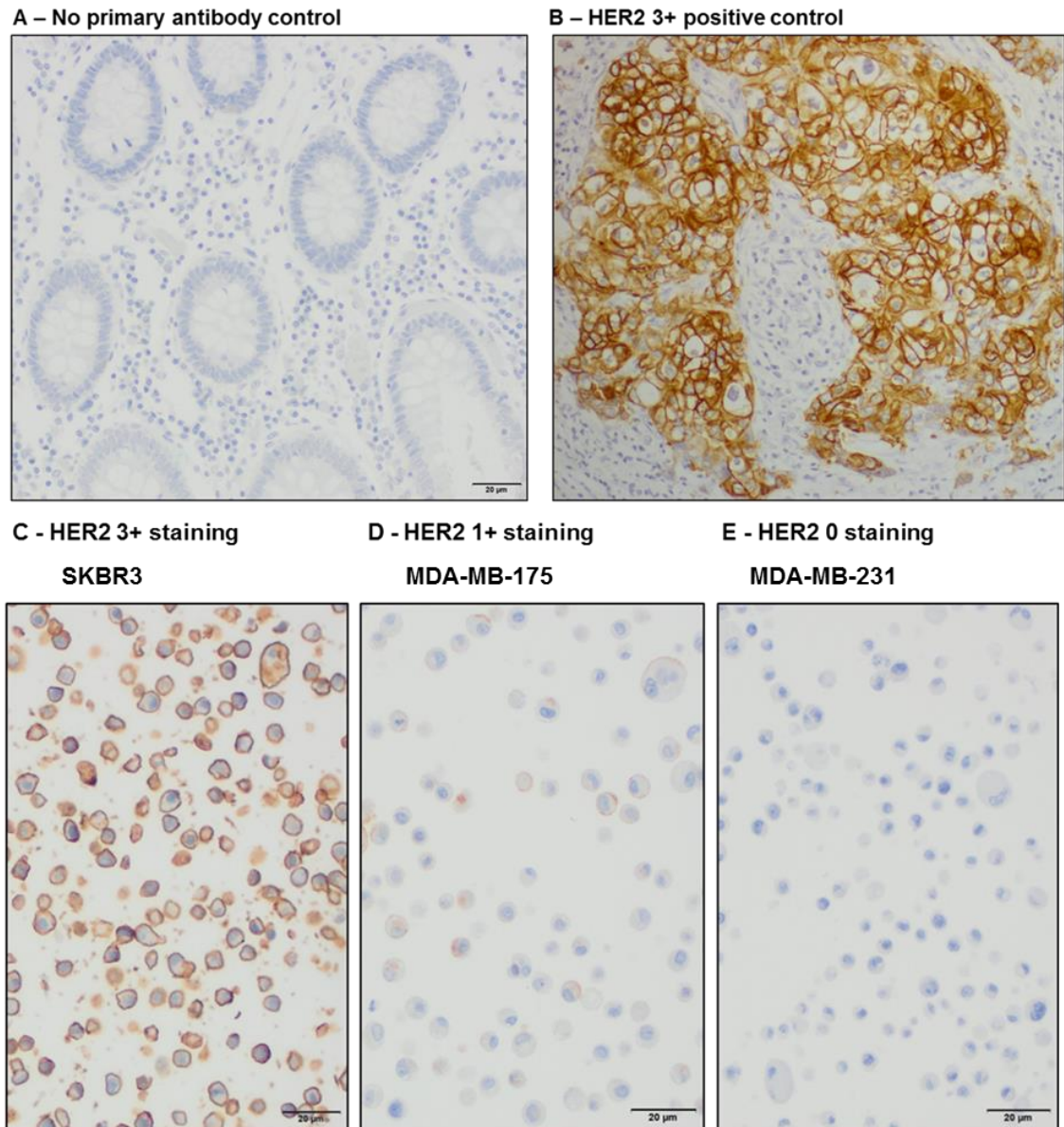


**Figure 4.5: HercepTest™ controls.**

Examples of the controls used with each experiment are shown. A, shows the no primary antibody control performed on a colon tissue section. B, HER2-positive control on HER 3+ graded tumour section. C, D and E show the manufacturer supplied controls. C, HER2 3+ staining of SKBR3 cells. D, HER2 1+ staining of MDA-MB-175 cells. E, HER2 0 staining of MDA-MB-231 cells.

The summary of Dr H Kourea's assessment of the tissue sections is shown in table 4.4. It has to be noted that some background staining was observed in a few cases for all antibodies. Antibody concentrations were adjusted for optimisation where possible. The HercepTest™ was performed on all HER2-positive tumours, but not yet on all HER2-negative tumours.

Group 3 (HER2/ER-negative) showed HER2 0 staining for all tumours with the C-terminal antibody and where performed also with the HercepTest™. Only the N-terminal antibody showed some discrepancies. It stained G3S1 and G3S8 as HER2 1+. HER2 0 and 1+ cases are considered HER2 negative. Additionally, cases G3S7 and G3S10 showed HER2 2+ staining. As equivocal cases are reflex tested for HER2 gene amplification. These cases were tested with CISH and the results will be presented in the next section. Overall the results from IHC matched the initial clinical classification of the group 3 tumours. Similar observations were made for group 4 (HER2-negative/ER-positive). The C- and N-terminal antibodies showed HER2 negative (HER2 0) staining for all tumours except G4S3, which showed a slight HER2 1+ staining. The HercepTest™ was performed on 4 tumours, of these G4S5 was HER2 1+ and G4S5 focally HER2 2+.

The two HER2 positive groups showed more complex results. In group 2 (HER2/ER-positive) the HercepTest™ showed HER2 3+ staining for 6 tumours, 3 tumours were HER2 2+ and one tumour was HER2 0. With the other two antibodies no HER2 3+ staining was observed with the exception of G2S2, G2S3 and G2S7. G2S2 showed focal HER2 3+ staining with HercepTest™, focal 2+ staining with the C-terminal antibody and 3+ with the N-terminal antibody. This tumour also showed HER2 3+ staining in tumour cells invading lymphatic vessels. In contrast G2S3 also showed focal HER2 3+ staining with the N-terminal antibody, however it only showed a HER2 2+ staining with the HercepTest™ and the C-terminal antibody. It should be noted that both G2S2 and G2S3 showed a heterogeneous population of tumour cells in regard to HER2 status. G2S7 showed 3+ staining with the HercepTest™ and the C-terminal antibody, but only a 2+ staining by the N-terminal antibody. Tumour heterogeneity was also observed in tumours G2S5 and 6. The tumour G2S10 showed a clear HER2 3+ status with the HercepTest™, however it the other antibodies showed no or only very weak staining. Additionally, one tumour G2S8 was assessed as HER2-negative by all antibodies.

## Chapter 4: Characterising HER2 in human breast tumours

**Table 4.4: Results from immunohistochemistry of 40 human primary ductal carcinomas.**

	ID	HercepTest™	C-terminal antibody	N-terminal antibody	Comment	IHC ID
<b>Group 2: ER+/HER2+</b>	G2S1	3	2	2(F)		IHC-4
	G2S2	3 (F)	2 (F), LVI 3+	3	Tum. heter.	
	G2S3	2(F)	2	3(F)	Tum. heter.	
	G2S4	2	1(F)	2	Tum. heter.	
	G2S5	3	2	2	Tum. heter.	IHC-2
	G2S6	2	2	2	Tum. heter.	
	G2S7	3	3	2		
	G2S8	0	1	2		IHC-3
	G2S9	3	2	2		
	G2S10	3	1	0		IHC-1
<b>Group 3: ER-/HER2-</b>	G3S1	NA	0	1		
	G3S2	NA	0	0		
	G3S3	NA	0	0		IHC-5
	G3S4	NA	0	0		
	G3S5	0	0	0		
	G3S6	0	0	0		
	G3S7	0	0	2		IHC-6
	G3S8	NA	0	1		
	G3S9	NA	0	0		
	G3S10	NA	0	2		IHC-7
<b>Group 4: ER+/HER2-</b>	G4S1	NA	0	0		
	G4S2	NA	0	0		
	G4S3	0	0	1		IHC--8
	G4S4	0	0	0		
	G4S5	2 (F)	0	0		IHC-9
	G4S6	1	0	0		IHC-10
	G4S7	NA	0	0		
	G4S8	NA	0	0		
	G4S9	NA	0	0		
	G4S10	NA	0	0		
<b>Group 5: ER-/HER2+</b>	G5S1	3	1	3		
	G5S2	0	0	0		IHC-11
	G5S3	3	2	3		
	G5S4	1	0	2	Tum. heter.	IHC-13
	G5S5	3	3	3		
	G5S6	3	1	3		IHC-12
	G5S7	3	0	3	Tum. heter.	IHC-14
	G5S8	2	2	2		
	G5S9	3	2	3		
	G5S10	1	0	3		IHC-15

“LVI”, lymphovascular space invasion; “F”, focal staining and “Tum. heter.”, tumour heterogeneity.

In group 5, six tumours were stained as HER2 3+ by the HercepTest™. These tumours also showed 3+ staining with the N-terminal antibody. However the C-terminal antibody only confirmed the 3+ staining for G5S5, the other tumours only showed weak staining. The other case of concordant staining was observed for G5S8, which showed HER2 2+ staining with all three antibodies. G5S2 showed no HER2 staining with any of the antibodies. HER2 negative

staining was observed with the HercepTest™ and the C-terminal antibody, but equivocal staining was observed with the N-terminal antibody for G5S4. G5S10 was also stained HER2 negative with the HercepTest™ and the C-terminal antibody, but it showed HER2 3+ staining with the N-terminal antibody. The HER2 staining of the tumour was heterogeneous in G5S4 and 7.

Some tumours showed borderline (HER2 2+) results or discrepancy between the staining results of the 3 antibodies. These discrepant cases as well as some HER2-negative tumours were used for further studies. For ease of use new ID's were assigned, these are indicated in table 4.4.

### **4.4.2. HER2 gene amplifications in human breast tumours**

This was the first time the *HER2* CISH pharmDx™ kit was successfully performed in our laboratory. To verify that the CISH worked and no unspecific staining took place different controls were used. Figure 4.6 shows the primary probe negative control for which an ER-negative, HER2-positive grade 3 ductal carcinoma section was used. It was part of the same Breast Cancer Now Tissue Bank cohort as the tested tissue sections. The negative control showed no *HER2* gene or centromere 17 signals. A normal breast tissue section is shown in figure 4.7. Both the *HER2* and CEN-17 probe are shown to bind specifically. Cells of normal ducts show two *HER2* gene and CEN-17 signals per nucleus. To further verify the correct positive staining with the assay two HER2 3+ ductal carcinomas (provided by the Department of Pathology of University of Patras, Patras, Greece) were included. Figure 4.8 shows images of the two positive controls. IHC-C1 was assessed to have a *HER2* gene amplification of 6.55 with a CEN-17 signal of 2.3 and thereby a *HER2*/CEN-17 ratio of 2.85. The second positive control, IHC-C2 was assessed to have a *HER2* gene amplification of 9.6 with a CEN-17 signal of 2.15 and thereby a *HER2*/CEN-17 ratio of 4.47. Both are clearly HER2-positive and confirm the previous clinical assessment and thereby our assay.

**No primary probe control**

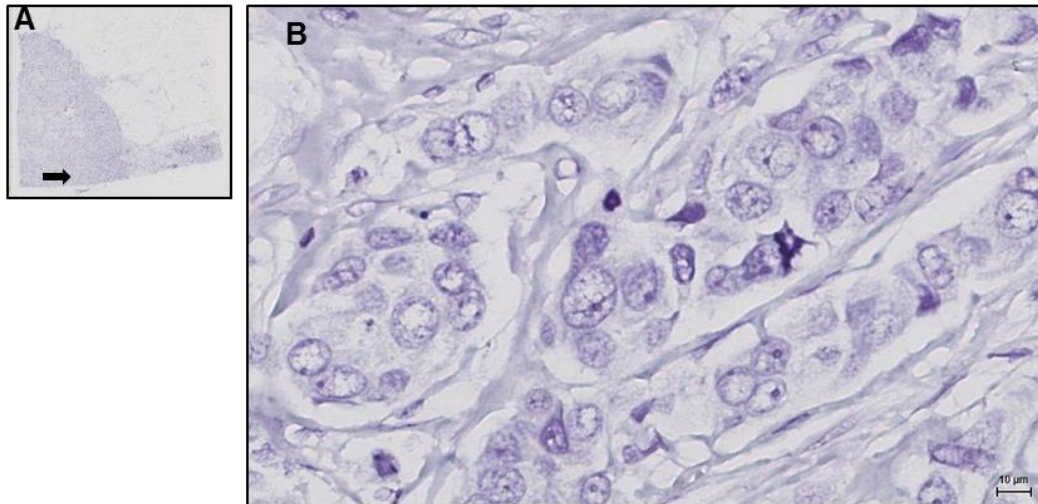


**Figure 4.6: *HER2* CISH pharmDx™: no primary probe control**

A, shows the whole tumour section stained without the primary probes. B, tumour is magnified and nuclei can be seen, but no staining for *HER2* or CEN-17 can be observed.

**Normal human breast tissue**

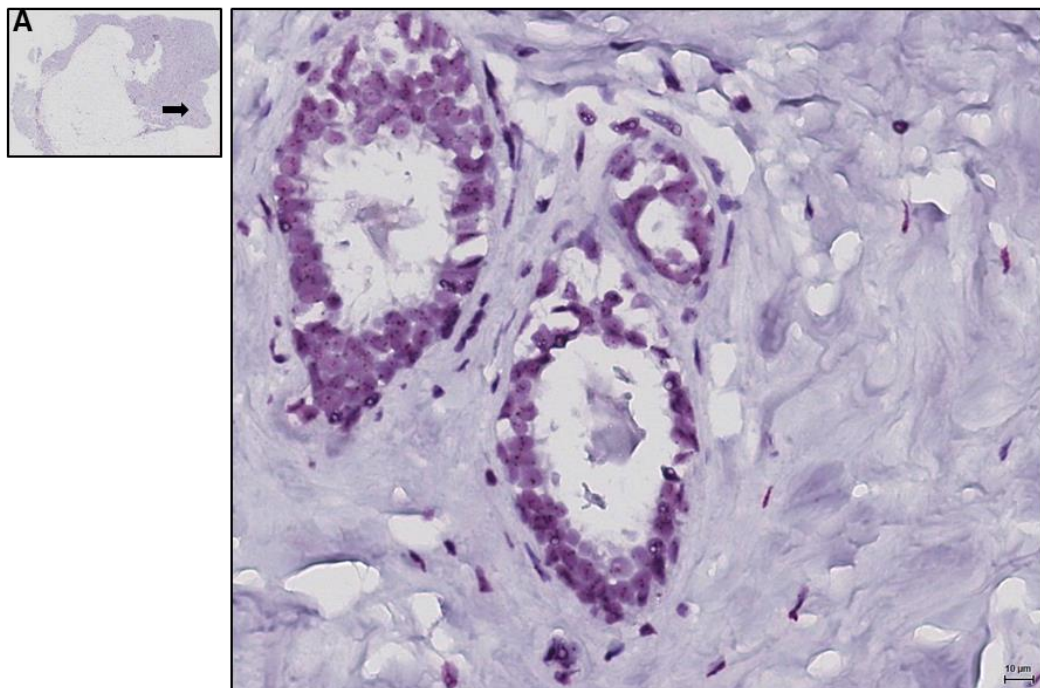
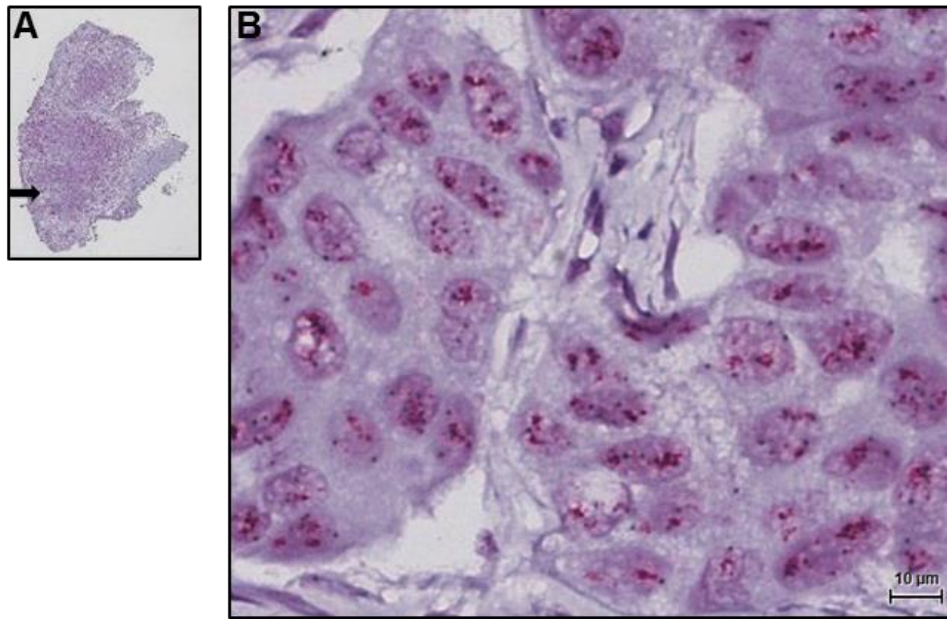


**Figure 4.7: *HER2* CISH staining on normal breast tissue.**

A, shows the whole tissue section. B, in the ductal cells both *HER2* and Cen-17 signals can be observed. Normal diploid signals can be observed. A few stromal cells nuclei can be observed, but they are too small to determine *HER2* gene status.

**IHC-C1; HER2 3+ positive breast tumour control**



**IHC-C2; HER2 3+ positive breast tumour control**

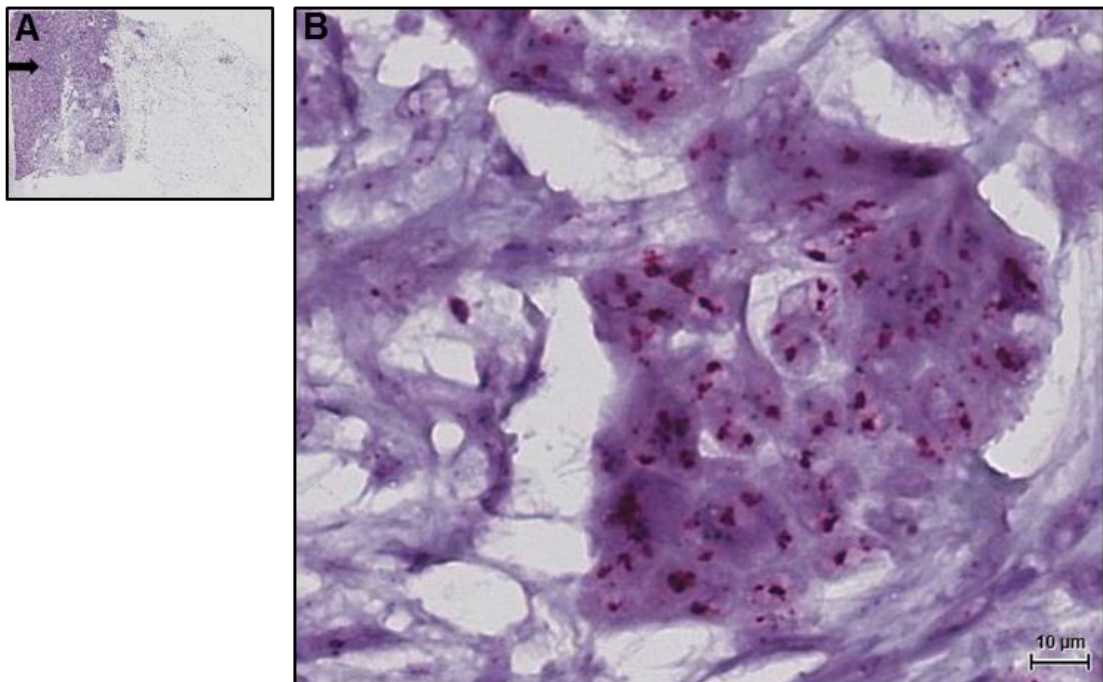


**Figure 4.8: *HER2* CISH staining showing *HER2* gene amplification on the *HER2* 3+ positive control tumours.**

A, shows the whole tissue section. B, in the ductal cells both *HER2* and Cen-17 signals can be observed. Normal diploid signals for centromere 17 (blue dots) can be observed, while large clusters of red signals corresponding to the *HER2* gene are seen, indicating *HER2* gene amplification.

Following the assessment of the controls, the staining of the 15 tumour cases was observed. The tissue sections from the Breast Cancer Now Tissue Bank originate from different hospitals throughout the UK. Although, the preservation of the tissue sections follows strict guidelines by the Breast Cancer Now Tissue Bank minor variations remain (Breast Cancer Now Tissue Bank, 2010). All samples were stained at the same time, but differences in tissue integrity and digestion of nuclei between tissues were observed. This could have impacted the assessment of borderline cases.

**Table 4.5: Results of the *HER2* CISH staining for the human invasive ductal carcinomas.**

Group	IHC-ID	<i>HER2</i> gene amplification	CEN-17	<i>HER2</i> /CEN-17	<i>HER2</i> status
<b>Group 2: ER+/HER2+</b>	IHC-1	2.98	1.65	1.95	B/-
	IHC-2	5.58	2.48	2.25	+
	IHC-3	5.2	2.3	2.26	+
	IHC-4	8.35	2.05	4.07	+
<b>Group 3: ER-/HER2-</b>	IHC-5	1.7	1.65	1.03	-
	IHC-6	2.7	1.75	1.5	-
	IHC-7	2	1.9	1.05	-
<b>Group 4: ER+/HER2-</b>	IHC-8	2.75	2.15	1.3	-
	IHC-9	3.05	2.05	1.49	-
	IHC-10	2.35	1.65	1.42	-
<b>Group 5: ER-/HER2+</b>	IHC-11	1.3	1.2	1.08	-
	IHC-12	5.2	1.7	3.06	+
	IHC-13	2.3	1.85	1.24	-
	IHC-14	4.13	1.9	2.43	+
	IHC-15	2.83	1.25	2.02	B/+

Table 4.5 summarises the CISH scores of the grade 3 invasive primary ductal carcinomas studied in this chapter. Four samples were originally grouped as ER/HER2-positive (group 2), 3 each were grouped as ER/HER2-negative and ER-positive/HER2-negative (group 3 and 4) and 5 samples were grouped as ER-negative/HER2-positive (group 5). The original HER2 status for the samples of group 2, 3 and 4 was confirmed by our CISH scoring, except for IHC-1, which was clinically assessed to be a HER2-positive tumour, but was HER2-negative to borderline in our CISH assay. However in group 5, only IHC-12 and ICH-14

were scored as HER2-positive by our CISH. The tumour sections IHC-11, 13 and 15 were originally assessed as HER2-positive, however by CISH IHC-11 and 13 were classified as HER2-negative. The tumour IHC-15 shows a *HER2/CEN-17* ratio of 2.02, which would make this a HER2 positive case, however this ratio is caused by loss of chromosome 17 centromere signals (CEN-17: 1.25). The *HER2* gene count is only 2.83 and with a normal CEN-17 signal of 2, a tumour would be clearly HER2 negative.

### **4.4.3. Comparison of HER2 protein levels and HER2 gene amplification in a cohort of human breast tumours**

In the two previous sections the outcomes from the IHC staining of tumour sections for the expression and localisation of HER2 proteins, and the outcome from the *HER2* CISH pharmDx™ assay for HER2 gene amplification were discussed. Here the tumours that have been scored by IHC and CISH were more closely examined. As was mentioned before, the tissue sections had been clinically assessed for their HER2 status before they were received from the Breast Cancer Now Tissue Bank. Table 4.5 shows an overview of the IHC and CISH results grouped according to the original tumour classification.

Group 2 are tumours that have been clinically assessed as HER2- and ER-positive. The CISH results for tumours IHC-2, 3 and 4 matched the clinical HER2-positive status. IHC-1 was HER2-negative to borderline by CISH. Figure 4.9 shows representative images of the IHC and CISH assays for IHC-1. A borderline case is generally assessed by a second method. It should be noted that although the *HER2/CEN-17* ratio was 1.95 - borderline, the *HER2* gene copy number per cell was actually less than 3 and this was suggested to be considered HER2-negative (Rakha *et al.*, 2015). The HercepTest™ confirmed the tumour as HER2-positive status (Figure 4.9, A). However the other two antibodies (C- and N-terminal) also showed a weak cytoplasmic positivity but no membranous staining, a finding that is scored as HER2-negative. IHC-2 and 4 are clearly HER2 positive by both CISH and HercepTest™, although the other antibodies only gave a score of HER2 2+. For IHC-2 tumour heterogeneity was

observed in the IHC experiments. IHC-4 is a case of strong *HER2*-gene amplification with a HER2 copy number of 8.35 per nucleus, this is also clearly visible in figure 4.11 III. Initial observation of the C-terminal staining (Figure 4.11 A) would indicate strong staining, however clinical HER2 scores are assigned according to the extent of complete membranous HER2 staining. It should be noted that the HercepTest™ also showed some diffuse cytoplasmic staining (Figure 4.11 A). IHC-3 is a very interesting case as it shows a clear HER2-positive score by CISH, but is HER2-negative by IHC (Figure 4.10). A general *HER2*-gene amplification was observed, however the strongest amplification was observed in clusters of tumour cells surrounded by stromal cells (Figure 4.10 IV). The tissue morphology is very similar to the area which showed HER2 2+ staining with the N-terminal antibody.

The group 3 (HER2/ER-negative) tumours were confirmed by CISH to be HER2-negative. The HercepTest™ has not yet been performed on IHC-5 and 7. All three tumours were scored HER2-negative for the C-terminal antibody. Only with the N-terminal antibody was a stronger HER2 2+ staining observed for IHC-6 and 7. Group 4 contains tumours with a HER2-negative and ER-positive status. IHC-8 and 10 were classified as HER2-negative by both CISH and IHC. They showed no more than a 1+ staining with one antibody. IHC-9 was also scored as HER2-negative by CISH and IHC, however it should be noted that the HercepTest™ showed focal HER2 2+ staining.

The tumours in group 5 were clinically assessed to be HER2-positive, but ER-negative. All three antibodies used showed no or minimal HER2 staining for IHC-11. The CISH assay also scored this tumour as HER2-negative (Figure 4.12 B). There is no indication in the tissue sections on why this tumour was initially assessed as HER2-positive. Similarly, IHC-13 was also graded 1+ by HercepTest™ and 0 with the C-terminal antibody. Only the N-terminal antibody gave a higher score of 2+ (Figure 4.13 A). The HER2-negative IHC staining matched the score of the CISH assay. The *HER2* gene was present at a normal level in most nuclei, however as can be observed in figure 4.13, IV in a few tumour cells *HER2*-gene amplification was shown. This matches the observation of tumour heterogeneity by IHC. The tumour IHC-15 only stained as HER2 3+ with the N-terminal antibody. Both the C-terminal antibody and the

HercepTest™ only stained the tumour weakly (Figure 4.15 A). The CISH score for this case was borderline to HER2 positive. Only a minor *HER2*-gene amplification was observed in some cells and the CEN-17 average indicated chromosome 17 monosomy. However some dispersed nuclei showed stronger *HER2*-gene amplification. An example is shown in 4.15 IV. IHC-12 and 14 had a HER2-positive CISH score. The results for IHC-14 are shown in figure 4.14. Both tumours showed HER2 3+ staining with the HercepTest™ and the N-terminal antibody. In contrast both only showed weak staining with the C-terminal antibody. It should be noted that IHC-14 showed focal staining with HercepTest™ and diffuse staining with the N-terminal antibody (Figure 4.14).

Table 4.6: Overview of results from HER2 IHC and CISH experiments.

Group	IHC-ID	HER2 gene amplification	CEN-17	HER2/CEN-17	HER2 status	HercepTest™	C-term. Antibody	N-term. Antibody
<b>Group 2: ER+/HER2+</b>	IHC-1	2.98	1.65	1.95	B/-	3	1	0
	IHC-2	5.58	2.48	2.25	+	3	2	2
	IHC-3	5.2	2.3	2.26	+	0	1	2
	IHC-4	8.35	2.05	4.07	+	3	2	2 (F)
<b>Group 3: ER-/HER2-</b>	IHC-5	1.7	1.65	1.03	-	NA	0	0
	IHC-6	2.7	1.75	1.5	-	0	0	2
	IHC-7	2	1.9	1.05	-	NA	0	2
<b>Group 4: ER+/HER2-</b>	IHC-8	2.75	2.15	1.3	-	0	0	1
	IHC-9	3.05	2.05	1.49	-	2 (F)	0	0
	IHC-10	2.35	1.65	1.42	-	1	0	0
<b>Group 5: ER-/HER2+</b>	IHC-11	1.3	1.2	1.08	-	0	0	0
	IHC-12	5.2	1.7	3.06	+	3	1	3
	IHC-13	2.3	1.85	1.24	-	1	0	2
	IHC-14	4.13	1.9	2.43	+	3	0	3
	IHC-15	2.83	1.25	2.02	B/+	1	0	3

“B”, borderline. “F”, focal staining. “NA”, not applicable.

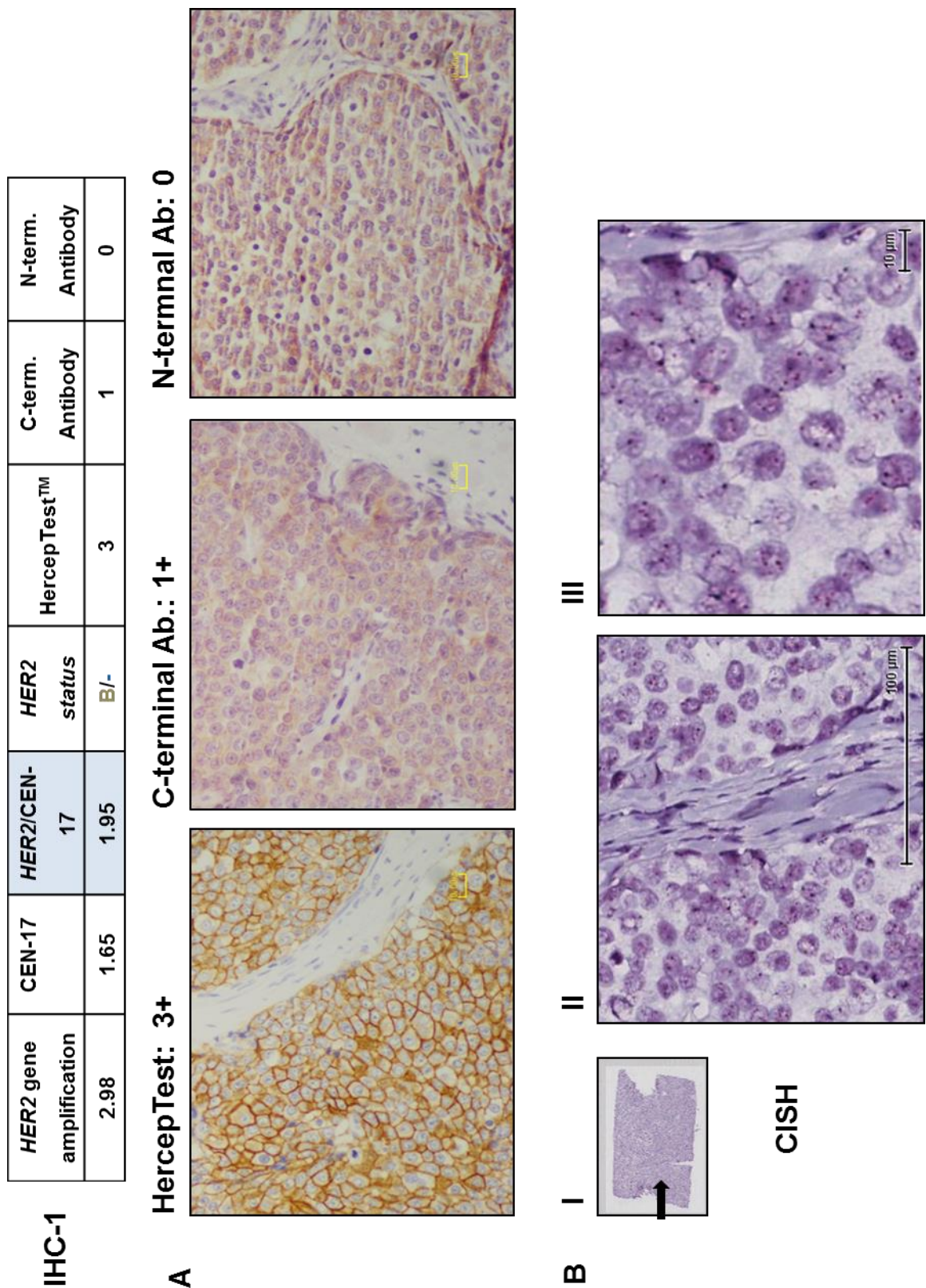


Figure 4.9: IHC and CISH images for the human breast cancer case IHC-1.

The table summarises the findings from IHC and CISH experiments. A, shows images of serial sections of the same tissue stained with the HercepTest™, C-terminal and N-terminal HER2 antibody. HER2 status is indicated for each image. B, shows images from CISH staining. I, shows the whole tissue section and the arrow indicates the area from which the images were taken. II, and III, show the same area at different magnifications.

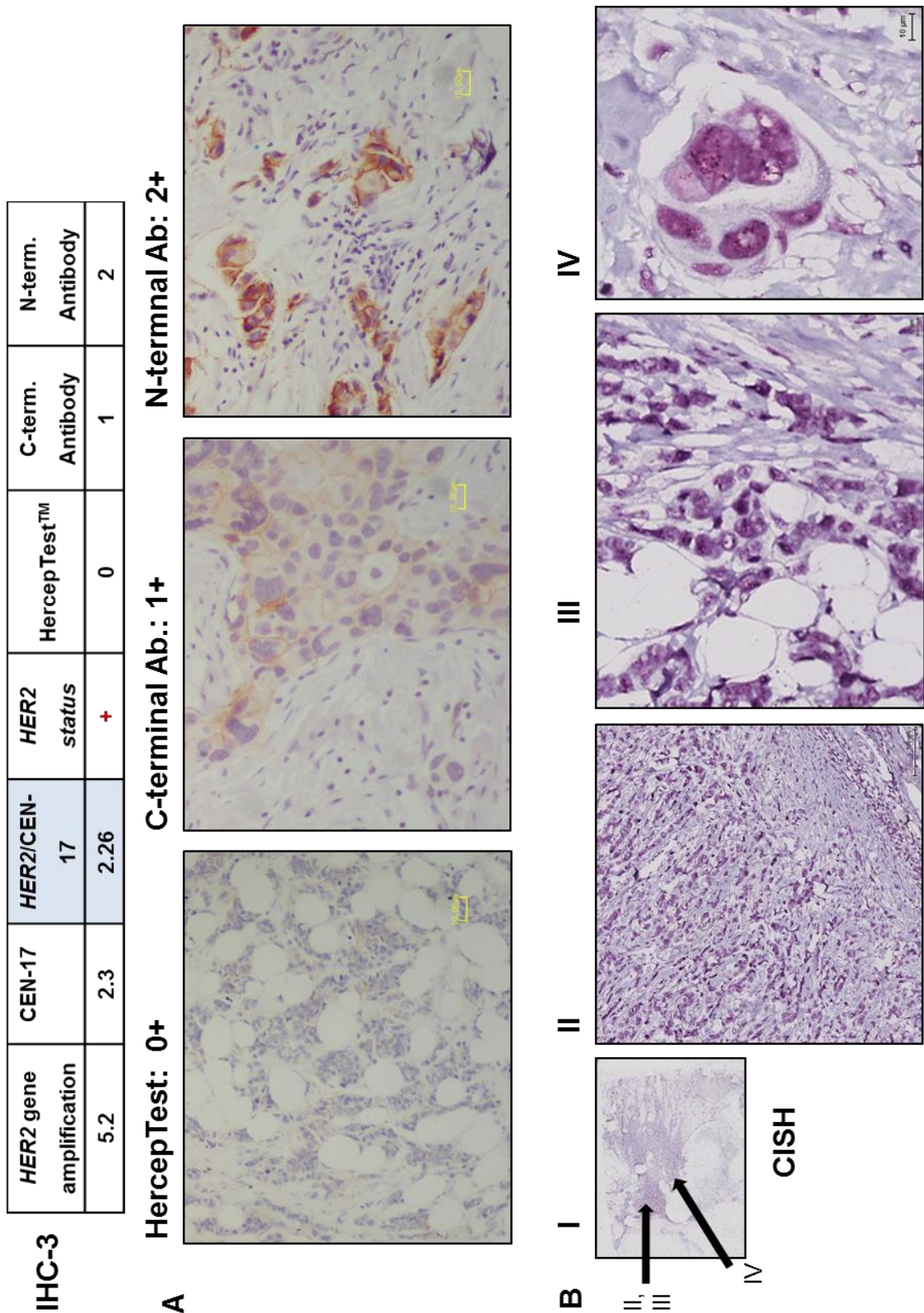


Figure 4.10: IHC and CISH images for the human breast cancer case IHC-3.

The table summarises the findings from IHC and CISH experiments. A, shows images of serial sections of the same tissue stained with the HercepTest™, C-terminal and N-terminal HER2 antibody. HER2 status is indicated for each image. B, shows images from CISH staining. I, shows the whole tissue section and the arrow indicates the area from which the images were taken. II, and III, show the same area at different magnifications. IV, shows high magnification of HER2-gene amplified cells.

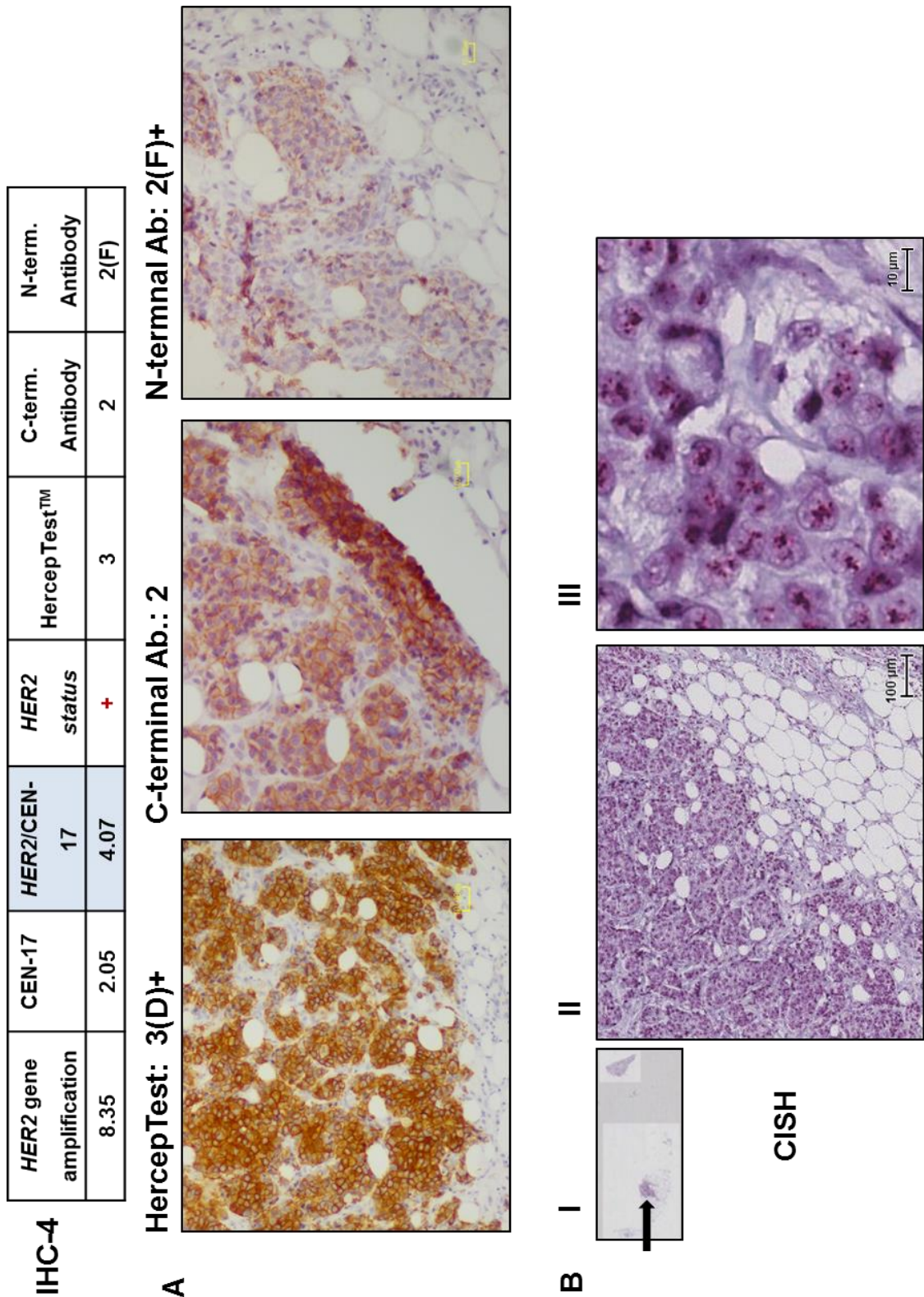


Figure 4.11: IHC and CISH images for the human breast cancer case IHC-4.

The table summarises the findings from IHC and CISH experiments. A, shows images of serial sections of the same tissue stained with the HercepTest™, C-terminal and N-terminal HER2 antibody. HER2 status is indicated for each image. “F”, indicates focal staining. B, shows images from CISH staining. I, shows the whole tissue section and the arrow indicates the area from which the images were taken. II, and III, show the same area at different magnifications.

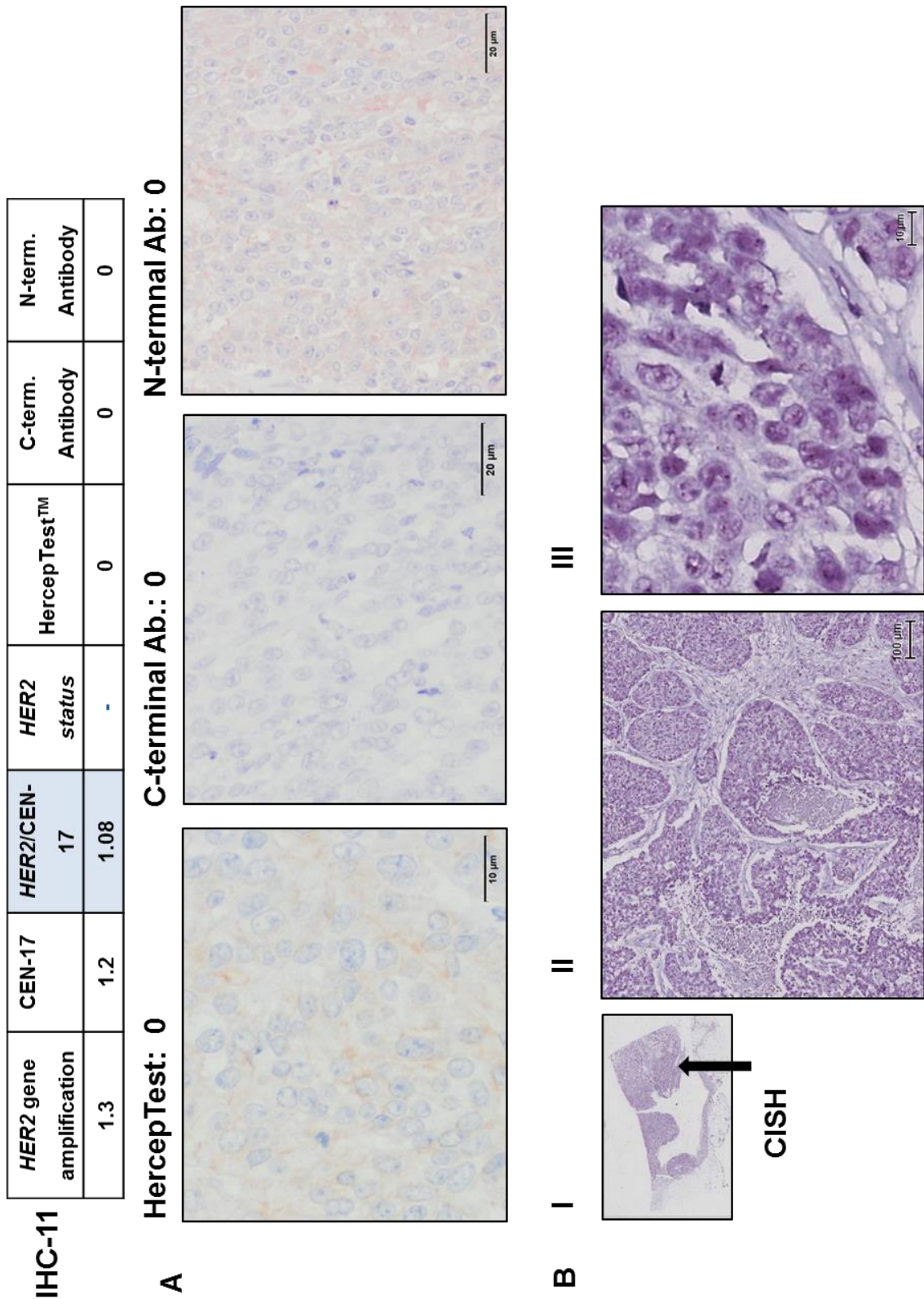


Figure 4.12: IHC and CISH images for the human breast cancer case IHC-11.

The table summarises the findings from IHC and CISH experiments. A, shows images of serial sections of the same tissue stained with the HercepTest™, C-terminal and N-terminal HER2 antibody. HER2 status is indicated for each image. B, shows images from CISH staining. I, shows the whole tissue section and the arrow indicates the area from which the images were taken. II, and III, show the same area at different magnifications displaying absence of amplification.

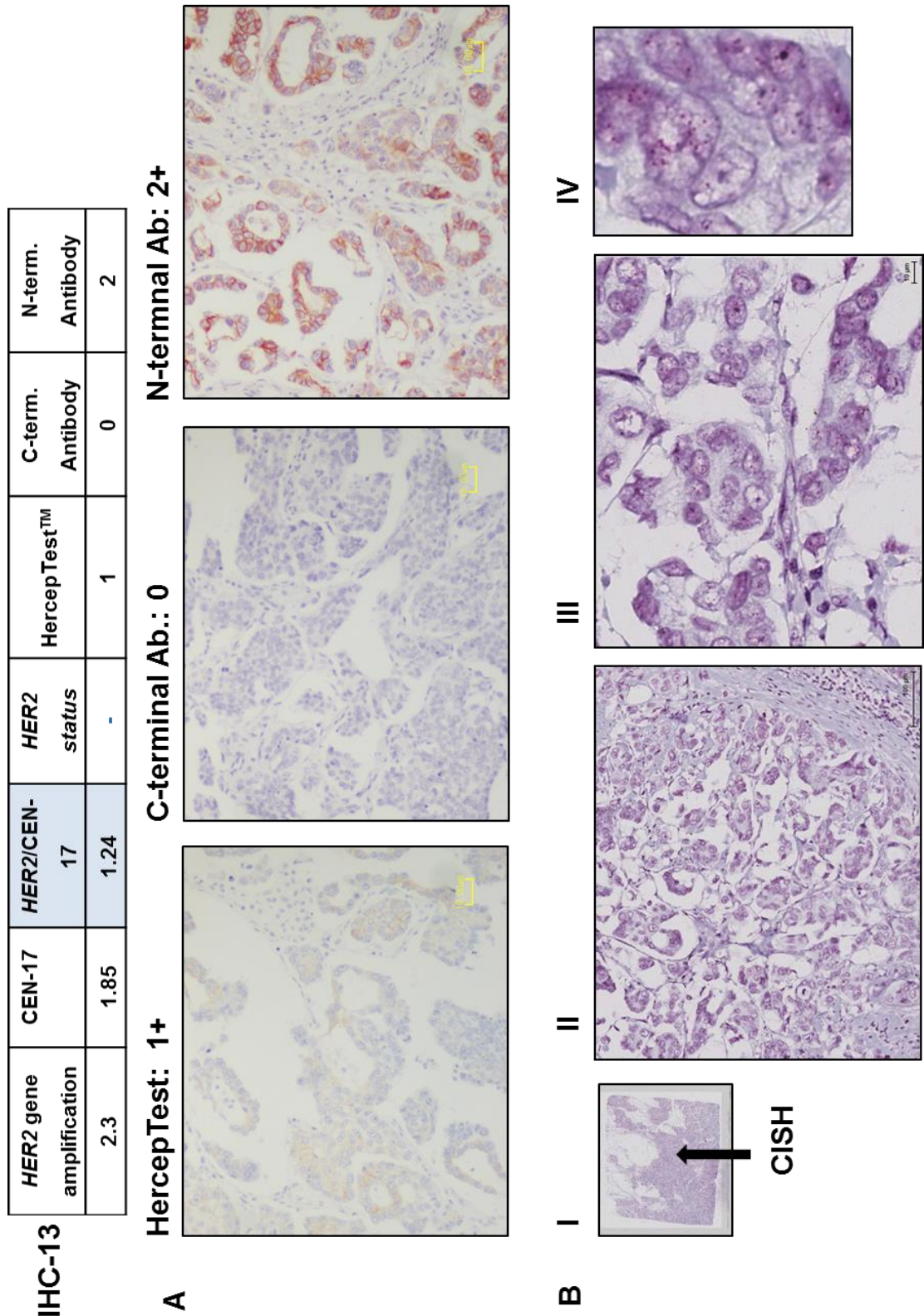


Figure 4.13: IHC and CISH images for the human breast cancer case IHC-13.

The table summarises the findings from IHC and CISH experiments. A, shows images of serial sections of the same tissue stained with the HercepTest™, C-terminal and N-terminal HER2 antibody. HER2 status is indicated for each image. B, shows images from CISH staining. I, shows the whole tissue section and the arrow indicates the area from which the images were taken. II, and III, show the same area at different magnifications. IV, shows nuclei with an increased *HER2* gene copy number.

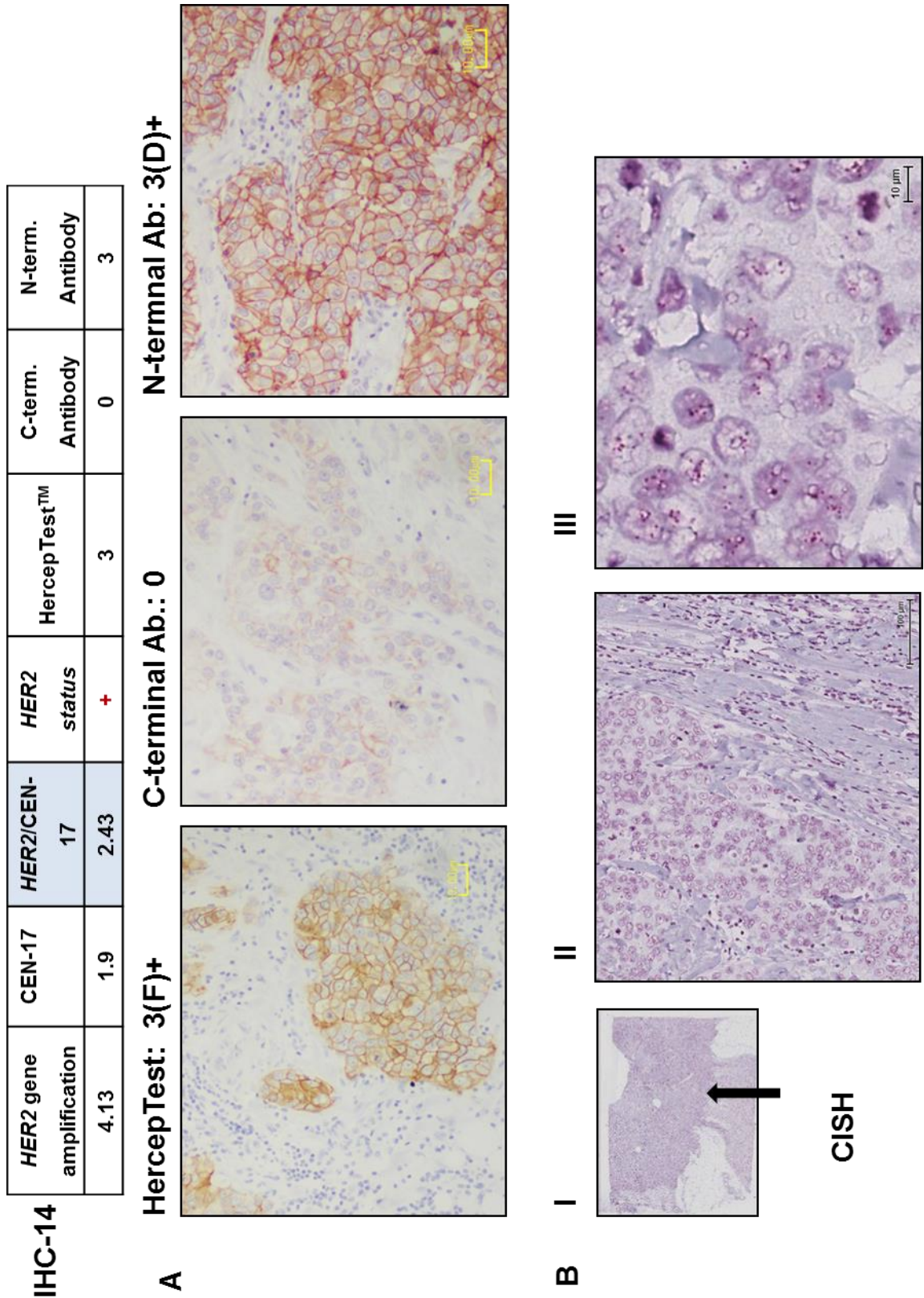


Figure 4.14: IHC and CISH images for the human breast cancer case IHC-14.

The table summarises the findings from IHC and CISH experiments. A, shows images of serial sections of the same tissue stained with the HercepTest™, C-terminal and N-terminal HER2 antibody. HER2 status is indicated for each image. “F”, indicates focal staining. B, shows images from CISH staining. I, shows the whole tissue section and the arrow indicates the area from which the images were taken. II, and III, show the same area at different magnifications.

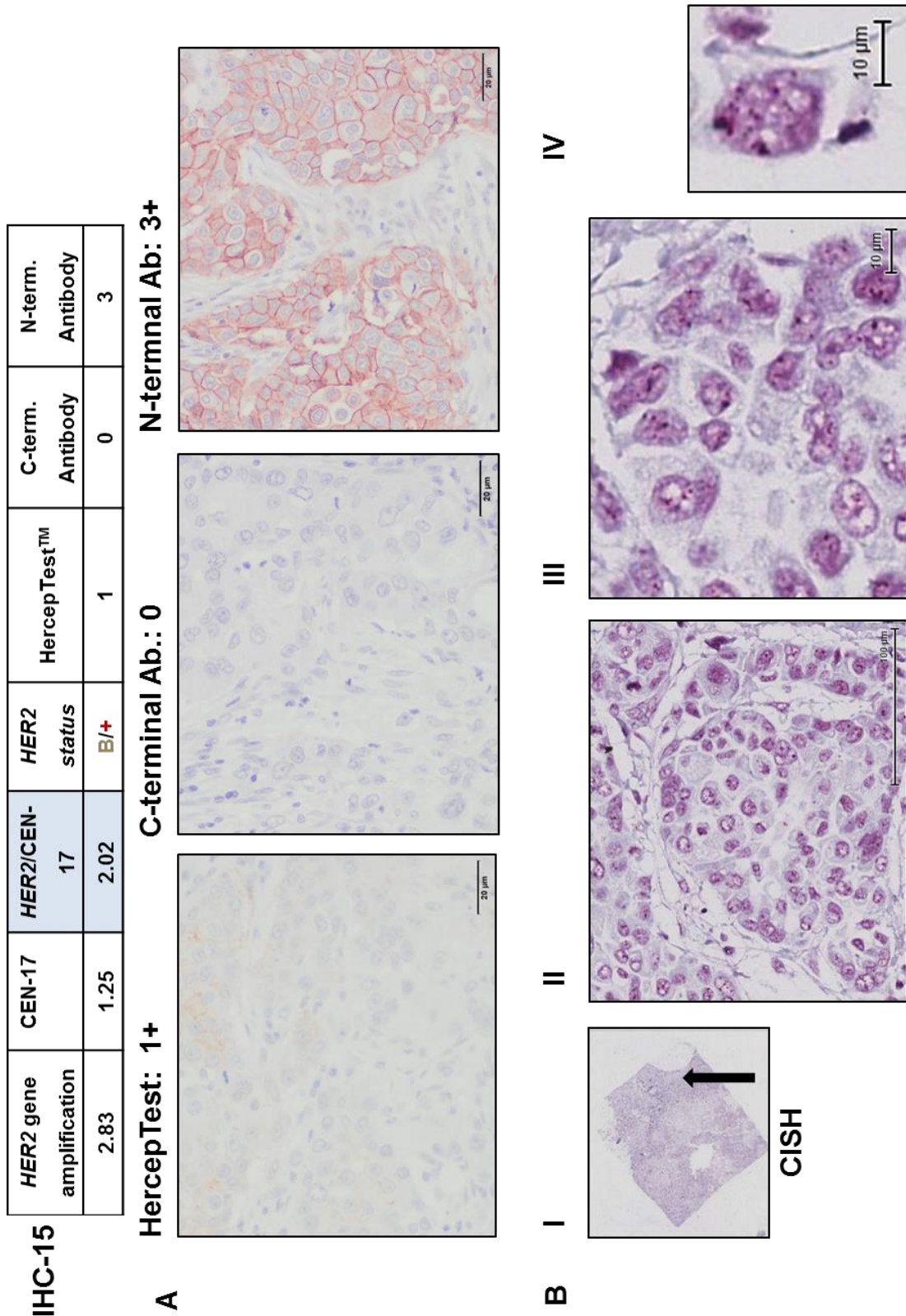
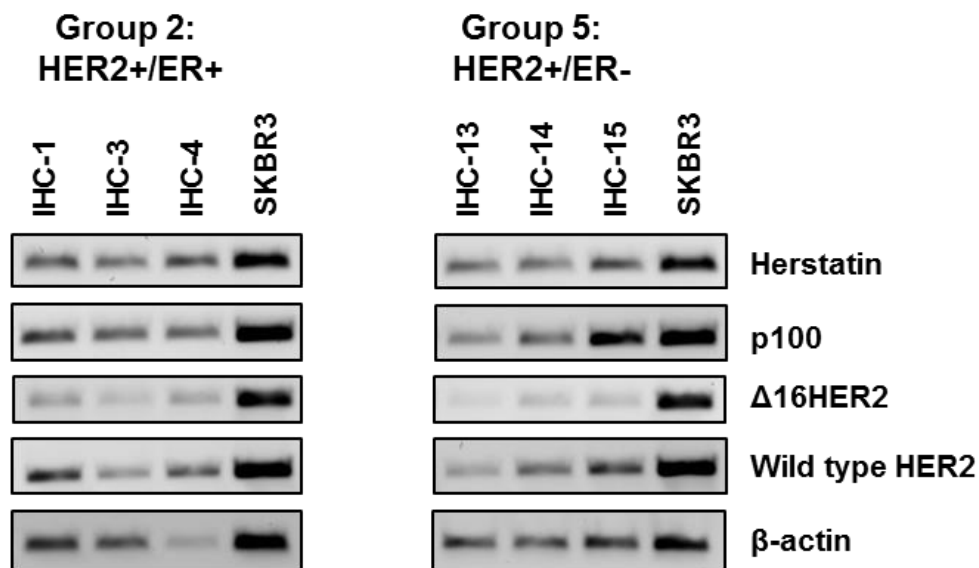


Figure 4.15: IHC and CISH images for the human breast cancer case IHC-15.

The table summarises the findings from IHC and CISH experiments. A, shows images of serial sections of the same tissue stained with the HercepTest™, C-terminal and N-terminal HER2 antibody. HER2 status is indicated for each image. B, shows images from CISH staining. I, shows the whole tissue section and the arrow indicates the area from which the images were taken. II, and III, show the same area at different magnifications. IV, shows an example of one single cell at high magnification with *HER2*-gene amplification.

**4.4.4. HER2 splice variant expression in selected, discrepant breast tumour cases**

In the previous sections a cohort of primary invasive ductal carcinomas were characterised. Discrepancies were observed between IHC and CISH results in a few tumour cases. To determine if these discrepancies might be due to HER2 splice variants PCRs were performed. From the HER2-/ER-positive breast tumour group samples IHC-1, 3 and 4 were used and from the HER2-positive/ER-negative breast tumour group samples IHC-13, 14 and 15 were used. The RNA quality of IHC-11 was not good enough to produce cDNA that could be used in this study. SKBR3 cDNA was included in each experiment as a control and for comparison. The levels of HER2 splice variants Herstatin, p100 and  $\Delta 16$ HER2 were determined by conventional PCR. Additionally, PCRs for wild type HER2 and the housekeeping gene  $\beta$ -actin were performed.



**Figure 4.16: HER2 splice variant levels in discrepant primary invasive ductal carcinoma cases.**

Three samples from group 2 and three samples from group 5 were used. PCRs used were performed for HER2 splice variants Herstatin, p100 and  $\Delta 16$ HER2, as well as wild type HER2 and the housekeeping gene  $\beta$ -actin.

Figure 4.16 shows the levels of the HER2 splice variants. The  $\beta$ -actin levels were comparable, only IHC-4 showed a decreased level of  $\beta$ -actin. Wild type HER2 was strongly expressed in IHC-1, 4, 14 and 15, but only weakly expressed in IHC-3 and IHC-13.  $\Delta$ 16HER2 was weakly expressed in all tumours and in a consistent ratio with wild type HER2. Herstatin is present in all samples, with the highest levels in IHC-1, 4 and 15. Similarly, p100 can also be observed in every tumour. The level is increased compared to the other tumours in IHC-1, but the strongest band can be observed for IHC-15. It should be noted that the PCRs for all three HER2 splice variants were carried out at the same cycle number.

**Table 4.7: Summary of CISH and IHC results for samples used in PCR.**

		<i>HER2</i> gene	<i>HER2</i> / CEN-17	HER2 status	Hercep Test™	C-term. Antibody	N-term. Antibody
<b>Group 2: HER2+/ ER+</b>	IHC-1	2.98	1.95	B/-	3	1	0
	IHC-3	5.2	2.26	+	0	1	2
	IHC-4	8.35	4.07	+	3	2	2(F)
<b>Group 5: HER2+/ ER-</b>	IHC-13	2.3	1.24	-	1	0	2
	IHC-14	4.13	2.43	+	3	0	3
	IHC-15	2.83	2.02	B/+	1	0	3

“B”, borderline. “F”, focal staining.

Comparing the PCR results to the results from the previous sections (Table 4.6) showed the following trends. The wild type HER2 levels detected by PCR roughly matched the observations made with the HercepTest™. Interesting observations can be made for levels of p100 and Herstatin. IHC-3 and 13 showed clear bands for p100 and Herstatin as well as a HER2 2+ score with the N-terminal antibody, but not the other antibodies. The highest level of p100 could be observed for IHC-15, which by IHC showed a 3+ score with the N-terminal antibody. Although wild type HER2 is expressed at the mRNA level, the HercepTest™ gave a very weak staining in this tumour.

## 4.5. Discussion

This chapter is part of a larger study that investigates the importance of HER2 splice variants in the assessment of breast cancer. For an optimal treatment of patients suffering from breast cancer, an accurate assessment of the main biomarkers (ER, PR and HER2) has to be made. The HER2 status is routinely clinically assessed and the methods used show a relatively high rate of accuracy [reviewed in (Sapino et al., 2013)]. However tumour heterogeneity and deviations between HER2 assessment methods can still be observed (Miller et al., 2004; Vance et al., 2009; Sapino et al., 2013; Carvajal-Hausdorf et al., 2015). As was discussed in the introduction, *HER2* genetic heterogeneity is defined as 5-50% of infiltrating tumour cells with a *HER2/CEN-17* ratio of  $\geq 2.2$  (Vance et al., 2009). Tumour heterogeneity can be subdivided in tumours with a localized subpopulation of HER2 overexpressing cells and in tumours which have two populations of cells that are present throughout the tumour (Sapino et al., 2013).

### ***4.5.1. Discrepant IHC and CISH staining in invasive ductal carcinomas***

In this study a cohort of primary invasive ductal carcinomas provided by the Breast Cancer Now Tissue Bank was characterised for their HER2 status with two clinically used tests. The HercepTest™ was used to study protein expression and localisation, and the *HER2* CISH pharmDx™ assay was used to measure *HER2*-gene amplification. Additionally, two HER2 antibodies with differing epitopes were utilised and compared to the HercepTest™. The tumours were characterised with the help of experienced clinical pathologist Dr H. Kourea. The findings in this study matched the initial clinical assessment for all HER2-negative tumours. Only IHC-9 showed a focal HER2 2+ score with the HercepTest™ and IHC-6 and 7 showed HER2 2+ staining with the N-terminal antibody. As is undertaken in clinic, these tumours were assessed for their

*HER2*-gene amplification status by CISH. They were clearly scored as HER2-negative, confirming their clinically determined HER2 status.

The two groups of HER2-positive tumours (group 2 and 5) showed more complex results. Twelve tumours showed HER2 3+ staining with the HercepTest™, but only one tumour showed 3+ staining with all antibodies. In the other breast tumours the antibodies gave mixed results. Seven HER2 positive tumours showed tumour heterogeneity. This might partially account for the different staining results with the 3 antibodies on the serial sections, as different parts of the heterogeneous tumour might be dominant in the different sections. HercepTest™ is a C-terminal antibody with an epitope only 20 amino acids downstream of the C-terminal antibody's epitope, however the other C-terminal antibody showed a weaker staining for most tumours. In all cases, except G2S7, the N-terminal antibody stained equally or stronger than the C-terminal antibody. Interestingly, two tumours stained 3+ with the N-terminal antibody but less with the other two antibodies. Concerning was the observation that some of the tumours were not HER2-positive by the IHC staining. Additionally, when HER2 status is evaluated in the clinic by IHC, only the HER2 membrane staining is taken into account. Dependent on the completeness of membrane staining and the extent in the tissue the HER2 score is determined. It is also important to note that HER2 has been shown to localise within the cytoplasm and the nucleus [reviewed in (Mills, 2012)]. In the present study no nuclear staining was observed. Cytoplasmic staining was observed to different extents in the majority of HER2 positive tumours. The strongest cytoplasmic staining was observed with the N-terminal antibody.

Next the *HER2*-gene amplification was assessed for part of the cohort. These included the tumour samples which were flagged up as discrepant by the IHC experiments. The HER2-negative tumours were also scored HER2-negative by the CISH assay. Five of nine originally HER2-positive tumours showed *HER2*-gene amplification by CISH. Two tumours showed borderline scoring (IHC-1, IHC-15) and two were scored HER2-negative. One of the tumours, IHC-3 was confirmed by CISH to have a HER2-positive score, however it showed no HER2 overexpression with the C-terminal antibodies and only a 2+ score with the N-terminal antibody. This patient was originally scored HER2-positive and would

have been accordingly treated. However, the protein level data suggests no overexpression of wild type HER2. The 2+ score with the N-terminal antibody might indicate the increased presence of truncated proteins such as p100 or Herstatin. As discussed in the main introduction p100 and Herstatin are HER2 protein variants that cannot induce downstream signalling and are considered tumour suppressors (Jackson *et al.*, 2013). Tumours with a HER2-positive CISH score, but HER2-negative IHC score are a minor group. Work by Kurozumi *et al.* found such a pattern in 1.8% of tested tumours. They correlated this observation with a worse survival rate than *HER2* gene and protein negative patients (Kurozumi *et al.*, 2016). It has not been sufficiently tested how HER2-negative patients respond to anti-HER2 therapy, it is likely that in this case the patient did not respond as expected to a HER2 targeting therapy; no follow up data for these patients is currently available.

In two cases the CISH assay clearly scored HER2-positive tumours as HER2-negative. These tumours, IHC-11 and 13 were also assessed as HER2 negative by IHC. IHC-11 showed no signs of HER2 genetic heterogeneity. For IHC-13 a few dispersed nuclei with a low-level HER2-gene amplification could be observed. This tumour stained 2+ with the N-terminal antibody, again suggesting the presence of truncated HER2 protein variants.

The two borderline cases IHC-1 and 15 are difficult to assess. They showed only very minimal HER2-gene amplification in combination with chromosome 17 monosomy. Dependent on assessment criteria they could also be classed as HER2-negative (Rakha *et al.*, 2015). IHC-1 was also stained HER2-negative with the C-and N-terminal antibody. However the HercepTest™ scored the tumour as HER2 3+. Dr Kourea reported tumour heterogeneity for the IHC stained tumour sections. This tumour might contain focal HER2-positive tumour areas that were not part of all serial sections. Furthermore this tumour might not contain *HER2*-gene amplification, but overexpress HER2 through alteration at the transcriptional and translational level. In the IHC-15 tumour dispersed nuclei with a stronger *HER2*-gene amplification could be observed on a background of HER2-negative tumour cells. This tumour showed weak staining with the C-terminal antibodies, but a 3+ staining with the N-terminal antibody; again

suggesting a tumour which might express other forms of HER2 proteins such as the HER2 splice variants p100 and Herstatin.

One major concern is that the tumour sections assessed are not representative of the whole breast tumours. This might be one of the reasons for discrepancies between findings in this study and the original clinical HER2-status, if a tumour is focally heterogeneous in regard to its HER2 status and different areas are assessed. In the here studied cohort of tumours some tumour heterogeneity was observed. However more concerning was the variability between the IHC results. One could argue that the C- and N-terminal antibodies have not been tested and optimised for clinical use like the HercepTest™ and might therefore give less reliable results. The results should still not be disregarded, as both antibodies worked on the positive controls of each experiment, although less intensely. The results for the N-terminal antibody are most interesting, as they might indicate the expression of HER2 splice variants. A study showed antibodies for the extracellular domain/N-terminus and intracellular domains/ C-terminus of HER2 to give discordant results in 15% of assessed breast tumours. They associated high extracellular domain/ intracellular domain levels with an increased disease free survival (Carvajal-Hausdorf et al., 2015). Increased levels of extracellular domain are likely to indicate HER2 protein variants with a truncated C-terminus, such as p100 and Herstatin. Furthermore, absence of N-terminal staining with strong C-terminal staining could indicate the presence of HER2 C-terminal fragments.

### ***4.5.2. Possible role of HER2 splice variants in discrepant breast cancer cases***

The discrepant IHC staining results indicate that these tumours may well express other HER2 protein variants. To address this question PCRs were performed to study the expression of the well-studied splice variants p100, Herstatin and  $\Delta 16$ HER2 in the same tumour samples. PCRs were performed on 6 tumours (IHC-1, 3, 4, 13, 14 and 15). The wild type HER2 mRNA levels matched the results from the HercepTest™ for most tumours. The exception was IHC-15

which showed a strong band in the PCR, but a 0 score with the HercepTest™. Δ16HER2 was present in all tumours, but only at a consistently low level. Both Herstatin and p100 could be observed in all tumours. As suggested in the above sections variations to the levels of p100 and Herstatin could be observed. Herstatin was most pronounced in IHC-1, 4 and 15. In the tumours IHC-3 and 13 where the N-terminal antibody gave the strongest staining with HER2 2+ scores, p100 and Herstatin were clearly present. Tumour IHC-15 showed the highest level of p100. Additionally, the PCR band for wild type HER2 was also strong. However, the mRNA level of wild type HER2 does not translate to the protein level, as the HercepTest™ only scores this tumour as 1+. In contrast the N-terminal antibody showed a 3+ staining and might indicate that p100 is translated. It can only be cautiously suggested that membranous N-terminal HER2 staining might be due to p100 or Herstatin. These two proteins are not anchored in the cell membrane, however they might interact and dimerize with wild type HER2 or another member of the ErbB protein family.

### **4.6. Summary**

In this chapter a cohort of invasive primary ductal carcinomas was characterized using IHC and CISH. The IHC results showed discordance between the three HER2-specific validated antibodies. Although the controls of the antibodies were consistently accurate, the C-terminal antibody did not stain most tumours that were stained by the other antibodies. Some discrepancies were also observed with the N-terminal antibody, however staining was more similar to the HercepTest™. Interestingly in two tumours the N-terminal antibody stained more strongly than the HercepTest™. Tumour heterogeneity could be observed in four of twenty HER2-positive tumours. In addition to IHC, CISH was performed to determine the *HER2*-gene amplification status in a subset of tumours. It confirmed the clinical HER2 status for most tumours. For four tumours CISH gave a borderline or HER2-negative score although they had been clinically assessed as HER2-positive. Of these one tumour (IHC-1) was scored HER2 3+ by HercepTest™ therefore confirming its clinical status. However the other two tumours (IHC-13 and IHC-15) were also HER2-negative

by HercepTest™. Interestingly IHC-15 is scored HER2 3+ with the N-terminal antibody. As the different results between N- and C-terminal antibodies might indicate the presence of HER2 protein variants. Through conventional PCR the levels of HER2 splice variants p100, Herstatin and  $\Delta$ 16HER2 was assessed. Indeed, when taking the housekeeping gene and the level of wild type HER2 into consideration, the levels of p100 and Herstatin mRNA were elevated in a few cases. Most notable is the strongly elevated level of p100 in IHC-15, which as mentioned above had a HER2 3+ score with the N-terminal antibody, but none of the C-terminal antibodies.

### **4.7. Further work**

This chapter discussed the first findings of a larger study undertaken by our research group to investigate the importance of HER2 splice variants in breast cancer. For completeness the HercepTest™ should be performed on the remaining HER2-negative cases. This work showed differences in IHC results depending on the antibodies used. As the differences between the antibodies might indicate the increased levels of HER2 protein variants, conventional PCRs were performed to measure their levels. Although this gave first indicative results, in a next step TaqMan™ qPCR will be performed to quantify the expression of HER2 splice variants in all tumours. Additionally, it would be useful if RNA could be derived from laser-capture sections of the serial sections characterized by IHC and CISH. Furthermore, western blots should be carried out with samples from these tumours to determine the presence of HER2 protein variants that are not due to the main HER2 splice variants. The experimental results should then be correlated to patient therapy and follow up information to identify any possible connections. This is of great interest, as it could be hypothesized that some breast tumours which are assessed as HER2-positive, but express a substantial amount of HER2 protein variants that will not respond to anti-HER2 therapies. Conversely, tumours with low levels of wild type HER2, but elevated levels of undetected HER2 protein variants could be classed as HER2-negative. This could prevent patients from being treated with anti-HER2 therapy, although they might benefit from receiving it.

For further studies it could be of interest to employ a gene-protein assay such as used by Kurozumi *et al.* to measure IHC and CISH on the same samples (Kurozumi *et al.*, 2016). Additionally, it would be interesting to extend work to include metastatic tumours with tissue biopsies from secondary tumours. In this chapter tumours were discussed that showed discordance between *HER2*-gene and protein status. It is not known how this pattern will change in secondary tumours and whether *HER2*-negative tumour cells with *HER2*-gene amplification might change their phenotype to express *HER2* proteins. The need for such studies was further highlighted by a systematic review showing the lack of sufficient knowledge (Turner and Di Leo, 2013).

Furthermore, it would be of great interest to determine where *HER2* splice variants occur in a tissue. For this an mRNA-FISH assay should be developed. This FISH assay would need to be very specific to distinguish between wild type *HER2* and its splice variants. First steps have been performed for such an assay. It is based on the FISH Tag RNA Multicolor kit (Thermo Scientific). This kit could allow the detection of multiple mRNAs in parallel. Plasmids carrying templates for wild type *HER2* and  $\Delta 16$ *HER2* probes have been generated. It would be suggested to develop this method for the use in cell lines and adapt it for tissue sections. Performing this assay successfully on human breast tumour sections would give insight into the localization and extend of splice variant expression, which cannot be assessed from qPCR.

## Chapter 5: Identification of novel HER2 splice variants

### 5.1. Introduction

The proto-oncogene *HER2* is located on chromosome 17q12. On the sense strand *HER2* is preceded by phenylethanolamine N-methyltransferase (*PNMT*) and followed by growth factor bound protein 7 (*GRB7*). The antisense strand encodes post-GPI attachment to protein 3 (*PGAP3*) which partially overlaps with the reading frame of some *HER2* transcripts. The reading frame of migration and invasion enhancer 1 (*MIEN1*) also partially overlaps with the 3' end of some *HER2* transcripts (Figure 5.1). As mentioned in chapter 1, *HER2* has two promoters, with the more recently discovered 2<sup>nd</sup> promoter initiating transcription of 4 (novel) exons, upstream of the normal exon 1. Additionally, one transcript has been described that starts from the novel exon 4 instead of normal exon 1 or novel exon 1 (Figure 5.2: ErbB2-201). The NCBI database considers the *HER2* gene to have 32 exons. The transcript on which most studies, including ours, are based is 27 exons long and uses the 1<sup>st</sup> promoter (Figure 5.2: ErbB2-008).



**Figure 5.1: Chromosomal location of *HER2* and surrounding genes.**

Derived from <http://www.ncbi.nlm.nih.gov/gene/2064>.

The web archive Ensembl (<http://www.ensembl.org/>) contains 22 *HER2* mRNA transcripts (Examples in figure 5.2) and NCBI AceView (<http://www.ncbi.nlm.nih.gov/IEB/Research/Acembly>) 23 *HER2* mRNA transcripts. Some of these are un-spliced and very short, others deviate by the length of the untranslated region. In some cases the evidence comes from only one clone from a tissue that is high in splicing events, such as the brain or

testis. Most of the variants found in the databases have not been studied further. Interestingly, of the three well studied HER2 splice variants, supporting transcripts can only be found for Herstatin (AceView: ERBB2, variant iAug10) and p100 (Ensembl ID: ENST00000578199) but not  $\Delta 16$ HER2. Of the 22 *HER2* mRNAs in Ensembl, 12 have been shown, or are predicted, to be translated into proteins. In western blot experiments our group detected more HER2 protein bands than can be attributed to known HER2 protein variants (Gautrey et al., 2015). Also, C- and N-terminal antibodies gave different spectrums of protein bands ranging from 55 kDa to 185 kDa. Knockdown experiments using HER2 specific siRNAs caused the disappearance of these bands, confirming their identity as HER2 protein variants. The potential number of functionally different HER2 proteins could have a major impact on the role of HER2 in cancer such as breast carcinoma.

Ensembl database:

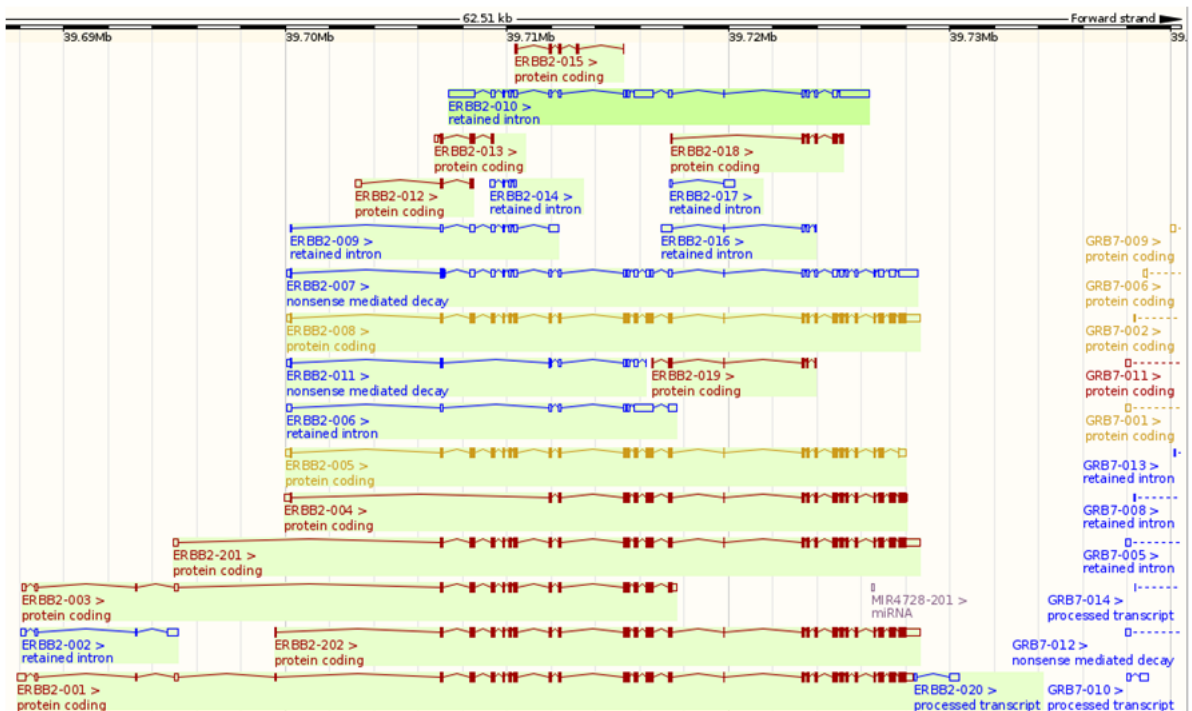


Figure 5.2: Transcript profile of the *HER2* (*ErbB2*) gene.

A snapshot of the Ensembl database shows the annotated *HER2* mRNA transcripts. Reference mRNA transcript is ErbB2-008.

In the previous chapters the focus was on the HER2 splice variant  $\Delta 16$ HER2. Here the existence of novel *HER2* mRNA transcripts was experimentally investigated. It was decided to use a PCR based approach to study possible

alternative splice variants of HER2 in breast cancer. Most HER2 protein variants studied so far, contain changes to the extracellular domain, therefore the focus of this study was on detecting changes to the mRNA sequence encoding the transmembrane and intracellular domain. Furthermore, the stability of any novel *HER2* mRNA transcript and the likelihood of translation into a novel HER2 protein variant were also investigated.

### **5.2. Aims**

The aims of this chapter were to:

- Identify novel HER2 transcripts
- Characterise the novel HER2 splice variant I25HER2
- Study the mRNA stability of I25HER2
- Observe the expression of I25HER2 in different normal human tissues
- Observe the expression of I25HER2 in a cohort of human breast tumours

### **5.3. Specific methodology**

#### ***5.3.1. In-silico predictions of I25HER2***

To predict the characteristics of potential protein product from any newly identified *HER2* transcripts, *in-silico* protein tools from the Swiss Bioinformatics Institute's Bioinformatics Resource Portal were used. The used mRNA sequences were translated into an amino acid sequence with the ExPASy translate tool ([http://web.expasy.org/cgi-bin/translate/dna\\_aa](http://web.expasy.org/cgi-bin/translate/dna_aa)). For the prediction of the molecular weight and isoelectric point, the ExPASy ProtParam (<http://web.expasy.org/protparam/>) was used.

The secondary structure of wild type HER2 and I25HER2 was predicted using the web resource of the Pôle BioInformatique Lyonnais: [https://npsa-prabi.ibcp.fr/cgi-bin/secpred\\_gor4.pl](https://npsa-prabi.ibcp.fr/cgi-bin/secpred_gor4.pl) [based on (Garnier et al., 1996)]. The

whole mRNA sequence was used for the prediction. The poly(A)-tail was not included, as its length is unknown.

### **5.3.2. RNA stability assay**

The rate of mRNA decay was studied using an RNA stability assay. For the RNA stability assay  $3 \times 10^5$  SKBR3 cells per well were seeded in 6 well plates with normal complete McCoy's medium. A 1 mg/mL Actinomycin D (Sigma) solution was prepared in DMSO. After 20 hours the medium was exchanged for complete McCoy's medium with 5  $\mu$ g/mL of Actinomycin D. The plates were immediately swirled for an even distribution of Actinomycin D on the cells. For time point 0 cells were harvested directly. Further cells were collected after 1, 2, 4, 6 and 8 hours. Cells were lysed in the ReliaPrep™ Cell Miniprep lysis buffer and stored overnight at -80°C. RNA was collected and reverse transcription performed as described before in sections 2.5.1 and 2.6.1.

### **5.3.3. Northern blot using NorthernMax®-Gly**

To determine to what extent intron 25 is retained in full length HER2 mRNA, northern blots were performed. The experiments were performed using the NorthernMax®-Gly kit (Life Technologies), based on the manufacturers recommendations. For details please refer to the manufacturer's instructions. This kit uses non-isotopic biotin labelled RNA probes to detect specific RNAs in RNA extracts from cells. Throughout the process RNase free conditions were ensured.

### **Generation of biotin labelled RNA probes**

Initially 83 bp long probes were used, but as these were found to not yield results, new longer probes were designed. PCRs were performed to produce templates for the generation of the new RNA probes, using cDNA from SKBR3

cells. Two probes were generated; one to capture general HER2 with a probe spanning exon 5 (size: 313 bp) and a second which encompasses parts of exon 25 and intron 25 (size: 311 bp) to detect intron 25 retention transcripts. The PCR was performed using the *Pfu* DNA Polymerase as described in section 3.3.6. Instead of 200 ng, 500 ng of cDNA were used in the PCR reactions. The primers used contain T7 promoter sequences. The T7 promoters are incorporated into the cDNA templates in an orientation that allows the production of RNA probes which are complementary to the mRNAs which were to be detected (Table 5.1). The PCR products were purified after separation on a 1% agarose gel (section 2.8.1) and used as a template for RNA synthesis.

**Table 5.1: Primers for the northern blot RNA probe DNA template.**

Name of Primer	Sequence
I25HER2_F	TCCCTCAACTGTCACCTCTCA
I25HER2_R with T7 promoter	TAATACGACTCACTATACAAATACATCGGA GCCAGCC
Wild type HER2_F	CTCCGATGTGTAAGGGCTCC
Wild Type HER2_R with T7 promoter	TAATACGACTCACTATAGGACAGGCAGTCA CACAGC

In the RNA synthesis step biotinylated CTP nucleotides (Invitrogen) were incorporated into the RNA probes. A reaction mix was prepared for each probe as described in table 5.2. The synthesis was carried out for 5 h at 37°C. The template DNA was degraded by TURBO™ DNase (Ambion) for 30 min at 37°C and the RNA was purified by phenol-chloroform extraction.

**Table 5.2: The T7 reaction mix for Northern blot RNA probe generation.**

Reagents	For a volume of 40 µL
10xBuffer	4 µL
RNaseOUT	2 µL
25 mM ATP, GTP and UTP mix	0.6 µL
10 mM CTP (1:4) mix	2 µL
T7 polymerase	4 µL
cDNA	0.3 to 1 µg
Nuclease free H <sub>2</sub> O	Fill up to 40 µL

## Northern blot

RNA from SKBR3 cells was used to detect the expression of *HER2* transcripts. To minimize unspecific interactions the GenElute Direct mRNA Mini prep kit (Sigma) was used, as it isolates the poly-adenylated mRNA fraction using oligo (dT) (for details see section 2.5.2). The mRNA (3 µg/lane) was mixed 1:1 with the glycoxal loading dye and denatured. The mRNA was size separated (5 V / cm electrode to electrode) on a 1% agarose gel together with a Millenium™ RNA marker (Ambion). The integrity and appropriate separation was briefly observed under UV light. Exposure was minimalised to keep damage to the mRNA minimal. For a size reference an image of the trans-illuminated gel and a ruler was taken. The assembly of the transfer is described in figure 5.1. A downward transfer of the mRNA onto a positively charged nylon BrightStar-Plus membrane (Life Technologies) was carried out for 2.5 h (Figure 5.3). After the transfer the mRNA was crosslinked at 254 nm UV light for 1 min with the membrane. During crosslinking of the mRNA, the successful transfer of mRNA can be observed.

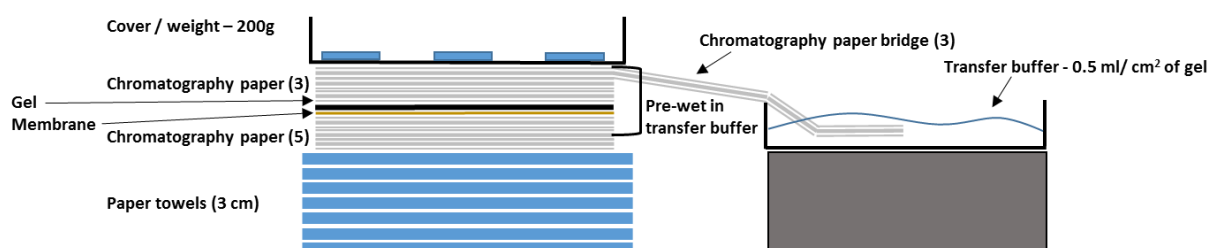


**Figure 5.3: Depiction of the northern blot transfer assembly.**

A stack (3 cm) of thick paper towels was prepared onto which 5 sheets of chromatography paper were placed. Three were pre-wet in the transfer buffer. Onto this the nylon BrightStar-Plus membrane was placed. Next the gel, followed by three pre-wet chromatography papers and the chromatography paper bridges were added. A tray with evenly spaced small weights (total 200 g) was placed on top. The buffer reservoir (0.5 mL/cm<sup>2</sup> of gel) is elevated to roughly the level of the membrane.

The membrane was cut into strips, so each 'mRNA lane' could be hybridized with the correct probe. The membranes were pre-hybridized at 68°C in ULTRAhyb buffer (10 mL/100 cm<sup>2</sup>) for 30 min in a hybridization oven. Next a

~16 h hybridization was performed. To optimise the binding of the probes to the mRNA, different concentrations of probes were used. The optimised concentrations were 10 ng (0.1 pmol) for the general HER2 probe and 30 ng (0.3 pmol) for the intron 25 retention probe. The probes were mixed with 1 mL of ULTRAhyb buffer and added to the membrane strips. Using the Low Stringency Wash Solution #1 (20 mL/100 cm<sup>2</sup>) a 10 min wash at RT and under agitation was performed. This was followed by two washes with High Stringency Wash Solution #2 (20 ml/100 cm<sup>2</sup>) for 15 min each at 68°C using agitation in a hybridization oven.

### **Detection of hybridization**

The Chemiluminescent Nucleic Acid Detection Module (Thermo Scientific) was used to detect the hybridized probes. The blocking and washing steps were carried out in 50 mL tubes (Greiner). The blocking and wash buffers were pre-warmed to 37°C. The membrane was blocked with 8 mL blocking buffer for 15 min. The blocking reagent was removed and fresh blocking buffer (8 mL) with Streptavidin/Horseradish peroxidase (25 µL) was added to the membrane strips and incubated for 15 min under agitation at RT. Next the membrane strips were washed 4 times with 4 x Wash Buffer. The membranes were then incubated in Substrate Equilibrium Buffer for 5 min at RT under agitation. Equal amounts of Luminol/Enhancer Solution and Substrate Working Solution were mixed. Excess liquid was removed from the membrane, the ECL mix was applied to it and incubated for 5 min. The ECL was then removed, and the films exposed to the chemiluminescence for 1 h.

## 5.4. Results

### 5.4.1. Identification of novel HER2 splicing events by PCR

As mentioned in section 5.1, the *HER2* gene has been reported to have two promoters and alternative first exons. The initial experiments were performed in the breast cancer cell line SKBR3, as these overexpress HER2 and produce all well studied HER2 splice variants. None of the 2<sup>nd</sup> promoter associated exons could be detected by PCR under these experimental conditions. However, a very short exon (51 bp) was found to be expressed in SKBR3 cells (Figure 5.4). This novel exon 6 is situated shortly upstream of the conventional exon 1.

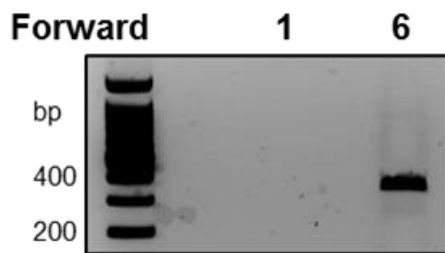


**Figure 5.4: Expression of exons upstream of normal exon 1.**

PCRs were performed on SKBR3 cDNA to amplify HER2 transcripts spanning from the upstream (novel) exon 1 or 6 to normal exon 3.

In the next step the existence of HER2 alternative splice variants was investigated. As all the established HER2 splice variants are generated by variations in the first 17 exons, this work focused on exons 17 to 27, which encode the transmembrane and intracellular domain. For completeness fellow PhD student M. Silipo investigated the first 16 exons. Specific forward and reverse primers covering exons 17 to 27 were used in a series of PCRs to amplify any intron retentions, exon skipping events or novel exons (Figure 5.5 A and B). The PCRs were performed on cDNA from SKBR3 cells. The reverse primer in exon 21 did not work, but the primers in the surrounding exons worked and should therefore amplify any variations in this area. In figure 5.5 A, two faint upper bands could be observed for the PCRs with forward primer in exon 25 and reverse primers in exons 26 and 27. Figure 5.5 B, the PCR with forward primer in exon 24 and reverse primer in exon 26 also shows a very faint band at ~ 650 bp. The upper bands were sequenced and confirmed to be due to the retention of the 291 bp sized intron 25. PCRs on cDNA from three separate

nuclear and cytoplasmic RNA fractions showed that intron 25 is present in the cytoplasm; opposed to transcripts containing both intron 25 and 26, which are only found in the nuclear fraction suggesting an only partially spliced transcript (Figure 5.5 C).

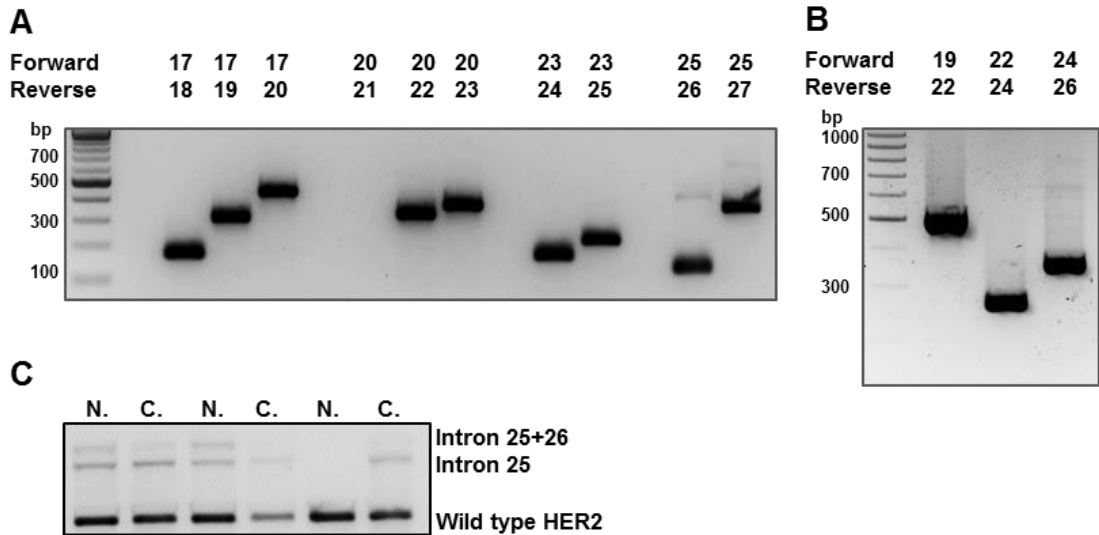


**Figure 5.5: The retention of intron 25 in HER2 transcripts.**

All PCRs were carried out using cDNA from SKBR3 cells. A, PCR based mapping of splicing events between exons 17 and the last exon 27. Reverse primer in exon 21 did not work. B, Three PCRs from exon 19 to 22, exon 22 to 24 and exon 24 to 26. C, Expression of wild type HER2 and intron 25 retention with or without intron 26 in cDNA from nuclear (N.) and cytoplasmic (C.) RNA fraction.

To understand the nature of the intron 25 containing mRNA, PCRs were performed using a reverse primer in intron 25 in combination with forward primers spanning the exons upstream, until conventional exon 1. The PCR with a forward primer in exon 1 did not yield a PCR product and amplifications from exon 2 and 3 were very faint. Two bands were observed for all PCRs with forward primers upstream from exon 12 (Figure 5.6 A and B), the upper bands were attributed to intron 12 (361 bp) retention, which was identified by fellow PhD student M. Silipo. The retention of intron 12 was also confirmed with a forward primer in intron 12 and a reverse primer in intron 25 (Figure 5.6 B and C), the intron 12 retention band was stronger in SKBR3, than MCF-7 cDNA. Intron 25 is not retained in transcripts skipping exon 16, therefore not part of  $\Delta 16$ HER2 (Figure 5.6 B and C).

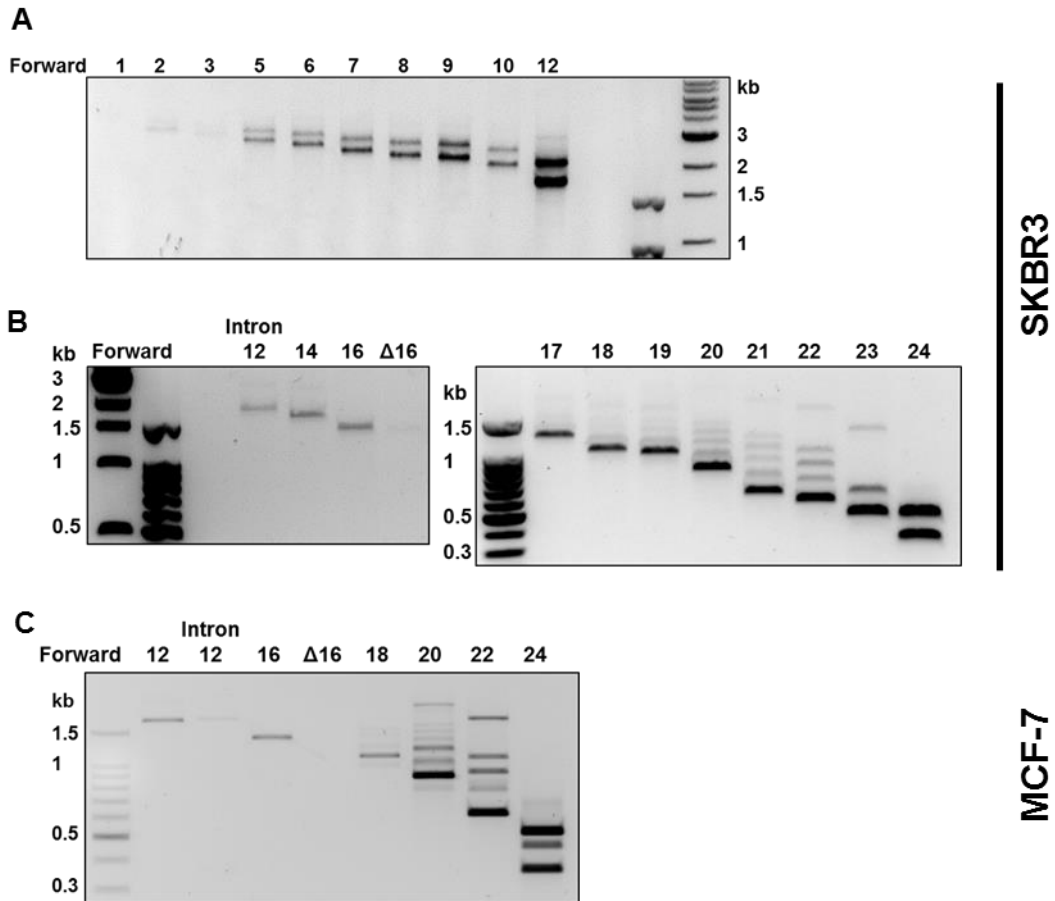


**Figure 5.6: Presence of intron 25 in *HER2* mRNA transcripts.**

PCR based mapping of the inclusion of intron 25 was performed. In A, and B, SKBR3 cDNA was used. A, Using forward primers in exons 1 to 12 with a reverse primer in intron 25. B, Using forward primers in intron 12 and exons 14 to 24 and exon 16 skipping ( $\Delta 16$ ) in combination with a reverse primer in intron 25. C, PCR using forward primers in exons 12 to 24, including exon 16 skipping ( $\Delta 16$ ) with intron 25 reverse primers performed on MCF-7 cDNA.

A very diffuse range of PCR products were amplified between exons 20 and 24, if a reverse primer in intron 25 was used (Figure 5.6 B and C). The bands above 1.5 kb match the predicted sizes of intron 23 (708 bp) retention. The strongest bands are due to intron 24 (155 bp) retention. However, this intron retention was not observed in the initial experiments (Figure 5.5 A). Figure 5.6 C shows the same area amplified with MCF-7 cDNA. A similar if not more complex range of PCR products were amplified. The additional fainter bands in both SKBR3 and MCF-7 were due to the sequential retention of introns. Surprisingly, compared to the expression profile in SKBR3 cells, in MCF-7 cells the PCRs that amplify from forward primers upstream of exon 20 are much fainter.

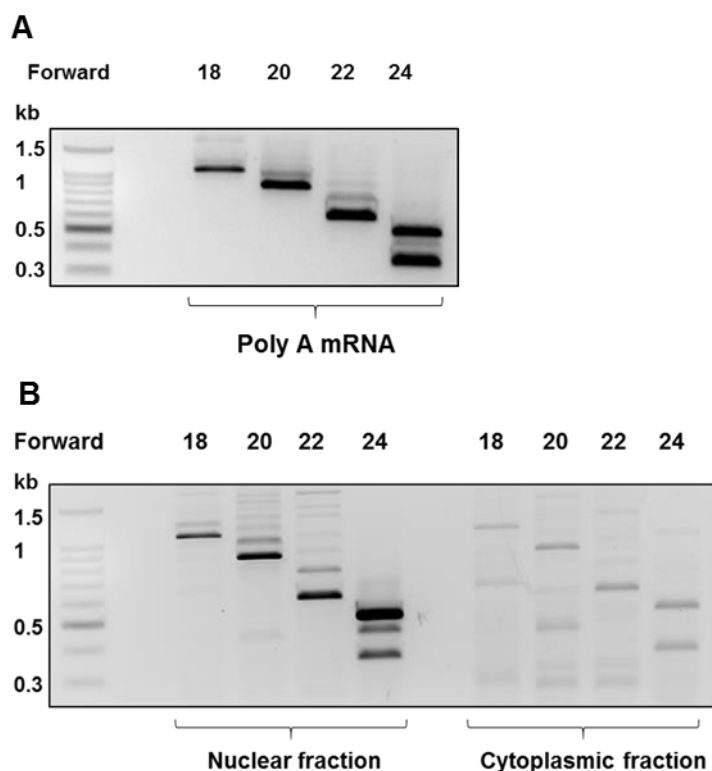


**Figure 5.7: Presence of intron 25 in *HER2* mRNA transcripts.**

PCR based mapping of the inclusion of intron 25 was performed. PCRs with forward primers in exon 18 to exon 24 with reverse primers in intron 25 were performed. A, for these PCRs cDNA from poly(A) enriched SKBR3 mRNA was used. B, for these PCRs cDNA from cell compartment fractionated nuclear and cytoplasmic SKBR3 mRNA was used.

To separate intermediate splice products from mature mRNAs, PCRs were performed on a three different RNA preparations. PCRs for the region of exon 18 to 24 were performed with cDNA from poly(A) enriched as well as nuclear and cytoplasmic fractions of SKBR3 mRNAs (Figure 5.7). The poly(A) enriched RNA, should primarily contain polyadenylated mRNA. The number of bands is strongly reduced in the PCRs using this cDNA, only the intron 24 retention band can be observed in the PCRs with forward primers in exons 22 and 24, and very faintly with the forward primer in exon 20 (Figure 5.7 A). PCRs performed on the nuclear RNA fraction show a very strong band for the retention of intron 24 when using a forward primer in exon 24, as well as additional fainter bands as previously observed with normal cDNA (Figure 5.7 B). The PCR products from the reactions using the cytoplasmic RNA fraction are faint. In the cytoplasmic fraction a number of bands that could be seen before totally disappear (Figure 5.7 B). However retention of intron 24 in combination with intron 25 can still be

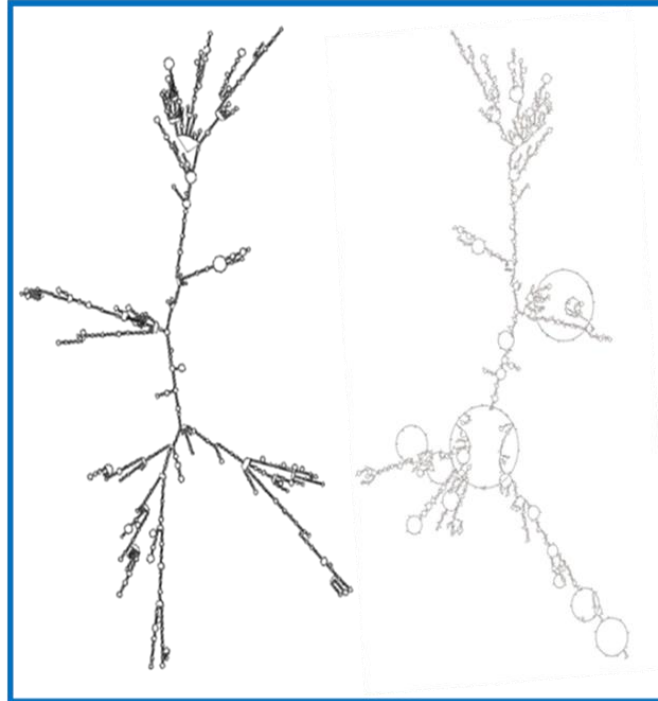
observed, but only if amplified from exon 24 to intron 25. The cytoplasmic fraction was expected to only contain mature mRNAs and for any intermediate splicing products to not be present.

### **5.4.2. *In-silico* predictions for I25HER2 mRNA and protein**

The PCR-based mapping of intron 25 retention indicated it to be primarily retained in an otherwise normal full length HER2 transcript. Intron 25 is 291 bp long and does not change the reading frame of the transcript. The intron also encodes a premature stop codon, which could cause this transcript to be a target of nonsense-mediated decay. An *in-silico* prediction of the mRNA secondary structure of I25HER2 and wild type HER2 was performed to assess the impact of the retained intron 25 on the overall secondary structure. As for the prediction of  $\Delta$ 16HER2, both the MFE and the centroid plain model were used. The MFE model predicted secondary structure of I25HER2 shows differences in some areas of the structure compared to the prediction for wild type HER2. The main differences are observed in the bottom half of the images in figure 5.8. The centroid model predicted a secondary structure for I25HER2 which is very different compared to wildtype HER2.

In the next step *in-silico* predictions for a translated I25HER2 protein was performed. The I25HER2 mRNA is predicted to translate into an 1110 amino acid long protein (ExpASy Bioinformatics Resource portal). Due to the stop codon in intron 25 it is predicted to lack the last 202 amino acids of the normal HER2 C-terminus and to instead contain a novel 57 amino acid long C-terminus (Figure 5.9, A). No sequence similarity can be observed when aligning the two C-termini.

Predicted wild type HER2 mRNA structure



MFE plain structure

Centroid plain structure

Predicted I25HER2 mRNA structure



MFE plain structure

Centroid plain structure

**Figure 5.8: *In-silico* predicted secondary structure of wild type HER2 and I25HER2 mRNA.**

Secondary mRNA structure predictions from two methods are shown, the minimum free energy (MFE) model and the centroid plain model. The predicted secondary structure for the full length mRNA transcripts are shown, but lacking the poly(A)-tail. Images were generated by the RNAfold web server, based on (Lorenz *et al.*, 2011).

A

SGGGDLTLGLEPSEEEAPRSPLAPSEGAGSDVFDGDLGMGAAKGLQSL  
 PTHDPSPLQRYSEDPTVPLPSETDGYVAPLTCSPQPEYVNQPDVRPQPP  
 SPREGPLPAARPAGATLERPKTLSPGKNGVVKDVFAGGAVENPEYLTP **Wild type HER2 C-terminus**  
 QGGAAPQPHPPAFSPAFDNLYYWDQDPPERGAPPSTFKGTPTAENPE  
 YLGLDVPV

VSALGHTVWLSAYLPQRWTRVPFSDVPSTVTSQGNPIIPTKNSYCLPTP **I25HER2 C-terminus**  
 VTPFSPR

B

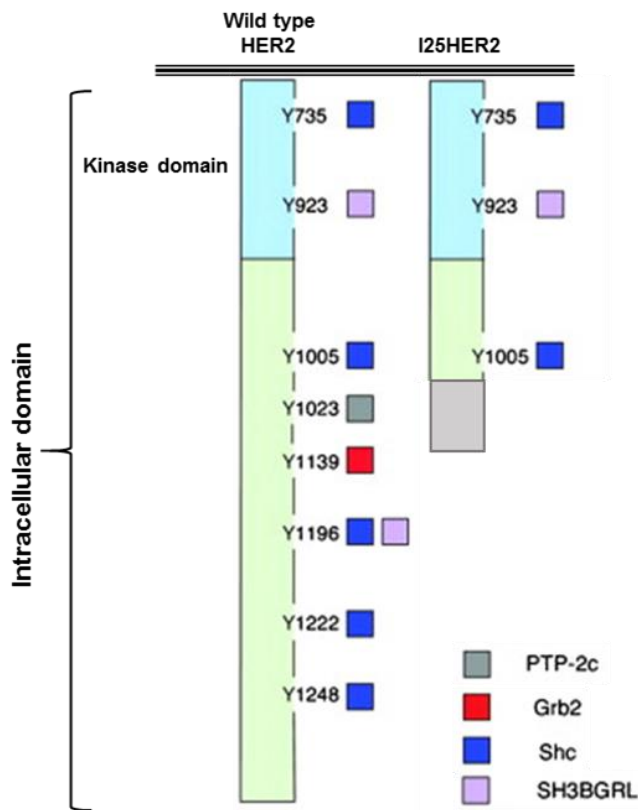


**Figure 5.9: Protein predictions for I25HER2.**

A, The C-terminus of wild type HER2 and I25HER2 is shown. I25HER2 protein sequence encoded by intron 25 was predicted by ExPASy translation tool ([http://web.expasy.org/cgi-bin/translate/dna\\_aa](http://web.expasy.org/cgi-bin/translate/dna_aa)). B, The phosphorylation and binding sites in wild type HER2 and I25HER2 are shown. It is indicated for which protein the phosphorylation sites function as binding motifs. Image was adapted from (Roskoski, 2013).

I25HER2 is predicted to have a molecular weight of 123.1 kDa and isoelectric point (pI) of 6.25 (ExPASy ProtParam). Wild type HER2 without post-translational modifications is 137.9 kDa in size and has a basal pI of 5.58. Due to extensive post-translational modifications of wild type HER2, it is normally 185 kDa in size. Therefore I25HER2 can be expected to be closer to 170 kDa in size. The C-terminus of wild type HER2 is highly phosphorylated especially at the tyrosines, which act as important binding sites for downstream effectors. The predicted I25HER2 protein lacks five of these binding sites and only contains 1 instead of 6 tyrosines in the alternate sequence (Figure 5.9, B).

## Chapter 5: Identification of novel HER2 splice variants

Protein secondary structure predictions were performed for wild type HER2 and I25HER2 (web resource of the Pôle BioInformatique). The secondary structure predicted for I25HER2 differs in its C-terminus from wild type HER2. The shorter I25HER2 sequence lacks an alpha helix and has a shorter random coil structure broken up by extended strands compared to wild type HER2 (Figure 5.10).



**Figure 5.10: Predicted secondary structures of wild type HER2 and I25HER2.**

Bellow the amino acid sequence the predicted secondary structure is indicated. The table indicates the secondary structures, their abbreviations and percentage of the total protein sequence. The purple bar indicates the start of the alternative C-terminal sequences. Based on the online prediction by: [https://npsa-prabi.ibcp.fr/cgi-bin/secpred\\_gor4.pl](https://npsa-prabi.ibcp.fr/cgi-bin/secpred_gor4.pl); (Garnier *et al.*, 1996).

5.4.3. Expression of I25HER2 in cell lines and tissue

To understand whether the expression of intron 25 retention is just a by-product of the aberrant overexpression of HER2 in the SKBR3 cancer cell line or if it is expressed more commonly the following experiments were performed. The level of intron 25 was observed in a number of breast cancer cell lines. Intron 25 retention was found to be present in all tested breast cancer cell lines and mostly in the same ratio to wild type HER2 (Figure 5.11, A). Except for one sample of normal breast tissue in which the intron 25 level was increased compared to wild type HER2.

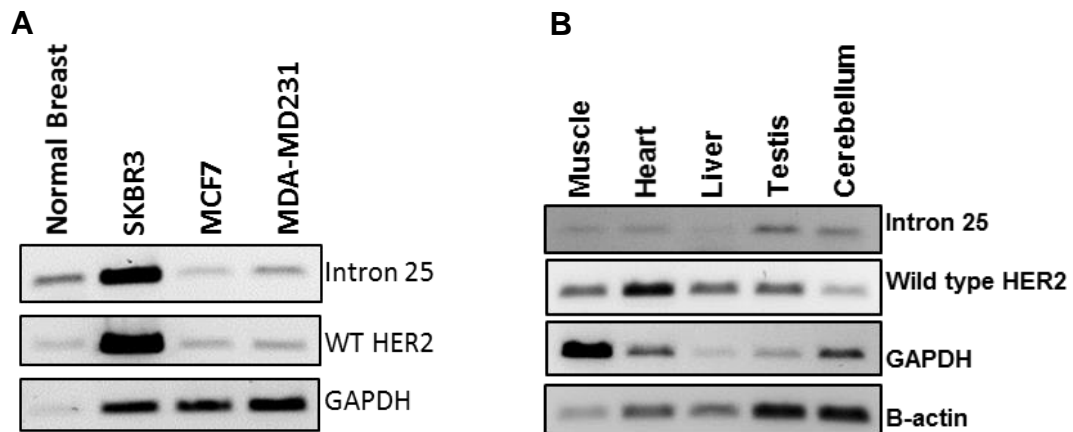


Figure 5.11: Expression of I25HER2 in a panel of human breast cancer cell lines (A) and normal human tissues (B).

Conventional PCR was performed to amplify Intron 25 HER2, wild type HER2 and the housekeeping genes GAPDH. A second housekeeping gene  $\beta$ -actin was included for the normal tissues, as GAPDH is differentially expressed in tissues.

A panel of normal human tissues was used to further study the splicing of intron 25. PCRs for intron 25 retention, wild type HER2 and two housekeeping genes were performed (Figure 5.11, B). The primers for intron 25 were located in exon 25 and intron 25. The intron retention could be observed in all of the studied tissue samples. The level of intron 25 did not correspond directly to the level of wild type HER2. In the heart sample intron 25 is only faintly expressed, whereas wild type HER2 is strongly expressed. In the cerebellum intron 25 is present nearly at the same level as wild type HER2. Overall the intron 25 retention is the most abundant in testis and cerebellum.

Furthermore, samples from the Breast Cancer Now Tissue Bank were used to study the relationship of intron 25 retention within breast cancer subtypes (Figure 5.12). A forward primer in exon 23 and a reverse primer in intron 25 were used to detect intron 25 retention. This combination was used not only to detect intron 25 or intron 24 and 25 retention, but to also show genomic DNA contamination which would be characterised by the additional inclusion of intron 23. The focus is on the intron 25 retention band, as combined intron retention of intron 24 and 25 could be caused by incompletely spliced mRNAs. No genomic bands were detected. Additionally, PCRs for wild type HER2 and the housekeeping gene  $\beta$ -actin were performed. Samples from two groups (Group 5 and 9) of HER2-positive/ER-negative grade 3 ductal carcinomas and one group (Group 3) of HER2/ER-negative grade 3 ductal carcinomas, as well as one group (Group 1) of normal breast tissue from breast reduction surgery were used. PCRs on five samples for each group were performed and SKBR3 was included as a positive control. It should be noted that although the same amounts of RNA were used to generate cDNA, fluctuations in expression of the housekeeping gene  $\beta$ -actin impair normalisation between samples. For most samples the ratio between wild type HER2 and intron 25 expression was consistent.

In the two groups of HER2 positive breast tumours four samples (G5-3, G5-4, G9-3, G9-4) showed a lower expression of wild type HER2 than expected for HER2 positive tumours. When comparing the tumour samples to SKBR3 and normalising by  $\beta$ -actin, the ratio between intron 25 retention and wild type HER2 seems consistent. In contrast variations in the ratio between intron 25 retention and wild type HER2 in both normal breast and ER/HER2-negative tumour samples were observed. As expected the level of wild type HER2 was very low in normal breast and HER/ER-negative tumour samples. In some HER2/ER-negative tumour samples (G3-3, G3-4, G3-5) wild type HER2 could not be detected. One normal breast sample, G1-4 had a slightly increased expression of wild type HER2. However in all samples of group 1 and 3 intron 25 retention could be observed. The samples G3-3, G3-4 and G3-5 should be noted as they show intron 25 retention, but wild type HER2 levels remain below detection limit. In most samples the retention of intron 24 and 25 remains in the same ratio to intron 25 retention and wild type HER2. Interesting exceptions are the

normal breast samples G1-1, G1-3 and G1-4 as well as the HER2/ER-negative tumour samples G3-3 and G3-4, which show no double intron retention.

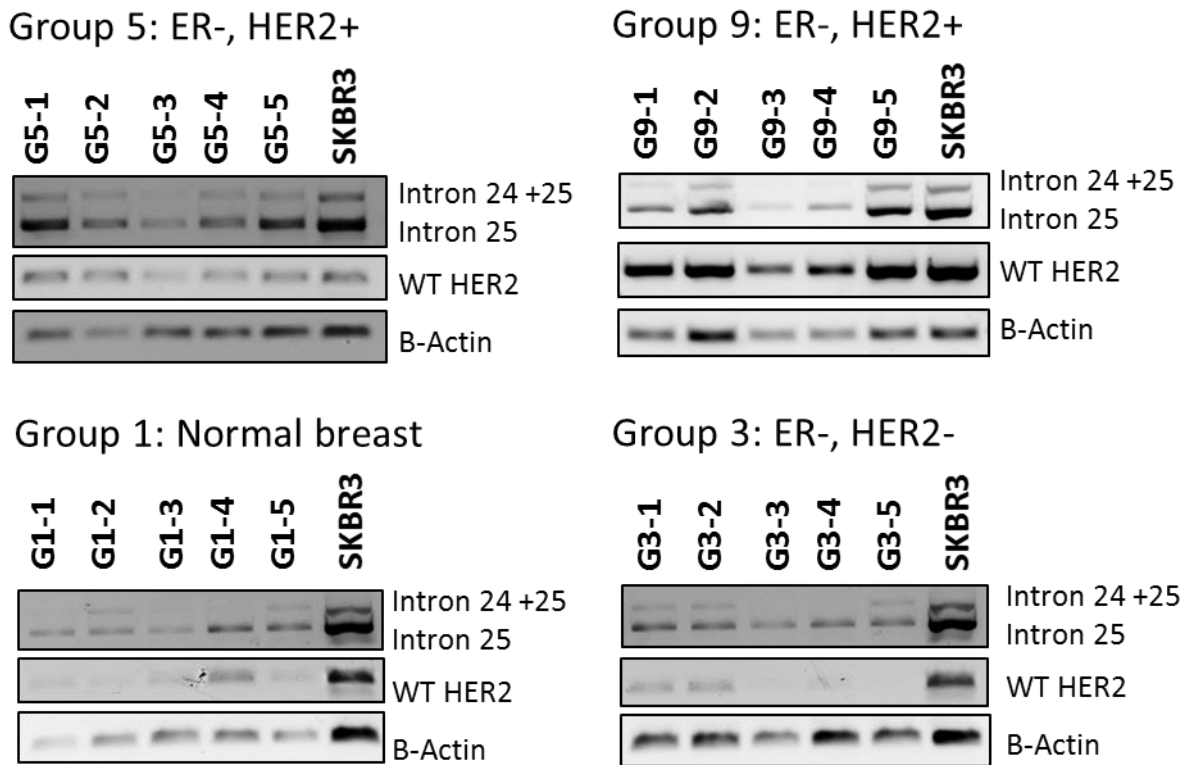


**Figure 5.12: Expression of I25HER2 in breast tumour and breast reduction samples.**

Conventional PCR was performed to amplify the retentions of HER2 introns 24 and double intron 24 and 25 retention. Wild type (WT) HER2 and the housekeeping gene  $\beta$ -actin were also amplified. Tissue samples were provided by the Breast Cancer Now Tissue Bank. The sample groups shown here are: Group 5 - grade 3, ER-negative, HER2-positive ductal carcinoma; Group 9 - grade 3, ER-negative, HER2-positive ductal carcinoma; Group 1 - normal breast from reduction surgery; Group 3 - grade 3, ER-negative, HER2-negative ductal carcinoma. The PCRs were performed on five samples of each sample group. SKBR3 was included as a positive control for HER2 expression.

**5.4.4. Stability of I25HER2 mRNA**

The novel HER2 transcript I25HER2 is likely to undergo nonsense-mediated decay as the retained intron encodes a premature stop codon (Silva and Romao, 2009). To study how stable the I25HER2 transcript is, a RNA stability or RNA decay assay was performed. Using Actinomycin D the transcription of mRNAs was impaired and the degradation of mRNAs observed over a time period of 8 hours. One representative experiment of three biological replicates is shown here (Figure 5.13). The levels of wild type HER2 and GAPDH stay relatively unaffected by the Actinomycin D treatment until 8 h after treatment. The levels of  $\Delta$ 16HER2 and intron 25 stay relatively stable for the first four hours and then decrease. Opposed to this, the levels of intron 12 retention decrease strongly within the first hour and are only very slightly detectable afterwards. This increased stability of intron 25 compared to intron 12 indicates that I25HER2 might evade the normal nonsense-mediated mRNA decay.

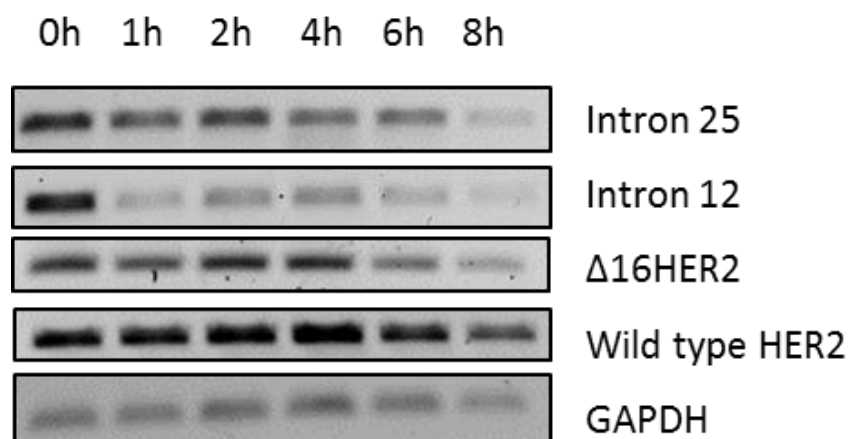


**Figure 5.13: RNA stability assay for HER2 transcripts.**

SKBR3 cells were treated with 5  $\mu$ g/mL Actinomycin D. At 0, 1, 2, 4, 6 and 8 hours post-treatment RNA was collected. Following reverse transcription PCRs were performed to detect the expression levels of intron 25 retention, intron 12 retention,  $\Delta$ 16HER2, wild type HER2 and GAPDH. One representative experiment of 3 biological replicates is shown.

Next, a non-isotopic northern blot was designed to study the expression of intron 25 and to better understand what *HER2* transcript it is part of. The positive control provided in the NorthernMax®-Gly kit was used, alongside the

HER2 specific probes. A strong band at ~ 1.5 kb was detected. This matches with the expected 1.4 kb of mouse GAPDH mRNA. One representative experiment is shown in figure 5.14. Very faint additional bands can be observed at stronger exposures. Given their size, these are expected to be due to unspecific binding to the RNA of the 28S and 18S ribosomal subunits.

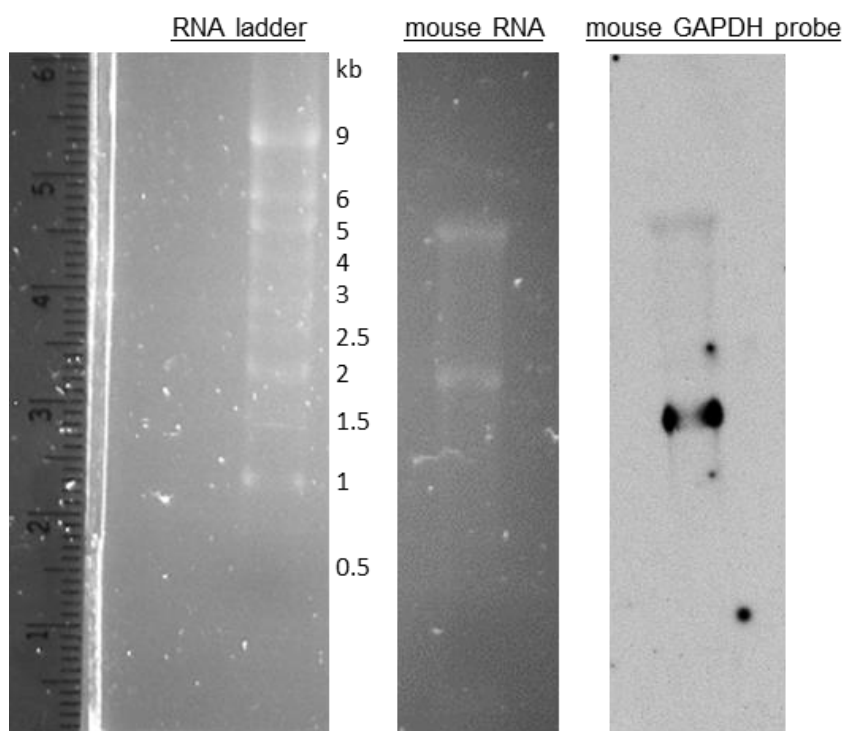


**Figure 5.14: Mouse GAPDH positive control for northern blot.**

Results of the positive control experiment for the northern blot is shown (n=2). The first panel shows the RNA ladder with a ruler aligned for comparison. The second panel shows the mouse RNA size separated on an agarose gel. The last panel show the northern analysis using the company provided mouse GAPDH RNA probe.

After establishing this basic northern blot in our laboratory, a series of optimisation steps were undertaken to detect human general HER2 and intron 25 retention. A RNA probe was designed to bind to exon 5 to detect all HER2 transcripts and a second probe was designed to target intron 25. To prevent unspecific binding of the RNA probes to ribosomal RNA and partially spliced pre-mRNAs, poly(A) enriched mRNA from the HER2 overexpressing SKBR3 cell line was used. A number of optimisation steps were carried out to detect

both general HER2 and intron 25 retention. Two experiments were performed in which the same pattern with the general HER2 probe was observed. However the assay had to be further optimized for intron 25 detection. In figure 5.15 the results from the last optimisations are shown. The first panel of figure 5.15 shows the size separated mRNA. The most abundant mRNAs are visible at approximately 9, 3, 2.4 and 1.4 kb. As poly(A) enriched mRNA was used in the assay no ribosomal RNAs (18S - 1.9 kb, 28S - 5 kb) can be observed. As no biotin-labelled RNA ladder of appropriate size exists, a ruler was aligned to later assign the correct size to the northern blot. The two northern blots in figure 5.14 show the corresponding hybridization of probes for general HER2 and intron 25. In the intron 25 blot two bands (8-9 kb and 2.8kb) were detected. With the general HER2 probe multiple bands were detected at 9, 4.5, 3 and 2.5 kb. Due to the signal strength of the dominant bands, fainter bands are difficult to determine. However there seems to be a faint band at 2.8 kb and one at 2 kb. The 9 kb bands are roughly the size of the main mRNA bands on the agarose gel and do not match any known *HER2* transcript. The 4.5 kb band detected by the general HER2 probe matches the size of wild type HER2. The 3 and 2.5 kb bands of the general HER2 plot, similar to the 9 kb band are very close in size to the most abundant RNAs on the agarose gel. The HER2 splice variant p100 was determined to be 2.3kb of size and could possibly correspond to the 2.5 kb band (Doherty *et al.*, 1999a). Additionally, with the intron 25 probe a second band that does not seem to match any of the mRNA bands of the agarose gel was detected. This band is 2.8 kb of size and could match a very faint band on the general HER2 blot. An intron 25 band was expected to overlap with a general HER2 band, as the general HER2 probe binds exon 5, which was shown in PCR to be part of I25HER2.

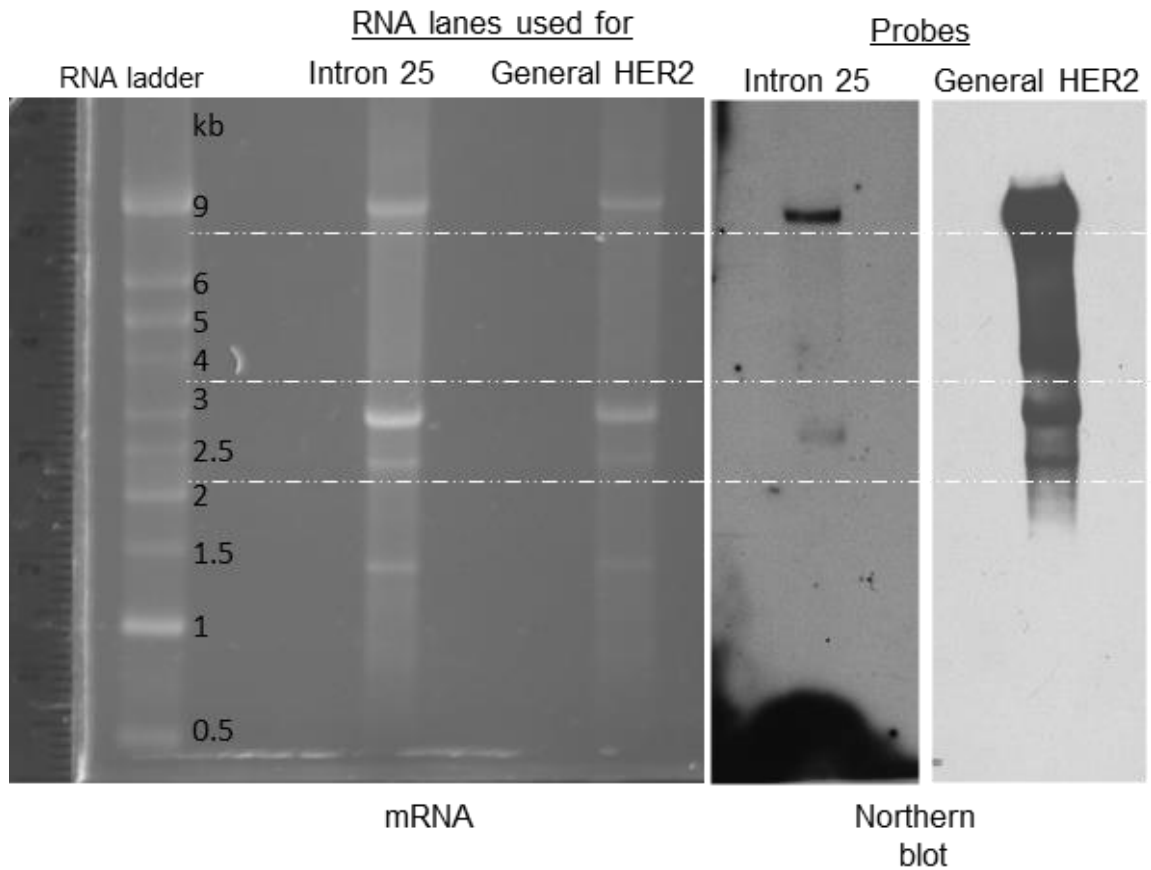


**Figure 5.15: Northern blot for I25HER2 and wild type HER2.**

Results of northern blot for general HER2 and intron 25 retention are shown. The first panel shows the agarose gel with the RNA ladder and two lines of poly(A) isolated RNA. For comparison a ruler was aligned. The next panels show the northern analysis with the general HER2 and intron 25 probes. For general HER2 4 bands can be detected and for intron 25 two bands.

## **5.5. Discussion**

Currently about 30% of breast cancers are diagnosed as HER2-positive. This subset of breast tumours is associated with a poor prognosis, although treatment with anti-HER2 drugs has improved the survival rates. As detailed in the introduction, resistance can occur both in adjuvant and neo-adjuvant HER2 targeted therapy in both primary and advanced metastatic breast cancer (Guarneri *et al.*, 2010). In chapter four breast cancer cases with discordant HER2 status profiles were discussed. The differences observed when using different HER2 antibodies highlight the importance of re-evaluating the clinical assessment of HER2 positivity. This highlights the need for a detailed analysis of the HER2 variants. In this chapter the existence of previously undescribed HER2 splice variants was investigated. A large number of *HER2* mRNA transcripts can be found in online databases (NCBI AceView and Ensembl), but they have not been studied further.

### **5.5.1. Intron 25 retention**

Our research group decided to re-investigate *HER2* transcript variants. In this thesis the focus was on the mRNA sequence encoding the transmembrane and intracellular domain of HER2, as the known three splice variants arise from changes to the first 16 exons. The retention of intron 25 (I25HER2) was detected in a number of cell lines and tissues. Intron retentions are often dismissed as intermediates of pre-mRNA splicing or unimportant by-products of aberrant splicing. This is a narrow view has been disputed by a number of intron retaining mRNAs that give rise to functional proteins [reviewed in (Hube and Francastel, 2015)]. HER2 itself has two functional splice variants that arise due to intron retention, p100 and Herstatin (Gebhardt *et al.*, 1998; Doherty *et al.*, 1999a).

Intron 25 encodes a premature stop/termination codon (PTC). PTCs are a main signal on mRNAs to initiate nonsense-mediated mRNA decay (NMD). NMD is normal cellular mechanism that limits the translation of C-terminally truncated

proteins with dominant-negative or gain-of-function variations [reviewed in (Silva and Romao, 2009)]. A transcript with a PTC more than 50-55 nts upstream of the last exon-exon junction will be recognised as a target of RNA decay (Nagy and Maquat, 1998). Therefore the recognition of a PTC is dependent on the recognition of exon-exon junctions and the splicing associated assembly of the exon junction complex (EJC). The EJC is a protein complex assembled 20-24 nt upstream of each exon-exon junction (Le Hir *et al.*, 2000). NMD takes place in the first round of translation from an mRNA. At this stage the cap-binding complex is still associated with the mRNA [reviewed in (Maquat, 2004)]. Each EJC is displaced from the mRNA as it is translated in the ribosome. If a PTC terminated the translation early, the remaining EJCs interact with the terminating ribosome and the SURF complex is formed which triggers the degradation of the mRNA [reviewed in (Popp and Maquat, 2013)]. In the case of intron 25 retention the next EJC is expected to be located more than 55 nt downstream of the PTC in intron 25. However there are cases where the transcripts are translated in spite of a premature stop codon. One example is the HER2 splice variant Herstatin, which retains the PTC containing intron 8 (Doherty *et al.*, 1999a). Another example is  $\beta$ -globulin in the disease  $\beta$ -thalassaemia. There mutations to  $\beta$ -globulin have been identified that result in a PTC in exon 1. These  $\beta$ -globulin variants are translated at a comparable level to the wild type (Romao *et al.*, 2000).

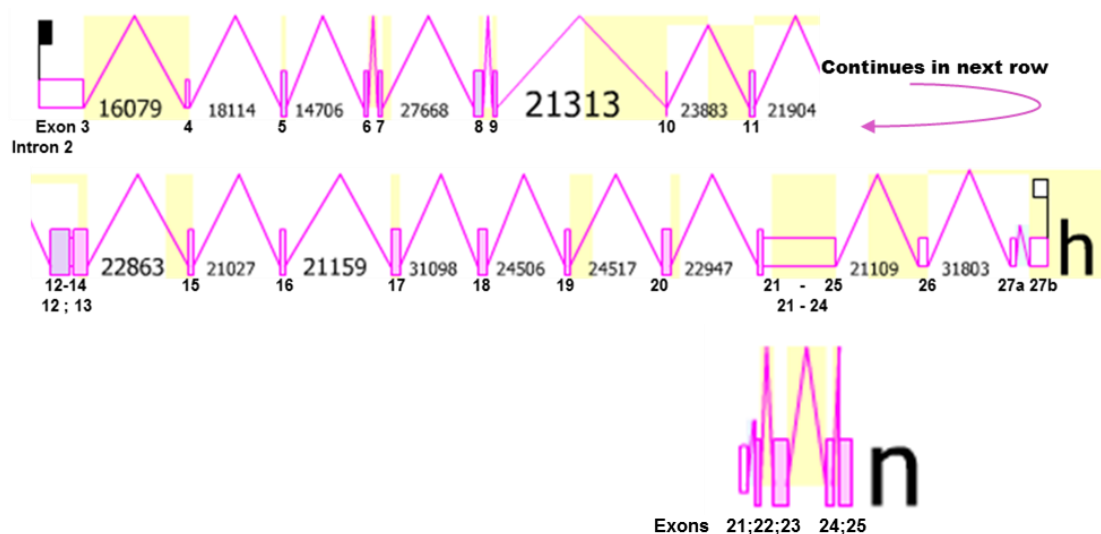


**Figure 5.16: Transcript profile of the *HER2* gene.**

A snapshot of two *HER2* mRNA transcripts from the NCBI AceView database are shown; variant “h” and “n”. Exons and retained introns are indicated on the images.

## Chapter 5: Identification of novel HER2 splice variants

Through PCRs performed on cDNA from different RNA preparations, it was possible to confirm the presence of intron 25 mRNA in the cytoplasm and as part of polyadenylated transcripts. Intron 25 retention is part of an mRNA transcript that is, as far as could be assessed, full length. Due to the length of the transcript, the PCR from exon 1 to intron 25 was not successful. Amplification was only possible from exon 3 to intron 25. The finding that intron 25 is not retained in exon 16 skipping ( $\Delta 16$ HER2) transcripts, further supports the assumption that intron 25 retention is not only a late spliced intron, but a specific transcript. The incorporation of intron 12 in a portion of intron 25 mRNAs was also observed. Intron 12 retention was observed by fellow PhD student M. Silipo in a number of cell lines and normal tissues (unpublished data). The retention of intron 12 has also been reported previously to Ensembl and NCBI AceView databases. Members of our research group, M. Silipo and MRes student S. Satam, also showed protein expression from this transcript using an intron 12 containing HER2 plasmid construct (manuscript under preparation).

**A**



**B**

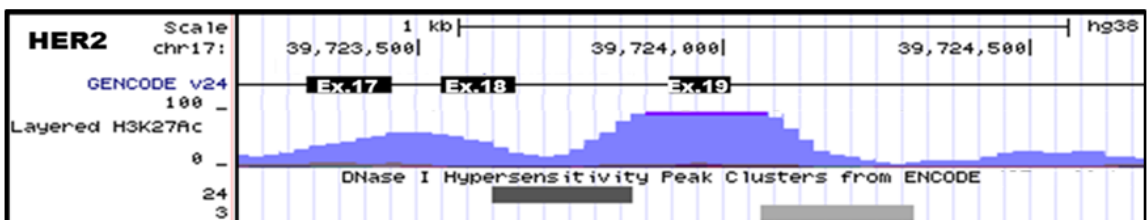


**Figure 5.17: Promoter related signatures around HER2 exons 17 to 19.**

A, shows a snapshot from the Ensembl database, which shows transcription factor binding sites in the region of *HER2* exons 17 to 19. B, shows a snapshot from the UCSC Genome browser, which indicates acetylation of the lysine 27 of histone H3 (H3K27Ac) and DNase I hypersensitivity clusters for the region of *HER2* exons 17 to 20 is shown.

Less clear are the results for PCRs covering the region downstream of exon 18 to intron 25, for which a diffuse band pattern is observed. These multiple bands may be partially spliced pre-mRNAs, as PCRs performed on cDNA from poly(A) enriched mRNA of HER2-positive SKBR3 cells show only a retention of intron 24 and 25. A similar pattern was observed in the HER2-low MCF-7 cells. It should be noted that the band intensity was stronger for amplifications from exon 20 onward. This is very interesting as a transcript, “n” has been described that, although incomplete in regard to the 3’ end of the sequence, has a 5’UTR starting in exon 21 (Figure 5.65). The region from exon 17 to exon 19 has also been annotated as a transcription factor binding site in the Ensembl database (Figure 5.17 A). For the same region an increased acetylation of the lysine 27 of histone H3 (H3K27Ac) and DNase I hypersensitivity clusters can be found on the UCSC Genome browser, which are associated with transcription initiation (Figure 5.17 B). This could support the transcription start site of variant ‘n’ in exon 21 and possibly a similar transcript in MCF-7 that also incorporates intron 25.

Another previously described transcript that might be linked to I25HER2 is variant “h”, which had been identified as a polyadenylated and capped transcript in trachea (NCBI AceView). Initially it was presumed that the PCR from exon 1 to intron 25 did not work because the large amplicon size impaired the PCR. Therefore I25HER2 was expected to still contain exon 1 although only amplification from exon 2 to intron 25 could be observed. A *HER2* variant “h” described in the AceView database was described to start in intron 2. This raises the question if I25HER2 might also have a later start point. Similar to variant “h” a subset of I25HER2 also retains intron 12. Lastly, increased retention of introns between exon 21 and 25 in I25HER2 was observed, which has also been described in variant “h”. Due to the start of transcript “h” being in intron 2 it was predicted to have a 2484 bp long 5’UTR and to only initiate translation in intron 12. Its translation was also predicted to be terminated in intron 21, giving rise to a 3955 bp long 3’UTR. Interestingly it was also shown to contain a partially spliced exon 27. A partially spliced exon 27 in I25HER2 could not be verified. Variant “h” has been suggested to have impaired protein translation efficacy, due to the presence of a shorter translated product upstream of the main open reading frame. The predicted protein “h” lacks both

the majority of the ligand binding domains and the last 271 amino acids of conventional HER2. Its predicted molecular weight is 41.3 kD (NCBI AceView).

### **5.5.1.1. *In-silico* predictions for I25HER2**

The previously described mRNA transcripts (variants “n” and “h”) and our finding regarding the different ways in which intron 25 can be incorporated into mRNAs show that there is possibly more than one I25HER2 transcript. Retention of additional introns or the use of a not previously described promoter are possibilities, but are unlikely to be the main, stable I25HER2 transcript. Therefore a transcript from exon 1 to exon 27 was used with only intron 25 retention for our *in-silico* predictions. Secondary mRNA structure predictions show that the retention of intron 25 causes an extensive change to the mRNA structure, especially in the centroid plain model. This could indicate I25HER2 mRNA to be differently processed, shuttled to the ribosomes and translated. A full length I25HER2 protein would be expected to only differ from wild type HER2 by its shorter alternative C-terminal tail. This could have a major impact on the downstream signalling ability of I25HER2, as the phosphorylation sites in the normal C-terminus are not part of I25HER2. These phosphorylated tyrosines are the main docking sites for downstream signalling molecules, so that neither the PI3K-AKT nor the ras-MAPK pathways are likely to be initiated in I25 HER2. In addition the I25HER2 C-terminus is short and has a slightly different secondary structure, which could impact not only its own downstream signalling, but also the transactivation of its dimerization partner. In the introduction it was described how the ErbB family members need to dimerise after ligand binding to induce downstream signalling [reviewed in (Roskoski, 2014)]. Considering the intricate interaction between the intracellular domains of the two ErbB interacting proteins (Collier *et al.*, 2013) such a drastic shortening of the C-terminus is very likely to impair that interaction.

**5.5.1.2. HER2 intron 25 retention levels in human tissues**

In this study it was shown that intron 25 is retained in breast cancer cell lines as well as normal breast tissue. Additionally, intron 25 was observed to be retained in other normal tissues. An indicator that I25HER2 is not only a by-product of HER2 splicing, is that the ratio between wild type HER2 and intron 25 retention is dependent on the tissue. Overall the intron 25 retention is the most abundant in testis and cerebellum. These tissues are known for a high level of alternative splicing (de la Grange *et al.*, 2010). Additionally, the expression of I25HER2 was studied in a small cohort of human grade 3 ductal breast carcinomas and normal breast tissues. In the HER2-positive breast tumour samples the ratio between wild type HER2 and intron 25 retention was mostly consistent. For three HER2-positive breast tumour samples HER2 (G5-2, G5-3, G5-4) IHC and CISH data is available from chapter 4 (Table 5.3). G5-3 and G5-4 showed a lower wild type HER2 expression than expected. For G5-3 this matches the IHC and CISH scoring. In case of G5-4 CISH score as well as two of three IHC methods indicated HER2 overexpression.

**Table 5.3: HER2 IHC and CISH score for four tumour samples used in intron 25 PCRs.**

<b>Sample ID</b>	<b>CISH ID</b>	<b>HercepTest</b>	<b>C-term. Antibody</b>	<b>N-term Antibody</b>	<b>HER2 CISH score</b>
<b>G3-1</b>	IHC-5	NA	0	0	1.03
<b>G5-2</b>	IHC-12	3	1*	3	3.06
<b>G5-3</b>	IHC-13	1*	0	2	1.24
<b>G5-4</b>	IHC-14	3(F)	0	3(D)*	2.42

In contrast variations in the ratio between intron 25 retention and wild type HER2 was observed in both normal breast and ER/HER2-negative tumour samples. As expected the level of wild type HER2 was very low or not detectable in normal breast and HER/ER-negative tumour samples. Only one normal breast sample (G1-4) showed a slightly increased level of wild type HER2. However in all normal breast and ER/HER2-negative tumour samples intron 25 retention could be observed. The samples G3-3, G3-4 and G3-5

should be noted as they show intron 25 retention, but wild type HER2 levels remain below detection limit.

### **5.5.1.3. Intron 25 stability**

To further assess if I25HER2 is likely to be translated into a protein an mRNA decay assay was performed. There it was shown that I25HER2 is degraded slowly, at a similar rate to  $\Delta$ 16HER2. A member of our group, MRes student S. Satam successfully transfected a HER2 construct containing intron 12 into breast cancer cells and showed its protein expression (unpublished data). Given that intron 25 was more stable than intron 12 in the RNA decay assay, it is very likely that I25HER2 mRNA will also be translated.

Before trying to detect I25HER2 at the protein level we wished to further understand the type of *HER2* transcript that intron 25 is retained in. For this a non-isotopic northern blot was established. The positive control experiment supplied by the manufacturer of the northern blot kit was carried out successfully. However, problems were encountered when adapting the protocol for the detection of general HER2 and intron 25. In two experiments the same binding pattern for general HER2 was observed. A number of bands sized: 9, 4.5, 3 and 2.5 kb were detected. Multiple bands were expected as all known HER2 splice variants are expected to contain exon 5, the binding site of the general HER2 probe. The 4.5 kb band corresponds to wild type HER2. Furthermore, HER2 splice variant p100 was determined to be 2.3 kb of size and could possibly correspond to the 2.5 kb band detected in the northern blot (Doherty *et al.*, 1999a). However, the specificity of the probes has to be put in question as three bands (9, 3 and 2.5 kb) are close in size to the main RNA bands observed on the agarose gel. The RNA used was enriched for poly(A) mRNA and the main bands in the agarose gel were therefore the most strongly expressed mRNAs in SKBR3 cells. Although HER2 is strongly overexpressed in SKBR3 cell, the ~9 kb sized band does not correspond to any known HER2 transcript. Only in one study in the ovarian cancer cell line SKOV-3, was a HER2 variant detected that had a similar size (Doherty *et al.*, 1999b). That

transcript also contained a very long 3'UTR. The sequence provided by the paper showed *HER2* to be translocated, as the 3'UTR contained elements from chromosome 3q26.2. *HER2* gene amplification can also be observed in SKBR3 cells, but there is no information on a similar translocation and associated increase in 3'UTR length.

The results from the northern blot for intron 25 are not conclusive. The process has undergone a number of optimisation steps. The result from the last optimized experiment was shown here. Two bands (8-9 kb and 2.8 kb) were detected in the intron 25 northern blot. One is very similar in size to the before discussed 9 kb band detected with the general HER2 probe. The other, 2.8 kb band does not share the size with the RNA bands, but matches a very faint general HER2 band. This was expected as the general HER2 probe binds exon 5, which was shown by PCR to be part of I25HER2. However the band size of 2.8 kb was unexpected, as the PCR work indicated I25HER2 to be part of a full length transcript of approximately 4.5 kb. Previously the possibility of an I25HER2 variant in MCF-7 cells, which starts around exon 20 was discussed. Depending on the 3'UTR length such a transcript could potentially account for the 2.8 kb northern blot band. The similar size of this band to the general HER2 band could be a coincident and the general HER2 band could actually correspond to Herstatin.

### **5.5.2. Summary**

In this study a novel intron retention variant of HER2 was identified. As I25HER2 is expressed in a number of tissues and its mRNA is stable, it is likely to be translated into a protein. Although the sample size was small, it is very interesting to note that I25HER2 expression is increased in normal breast tissue and HER2-negative breast tumours, as well as some HER2-positive tumours. It could be suggested that due to the truncated c-terminus I25HER2 is a functionally impaired HER2 protein variant.

### **5.5.3. Further work**

The main aim of any future work would be to identify any other novel HER2 variants and to better characterise I25HER2. It would be necessary to optimise the northern blot assay further. Plasmids with templates for human GAPDH, general HER2 and I25HER2 northern blot probes have been generated and will be used in future studies. A main issue is the lack of a biotinylated RNA ladder of the appropriate size to accurately determine the size of northern blot bands. A pre-stained RNA ladder (DynaMarker® Prestained Marker for RNA High, BioDynamics Laboratory) that can be transferred onto the nitrocellulose membrane was acquired, to be used in future work. To verify if the bands observed in the northern blot are specific different sources of mRNA should be tested. It would also be best to use previously tested HER2 probes, to see if the pattern observed in this work is reproducible with a different probe and possibly northern blot system. If the probes were for identical regions, the results would indicate how specific this non-isotopic northern blot was. An optimised northern blot assay would also be of use for the study of other novel splice variants.

To better understand *HER2* transcripts in general, we would suggest to perform a 3'/5' RACE (rapid amplification cDNA ends). The basic method has been modified and improved by some companies (e.g. FirstChoice® RLM-RACE kit by Thermo Scientific) and could be adapted to identify novel HER2 variants as well as the exact 3' and 5' usage of known HER2 variants, including I25HER2.

## Chapter 5: Identification of novel HER2 splice variants

The existence of alternative promoters and first exons was discussed previously. A 5' RACE would be especially interesting in regard to alternative poly(A) sites, which have not been previously investigated in HER2. Work in recent years have shown them to be important for the splicing of the transcript in general and the further processing of mRNAs (Elkon *et al.*, 2013; Li *et al.*, 2015a).

Once I25HER2 transcript has been sufficiently characterised, an I25HER2 plasmid construct should be designed. It could then be expressed in cells and the translated protein could be studied in regard to its localisation, ability to dimerize and induce downstream signalling. Depending on the results, an antibody could be designed and further expression studies in human tumour samples would be performed. A similar approach would be used if other HER2 mRNA transcripts were identified.

## Chapter 6: Conclusion and outlook

### 6.1. Conclusion

The topic of the research presented in this thesis is the breast cancer proto-oncogene and therapy target *HER2*. Different interlinking aspects were studied in this project. The focus of the first result chapter was  $\Delta 16$ HER2. A number of studies have indicated that the oncogenic *HER2* splice variant  $\Delta 16$ HER2 might be a driver of breast tumour formation (Castiglioni *et al.*, 2006; Marchini *et al.*, 2011; Alajati *et al.*, 2013). *In-vitro* and *in-vivo* experiments have suggested that  $\Delta 16$ HER2 driven breast tumours show an expression profile similar to ER-negative, high grade metastatic breast tumours (Alajati *et al.*, 2013). It has been further suggested that these tumours have a histology and karyotype distinct from wild type *HER2* driven tumours (Castagnoli *et al.*, 2014).

To better understand this driver of tumour formation the mechanisms regulating its production were investigated. Four key splicing factors (SRSF3, hnRNPs F, H & K) were identified that regulate the splicing process yielding  $\Delta 16$ HER2, as well as a hnRNP K binding site in the  $\Delta 16$ HER2 splice region. These splicing factors were also found to affect the splicing process of the tumour suppressor *HER2* splice variant p100. Part of the work presented here indicated that hnRNP F/H might not only enhance exon 16 inclusion in the *HER2* mRNA, but itself be induced by *HER2* signalling.

*HER2* as well as *HER2* signalling has been shown to interact with the other main biomarkers of breast cancer, ER and PR (Oh *et al.*, 2001; Beguelin *et al.*, 2010; Diaz Flaque *et al.*, 2013; Giuliano *et al.*, 2013; Grabinski *et al.*, 2014). In chapter three an additional possible way of interaction was studied. The aim was to investigate whether progesterone induced *HER2* expression and affected the alternative splicing pattern of *HER2*. Progesterone was observed to induce *HER2* expression but not affect the alternative splicing pattern.

Most studies only focus on studying one *HER2* protein variant. However, to understand the impact that the coexistence of *HER2* protein variants and how

they interact might have on therapy success, different approaches have to be considered. As an initial step, in chapter four a cohort of invasive primary ductal carcinomas was characterized by IHC and CISH. A N- and a C-terminal antibody were used in addition to clinically used HercepTest™. Some discrepancies were observed between the IHC staining's as well as between the initial clinical assessment and the results of the IHC and CISH study. Tumour heterogeneity was observed in 35% of HER2-positive tumours. Four HER2-positive tumours showed HER2-negative to borderline scores by CISH. Of these only one was scored 3+ by the HercepTest™. The other two were HER2-negative on the protein level however one, tumour IHC-15 was interesting as it scored HER2 3+ with the N-terminal antibody. To investigate whether some of these discrepant results are due to HER2 splice variants, conventional PCRs were performed. Indeed, p100 and Herstatin levels were elevated in some tumours, most strongly in IHC-15.

As mentioned above, all HER2 protein variants arising from alternative mRNA processing, translation initiation as well as proteolytic cleavage, should be investigated in conjunction. Moreover, in the final results chapter of this thesis the existence of novel HER2 splice variants was investigated. An intron retention splice variant, named I25HER2 was identified. It was found to be present in both normal tissues and human breast tumour tissues. Interestingly, although the sample size was small I25HER2 levels were elevated in normal and HER-negative tumours. Additionally, experimental evidence suggests the mRNA stability of I25HER2 to be similar to  $\Delta$ 16HER2. I25HER2 is therefore likely to be translated into a protein, which is likely to be functionally impaired and could possibly downregulate the function of wild type HER2.

In conclusion, this work identified key splicing regulators through which the production of HER2 splice variants  $\Delta$ 16HER2 and p100 is regulated. The research also identified a novel HER2 splice variant.

### **6.2. Outlook**

Taking the findings of this PhD thesis forward, the main aim will be to devise a study that characterizes HER2 in all its forms in breast cancer. This will be of relevance to define potential breast cancer subtypes and inform clinical HER2 assessment methods. Such a study would also show at what levels and in what combinations HER2 protein variants can be found in human breast tumours. This could be explored by studying the mechanistic of HER2 splice variant interactions in basic cell line models. Here key splicing regulators of  $\Delta 16$ HER2 were identified. In future studies this work would be expanded to include the other HER2 splice variants. Understanding the role of HER2 protein variants and how they are produced would give an opportunity to potentially develop new treatment strategies.

As research in tumour biology expands new aspects have to be considered. Of particular interest for future work would be the microenvironment of breast tumour cells and their interaction with the immune system. Functional studies are mostly done in cell line models and to some extent in mice. However, alternative splicing has been shown to be affected by environmental influences (Pagliarini *et al.*, 2015) and therefore findings in 2D cell line models might not translate directly into 3D-models or actual mechanisms in human tumours. In future work it would be very interesting to investigate different tumour cell line models, their interaction with stromal cells and the effect on expression and alternative splicing of HER2.

**References**

Aigner, A., Juhl, H., Malerczyk, C., Tkybusch, A., Benz, C.C. and Czubayko, F. (2001) 'Expression of a truncated 100 kDa HER2 splice variant acts as an endogenous inhibitor of tumour cell proliferation', *Oncogene*, 20(17), pp. 2101-11.

Aksamitiene, E., Kiyatkin, A. and Kholodenko, B.N. (2012) 'Cross-talk between mitogenic Ras/MAPK and survival PI3K/Akt pathways: a fine balance', *Biochem Soc Trans*, 40(1), pp. 139-46.

Alajati, A., Sausgruber, N., Aceto, N., Duss, S., Sarret, S., Voshol, H., Bonenfant, D. and Bentires-Alj, M. (2013) 'Mammary tumor formation and metastasis evoked by a HER2 splice variant', *Cancer Res*, 73(17), pp. 5320-7.

Allouche, A., Nolens, G., Tancredi, A., Delacroix, L., Mardaga, J., Fridman, V., Winkler, R., Boniver, J., Delvenne, P. and Begon, D.Y. (2008) 'The combined immunodetection of AP-2alpha and YY1 transcription factors is associated with ERBB2 gene overexpression in primary breast tumors', *Breast Cancer Res*, 10(1), p. R9.

Aloraifi, F., Boland, M.R., Green, A.J. and Geraghty, J.G. (2015) 'Gene analysis techniques and susceptibility gene discovery in non-BRCA1/BRCA2 familial breast cancer', *Surg Oncol*, 24(2), pp. 100-9.

Amiri-Kordestani, L., Wedam, S., Zhang, L., Tang, S., Tilley, A., Ibrahim, A., Justice, R., Pazdur, R. and Cortazar, P. (2014) 'First FDA approval of neoadjuvant therapy for breast cancer: pertuzumab for the treatment of patients with HER2-positive breast cancer', *Clin Cancer Res*, 20(21), pp. 5359-64.

*Anatomy of the human breast.*  
[http://www.myvmc.com/uploads/VMC/PagelImages/2898\\_breasts\\_normal\\_prof\\_450\\_v2.jpg](http://www.myvmc.com/uploads/VMC/PagelImages/2898_breasts_normal_prof_450_v2.jpg): virtualmedicalcentre (Accessed: 19/04/2016).

Anderson, W.F., Schairer, C., Chen, B.E., Hance, K.W. and Levine, P.H. (2005) 'Epidemiology of inflammatory breast cancer (IBC)', *Breast Dis*, 22, pp. 9-23.

Arkhipov, A., Shan, Y., Das, R., Endres, N.F., Eastwood, M.P., Wemmer, D.E., Kuriyan, J. and Shaw, D.E. (2013) 'Architecture and membrane interactions of the EGF receptor', *Cell*, 152(3), pp. 557-69.

Arteaga, C.L., Johnson, M.D., Todderud, G., Coffey, R.J., Carpenter, G. and Page, D.L. (1991) 'Elevated content of the tyrosine kinase substrate

## References

phospholipase C-gamma 1 in primary human breast carcinomas', *Proc Natl Acad Sci U S A*, 88(23), pp. 10435-9.

Azios, N.G., Romero, F.J., Denton, M.C., Doherty, J.K. and Clinton, G.M. (2001) 'Expression of herstatin, an autoinhibitor of HER-2/neu, inhibits transactivation of HER-3 by HER-2 and blocks EGF activation of the EGF receptor', *Oncogene*, 20(37), pp. 5199-209.

Balasubramani, M., Day, B.W., Schoen, R.E. and Getzenberg, R.H. (2006) 'Altered expression and localization of creatine kinase B, heterogeneous nuclear ribonucleoprotein F, and high mobility group box 1 protein in the nuclear matrix associated with colon cancer', *Cancer Res*, 66(2), pp. 763-9.

Ballare, C., Uhrig, M., Bechtold, T., Sancho, E., Di Domenico, M., Migliaccio, A., Auricchio, F. and Beato, M. (2003) 'Two domains of the progesterone receptor interact with the estrogen receptor and are required for progesterone activation of the c-Src/Erk pathway in mammalian cells', *Mol Cell Biol*, 23(6), pp. 1994-2008.

Barboro, P., Ferrari, N. and Balbi, C. (2014) 'Emerging roles of heterogeneous nuclear ribonucleoprotein K (hnRNP K) in cancer progression', *Cancer Lett*, 352(2), pp. 152-9.

Barros, F.F., Powe, D.G., Ellis, I.O. and Green, A.R. (2010) 'Understanding the HER family in breast cancer: interaction with ligands, dimerization and treatments', *Histopathology*, 56(5), pp. 560-72.

Baxi, S.M., Tan, W., Murphy, S.T., Smeal, T. and Yin, M.J. (2012) 'Targeting 3-phosphoinoside-dependent kinase-1 to inhibit insulin-like growth factor-I induced AKT and p70 S6 kinase activation in breast cancer cells', *PLoS One*, 7(10), p. e48402.

Beguelin, W., Diaz Flaque, M.C., Proietti, C.J., Cayrol, F., Rivas, M.A., Tkach, M., Rosemblyt, C., Tocci, J.M., Charreau, E.H., Schillaci, R. and Elizalde, P.V. (2010) 'Progesterone receptor induces ErbB-2 nuclear translocation to promote breast cancer growth via a novel transcriptional effect: ErbB-2 function as a coactivator of Stat3', *Mol Cell Biol*, 30(23), pp. 5456-72.

Berget, S.M. (1995) 'Exon recognition in vertebrate splicing', *J Biol Chem*, 270(6), pp. 2411-4.

Berget, S.M., Moore, C. and Sharp, P.A. (1977) 'Spliced segments at the 5' terminus of adenovirus 2 late mRNA.', *Proc Natl Acad Sci U S A*, 74, pp. 3171-3175.

Berglund, J.A., Chua, K., Abovich, N., Reed, R. and Rosbash, M. (1997) 'The splicing factor BBP interacts specifically with the pre-mRNA branchpoint sequence UACUAAC', *Cell*, 89(5), pp. 781-7.

## References

Bianchini, G. and Gianni, L. (2014) 'The immune system and response to HER2-targeted treatment in breast cancer', *Lancet Oncol*, 15(2), pp. e58-68.

Bjornstrom, L. and Sjoberg, M. (2005) 'Mechanisms of estrogen receptor signaling: convergence of genomic and nongenomic actions on target genes', *Mol Endocrinol*, 19(4), pp. 833-42.

Breast Cancer Now Tissue Bank (2010) *SOP: Tissue processing for paraffin wax embedding*. [Online]. Available at: <https://www.breastcancertissuebank.org/sites/default/files/BCNTB-SOP-002%20Tissue%20processing.pdf> (Accessed: 23/08/2016).

*Breast Cancer, A Lobular Disease* (2011). London: Springer.

Brunet, A., Bonni, A., Zigmond, M.J., Lin, M.Z., Juo, P., Hu, L.S., Anderson, M.J., Arden, K.C., Blenis, J. and Greenberg, M.E. (1999) 'Akt promotes cell survival by phosphorylating and inhibiting a Forkhead transcription factor', *Cell*, 96(6), pp. 857-68.

Burge, L., Tuschl, T. and Sharp, P. (1999) '20 Splicing of Precursors to mRNAs by the Spliceosomes.', in *The RNA World*. 2 edn. North America: Cold Spring Harbor Monograph Archive.

Burgess, A.W., Cho, H.S., Eigenbrot, C., Ferguson, K.M., Garrett, T.P., Leahy, D.J., Lemmon, M.A., Sliwkowski, M.X., Ward, C.W. and Yokoyama, S. (2003) 'An open-and-shut case? Recent insights into the activation of EGF/ErbB receptors', *Mol Cell*, 12(3), pp. 541-52.

Burriss, H.A., 3rd (2013) 'Overcoming acquired resistance to anticancer therapy: focus on the PI3K/AKT/mTOR pathway', *Cancer Chemother Pharmacol*, 71(4), pp. 829-42.

Cailleau, R., Young, R., Olive, M. and Reeves, W.J., Jr. (1974) 'Breast tumor cell lines from pleural effusions', *J Natl Cancer Inst*, 53(3), pp. 661-74.

Campbell, I.G., Russell, S.E., Choong, D.Y., Montgomery, K.G., Ciavarella, M.L., Hooi, C.S., Cristiano, B.E., Pearson, R.B. and Phillips, W.A. (2004) 'Mutation of the PIK3CA gene in ovarian and breast cancer', *Cancer Res*, 64(21), pp. 7678-81.

Cancer Research UK (2014a) *Breast cancer incidence by age (female)* (Accessed: 01/10/2014).

Cancer Research UK (2014b) *Breast cancer incidence statistics*. Available at: <http://www.cancerresearchuk.org/health-professional/cancer-statistics/statistics-by-cancer-type/breast-cancer/incidence-invasive#heading-Zero> (Accessed: 30/09/2015).

## References

Cancer Research UK (2014c) *Breast cancer mortality statistics*. Available at: <http://www.cancerresearchuk.org/health-professional/cancer-statistics/statistics-by-cancer-type/breast-cancer/mortality#heading-Zero> (Accessed: 30/09/2015).

Cancer Research UK (2014d) 'Cancer Incidence and Mortality in the UK (2012)'. Cancer Research UK. Available at: [http://publications.cancerresearchuk.org/downloads/Product/CS\\_REPORT\\_TO\\_P10INCMORT.pdf](http://publications.cancerresearchuk.org/downloads/Product/CS_REPORT_TO_P10INCMORT.pdf) (Accessed: 11.02.2015).

Cancer Research UK (2014e) *TNM breast cancer staging* (Accessed: 02/10/2015).

Caputi, M. and Zahler, A.M. (2001) 'Determination of the RNA binding specificity of the heterogeneous nuclear ribonucleoprotein (hnRNP) H/H'/F/2H9 family', *J Biol Chem*, 276(47), pp. 43850-9.

Carpenter, C.L., Auger, K.R., Chanudhuri, M., Yoakim, M., Schaffhausen, B., Shoelson, S. and Cantley, L.C. (1993) 'Phosphoinositide 3-kinase is activated by phosphopeptides that bind to the SH2 domains of the 85-kDa subunit', *J Biol Chem*, 268(13), pp. 9478-83.

Carpenter, R.L., Paw, I., Dewhirst, M.W. and Lo, H.W. (2014) 'Akt phosphorylates and activates HSF-1 independent of heat shock, leading to Slug overexpression and epithelial-mesenchymal transition (EMT) of HER2-overexpressing breast cancer cells', *Oncogene*.

Cartegni, L., Chew, S.L. and Krainer, A.R. (2002) 'Listening to silence and understanding nonsense: exonic mutations that affect splicing', *Nat Rev Genet*, 3(4), pp. 285-98.

Carvajal-Hausdorf, D.E., Schalper, K.A., Pusztai, L., Psyrrri, A., Kalogeras, K.T., Kotoula, V., Fountzilas, G. and Rimm, D.L. (2015) 'Measurement of Domain-Specific HER2 (ERBB2) Expression May Classify Benefit From Trastuzumab in Breast Cancer', *J Natl Cancer Inst*, 107(8).

Castagnoli, L., Iezzi, M., Ghedini, G.C., Ciravolo, V., Marzano, G., Lamolinara, A., Zappasodi, R., Gasparini, P., Campiglio, M., Amici, A., Chiodoni, C., Palladini, A., Lollini, P.L., Triulzi, T., Menard, S., Nanni, P., Tagliabue, E. and Pupa, S.M. (2014) 'Activated d16HER2 homodimers and SRC kinase mediate optimal efficacy for trastuzumab', *Cancer Res*, 74(21), pp. 6248-59.

Castaneda, C.A., Cortes-Funes, H., Gomez, H.L. and Ciruelos, E.M. (2010) 'The phosphatidyl inositol 3-kinase/AKT signaling pathway in breast cancer', *Cancer Metastasis Rev*, 29(4), pp. 751-9.

Castiglioni, F., Tagliabue, E., Campiglio, M., Pupa, S.M., Balsari, A. and Menard, S. (2006) 'Role of exon-16-deleted HER2 in breast carcinomas', *Endocrine-Related Cancer*, 13(1), pp. 221-32.

## References

- Chakrabarty, A., Bhola, N.E., Sutton, C., Ghosh, R., Kuba, M.G., Dave, B., Chang, J.C. and Arteaga, C.L. (2013) 'Trastuzumab-resistant cells rely on a HER2-PI3K-FoxO-survivin axis and are sensitive to PI3K inhibitors', *Cancer Res*, 73(3), pp. 1190-200.
- Chan, H.J., Petrossian, K. and Chen, S. (2015) 'Structural and functional characterization of aromatase, estrogen receptor, and their genes in endocrine-responsive and -resistant breast cancer cells', *J Steroid Biochem Mol Biol*.
- Chandarlapaty, S., Scaltriti, M., Angelini, P., Ye, Q., Guzman, M., Hudis, C.A., Norton, L., Solit, D.B., Arribas, J., Baselga, J. and Rosen, N. (2010) 'Inhibitors of HSP90 block p95-HER2 signaling in Trastuzumab-resistant tumors and suppress their growth', *Oncogene*, 29(3), pp. 325-34.
- Chen, H., Sun, J.G., Cao, X.W., Ma, X.G., Xu, J.P., Luo, F.K. and Chen, Z.T. (2009) 'Preliminary validation of ERBB2 expression regulated by miR-548d-3p and miR-559', *Biochem Biophys Res Commun*, 385(4), pp. 596-600.
- Chen, R.H., Sarnecki, C. and Blenis, J. (1992) 'Nuclear localization and regulation of erk- and rsk-encoded protein kinases', *Mol Cell Biol*, 12(3), pp. 915-27.
- Chia, K.M., Liu, J., Francis, G.D. and Naderi, A. (2011) 'A feedback loop between androgen receptor and ERK signaling in estrogen receptor-negative breast cancer', *Neoplasia*, 13(2), pp. 154-66.
- Chikarmane, S.A., Tirumani, S.H., Howard, S.A., Jagannathan, J.P. and DiPiro, P.J. (2015) 'Metastatic patterns of breast cancer subtypes: what radiologists should know in the era of personalized cancer medicine', *Clin Radiol*, 70(1), pp. 1-10.
- Chow, L.T., Gelinas, R.E., T.R., B. and Roberts, R.J. (1977) 'An amazing sequence arrangement at the 5' ends of adenovirus 2 messenger RNA.', *Cell*, 12, pp. 1-8.
- Chrestensen, C.A., Shuman, J.K., Eschenroeder, A., Worthington, M., Gram, H. and Sturgill, T.W. (2007) 'MNK1 and MNK2 regulation in HER2-overexpressing breast cancer lines', *J Biol Chem*, 282(7), pp. 4243-52.
- Ciarlo, M., Benelli, R., Barbieri, O., Minghelli, S., Barboro, P., Balbi, C. and Ferrari, N. (2012) 'Regulation of neuroendocrine differentiation by AKT/hnRNPK/AR/beta-catenin signaling in prostate cancer cells', *Int J Cancer*, 131(3), pp. 582-90.
- Ciocca, D.R., Arrigo, A.P. and Calderwood, S.K. (2013) 'Heat shock proteins and heat shock factor 1 in carcinogenesis and tumor development: an update', *Arch Toxicol*, 87(1), pp. 19-48.

## References

Cittelly, D.M., Das, P.M., Salvo, V.A., Fonseca, J.P., Burow, M.E. and Jones, F.E. (2010a) 'Oncogenic HER2{Delta}16 suppresses miR-15a/16 and deregulates BCL-2 to promote endocrine resistance of breast tumors', *Carcinogenesis*, 31(12), pp. 2049-57.

Cittelly, D.M., Das, P.M., Spoelstra, N.S., Edgerton, S.M., Richer, J.K., Thor, A.D. and Jones, F.E. (2010b) 'Downregulation of miR-342 is associated with tamoxifen resistant breast tumors', *Mol Cancer*, 9, p. 317.

Collaborative Group on Hormonal Factors in Breast, C. (1996) 'Breast cancer and hormonal contraceptives: collaborative reanalysis of individual data on 53 297 women with breast cancer and 100 239 women without breast cancer from 54 epidemiological studies', *Lancet*, 347(9017), pp. 1713-27.

Collaborative Group on Hormonal Factors in Breast, C. (2002) 'Breast cancer and breastfeeding: collaborative reanalysis of individual data from 47 epidemiological studies in 30 countries, including 50302 women with breast cancer and 96973 women without the disease', *Lancet*, 360(9328), pp. 187-95.

Collaborative Group on Hormonal Factors in Breast, C. (2012) 'Menarche, menopause, and breast cancer risk: individual participant meta-analysis, including 118 964 women with breast cancer from 117 epidemiological studies', *Lancet Oncol*, 13(11), pp. 1141-51.

Collier, T.S., Diraviyam, K., Monsey, J., Shen, W., Sept, D. and Bose, R. (2013) 'Carboxyl group footprinting mass spectrometry and molecular dynamics identify key interactions in the HER2-HER3 receptor tyrosine kinase interface', *J Biol Chem*, 288(35), pp. 25254-64.

Contino, F., Mazarella, C., Ferro, A., Lo Presti, M., Roz, E., Lupo, C., Perconti, G., Giallongo, A. and Feo, S. (2013) 'Negative transcriptional control of ERBB2 gene by MBP-1 and HDAC1: diagnostic implications in breast cancer', *BMC Cancer*, 13, p. 81.

Cooper, A.P. (1840) *The Anatomy of the Breast*. London: Longman.

Cork, D.M., Lennard, T.W. and Tyson-Capper, A.J. (2008) 'Alternative splicing and the progesterone receptor in breast cancer', *Breast Cancer Res*, 10(3), p. 207.

Cramer, P., Srebrow, A., Kadener, S., Werbajh, S., de la Mata, M., Melen, G., Nogues, G. and Kornblihtt, A.R. (2001) 'Coordination between transcription and pre-mRNA processing', *FEBS Lett*, 498(2-3), pp. 179-82.

Creighton, C.J., Hilger, A.M., Murthy, S., Rae, J.M., Chinnaiyan, A.M. and El-Ashry, D. (2006) 'Activation of mitogen-activated protein kinase in estrogen receptor alpha-positive breast cancer cells in vitro induces an in vivo molecular

## References

phenotype of estrogen receptor alpha-negative human breast tumors', *Cancer Res*, 66(7), pp. 3903-11.

Cui, M., Allen, M.A., Larsen, A., Macmorris, M., Han, M. and Blumenthal, T. (2008) 'Genes involved in pre-mRNA 3'-end formation and transcription termination revealed by a lin-15 operon Muv suppressor screen', *Proc Natl Acad Sci U S A*, 105(43), pp. 16665-70.

Cyphert, T.J., Suchanek, A.L., Griffith, B.N. and Salati, L.M. (2013) 'Starvation actively inhibits splicing of glucose-6-phosphate dehydrogenase mRNA via a bifunctional ESE/ESS element bound by hnRNP K', *Biochim Biophys Acta*, 1829(9), pp. 905-15.

Dankort, D., Maslikowski, B., Warner, N., Kanno, N., Kim, H., Wang, Z., Moran, M.F., Oshima, R.G., Cardiff, R.D. and Muller, W.J. (2001) 'Grb2 and Shc adapter proteins play distinct roles in Neu (ErbB-2)-induced mammary tumorigenesis: implications for human breast cancer', *Mol Cell Biol*, 21(5), pp. 1540-51.

Dankort, D.L., Wang, Z., Blackmore, V., Moran, M.F. and Muller, W.J. (1997) 'Distinct tyrosine autophosphorylation sites negatively and positively modulate neu-mediated transformation', *Mol Cell Biol*, 17(9), pp. 5410-25.

Datta, S.R., Dudek, H., Tao, X., Masters, S., Fu, H., Gotoh, Y. and Greenberg, M.E. (1997) 'Akt phosphorylation of BAD couples survival signals to the cell-intrinsic death machinery', *Cell*, 91(2), pp. 231-41.

David, C.J. and Manley, J.L. (2010) 'Alternative pre-mRNA splicing regulation in cancer: pathways and programs unhinged', *Genes Dev*, 24(21), pp. 2343-64.

de Klerk, E. and t Hoen, P.A. (2015) 'Alternative mRNA transcription, processing, and translation: insights from RNA sequencing', *Trends Genet*, 31(3), pp. 128-39.

de la Grange, P., Gratadou, L., Delord, M., Dutertre, M. and Auboeuf, D. (2010) 'Splicing factor and exon profiling across human tissues', *Nucleic Acids Res*, 38(9), pp. 2825-38.

de la Mata, M., Alonso, C.R., Kadener, S., Fededa, J.P., Blaustein, M., Pelisch, F., Cramer, P., Bentley, D. and Kornblihtt, A.R. (2003) 'A slow RNA polymerase II affects alternative splicing in vivo', *Mol Cell*, 12(2), pp. 525-32.

De Luca, A., Maiello, M.R., D'Alessio, A., Pergameno, M. and Normanno, N. (2012) 'The RAS/RAF/MEK/ERK and the PI3K/AKT signalling pathways: role in cancer pathogenesis and implications for therapeutic approaches', *Expert Opin Ther Targets*, 16 Suppl 2, pp. S17-27.

## References

Dejgaard, K. and Leffers, H. (1996) 'Characterisation of the nucleic-acid-binding activity of KH domains. Different properties of different domains', *Eur J Biochem*, 241(2), pp. 425-31.

*Development of ductal carcinoma.* (2014) <http://aegiscreative.com/wp-content/uploads/2014/01/Figure-2.png>: Aegis creative. Available at: <http://aegiscreative.com/wp-content/uploads/2014/01/Figure-2.png> (Accessed: 19/04/2016).

Di Fiore, P.P., Pierce, J.H., Kraus, M.H., Segatto, O., King, C.R. and Aaronson, S.A. (1987) 'erbB-2 is a potent oncogene when overexpressed in NIH/3T3 cells', *Science*, 237(4811), pp. 178-82.

Diaz Flaque, M.C., Galigniana, N.M., Beguelin, W., Vicario, R., Proietti, C.J., Russo, R.C., Rivas, M.A., Tkach, M., Guzman, P., Roa, J.C., Maronna, E., Pineda, V., Munoz, S., Mercogliano, M.F., Charreau, E.H., Yankilevich, P., Schillaci, R. and Elizalde, P.V. (2013) 'Progesterone receptor assembly of a transcriptional complex along with activator protein 1, signal transducer and activator of transcription 3 and ErbB-2 governs breast cancer growth and predicts response to endocrine therapy', *Breast Cancer Res*, 15(6), p. R118.

Diermeier-Daucher, S., Ortmann, O., Buchholz, S. and Brockhoff, G. (2012) 'Trifunctional antibody ertumaxomab: Non-immunological effects on Her2 receptor activity and downstream signaling', *MAbs*, 4(5), pp. 614-22.

Dillon, A. (2012) '1-48', *NICE technology appraisal guidance 257; Lapatinib or trastuzumab in combination with an aromatase inhibitor for the first-line treatment of metastatic hormone-receptor-positive breast cancer that overexpresses HER2.* Available at: <http://www.nice.org.uk/nicemedia/live/13777/59707/59707.pdf> (Accessed: 07/10/2013).

Dillon, M.F., Stafford, A.T., Kelly, G., Redmond, A.M., McIlroy, M., Crotty, T.B., McDermott, E., Hill, A.D. and Young, L.S. (2008) 'Cyclooxygenase-2 predicts adverse effects of tamoxifen: a possible mechanism of role for nuclear HER2 in breast cancer patients', *Endocr Relat Cancer*, 15(3), pp. 745-53.

Dillon, R.L., Brown, S.T., Ling, C., Shioda, T. and Muller, W.J. (2007) 'An EGR2/CITED1 transcription factor complex and the 14-3-3sigma tumor suppressor are involved in regulating ErbB2 expression in a transgenic-mouse model of human breast cancer', *Mol Cell Biol*, 27(24), pp. 8648-57.

Dimova, D.K. and Dyson, N.J. (2005) 'The E2F transcriptional network: old acquaintances with new faces', *Oncogene*, 24(17), pp. 2810-26.

Ding, Y., Chan, C.Y. and Lawrence, C.E. (2005) 'RNA secondary structure prediction by centroids in a Boltzmann weighted ensemble', *RNA*, 11(8), pp. 1157-66.

## References

- Dittrich, A., Gautrey, H., Browell, D. and Tyson-Capper, A. (2014) 'The HER2 Signaling Network in Breast Cancer-Like a Spider in its Web', *J Mammary Gland Biol Neoplasia*.
- Doherty, J.K., Bond, C., Jardim, A., Adelman, J.P. and Clinton, G.M. (1999a) 'The HER-2/neu receptor tyrosine kinase gene encodes a secreted autoinhibitor', *Proc Natl Acad Sci U S A*, 96(19), pp. 10869-74.
- Doherty, J.K., Bond, C.T., Hua, W., Adelman, J.P. and Clinton, G.M. (1999b) 'An alternative HER-2/neu transcript of 8 kb has an extended 3'UTR and displays increased stability in SKOV-3 ovarian carcinoma cells', *Gynecol Oncol*, 74(3), pp. 408-15.
- Dreyfuss, G., Matunis, M.J., Pinol-Roma, S. and Burd, C.G. (1993) 'hnRNP proteins and the biogenesis of mRNA', *Annu Rev Biochem*, 62, pp. 289-321.
- Eisenberg, A., Biener, E., Charlier, M., Krishnan, R.V., Djiane, J., Herman, B. and Gertler, A. (2004) 'Transactivation of erbB2 by short and long isoforms of leptin receptors', *FEBS Lett*, 565(1-3), pp. 139-42.
- Elkon, R., Ugalde, A.P. and Agami, R. (2013) 'Alternative cleavage and polyadenylation: extent, regulation and function', *Nat Rev Genet*, 14(7), pp. 496-506.
- Epis, M.R., Giles, K.M., Barker, A., Kendrick, T.S. and Leedman, P.J. (2009) 'miR-331-3p regulates ERBB-2 expression and androgen receptor signaling in prostate cancer', *J Biol Chem*, 284(37), pp. 24696-704.
- Eroles, P., Bosch, A., Perez-Fidalgo, J.A. and Lluch, A. (2012) 'Molecular biology in breast cancer: intrinsic subtypes and signaling pathways', *Cancer Treat Rev*, 38(6), pp. 698-707.
- Escher, C., Cymer, F. and Schneider, D. (2009) 'Two GxxxG-like motifs facilitate promiscuous interactions of the human ErbB transmembrane domains', *J Mol Biol*, 389(1), pp. 10-6.
- Evans, D.G., Shenton, A., Woodward, E., Lalloo, F., Howell, A. and Maher, E.R. (2008) 'Penetrance estimates for BRCA1 and BRCA2 based on genetic testing in a Clinical Cancer Genetics service setting: risks of breast/ovarian cancer quoted should reflect the cancer burden in the family', *BMC Cancer*, 8, p. 155.
- Fairbrother, W.G. and Chasin, L.A. (2000) 'Human genomic sequences that inhibit splicing', *Mol Cell Biol*, 20(18), pp. 6816-25.
- Fan, Y.X., Wong, L., Ding, J., Spiridonov, N.A., Johnson, R.C. and Johnson, G.R. (2008) 'Mutational activation of ErbB2 reveals a new protein kinase autoinhibition mechanism', *J Biol Chem*, 283(3), pp. 1588-96.

## References

Faustino, N.A. and Cooper, T.A. (2003) 'Pre-mRNA splicing and human disease', *Genes Dev*, 17(4), pp. 419-37.

FDA (2016) *List of Cleared or Approved Companion Diagnostic Devices (In Vitro and Imaging Tools)*. Available at: <http://www.fda.gov/MedicalDevices/ProductsandMedicalProcedures/InVitroDiagnostics/ucm301431.htm> (Accessed: 17/06/2016).

Ferracin, M., Bassi, C., Pedriali, M., Pagotto, S., D'Abundo, L., Zagatti, B., Corra, F., Musa, G., Callegari, E., Lupini, L., Volpato, S., Querzoli, P. and Negrini, M. (2013) 'miR-125b targets erythropoietin and its receptor and their expression correlates with metastatic potential and ERBB2/HER2 expression', *Mol Cancer*, 12(1), p. 130.

Fiorio, E., Mercanti, A., Terrasi, M., Micciolo, R., Remo, A., Auriemma, A., Molino, A., Parolin, V., Di Stefano, B., Bonetti, F., Giordano, A., Cetto, G.L. and Surmacz, E. (2008) 'Leptin/HER2 crosstalk in breast cancer: in vitro study and preliminary in vivo analysis', *BMC Cancer*, 8, p. 305.

Fong, N., Kim, H., Zhou, Y., Ji, X., Qiu, J., Saldi, T., Diener, K., Jones, K., Fu, X.D. and Bentley, D.L. (2014) 'Pre-mRNA splicing is facilitated by an optimal RNA polymerase II elongation rate', *Genes Dev*, 28(23), pp. 2663-76.

Fourmann, J.B., Schmitzova, J., Christian, H., Urlaub, H., Ficner, R., Boon, K.L., Fabrizio, P. and Luhrmann, R. (2013) 'Dissection of the factor requirements for spliceosome disassembly and the elucidation of its dissociation products using a purified splicing system', *Genes Dev*, 27(4), pp. 413-28.

Fox-Walsh, K.L., Dou, Y., Lam, B.J., Hung, S.P., Baldi, P.F. and Hertel, K.J. (2005) 'The architecture of pre-mRNAs affects mechanisms of splice-site pairing', *Proc Natl Acad Sci U S A*, 102(45), pp. 16176-81.

Fresno Vara, J.A., Casado, E., de Castro, J., Cejas, P., Belda-Iniesta, C. and Gonzalez-Baron, M. (2004) 'PI3K/Akt signalling pathway and cancer', *Cancer Treat Rev*, 30(2), pp. 193-204.

Fruman, D.A. and Rommel, C. (2014) 'PI3K and cancer: lessons, challenges and opportunities', *Nat Rev Drug Discov*, 13(2), pp. 140-56.

Gampenrieder, S.P., Rinnerthaler, G. and Greil, R. (2013) 'Neoadjuvant Chemotherapy and Targeted Therapy in Breast Cancer: Past, Present, and Future', *J Oncol*, 2013, p. 732047.

Gangopadhyay, S., Nandy, A., Hor, P. and Mukhopadhyay, A. (2013) 'Breast cancer stem cells: a novel therapeutic target', *Clin Breast Cancer*, 13(1), pp. 7-15.

## References

- Garnier, J., Gibrat, J.F. and Robson, B. (1996) 'GOR method for predicting protein secondary structure from amino acid sequence', *Methods Enzymol*, 266, pp. 540-53.
- Garrett, J.T. and Arteaga, C.L. (2011) 'Resistance to HER2-directed antibodies and tyrosine kinase inhibitors: mechanisms and clinical implications', *Cancer Biol Ther*, 11(9), pp. 793-800.
- Gathirua-Mwangi, W.G., Zollinger, T.W., Murage, M.J., Pradhan, K.R. and Champion, V.L. (2015) 'Adult BMI change and risk of Breast Cancer: National Health and Nutrition Examination Survey (NHANES) 2005-2010', *Breast Cancer*.
- Gautrey, H., Jackson, C., Dittrich, A.L., Browell, D., Lennard, T. and Tyson-Capper, A. (2015) 'SRSF3 and hnRNP H1 regulate a splicing hotspot of HER2 in breast cancer cells', *RNA Biol*, 12(10), pp. 1139-51.
- Gebhardt, F., Zanker, K.S. and Brandt, B. (1998) 'Differential expression of alternatively spliced c-erbB-2 mRNA in primary tumors, lymph node metastases, and bone marrow micrometastases from breast cancer patients', *Biochem Biophys Res Commun*, 247(2), pp. 319-23.
- Geuens, T., Bouhy, D. and Timmerman, V. (2016) 'The hnRNP family: insights into their role in health and disease', *Hum Genet*, 135(8), pp. 851-67.
- Ghosh, A., Awasthi, S. and Hamburger, A.W. (2013) 'ErbB3-binding protein EBP1 decreases ErbB2 levels via a transcriptional mechanism', *Oncol Rep*, 29(3), pp. 1161-6.
- Gierisch, J.M., Coeytaux, R.R., Urrutia, R.P., Havrilesky, L.J., Moorman, P.G., Lowery, W.J., Dinan, M., McBroom, A.J., Hasselblad, V., Sanders, G.D. and Myers, E.R. (2013) 'Oral contraceptive use and risk of breast, cervical, colorectal, and endometrial cancers: a systematic review', *Cancer Epidemiol Biomarkers Prev*, 22(11), pp. 1931-43.
- Gilbert, W. (1978) 'Why genes in pieces?', *Nature*, 271(5645), p. 501.
- Giuliano, M., Trivedi, M.V. and Schiff, R. (2013) 'Bidirectional Crosstalk between the Estrogen Receptor and Human Epidermal Growth Factor Receptor 2 Signaling Pathways in Breast Cancer: Molecular Basis and Clinical Implications', *Breast Care (Basel)*, 8(4), pp. 256-262.
- Gougelet, A., Bouclier, C., Marsaud, V., Maillard, S., Mueller, S.O., Korach, K.S. and Renoir, J.M. (2005) 'Estrogen receptor alpha and beta subtype expression and transactivation capacity are differentially affected by receptor-, hsp90- and immunophilin-ligands in human breast cancer cells', *J Steroid Biochem Mol Biol*, 94(1-3), pp. 71-81.

## References

- Grabinski, N., Mollmann, K., Milde-Langosch, K., Muller, V., Schumacher, U., Brandt, B., Pantel, K. and Jucker, M. (2014) 'AKT3 regulates ErbB2, ErbB3 and estrogen receptor alpha expression and contributes to endocrine therapy resistance of ErbB2 breast tumor cells from Balb-neuT mice', *Cell Signal*.
- Graveley, B.R. (2005) 'Mutually exclusive splicing of the insect Dscam pre-mRNA directed by competing intronic RNA secondary structures', *Cell*, 123(1), pp. 65-73.
- Guarino, M. (2010) 'Src signaling in cancer invasion', *J Cell Physiol*, 223(1), pp. 14-26.
- Guarneri, V., Barbieri, E., Dieci, M.V., Piacentini, F. and Conte, P. (2010) 'Anti-HER2 neoadjuvant and adjuvant therapies in HER2 positive breast cancer', *Cancer Treat Rev*, 36 Suppl 3, pp. S62-6.
- Guha, M., Fang, J.K., Monks, R., Birnbaum, M.J. and Avadhani, N.G. (2010) 'Activation of Akt is essential for the propagation of mitochondrial respiratory stress signaling and activation of the transcriptional coactivator heterogeneous ribonucleoprotein A2', *Mol Biol Cell*, 21(20), pp. 3578-89.
- Guy, C.T., Webster, M.A., Schaller, M., Parsons, T.J., Cardiff, R.D. and Muller, W.J. (1992) 'Expression of the neu protooncogene in the mammary epithelium of transgenic mice induces metastatic disease', *Proc Natl Acad Sci U S A*, 89(22), pp. 10578-82.
- Hagan, C.R., Regan, T.M., Dressing, G.E. and Lange, C.A. (2011) 'ck2-dependent phosphorylation of progesterone receptors (PR) on Ser81 regulates PR-B isoform-specific target gene expression in breast cancer cells', *Mol Cell Biol*, 31(12), pp. 2439-52.
- Hahn, S. (2004) 'Structure and mechanism of the RNA polymerase II transcription machinery', *Nat Struct Mol Biol*, 11(5), pp. 394-403.
- Haluska, P., Carboni, J.M., TenEyck, C., Attar, R.M., Hou, X., Yu, C., Sagar, M., Wong, T.W., Gottardis, M.M. and Erlichman, C. (2008) 'HER receptor signaling confers resistance to the insulin-like growth factor-I receptor inhibitor, BMS-536924', *Mol Cancer Ther*, 7(9), pp. 2589-98.
- Hartman, Z., Zhao, H. and Agazie, Y.M. (2013) 'HER2 stabilizes EGFR and itself by altering autophosphorylation patterns in a manner that overcomes regulatory mechanisms and promotes proliferative and transformation signaling', *Oncogene*, 32(35), pp. 4169-80.
- Hassiotou, F. and Geddes, D. (2013) 'Anatomy of the human mammary gland: Current status of knowledge', *Clin Anat*, 26(1), pp. 29-48.

## References

- He, X.H., Zhu, W., Yuan, P., Jiang, S., Li, D., Zhang, H.W. and Liu, M.F. (2016) 'miR-155 downregulates ErbB2 and suppresses ErbB2-induced malignant transformation of breast epithelial cells', *Oncogene*.
- Honore, B., Baandrup, U. and Vorum, H. (2004) 'Heterogeneous nuclear ribonucleoproteins F and H/H' show differential expression in normal and selected cancer tissues', *Exp Cell Res*, 294(1), pp. 199-209.
- Honore, B., Rasmussen, H.H., Vorum, H., Dejgaard, K., Liu, X., Gromov, P., Madsen, P., Gesser, B., Tommerup, N. and Celis, J.E. (1995) 'Heterogeneous nuclear ribonucleoproteins H, H', and F are members of a ubiquitously expressed subfamily of related but distinct proteins encoded by genes mapping to different chromosomes', *J Biol Chem*, 270(48), pp. 28780-9.
- Hope, N.R. and Murray, G.I. (2011) 'The expression profile of RNA-binding proteins in primary and metastatic colorectal cancer: relationship of heterogeneous nuclear ribonucleoproteins with prognosis', *Hum Pathol*, 42(3), pp. 393-402.
- Hopkins, B.D., Hodakoski, C., Barrows, D., Mense, S.M. and Parsons, R.E. (2014) 'PTEN function: the long and the short of it', *Trends Biochem Sci*.
- Hu, P., Feng, J., Zhou, T., Wang, J., Jing, B., Yu, M., Hu, M., Zhang, X., Shen, B. and Guo, N. (2005) 'In vivo identification of the interaction site of ErbB2 extracellular domain with its autoinhibitor', *J Cell Physiol*, 205(3), pp. 335-43.
- Hu, P., Zhou, T., Qian, L., Wang, J., Shi, M., Yu, M., Yang, Y., Zhang, X., Shen, B. and Guo, N. (2006) 'Sequestering ErbB2 in endoplasmic reticulum by its autoinhibitor from translocation to cell surface: an autoinhibition mechanism of ErbB2 expression', *Biochem Biophys Res Commun*, 342(1), pp. 19-27.
- Huang, L., Ren, J., Chen, D., Li, Y., Kharbanda, S. and Kufe, D. (2003) 'MUC1 cytoplasmic domain coactivates Wnt target gene transcription and confers transformation', *Cancer Biol Ther*, 2(6), pp. 702-6.
- Huang, X., Gao, L., Wang, S., McManaman, J.L., Thor, A.D., Yang, X., Esteva, F.J. and Liu, B. (2010) 'Heterotrimerization of the growth factor receptors erbB2, erbB3, and insulin-like growth factor-i receptor in breast cancer cells resistant to herceptin', *Cancer Res*, 70(3), pp. 1204-14.
- Hube, F. and Francastel, C. (2015) 'Mammalian introns: when the junk generates molecular diversity', *Int J Mol Sci*, 16(3), pp. 4429-52.
- Hudziak, R.M., Schlessinger, J. and Ullrich, A. (1987) 'Increased expression of the putative growth factor receptor p185HER2 causes transformation and tumorigenesis of NIH 3T3 cells', *Proc Natl Acad Sci U S A*, 84(20), pp. 7159-63.

## References

- Hurley, W.L. (1989) 'Mammary gland function during involution', *J Dairy Sci*, 72(6), pp. 1637-46.
- Hurvitz, S.A., Hu, Y., O'Brien, N. and Finn, R.S. (2013) 'Current approaches and future directions in the treatment of HER2-positive breast cancer', *Cancer Treat Rev*, 39(3), pp. 219-29.
- Hutson, S.W., Cowen, P.N. and Bird, C.C. (1985) 'Morphometric studies of age related changes in normal human breast and their significance for evolution of mammary cancer', *J Clin Pathol*, 38(3), pp. 281-7.
- Inoki, K., Li, Y., Zhu, T., Wu, J. and Guan, K.L. (2002) 'TSC2 is phosphorylated and inhibited by Akt and suppresses mTOR signalling', *Nat Cell Biol*, 4(9), pp. 648-57.
- Jackson, C., Browell, D., Gautrey, H. and Tyson-Capper, A. (2013) 'Clinical Significance of HER-2 Splice Variants in Breast Cancer Progression and Drug Resistance', *Int J Cell Biol*, 2013, p. 973584.
- Jang, H.N., Lee, M., Loh, T.J., Choi, S.W., Oh, H.K., Moon, H., Cho, S., Hong, S.E., Kim do, H., Sheng, Z., Green, M.R., Park, D., Zheng, X. and Shen, H. (2014) 'Exon 9 skipping of apoptotic caspase-2 pre-mRNA is promoted by SRSF3 through interaction with exon 8', *Biochim Biophys Acta*, 1839(1), pp. 25-32.
- Jhabvala-Romero, F., Evans, A., Guo, S., Denton, M. and Clinton, G.M. (2003) 'Herstatin inhibits heregulin-mediated breast cancer cell growth and overcomes tamoxifen resistance in breast cancer cells that overexpress HER-2', *Oncogene*, 22(50), pp. 8178-86.
- Jia, M., Dahlman-Wright, K. and Gustafsson, J.A. (2015) 'Estrogen receptor alpha and beta in health and disease', *Best Pract Res Clin Endocrinol Metab*, 29(4), pp. 557-68.
- Jia, R., Li, C., McCoy, J.P., Deng, C.X. and Zheng, Z.M. (2010) 'SRp20 is a proto-oncogene critical for cell proliferation and tumor induction and maintenance', *Int J Biol Sci*, 6(7), pp. 806-26.
- Ju, J.H., Yang, W., Oh, S., Nam, K., Lee, K.M., Noh, D.Y. and Shin, I. (2013) 'HER2 stabilizes survivin while concomitantly down-regulating survivin gene transcription by suppressing Notch cleavage', *Biochem J*, 451(1), pp. 123-34.
- Junttila, T.T., Akita, R.W., Parsons, K., Fields, C., Lewis Phillips, G.D., Friedman, L.S., Sampath, D. and Sliwkowski, M.X. (2009) 'Ligand-independent HER2/HER3/PI3K complex is disrupted by trastuzumab and is effectively inhibited by the PI3K inhibitor GDC-0941', *Cancer Cell*, 15(5), pp. 429-40.

## References

Jura, N., Endres, N.F., Engel, K., Deindl, S., Das, R., Lamers, M.H., Wemmer, D.E., Zhang, X. and Kuriyan, J. (2009) 'Mechanism for activation of the EGF receptor catalytic domain by the juxtamembrane segment', *Cell*, 137(7), pp. 1293-307.

Jurica, M.S. and Moore, M.J. (2003) 'Pre-mRNA splicing: awash in a sea of proteins', *Mol Cell*, 12(1), pp. 5-14.

Justman, Q.A. and Clinton, G.M. (2002) 'Herstatin, an autoinhibitor of the human epidermal growth factor receptor 2 tyrosine kinase, modulates epidermal growth factor signaling pathways resulting in growth arrest', *J Biol Chem*, 277(23), pp. 20618-24.

Kalra, J., Sutherland, B.W., Stratford, A.L., Dragowska, W., Gelmon, K.A., Dedhar, S., Dunn, S.E. and Bally, M.B. (2010) 'Suppression of Her2/neu expression through ILK inhibition is regulated by a pathway involving TWIST and YB-1', *Oncogene*, 29(48), pp. 6343-56.

Kampa, M., Pelekanou, V., Notas, G., Stathopoulos, E.N. and Castanas, E. (2013) 'The estrogen receptor: two or more molecules, multiple variants, diverse localizations, signaling and functions. Are we undergoing a paradigm-shift as regards their significance in breast cancer?', *Hormones (Athens)*, 12(1), pp. 69-85.

Kastner, P., Krust, A., Turcotte, B., Stropp, U., Tora, L., Gronemeyer, H. and Chambon, P. (1990) 'Two distinct estrogen-regulated promoters generate transcripts encoding the two functionally different human progesterone receptor forms A and B', *EMBO J*, 9(5), pp. 1603-14.

Kasza, A. (2013) 'Signal-dependent Elk-1 target genes involved in transcript processing and cell migration', *Biochim Biophys Acta*, 1829(10), pp. 1026-33.

Kato, S., Endoh, H., Masuhiro, Y., Kitamoto, T., Uchiyama, S., Sasaki, H., Masushige, S., Gotoh, Y., Nishida, E., Kawashima, H., Metzger, D. and Chambon, P. (1995) 'Activation of the estrogen receptor through phosphorylation by mitogen-activated protein kinase', *Science*, 270(5241), pp. 1491-4.

Kelemen, O., Convertini, P., Zhang, Z., Wen, Y., Shen, M., Falaleeva, M. and Stamm, S. (2013) 'Function of alternative splicing', *Gene*, 514(1), pp. 1-30.

Key, T.J., Appleby, P.N., Reeves, G.K., Roddam, A., Dorgan, J.F., Longcope, C., Stanczyk, F.Z., Stephenson, H.E., Jr., Falk, R.T., Miller, R., Schatzkin, A., Allen, D.S., Fentiman, I.S., Key, T.J., Wang, D.Y., Dowsett, M., Thomas, H.V., Hankinson, S.E., Toniolo, P., Akhmedkhanov, A., Koenig, K., Shore, R.E., Zeleniuch-Jacquotte, A., Berrino, F., Muti, P., Micheli, A., Krogh, V., Sieri, S., Pala, V., Venturelli, E., Secreto, G., Barrett-Connor, E., Laughlin, G.A., Kabuto, M., Akiba, S., Stevens, R.G., Neriishi, K., Land, C.E., Cauley, J.A., Kuller, L.H.,

## References

- Cummings, S.R., Helzlsouer, K.J., Alberg, A.J., Bush, T.L., Comstock, G.W., Gordon, G.B., Miller, S.R., Longcope, C. and Endogenous Hormones Breast Cancer Collaborative, G. (2003) 'Body mass index, serum sex hormones, and breast cancer risk in postmenopausal women', *J Natl Cancer Inst*, 95(16), pp. 1218-26.
- Kim, J., Park, R.Y., Chen, J.K., Kim, J., Jeong, S. and Ohn, T. (2014) 'Splicing factor SRSF3 represses the translation of programmed cell death 4 mRNA by associating with the 5'-UTR region', *Cell Death Differ*, 21(3), pp. 481-90.
- Koletsa, T., Kostopoulos, I., Charalambous, E., Christoforidou, B., Nenopoulou, E. and Kotoula, V. (2008) 'A splice variant of HER2 corresponding to Herstatin is expressed in the noncancerous breast and in breast carcinomas', *Neoplasia*, 10(7), pp. 687-96.
- Konecny, G.E., Pegram, M.D., Venkatesan, N., Finn, R., Yang, G., Rahmeh, M., Untch, M., Rusnak, D.W., Spehar, G., Mullin, R.J., Keith, B.R., Gilmer, T.M., Berger, M., Podratz, K.C. and Slamon, D.J. (2006) 'Activity of the dual kinase inhibitor lapatinib (GW572016) against HER-2-overexpressing and trastuzumab-treated breast cancer cells', *Cancer Res*, 66(3), pp. 1630-9.
- Kovacs, E., Zorn, J.A., Huang, Y., Barros, T. and Kuriyan, J. (2015) 'A structural perspective on the regulation of the epidermal growth factor receptor', *Annu Rev Biochem*, 84, pp. 739-64.
- Kralovicova, J., Patel, A., Searle, M. and Vorechovsky, I. (2015) 'The role of short RNA loops in recognition of a single-hairpin exon derived from a mammalian-wide interspersed repeat', *RNA Biol*, 12(1), pp. 54-69.
- Kubba, A.A. (2003) 'Breast cancer and the pill', *J R Soc Med*, 96(6), pp. 280-3.
- Kufe, D.W. (2013) 'MUC1-C oncoprotein as a target in breast cancer: activation of signaling pathways and therapeutic approaches', *Oncogene*, 32(9), pp. 1073-81.
- Kurozumi, S., Padilla, M., Kurosumi, M., Matsumoto, H., Kenichi, I., Horiguchi, J., Takeyoshi, I., Oyama, T., Ranger-Moore, J., Allred, D.C., Dennis, E. and Nitta, H. (2016) 'HER2 intratumoral heterogeneity analyses by concurrent HER2 gene and protein assessment for the prognosis of HER2 negative invasive breast cancer patients', *Breast Cancer Research and Treatment*, 158(1), pp. 99-111.
- Kuyama, H., Nakajima, C., Kaneshiro, K., Hamana, C., Terasawa, K. and Tanaka, K. (2014) 'Characterization of N- and C-termini of HER2 protein by mass spectrometry-based sequencing: Observation of two types of N-terminal sequence', *International Journal of Mass Spectrometry*, 373, pp. 81-87.

## References

- Kwong, K.Y. and Hung, M.C. (1998) 'A novel splice variant of HER2 with increased transformation activity', *Mol Carcinog*, 23(2), pp. 62-8.
- Lal, S., Allan, A., Markovic, D., Walker, R., Macartney, J., Europe-Finner, N., Tyson-Capper, A. and Grammatopoulos, D.K. (2013) 'Estrogen alters the splicing of type 1 corticotropin-releasing hormone receptor in breast cancer cells', *Sci Signal*, 6(282), p. ra53.
- Lazrek, Y., Dubreuil, O., Garambois, V., Gaborit, N., Larbouret, C., Le Clorennec, C., Thomas, G., Leconet, W., Jarlier, M., Pugniere, M., Vie, N., Robert, B., Monnet, C., Bouayadi, K., Kharrat, H., Mondon, P., Pelegrin, A. and Chardes, T. (2013) 'Anti-HER3 domain 1 and 3 antibodies reduce tumor growth by hindering HER2/HER3 dimerization and AKT-induced MDM2, XIAP, and FoxO1 phosphorylation', *Neoplasia*, 15(3), pp. 335-47.
- Le Hir, H., Izaurralde, E., Maquat, L.E. and Moore, M.J. (2000) 'The spliceosome deposits multiple proteins 20-24 nucleotides upstream of mRNA exon-exon junctions', *EMBO J*, 19(24), pp. 6860-9.
- Le Romancer, M., Poulard, C., Cohen, P., Sentis, S., Renoir, J.M. and Corbo, L. (2011) 'Cracking the estrogen receptor's posttranslational code in breast tumors', *Endocr Rev*, 32(5), pp. 597-622.
- Lee, C.K., Davies, L., GebSKI, V.J., Lord, S.J., Di Leo, A., Johnston, S., Geyer, C., Jr., Cameron, D., Press, M.F., Ellis, C., Loi, S., Marschner, I., Simes, J. and de Souza, P. (2016) 'Serum Human Epidermal Growth Factor 2 Extracellular Domain as a Predictive Biomarker for Lapatinib Treatment Efficacy in Patients With Advanced Breast Cancer', *J Clin Oncol*.
- Lee, Y. and Rio, D.C. (2015) 'Mechanisms and Regulation of Alternative Pre-mRNA Splicing', *Annu Rev Biochem*, 84, pp. 291-323.
- Lefave, C.V., Squatrito, M., Vorlova, S., Rocco, G.L., Brennan, C.W., Holland, E.C., Pan, Y.X. and Cartegni, L. (2011) 'Splicing factor hnRNPH drives an oncogenic splicing switch in gliomas', *EMBO J*, 30(19), pp. 4084-97.
- Lei, K., Chen, L., Georgiou, E.X., Sooranna, S.R., Khanjani, S., Brosens, J.J., Bennett, P.R. and Johnson, M.R. (2012) 'Progesterone acts via the nuclear glucocorticoid receptor to suppress IL-1beta-induced COX-2 expression in human term myometrial cells', *PLoS One*, 7(11), p. e50167.
- Lemmon, M.A. and Schlessinger, J. (2010) 'Cell signaling by receptor tyrosine kinases', *Cell*, 141(7), pp. 1117-34.
- Lennon, S., Barton, C., Banken, L., Gianni, L., Marty, M., Baselga, J. and Leyland-Jones, B. (2009) 'Utility of serum HER2 extracellular domain assessment in clinical decision making: pooled analysis of four trials of trastuzumab in metastatic breast cancer', *J Clin Oncol*, 27(10), pp. 1685-93.

## References

- Leone, G., DeGregori, J., Sears, R., Jakoi, L. and Nevins, J.R. (1997) 'Myc and Ras collaborate in inducing accumulation of active cyclin E/Cdk2 and E2F', *Nature*, 387(6631), pp. 422-6.
- Leonhardt, S.A., Boonyaratanakornkit, V. and Edwards, D.P. (2003) 'Progesterone receptor transcription and non-transcription signaling mechanisms', *Steroids*, 68(10-13), pp. 761-70.
- Lev Maor, G., Yearim, A. and Ast, G. (2015) 'The alternative role of DNA methylation in splicing regulation', *Trends Genet*, 31(5), pp. 274-80.
- Lewis Phillips, G.D., Li, G., Dugger, D.L., Crocker, L.M., Parsons, K.L., Mai, E., Blattler, W.A., Lambert, J.M., Chari, R.V., Lutz, R.J., Wong, W.L., Jacobson, F.S., Koeppen, H., Schwall, R.H., Kenkare-Mitra, S.R., Spencer, S.D. and Sliwkowski, M.X. (2008) 'Targeting HER2-positive breast cancer with trastuzumab-DM1, an antibody-cytotoxic drug conjugate', *Cancer Res*, 68(22), pp. 9280-90.
- Li, W., You, B., Hoque, M., Zheng, D., Luo, W., Ji, Z., Park, J.Y., Gunderson, S.I., Kalsotra, A., Manley, J.L. and Tian, B. (2015a) 'Systematic profiling of poly(A)+ transcripts modulated by core 3' end processing and splicing factors reveals regulatory rules of alternative cleavage and polyadenylation', *PLoS Genet*, 11(4), p. e1005166.
- Li, X.W., Shi, B.Y., Yang, Q.L., Wu, J., Wu, H.M., Wang, Y.F., Wu, Z.J., Fan, Y.M. and Wang, Y.P. (2015b) 'Epigenetic regulation of CDH1 exon 8 alternative splicing in gastric cancer', *BMC Cancer*, 15, p. 954.
- Li, Y., Yu, W.H., Ren, J., Chen, W., Huang, L., Kharbanda, S., Loda, M. and Kufe, D. (2003) 'Heregulin targets gamma-catenin to the nucleolus by a mechanism dependent on the DF3/MUC1 oncoprotein', *Mol Cancer Res*, 1(10), pp. 765-75.
- Liang, W.W. and Cheng, S.C. (2015) 'A novel mechanism for Prp5 function in prespliceosome formation and proofreading the branch site sequence', *Genes Dev*, 29(1), pp. 81-93.
- Lin Fde, M., Pincerato, K.M., Bacchi, C.E., Baracat, E.C. and Carvalho, F.M. (2012) 'Coordinated expression of oestrogen and androgen receptors in HER2-positive breast carcinomas: impact on proliferative activity', *J Clin Pathol*, 65(1), pp. 64-8.
- Lorenz, R., Bernhart, S.H., Honer Zu Siederdisen, C., Tafer, H., Flamm, C., Stadler, P.F. and Hofacker, I.L. (2011) 'ViennaRNA Package 2.0', *Algorithms Mol Biol*, 6, p. 26.
- Maddams, J., Utley, M. and Moller, H. (2012) 'Projections of cancer prevalence in the United Kingdom, 2010-2040', *Br J Cancer*, 107(7), pp. 1195-202.

## References

- Mandal, M., Vadlamudi, R., Nguyen, D., Wang, R.A., Costa, L., Bagheri-Yarmand, R., Mendelsohn, J. and Kumar, R. (2001) 'Growth factors regulate heterogeneous nuclear ribonucleoprotein K expression and function', *J Biol Chem*, 276(13), pp. 9699-704.
- Maquat, L.E. (2004) 'Nonsense-mediated mRNA decay: splicing, translation and mRNP dynamics', *Nat Rev Mol Cell Biol*, 5(2), pp. 89-99.
- Marchini, C., Gabrielli, F., Iezzi, M., Zenobi, S., Montani, M., Pietrella, L., Kalogris, C., Rossini, A., Ciravolo, V., Castagnoli, L., Tagliabue, E., Pupa, S.M., Musiani, P., Monaci, P., Menard, S. and Amici, A. (2011) 'The human splice variant Delta16HER2 induces rapid tumor onset in a reporter transgenic mouse', *PLoS One*, 6(4), p. e18727.
- Marino, M., Galluzzo, P. and Ascenzi, P. (2006) 'Estrogen signaling multiple pathways to impact gene transcription', *Curr Genomics*, 7(8), pp. 497-508.
- Martinez-Contreras, R., Fiset, J.F., Nasim, F.U., Madden, R., Cordeau, M. and Chabot, B. (2006) 'Intronic binding sites for hnRNP A/B and hnRNP F/H proteins stimulate pre-mRNA splicing', *PLoS Biol*, 4(2), p. e21.
- Matera, A.G. and Wang, Z. (2014) 'A day in the life of the spliceosome', *Nat Rev Mol Cell Biol*, 15(2), pp. 108-21.
- Matsui, K., Sugimori, K., Motomura, H., Ejiri, N., Tsukada, K. and Kitajima, I. (2006) 'PEA3 cooperates with c-Jun in regulation of HER2/neu transcription', *Oncol Rep*, 16(1), pp. 153-8.
- Matsushita, C., Tamagaki, H., Miyazawa, Y., Aimoto, S., Smith, S.O. and Sato, T. (2013) 'Transmembrane helix orientation influences membrane binding of the intracellular juxtamembrane domain in Neu receptor peptides', *Proc Natl Acad Sci U S A*, 110(5), pp. 1646-51.
- Mayo, L.D. and Donner, D.B. (2001) 'A phosphatidylinositol 3-kinase/Akt pathway promotes translocation of Mdm2 from the cytoplasm to the nucleus', *Proc Natl Acad Sci U S A*, 98(20), pp. 11598-603.
- McManaman, J.L. and Neville, M.C. (2003) 'Mammary physiology and milk secretion', *Adv Drug Deliv Rev*, 55(5), pp. 629-41.
- Mendillo, M.L., Santagata, S., Koeva, M., Bell, G.W., Hu, R., Tamimi, R.M., Fraenkel, E., Ince, T.A., Whitesell, L. and Lindquist, S. (2012) 'HSF1 drives a transcriptional program distinct from heat shock to support highly malignant human cancers', *Cell*, 150(3), pp. 549-62.
- Merendino, L., Guth, S., Bilbao, D., Martinez, C. and Valcarcel, J. (1999) 'Inhibition of msl-2 splicing by Sex-lethal reveals interaction between U2AF35 and the 3' splice site AG', *Nature*, 402(6763), pp. 838-41.

## References

- Micalizzi, D.S., Farabaugh, S.M. and Ford, H.L. (2010) 'Epithelial-mesenchymal transition in cancer: parallels between normal development and tumor progression', *J Mammary Gland Biol Neoplasia*, 15(2), pp. 117-34.
- Michlewski, G. and Caceres, J.F. (2010) 'RNase-assisted RNA chromatography', *RNA*, 16(8), pp. 1673-8.
- Miller, D.V., Jenkins, R.B., Lingle, W.L., Davidson, N.E., Kaufman, P.A., Martino, S., Dakhil, S.R. and Perez, E.A. (2004) 'Focal HER2/neu amplified clones partially account for discordance between immunohistochemistry and fluorescence in-situ hybridization results: data from NCCTG N9831 Intergroup Adjuvant Trial', *Journal of Clinical Oncology*, 22(14\_suppl 568).
- Mills, I.G. (2012) 'Nuclear translocation and functions of growth factor receptors', *Semin Cell Dev Biol*, 23(2), pp. 165-71.
- Mineev, K.S., Bocharov, E.V., Pustovalova, Y.E., Bocharova, O.V., Chupin, V.V. and Arseniev, A.S. (2010) 'Spatial structure of the transmembrane domain heterodimer of ErbB1 and ErbB2 receptor tyrosine kinases', *J Mol Biol*, 400(2), pp. 231-43.
- Mitra, D., Brumlik, M.J., Okamgba, S.U., Zhu, Y., Duplessis, T.T., Parvani, J.G., Lesko, S.M., Brogi, E. and Jones, F.E. (2009) 'An oncogenic isoform of HER2 associated with locally disseminated breast cancer and trastuzumab resistance', *Mol Cancer Ther*, 8(8), pp. 2152-62.
- Mittendorf, E.A., Holmes, J.P., Ponniah, S. and Peoples, G.E. (2008) 'The E75 HER2/neu peptide vaccine', *Cancer Immunol Immunother*, 57(10), pp. 1511-21.
- Mohammed, H., Russell, I.A., Stark, R., Rueda, O.M., Hickey, T.E., Tarulli, G.A., Serandour, A.A., Birrell, S.N., Bruna, A., Saadi, A., Menon, S., Hadfield, J., Pugh, M., Raj, G.V., Brown, G.D., D'Santos, C., Robinson, J.L., Silva, G., Launchbury, R., Perou, C.M., Stingl, J., Caldas, C., Tilley, W.D. and Carroll, J.S. (2015) 'Progesterone receptor modulates ERalpha action in breast cancer', *Nature*, 523(7560), pp. 313-7.
- Moore, M.J. and Sharp, P.A. (1993) 'Evidence for two active sites in the spliceosome provided by stereochemistry of pre-mRNA splicing', *Nature*, 365(6444), pp. 364-8.
- Mukhopadhyay, P., Chakraborty, S., Ponnusamy, M.P., Lakshmanan, I., Jain, M. and Batra, S.K. (2011) 'Mucins in the pathogenesis of breast cancer: implications in diagnosis, prognosis and therapy', *Biochim Biophys Acta*, 1815(2), pp. 224-40.
- Mulac-Jericevic, B. and Conneely, O.M. (2004) 'Reproductive tissue selective actions of progesterone receptors', *Reproduction*, 128(2), pp. 139-46.

## References

Naccarato, A.G., Viacava, P., Vignati, S., Fanelli, G., Bonadio, A.G., Montruccoli, G. and Bevilacqua, G. (2000) 'Bio-morphological events in the development of the human female mammary gland from fetal age to puberty', *Virchows Arch*, 436(5), pp. 431-8.

Naderi, A. and Hughes-Davies, L. (2008) 'A functionally significant cross-talk between androgen receptor and ErbB2 pathways in estrogen receptor negative breast cancer', *Neoplasia*, 10(6), pp. 542-8.

Naftelberg, S., Schor, I.E., Ast, G. and Kornblihtt, A.R. (2015) 'Regulation of alternative splicing through coupling with transcription and chromatin structure', *Annu Rev Biochem*, 84, pp. 165-98.

Nagy, E. and Maquat, L.E. (1998) 'A rule for termination-codon position within intron-containing genes: when nonsense affects RNA abundance', *Trends Biochem Sci*, 23(6), pp. 198-9.

Nagy, P., Friedlander, E., Tanner, M., Kapanen, A.I., Carraway, K.L., Isola, J. and Jovin, T.M. (2005) 'Decreased accessibility and lack of activation of ErbB2 in JIMT-1, a herceptin-resistant, MUC4-expressing breast cancer cell line', *Cancer Res*, 65(2), pp. 473-82.

Nahta, R., Yuan, L.X., Zhang, B., Kobayashi, R. and Esteva, F.J. (2005) 'Insulin-like growth factor-I receptor/human epidermal growth factor receptor 2 heterodimerization contributes to trastuzumab resistance of breast cancer cells', *Cancer Res*, 65(23), pp. 11118-28.

National Cancer Institute (2012) *Inflammatory Breast Cancer* (Accessed: 01/10/2015).

National Health Service (2013) *New Drugs Online Report for pertuzumab*. Available at: [http://www.ukmi.nhs.uk/applications/ndo/record\\_view\\_open.asp?newDrugID=4894](http://www.ukmi.nhs.uk/applications/ndo/record_view_open.asp?newDrugID=4894) (Accessed: 07/10/2013).

National Institute for health and Care Excellence (2015) *Trastuzumab emtansine for treating HER2-positive, unresectable locally advanced or metastatic breast cancer after treatment with trastuzumab and a taxane*. Available at: <https://www.nice.org.uk/guidance/ta371> (Accessed: 08/01/2016).

Nezu, M., Sasaki, H., Kuwahara, Y., Ochiya, T., Yamada, Y., Sakamoto, H., Tashiro, H., Yamazaki, M., Ikeuchi, T., Saito, Y. and Terada, M. (1999) 'Identification of a novel promoter and exons of the c-ERBB-2 gene', *Biochem Biophys Res Commun*, 258(3), pp. 499-505.

NICE (2002) *Guidance on the use of trastuzumab for the treatment of advanced breast cancer*. Available at: <https://nice.org.uk/guidance/TA43>.

## References

NICE (2009) *Early and locally advanced breast cancer: diagnosis and treatment*. [Online]. Available at: <http://nice.org.uk/guidance/cg80>.

NIH (2013) *FDA Approval for Trastuzumab*. Available at: <https://cancer.gov/about-cancer/treatment/drugs/fda-trastuzumab> (Accessed: 22.02.2017).

Niwa, M. and Berget, S.M. (1991) 'Mutation of the AAUAAA polyadenylation signal depresses in vitro splicing of proximal but not distal introns', *Genes Dev*, 5(11), pp. 2086-95.

Nolens, G., Pignon, J.C., Koopmansch, B., Elmoualij, B., Zorzi, W., De Pauw, E. and Winkler, R. (2009) 'Ku proteins interact with activator protein-2 transcription factors and contribute to ERBB2 overexpression in breast cancer cell lines', *Breast Cancer Res*, 11(6), p. R83.

Notari, M., Neviani, P., Santhanam, R., Blaser, B.W., Chang, J.S., Galletta, A., Willis, A.E., Roy, D.C., Caligiuri, M.A., Marcucci, G. and Perrotti, D. (2006) 'A MAPK/HNRPK pathway controls BCR/ABL oncogenic potential by regulating MYC mRNA translation', *Blood*, 107(6), pp. 2507-16.

O'Neill, F., Madden, S.F., Clynes, M., Crown, J., Doolan, P., Aherne, S.T. and O'Connor, R. (2013) 'A gene expression profile indicative of early stage HER2 targeted therapy response', *Mol Cancer*, 12, p. 69.

Oakman, C., Sapino, A., Marchio, C., Pestrin, M., Biganzoli, L. and Di Leo, A. (2010) 'Chemotherapy with or without trastuzumab', *Ann Oncol*, 21 Suppl 7, pp. vii112-9.

Oh, A.S., Lorant, L.A., Holloway, J.N., Miller, D.L., Kern, F.G. and El-Ashry, D. (2001) 'Hyperactivation of MAPK induces loss of ERalpha expression in breast cancer cells', *Mol Endocrinol*, 15(8), pp. 1344-59.

Ohlschlegel, C., Zahel, K., Kradofer, D., Hell, M. and Jochum, W. (2011) 'HER2 genetic heterogeneity in breast carcinoma', *J Clin Pathol*, 64(12), pp. 1112-6.

Orban, T.I. and Olah, E. (2003) 'Emerging roles of BRCA1 alternative splicing', *Mol Pathol*, 56(4), pp. 191-7.

Ortuno-Pineda, C., Galindo-Rosales, J.M., Calderon-Salinas, J.V., Villegas-Sepulveda, N., Saucedo-Cardenas, O., De Nova-Ocampo, M. and Valdes, J. (2012) 'Binding of hnRNP H and U2AF65 to respective G-codes and a poly-uridine tract collaborate in the N50-5' ss selection of the REST N exon in H69 cells', *PLoS One*, 7(7), p. e40315.

Ostareck, D.H., Ostareck-Lederer, A., Wilm, M., Thiele, B.J., Mann, M. and Hentze, M.W. (1997) 'mRNA silencing in erythroid differentiation: hnRNP K and

## References

hnRNP E1 regulate 15-lipoxygenase translation from the 3' end', *Cell*, 89(4), pp. 597-606.

Pagliarini, V., Naro, C. and Sette, C. (2015) 'Splicing Regulation: A Molecular Device to Enhance Cancer Cell Adaptation', *Biomed Res Int*, 2015, p. 543067.

Pal, S., Gupta, R. and Davuluri, R.V. (2012) 'Alternative transcription and alternative splicing in cancer', *Pharmacol Ther*, 136(3), pp. 283-94.

Pang, W.W. and Hartmann, P.E. (2007) 'Initiation of human lactation: secretory differentiation and secretory activation', *J Mammary Gland Biol Neoplasia*, 12(4), pp. 211-21.

Park, S.K. and Jeong, S. (2016) 'SRSF3 represses the expression of PDCD4 protein by coordinated regulation of alternative splicing, export and translation', *Biochem Biophys Res Commun*, 470(2), pp. 431-8.

Parkin, D.M., Boyd, L. and Walker, L.C. (2011) '16. The fraction of cancer attributable to lifestyle and environmental factors in the UK in 2010', *Br J Cancer*, 105 Suppl 2, pp. S77-81.

Pedersen, K., Angelini, P., Laos, S., Bach-Faig, A., Cunningham, M.P., Ferrer-Ramón, C., Luque-García, A., García-Castillo, J., Parra-Palau, J.L., Scaltriti, M., Ramón y Cajal, S., Baselga, J. and Arribas, J. (2009) 'A Naturally Occurring HER2 Carboxy-Terminal Fragment Promotes Mammary Tumor Growth and Metastasis', *Molecular and Cellular Biology*, 29(12), pp. 3319-3331.

Pinder, S.E. (2010) 'Ductal carcinoma in situ (DCIS): pathological features, differential diagnosis, prognostic factors and specimen evaluation', *Mod Pathol*, 23 Suppl 2, pp. S8-13.

Popp, M.W. and Maquat, L.E. (2013) 'Organizing principles of mammalian nonsense-mediated mRNA decay', *Annu Rev Genet*, 47, pp. 139-65.

Proud, C.G. (2009) 'mTORC1 signalling and mRNA translation', *Biochem Soc Trans*, 37(Pt 1), pp. 227-31.

Qian, L., Chen, L., Shi, M., Yu, M., Jin, B., Hu, M., Xia, Q., Zhang, X., Shen, B. and Guo, N. (2006) 'A novel cis-acting element in Her2 promoter regulated by Stat3 in mammary cancer cells', *Biochem Biophys Res Commun*, 345(2), pp. 660-8.

Ragunathan, P.L. and Guthrie, C. (1998) 'RNA unwinding in U4/U6 snRNPs requires ATP hydrolysis and the DEIH-box splicing factor Brr2', *Curr Biol*, 8(15), pp. 847-55.

## References

Rahman, M.A., Azuma, Y., Nasrin, F., Takeda, J., Nazim, M., Bin Ahsan, K., Masuda, A., Engel, A.G. and Ohno, K. (2015) 'SRSF1 and hnRNP H antagonistically regulate splicing of COLQ exon 16 in a congenital myasthenic syndrome', *Sci Rep*, 5, p. 13208.

Rakha, E.A., Pinder, S.E., Bartlett, J.M., Ibrahim, M., Starczynski, J., Carder, P.J., Provenzano, E., Hanby, A., Hales, S., Lee, A.H., Ellis, I.O. and National Coordinating Committee for Breast, P. (2015) 'Updated UK Recommendations for HER2 assessment in breast cancer', *J Clin Pathol*, 68(2), pp. 93-9.

Rakha, E.A., Reis-Filho, J.S., Baehner, F., Dabbs, D.J., Decker, T., Eusebi, V., Fox, S.B., Ichihara, S., Jacquemier, J., Lakhani, S.R., Palacios, J., Richardson, A.L., Schnitt, S.J., Schmitt, F.C., Tan, P.H., Tse, G.M., Badve, S. and Ellis, I.O. (2010) 'Breast cancer prognostic classification in the molecular era: the role of histological grade', *Breast Cancer Res*, 12(4), p. 207.

Revil, T., Pelletier, J., Toutant, J., Cloutier, A. and Chabot, B. (2009) 'Heterogeneous nuclear ribonucleoprotein K represses the production of pro-apoptotic Bcl-xS splice isoform', *J Biol Chem*, 284(32), pp. 21458-67.

Rhodes, L.V., Short, S.P., Neel, N.F., Salvo, V.A., Zhu, Y., Elliott, S., Wei, Y., Yu, D., Sun, M., Muir, S.E., Fonseca, J.P., Bratton, M.R., Segar, C., Tilghman, S.L., Sobolik-Delmaire, T., Horton, L.W., Zaja-Milatovic, S., Collins-Burow, B.M., Wadsworth, S., Beckman, B.S., Wood, C.E., Fuqua, S.A., Nephew, K.P., Dent, P., Worthylake, R.A., Curiel, T.J., Hung, M.C., Richmond, A. and Burow, M.E. (2011) 'Cytokine receptor CXCR4 mediates estrogen-independent tumorigenesis, metastasis, and resistance to endocrine therapy in human breast cancer', *Cancer Res*, 71(2), pp. 603-13.

Richer, J.K., Jacobsen, B.M., Manning, N.G., Abel, M.G., Wolf, D.M. and Horwitz, K.B. (2002) 'Differential gene regulation by the two progesterone receptor isoforms in human breast cancer cells', *J Biol Chem*, 277(7), pp. 5209-18.

Rizzolo, P., Silvestri, V., Falchetti, M. and Ottini, L. (2011) 'Inherited and acquired alterations in development of breast cancer', *Appl Clin Genet*, 4, pp. 145-58.

*RNA and Cancer*. (2013) Springer-Verlag(Accessed: 10/09/2015).

Robberson, B.L., Cote, G.J. and Berget, S.M. (1990) 'Exon definition may facilitate splice site selection in RNAs with multiple exons', *Mol Cell Biol*, 10(1), pp. 84-94.

Romao, L., Inacio, A., Santos, S., Avila, M., Faustino, P., Pacheco, P. and Lavinha, J. (2000) 'Nonsense mutations in the human beta-globin gene lead to unexpected levels of cytoplasmic mRNA accumulation', *Blood*, 96(8), pp. 2895-901.

## References

- Romeo, Y., Zhang, X. and Roux, P.P. (2012) 'Regulation and function of the RSK family of protein kinases', *Biochem J*, 441(2), pp. 553-69.
- Roskoski, R., Jr. (2013) 'The ErbB/HER family of protein-tyrosine kinases and cancer', *Pharmacol Res*, 79C, pp. 34-74.
- Roskoski, R., Jr. (2014) 'ErbB/HER protein-tyrosine kinases: Structures and small molecule inhibitors', *Pharmacol Res*, 87, pp. 42-59.
- Russo, J. and Russo, I.H. (2004) 'Development of the human breast', *Maturitas*, 49(1), pp. 2-15.
- Sapino, A., Goia, M., Recupero, D. and Marchio, C. (2013) 'Current Challenges for HER2 Testing in Diagnostic Pathology: State of the Art and Controversial Issues', *Front Oncol*, 3, p. 129.
- Sasso, M., Bianchi, F., Ciravolo, V., Tagliabue, E. and Campiglio, M. (2011) 'HER2 splice variants and their relevance in breast cancer', *Journal of Nucleic Acids Investigation*, 2(1), pp. 52-59.
- Schillaci, R., Guzman, P., Cayrol, F., Beguelin, W., Diaz Flaque, M.C., Proietti, C.J., Pineda, V., Palazzi, J., Frahm, I., Charreau, E.H., Maronna, E., Roa, J.C. and Elizalde, P.V. (2012) 'Clinical relevance of ErbB-2/HER2 nuclear expression in breast cancer', *BMC Cancer*, 12, p. 74.
- Schneeweiss, A., Chia, S., Hickish, T., Harvey, V., Eniu, A., Hegg, R., Tausch, C., Seo, J.H., Tsai, Y.F., Ratnayake, J., McNally, V., Ross, G. and Cortes, J. (2013) 'Pertuzumab plus trastuzumab in combination with standard neoadjuvant anthracycline-containing and anthracycline-free chemotherapy regimens in patients with HER2-positive early breast cancer: a randomized phase II cardiac safety study (TRYPHAENA)', *Ann Oncol*, 24(9), pp. 2278-84.
- Schrohl, A.S., Pedersen, H.C., Jensen, S.S., Nielsen, S.L. and Brunner, N. (2011) 'Human epidermal growth factor receptor 2 (HER2) immunoreactivity: specificity of three pharmacodiagnostic antibodies', *Histopathology*, 59(5), pp. 975-83.
- Schulz, R., Steller, F., Scheel, A.H., Ruschoff, J., Reinert, M.C., Dobbstein, M., Marchenko, N.D. and Moll, U.M. (2014) 'HER2/ErbB2 activates HSF1 and thereby controls HSP90 clients including MIF in HER2-overexpressing breast cancer', *Cell Death Dis*, 5, p. e980.
- Scimeca, M., Antonacci, C., Colombo, D., Bonfiglio, R., Buonomo, O.C. and Bonanno, E. (2016) 'Emerging prognostic markers related to mesenchymal characteristics of poorly differentiated breast cancers', *Tumour Biol*, 37(4), pp. 5427-35.

## References

- Scott, G.K., Goga, A., Bhaumik, D., Berger, C.E., Sullivan, C.S. and Benz, C.C. (2007) 'Coordinate suppression of ERBB2 and ERBB3 by enforced expression of micro-RNA miR-125a or miR-125b', *J Biol Chem*, 282(2), pp. 1479-86.
- Scott, G.K., Marx, C., Berger, C.E., Saunders, L.R., Verdin, E., Schafer, S., Jung, M. and Benz, C.C. (2008) 'Destabilization of ERBB2 transcripts by targeting 3' untranslated region messenger RNA associated HuR and histone deacetylase-6', *Mol Cancer Res*, 6(7), pp. 1250-8.
- Scott, G.K., Robles, R., Park, J.W., Montgomery, P.A., Daniel, J., Holmes, W.E., Lee, J., Keller, G.A., Li, W.L., Fendly, B.M. and et al. (1993) 'A truncated intracellular HER2/neu receptor produced by alternative RNA processing affects growth of human carcinoma cells', *Mol Cell Biol*, 13(4), pp. 2247-57.
- Segatto, O., King, C.R., Pierce, J.H., Di Fiore, P.P. and Aaronson, S.A. (1988) 'Different structural alterations upregulate in vitro tyrosine kinase activity and transforming potency of the erbB-2 gene', *Mol Cell Biol*, 8(12), pp. 5570-4.
- Shamieh, L.S., Evans, A.J., Denton, M.C. and Clinton, G.M. (2004) 'Receptor binding specificities of Herstatin and its intron 8-encoded domain', *FEBS Lett*, 568(1-3), pp. 163-6.
- Sharma, S., Kohlstaedt, L.A., Damianov, A., Rio, D.C. and Black, D.L. (2008) 'Polypyrimidine tract binding protein controls the transition from exon definition to an intron defined spliceosome', *Nat Struct Mol Biol*, 15(2), pp. 183-91.
- Sharp, P.A. (1994) 'Split genes and RNA splicing', *Cell*, 77(6), pp. 805-15.
- Sharp, P.A. (2005) 'The discovery of split genes and RNA splicing', *Trends Biochem Sci*, 30(6), pp. 279-81.
- Siegel, P.M., Dankort, D.L., Hardy, W.R. and Muller, W.J. (1994) 'Novel activating mutations in the neu proto-oncogene involved in induction of mammary tumors', *Mol Cell Biol*, 14(11), pp. 7068-77.
- Siegel, P.M. and Muller, W.J. (1996) 'Mutations affecting conserved cysteine residues within the extracellular domain of Neu promote receptor dimerization and activation', *Proc Natl Acad Sci U S A*, 93(17), pp. 8878-83.
- Siegel, P.M., Ryan, E.D., Cardiff, R.D. and Muller, W.J. (1999) 'Elevated expression of activated forms of Neu/ErbB-2 and ErbB-3 are involved in the induction of mammary tumors in transgenic mice: implications for human breast cancer', *EMBO J*, 18(8), pp. 2149-64.
- Siegfried, Z., Bonomi, S., Ghigna, C. and Karni, R. (2013) 'Regulation of the Ras-MAPK and PI3K-mTOR Signalling Pathways by Alternative Splicing in Cancer', *Int J Cell Biol*, 2013, p. 568931.

## References

Silipo, M., Gautrey, H. and Tyson-Capper, A. (2015) 'Deregulation of splicing factors and breast cancer development', *J Mol Cell Biol*, 7(5), pp. 388-401.

Silva, A.L. and Romao, L. (2009) 'The mammalian nonsense-mediated mRNA decay pathway: to decay or not to decay! Which players make the decision?', *FEBS Lett*, 583(3), pp. 499-505.

Singletary, S.E. and Connolly, J.L. (2006) 'Breast cancer staging: working with the sixth edition of the AJCC Cancer Staging Manual', *CA Cancer J Clin*, 56(1), pp. 37-47; quiz 50-1.

Sistonen, L., Holtta, E., Lehvaslaiho, H., Lehtola, L. and Alitalo, K. (1989) 'Activation of the neu tyrosine kinase induces the fos/jun transcription factor complex, the glucose transporter and ornithine decarboxylase', *J Cell Biol*, 109(5), pp. 1911-9.

Slamon, D.J., Clark, G.M., Wong, S.G., Levin, W.J., Ullrich, A. and McGuire, W.L. (1987) 'Human breast cancer: correlation of relapse and survival with amplification of the HER-2/neu oncogene', *Science*, 235(4785), pp. 177-82.

Slamon, D.J., Godolphin, W., Jones, L.A., Holt, J.A., Wong, S.G., Keith, D.E., Levin, W.J., Stuart, S.G., Udove, J., Ullrich, A. and et al. (1989) 'Studies of the HER-2/neu proto-oncogene in human breast and ovarian cancer', *Science*, 244(4905), pp. 707-12.

Soma, D., Kitayama, J., Yamashita, H., Miyato, H., Ishikawa, M. and Nagawa, H. (2008) 'Leptin augments proliferation of breast cancer cells via transactivation of HER2', *J Surg Res*, 149(1), pp. 9-14.

Song, K.Y., Choi, H.S., Law, P.Y., Wei, L.N. and Loh, H.H. (2012) 'Post-transcriptional regulation of mu-opioid receptor: role of the RNA-binding proteins heterogeneous nuclear ribonucleoprotein H1 and F', *Cell Mol Life Sci*, 69(4), pp. 599-610.

Song, K.Y., Choi, H.S., Law, P.Y., Wei, L.N. and Loh, H.H. (2016) 'Post-Transcriptional Regulation of the Human Mu-Opioid Receptor (MOR) by Morphine-Induced RNA Binding Proteins hnRNP K and PCBP1', *J Cell Physiol*.

Soule, H.D., Vazquez, J., Long, A., Albert, S. and Brennan, M. (1973) 'A human cell line from a pleural effusion derived from a breast carcinoma', *J Natl Cancer Inst*, 51(5), pp. 1409-16.

Srebrow, A. and Kornblihtt, A.R. (2006) 'The connection between splicing and cancer', *J Cell Sci*, 119(Pt 13), pp. 2635-41.

Sridharan, S. and Basu, A. (2011) 'S6 kinase 2 promotes breast cancer cell survival via Akt', *Cancer Res*, 71(7), pp. 2590-9.

## References

- Stickeler, E., Kittrell, F., Medina, D. and Berget, S.M. (1999) 'Stage-specific changes in SR splicing factors and alternative splicing in mammary tumorigenesis', *Oncogene*, 18(24), pp. 3574-82.
- Suami, H., Pan, W.R., Mann, G.B. and Taylor, G.I. (2008) 'The lymphatic anatomy of the breast and its implications for sentinel lymph node biopsy: a human cadaver study', *Ann Surg Oncol*, 15(3), pp. 863-71.
- Subbaramaiah, K., Norton, L., Gerald, W. and Dannenberg, A.J. (2002) 'Cyclooxygenase-2 is overexpressed in HER-2/neu-positive breast cancer: evidence for involvement of AP-1 and PEA3', *J Biol Chem*, 277(21), pp. 18649-57.
- Subik, K., Lee, J.F., Baxter, L., Strzepek, T., Costello, D., Crowley, P., Xing, L., Hung, M.C., Bonfiglio, T., Hicks, D.G. and Tang, P. (2010) 'The Expression Patterns of ER, PR, HER2, CK5/6, EGFR, Ki-67 and AR by Immunohistochemical Analysis in Breast Cancer Cell Lines', *Breast Cancer (Auckl)*, 4, pp. 35-41.
- Sun, J.S. and Manley, J.L. (1995) 'A novel U2-U6 snRNA structure is necessary for mammalian mRNA splicing', *Genes Dev*, 9(7), pp. 843-54.
- Tai, W., Mahato, R. and Cheng, K. (2010) 'The role of HER2 in cancer therapy and targeted drug delivery', *J Control Release*, 146(3), pp. 264-75.
- Takimoto, M., Tomonaga, T., Matunis, M., Avigan, M., Krutzsch, H., Dreyfuss, G. and Levens, D. (1993) 'Specific binding of heterogeneous ribonucleoprotein particle protein K to the human c-myc promoter, in vitro', *J Biol Chem*, 268(24), pp. 18249-58.
- Tal, M., King, C.R., Kraus, M.H., Ullrich, A., Schlessinger, J. and Givol, D. (1987) 'Human HER2 (neu) promoter: evidence for multiple mechanisms for transcriptional initiation', *Mol Cell Biol*, 7(7), pp. 2597-601.
- Tang, Y., Horikawa, I., Ajiro, M., Robles, A.I., Fujita, K., Mondal, A.M., Stauffer, J.K., Zheng, Z.M. and Harris, C.C. (2013) 'Downregulation of splicing factor SRSF3 induces p53beta, an alternatively spliced isoform of p53 that promotes cellular senescence', *Oncogene*, 32(22), pp. 2792-8.
- Tania, M., Khan, M.A. and Fu, J. (2014) 'Epithelial to mesenchymal transition inducing transcription factors and metastatic cancer', *Tumour Biol*.
- Taraborrelli, S. (2015) 'Physiology, production and action of progesterone', *Acta Obstet Gynecol Scand*, 94 Suppl 161, pp. 8-16.
- Tazi, J., Bakkour, N. and Stamm, S. (2009) 'Alternative splicing and disease', *Biochimica et Biophysica Acta - Molecular Basis of Disease*, 1792(1), pp. 14-26.

## References

Tice, J.A., Miglioretti, D.L., Li, C.S., Vachon, C.M., Gard, C.C. and Kerlikowske, K. (2015) 'Breast Density and Benign Breast Disease: Risk Assessment to Identify Women at High Risk of Breast Cancer', *J Clin Oncol*, 33(28), pp. 3137-43.

Torres, M.P., Chakraborty, S., Soucek, J. and Batra, S.K. (2012) 'Mucin-based targeted pancreatic cancer therapy', *Curr Pharm Des*, 18(17), pp. 2472-81.

Trempe, G.L. (1976) 'Human breast cancer in culture', *Recent Results Cancer Res*, (57), pp. 33-41.

Triulzi, T., Bianchi, G.V. and Tagliabue, E. (2016) 'Predictive biomarkers in the treatment of HER2-positive breast cancer: an ongoing challenge', *Future Oncol*, 12(11), pp. 1413-28.

Tse, C., Gauchez, A.S., Jacot, W. and Lamy, P.J. (2012) 'HER2 shedding and serum HER2 extracellular domain: biology and clinical utility in breast cancer', *Cancer Treat Rev*, 38(2), pp. 133-42.

Turner, N.H. and Di Leo, A. (2013) 'HER2 discordance between primary and metastatic breast cancer: assessing the clinical impact', *Cancer Treat Rev*, 39(8), pp. 947-57.

Turpin, J., Ling, C., Crosby, E.J., Hartman, Z.C., Simond, A.M., Chodosh, L.A., Rennhack, J.P., Andrechek, E.R., Ozcelik, J., Hallett, M., Mills, G.B., Cardiff, R.D., Gray, J.W., Griffith, O.L. and Muller, W.J. (2016) 'The ErbB2DeltaEx16 splice variant is a major oncogenic driver in breast cancer that promotes a pro-metastatic tumor microenvironment', *Oncogene*.

Twyffels, L., Gueydan, C. and Kruys, V. (2011) 'Shuttling SR proteins: more than splicing factors', *FEBS J*, 278(18), pp. 3246-55.

U.S. Food and Drug Administration (2007) *TYKERB (lapatinib) tablets Initial U.S. Approval: 2007.* Available at: [http://www.accessdata.fda.gov/drugsatfda\\_docs/label/2010/022059s007lbl.pdf](http://www.accessdata.fda.gov/drugsatfda_docs/label/2010/022059s007lbl.pdf) (Accessed: 07/10/2013).

U.S. Food and Drug Administration (2012) *U.S. BLA: Pertuzumab* Genentech, Inc. Available at: [http://www.accessdata.fda.gov/drugsatfda\\_docs/label/2012/125409lbl.pdf](http://www.accessdata.fda.gov/drugsatfda_docs/label/2012/125409lbl.pdf) (Accessed: 07/10/2013).

U.S. Food and Drug Administration (2013) *Ado-Trastuzumab Emtansine.* Available at: <http://www.fda.gov/drugs/informationondrugs/approveddrugs/ucm340913.htm> (Accessed: 07/10/2013).

## References

- Ueki, K., Matsuda, S., Tobe, K., Gotoh, Y., Tamemoto, H., Yachi, M., Akanuma, Y., Yazaki, Y., Nishida, E. and Kadowaki, T. (1994) 'Feedback regulation of mitogen-activated protein kinase kinase activity of c-Raf-1 by insulin and phorbol ester stimulation', *J Biol Chem*, 269(22), pp. 15756-61.
- Uren, P.J., Bahrami-Samani, E., de Araujo, P.R., Vogel, C., Qiao, M., Burns, S.C., Smith, A.D. and Penalva, L.O. (2016) 'High-throughput analyses of hnRNP H1 dissects its multi-functional aspect', *RNA Biol*, 13(4), pp. 400-11.
- Vance, G.H., Barry, T.S., Bloom, K.J., Fitzgibbons, P.L., Hicks, D.G., Jenkins, R.B., Persons, D.L., Tubbs, R.R., Hammond, M.E. and College of American, P. (2009) 'Genetic heterogeneity in HER2 testing in breast cancer: panel summary and guidelines', *Arch Pathol Lab Med*, 133(4), pp. 611-2.
- Venables, J.P., Koh, C.S., Froehlich, U., Lapointe, E., Couture, S., Inkel, L., Bramard, A., Paquet, E.R., Watier, V., Durand, M., Lucier, J.F., Gervais-Bird, J., Tremblay, K., Prinos, P., Klinck, R., Elela, S.A. and Chabot, B. (2008) 'Multiple and specific mRNA processing targets for the major human hnRNP proteins', *Mol Cell Biol*, 28(19), pp. 6033-43.
- Venturutti, L., Cordo Russo, R.I., Rivas, M.A., Mercogliano, M.F., Izzo, F., Oakley, R.H., Pereyra, M.G., De Martino, M., Proietti, C.J., Yankilevich, P., Roa, J.C., Guzman, P., Cortese, E., Allemand, D.H., Huang, T.H., Charreau, E.H., Cidlowski, J.A., Schillaci, R. and Elizalde, P.V. (2016) 'MiR-16 mediates trastuzumab and lapatinib response in ErbB-2-positive breast and gastric cancer via its novel targets CCNJ and FUBP1', *Oncogene*.
- Vernimmen, D., Begon, D., Salvador, C., Gofflot, S., Grootelaes, M. and Winkler, R. (2003a) 'Identification of HTF (HER2 transcription factor) as an AP-2 (activator protein-2) transcription factor and contribution of the HTF binding site to ERBB2 gene overexpression', *Biochem J*, 370(Pt 1), pp. 323-9.
- Vernimmen, D., Gueders, M., Pisvin, S., Delvenne, P. and Winkler, R. (2003b) 'Different mechanisms are implicated in ERBB2 gene overexpression in breast and in other cancers', *Br J Cancer*, 89(5), pp. 899-906.
- Vogel, C.L., Cobleigh, M.A., Tripathy, D., Gutheil, J.C., Harris, L.N., Fehrenbacher, L., Slamon, D.J., Murphy, M., Novotny, W.F., Burchmore, M., Shak, S., Stewart, S.J. and Press, M. (2002) 'Efficacy and safety of trastuzumab as a single agent in first-line treatment of HER2-overexpressing metastatic breast cancer', *J Clin Oncol*, 20(3), pp. 719-26.
- Vorherr, H. (1974) 'The Breast, Morphology, Physiology And Lactation', in *The Breast*. New York: Academic Press.
- Vu, N.T., Park, M.A., Shultz, J.C., Goehle, R.W., Hoferlin, L.A., Shultz, M.D., Smith, S.A., Lynch, K.W. and Chalfant, C.E. (2013) 'hnRNP U enhances

## References

caspase-9 splicing and is modulated by AKT-dependent phosphorylation of hnRNP L', *J Biol Chem*, 288(12), pp. 8575-84.

Wang, E., Aslanzadeh, V., Papa, F., Zhu, H., de la Grange, P. and Cambi, F. (2012a) 'Global profiling of alternative splicing events and gene expression regulated by hnRNPH/F', *PLoS One*, 7(12), p. e51266.

Wang, S.C., Lien, H.C., Xia, W.Y., Chen, I.F., Lo, H.W., Wang, Z.Q., Ali-Seyed, M., Lee, D.F., Bartholomeusz, G., Fu, O.Y., Giri, D.K. and Hung, M.C. (2004) 'Binding at and transactivation of the COX-2 promoter by nuclear tyrosine kinase receptor ErbB-2', *Cancer Cell*, 6(3), pp. 251-261.

Wang, Y., Ma, M., Xiao, X. and Wang, Z. (2012b) 'Intronic splicing enhancers, cognate splicing factors and context-dependent regulation rules', *Nat Struct Mol Biol*, 19(10), pp. 1044-52.

Wang, Z., Murigneux, V. and Le Hir, H. (2014) 'Transcriptome-wide modulation of splicing by the exon junction complex', *Genome Biol*, 15(12), p. 551.

Ward, T.M., Iorns, E., Liu, X., Hoe, N., Kim, P., Singh, S., Dean, S., Jegg, A.M., Gallas, M., Rodriguez, C., Lippman, M., Landgraf, R. and Pegram, M.D. (2013) 'Truncated p110 ERBB2 induces mammary epithelial cell migration, invasion and orthotopic xenograft formation, and is associated with loss of phosphorylated STAT5', *Oncogene*, 32(19), pp. 2463-74.

Wei, C.C., Guo, D.F., Zhang, S.L., Ingelfinger, J.R. and Chan, J.S. (2005) 'Heterogenous nuclear ribonucleoprotein F modulates angiotensinogen gene expression in rat kidney proximal tubular cells', *J Am Soc Nephrol*, 16(3), pp. 616-28.

Weigelt, B., Horlings, H.M., Kreike, B., Hayes, M.M., Hauptmann, M., Wessels, L.F., de Jong, D., Van de Vijver, M.J., Van't Veer, L.J. and Peterse, J.L. (2008) 'Refinement of breast cancer classification by molecular characterization of histological special types', *J Pathol*, 216(2), pp. 141-50.

White, R., Gonsior, C., Bauer, N.M., Kramer-Albers, E.M., Luhmann, H.J. and Trotter, J. (2012) 'Heterogeneous nuclear ribonucleoprotein (hnRNP) F is a novel component of oligodendroglial RNA transport granules contributing to regulation of myelin basic protein (MBP) synthesis', *J Biol Chem*, 287(3), pp. 1742-54.

Will, C.L. and Luhrmann, R. (2011) 'Spliceosome structure and function', *Cold Spring Harb Perspect Biol*, 3(7).

World Health Organisation (2014) 'WHO position paper on mammography screening'. Geneva, Switzerland: WHO Press. Available at: [http://apps.who.int/iris/bitstream/10665/137339/1/9789241507936\\_eng.pdf?ua=1&ua=1](http://apps.who.int/iris/bitstream/10665/137339/1/9789241507936_eng.pdf?ua=1&ua=1).

## References

World Health Organisation (2015) *Cancer Key facts*. Available at: <http://www.who.int/mediacentre/factsheets/fs297/en/> (Accessed: 30/09/2015).

Worthington, J., Bertani, M., Chan, H.L., Gerrits, B. and Timms, J.F. (2010) 'Transcriptional profiling of ErbB signalling in mammary luminal epithelial cells--interplay of ErbB and IGF1 signalling through IGFBP3 regulation', *BMC Cancer*, 10, p. 490.

Wu, S., Romfo, C.M., Nilsen, T.W. and Green, M.R. (1999) 'Functional recognition of the 3' splice site AG by the splicing factor U2AF35', *Nature*, 402(6763), pp. 832-5.

Wu, Y., Elshimali, Y., Sarkissyan, M., Mohamed, H., Clayton, S. and Vadgama, J.V. (2012) 'Expression of FOXO1 is associated with GATA3 and Annexin-1 and predicts disease-free survival in breast cancer', *Am J Cancer Res*, 2(1), pp. 104-15.

Wu, Y., Shang, X., Sarkissyan, M., Slamon, D. and Vadgama, J.V. (2010) 'FOXO1A is a target for HER2-overexpressing breast tumors', *Cancer Res*, 70(13), pp. 5475-85.

Xiao, X., Wang, Z., Jang, M., Nutiu, R., Wang, E.T. and Burge, C.B. (2009) 'Splice site strength-dependent activity and genetic buffering by poly-G runs', *Nat Struct Mol Biol*, 16(10), pp. 1094-100.

Xie, D., Shu, X.O., Deng, Z., Wen, W.Q., Creek, K.E., Dai, Q., Gao, Y.T., Jin, F. and Zheng, W. (2000) 'Population-based, case-control study of HER2 genetic polymorphism and breast cancer risk', *J Natl Cancer Inst*, 92(5), pp. 412-7.

Yang, L., Li, Y. and Zhang, Y. (2014) 'Identification of prolidase as a high affinity ligand of the ErbB2 receptor and its regulation of ErbB2 signaling and cell growth', *Cell Death Dis*, 5, p. e1211.

Yilmaz, M. and Christofori, G. (2009) 'EMT, the cytoskeleton, and cancer cell invasion', *Cancer Metastasis Rev*, 28(1-2), pp. 15-33.

Yordy, J.S. and Muise-Helmericks, R.C. (2000) 'Signal transduction and the Ets family of transcription factors', *Oncogene*, 19(55), pp. 6503-13.

Yoshida, K. and Miki, Y. (2004) 'Role of BRCA1 and BRCA2 as regulators of DNA repair, transcription, and cell cycle in response to DNA damage', *Cancer Sci*, 95(11), pp. 866-71.

Zardavas, D., Cameron, D., Krop, I. and Piccart, M. (2013) 'Beyond trastuzumab and lapatinib', *Am Soc Clin Oncol Educ Book*, pp. 2-11.

## References

- Zhang, C., Krainer, A.R. and Zhang, M.Q. (2007) 'Evolutionary impact of limited splicing fidelity in mammalian genes', *Trends Genet*, 23(10), pp. 484-8.
- Zhang, J., Kuo, C.C. and Chen, L. (2011) 'GC content around splice sites affects splicing through pre-mRNA secondary structures', *BMC Genomics*, 12, p. 90.
- Zhang, T., Zhang, H., Wang, Y. and McGown, L.B. (2012) 'Capture and identification of proteins that bind to a GGA-rich sequence from the ERBB2 gene promoter region', *Anal Bioanal Chem*, 404(6-7), pp. 1867-76.
- Zheng, F., Yue, C., Li, G., He, B., Cheng, W., Wang, X., Yan, M., Long, Z., Qiu, W., Yuan, Z., Xu, J., Liu, B., Shi, Q., Lam, E.W., Hung, M.C. and Liu, Q. (2016) 'Nuclear AURKA acquires kinase-independent transactivating function to enhance breast cancer stem cell phenotype', *Nat Commun*, 7, p. 10180.
- Zorio, D.A. and Blumenthal, T. (1999) 'Both subunits of U2AF recognize the 3' splice site in *Caenorhabditis elegans*', *Nature*, 402(6763), pp. 835-8.
- Zuker, M. and Stiegler, P. (1981) 'Optimal computer folding of large RNA sequences using thermodynamics and auxiliary information', *Nucleic Acids Res*, 9(1), pp. 133-48.
- Zuo, T., Wang, L., Morrison, C., Chang, X., Zhang, H., Li, W., Liu, Y., Wang, Y., Liu, X., Chan, M.W., Liu, J.Q., Love, R., Liu, C.G., Godfrey, V., Shen, R., Huang, T.H., Yang, T., Park, B.K., Wang, C.Y., Zheng, P. and Liu, Y. (2007) 'FOXP3 is an X-linked breast cancer suppressor gene and an important repressor of the HER-2/ErbB2 oncogene', *Cell*, 129(7), pp. 1275-86.

## Appendix

### Publications

- Dittrich A., Gautrey H., Browell D. and Tyson-Capper A. (2014) The HER2 Signalling Network in Breast Cancer—Like a Spider in its Web. *J Mammary Gland Biol Neoplasia* 19 (3-4)
- Gautrey H., Jackson C., Dittrich A., Browell D., Lennard T. and Tyson-Capper A. (2015) SRSF3 and hnRNPH1 regulate a splicing hotspot of HER2 in breast cancer cells. *RNA Biol* 12 (10)
- Dittrich A., Gautrey H. and Tyson-Capper A. Regulatory mechanisms of the  $\Delta 16$ HER2 splicing event. (manuscript in preparation)
- Dittrich A., Gautrey H., Kourea H. and Tyson-Capper A. Associations between HER2 splice variants and breast tumour heterogeneity. (manuscript in preparation)

### Presentations

- |                      |  |
|----------------------|--|
| <b>July 2016</b>     | <b>Tumour promoting HER2 Splice Variant <math>\Delta 16</math>HER2: Regulation and Implication in Breast Cancer</b><br><br><u>Oral presentation</u> , 24th Biennial Congress of the European Association for Cancer Research, Manchester, UK |
| <b>March 2016</b>    | <b>Tumour promoting HER2 Splice Variant <math>\Delta 16</math>HER2: Regulation and Implication in Breast Cancer</b><br><br><u>Oral presentation</u> , Postgraduate Cancer Research Conference, Newcastle University, UK                      |
| <b>March 2016</b>    | <b>Tumour promoting HER2 Splice Variant <math>\Delta 16</math>HER2: Regulation and Implication in Breast Cancer</b><br><br><u>Oral presentation</u> , ICM Student Seminar, Newcastle University, UK  |
| <b>March 2015</b>    | <b>HER2 splice variants: the known and the novel</b><br><br><u>Poster presentation</u> , 1 <sup>st</sup> Course: Post-transcriptional gene regulation, Paris, France   |
| <b>November 2014</b> | <b>HER2: Regulation of alternative splicing and novel splice variants</b>  |

## Appendix

Oral presentation, ICM Student Seminar, Newcastle University, UK

**June 2014**

**My PhD Project**

Three Minutes Thesis, ICM Research Day, Newcastle University, UK

**January 2014**

**Defining how HER2 splicing hotspots are regulated in breast cancer cells**

Oral presentation, RNA UK 2014 conference, Cumbria, UK

### **Awards**

- EACR24 Meeting bursary 2016
- Wellcome Trust Institutional Strategic Grant Offering – small grant